Università degli Studi di Torino

Doctoral School of the University of Torino

PhD Programme in Chemical and Materials Sciences XXXIV Cycle

Study of micro and nano-structured materials aimed to anions, heavy metals and herbicides abatement in water treatment

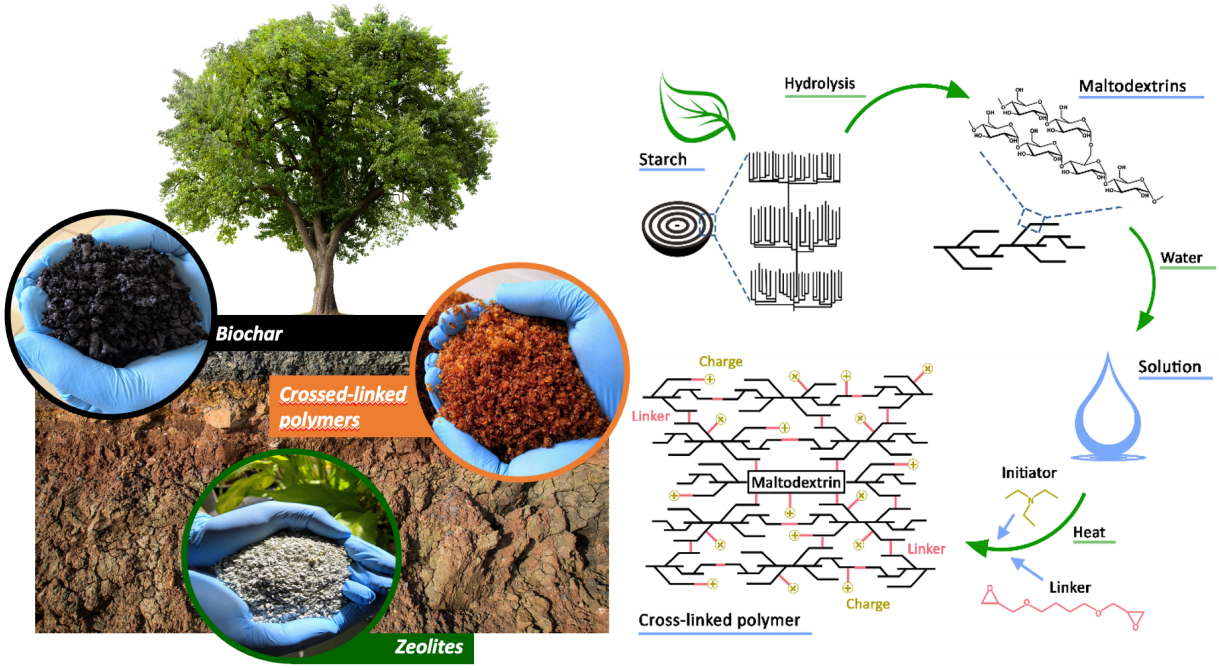

Giulia Costamagna

Supervisor:

Prof. Marco Ginepro

Università degli Studi di Torino

Doctoral School of the University of Torino

PhD Programme in Chemical and Materials Sciences XXXVI cycle

Study of micro and nano-structured materials aimed to anions, heavy metals and herbicides abatement in water treatment

Candidate: **Giulia Costamagna**

Supervisor: Prof. **Marco Ginepro**

Jury Members: Prof. **Silvia Berto**

Università degli Studi di Torino

Dipartimento di Chimica

Prof. **Gianpiero Adami**

Università di Trieste

Dipartimento di Chimica e Tecnologia del Farmaco

Prof. **Daniele Massa**

CREA: Consiglio per la Ricerca Agricola e l'analisi dell'economia agraria

Head of the Doctoral School: Prof. Alberto Rizzuti

PhD Programme Coordinator: Prof. Bartolomeo Civalleri

Torino, 2022

Abstract

Water pollution is an increasingly critical phenomenon on a global level. The main cause of contamination is attributed to untreated industrial and urban wastewater. In recent years, there has been an increase in environmental and public health problems associated with environmental pollution by heavy metals.

This thesis work focused on the research and development of zeolite, maltodextrin nanosponges and biochar, for pollutants removal in wastewater, through sustainable approach and synthesis methods for a future scaling up.

Within Cuneo and Piacenza's area there are many SMEs which target the animal husbandry business. Consequently, those SMEs need the disposal of zootechnical sewage. Data gathered by the Italian National Livestock Registry database shows a high percentage of intensive farming, mainly cattle, swine and poultry. Livestock waste is mainly composed of nitrogen substances which are notorious for being highly pollutants: those substances are responsible for air pollution as well as soil and water contamination. The European community, issued Directive 91/676/CEE, also known as the nitrate's directive, it has established what are the spreading and discharge limits (170 kg N/ha) of animal waste into crops to avoid water pollution. Anaerobic digestion has become increasingly more important within wastewater recovery in recent decades. The aforementioned methodology allows organic substances to be decomposed in absence of oxygen through specific microorganisms, achieving products with high added value such as biomethane, electrical and thermal energy. At the end of the digestion the main products are heat, biogas, composed mostly of CH_4 and CO_2, and digestate, consisting of undecomposed fraction. Biogas serves as a fuel to produce electricity while digestate can be separated into a solid and a liquid fraction. By the end of anaerobic digestion process, most of organic nitrogen has been reduced to ammoniacal nitrogen. Nitrifying bacteria oxidize ammoniacal nitrogen to form nitrates, which are responsible of water eutrophication. Given the difficulty of managing large, centralized purification plants, a localized purification system on a small scale based on natural zeolites is proposed, since they have a high cation exchange capacity and water retention. The first part of this thesis is aimed to evaluate the retaining efficacy of the ammonium ion in competition with other cations, mainly the omnipresent potassium ion in plant matter and consequently in the digestate. Knowing the composition of the digestate, the goal is to identify the amount of zeolite required to have an ammonium ion abatement of at least 60 %, such as to fall within the regulatory parameters which allows the use of greater amount of digestate into fields. The competition between ammonium and potassium ions in zeolite has been studied, by varying the ratio between the two ions. Subsequently the ammonium abatement effectiveness in these conditions has been quantified, both on synthetic samples prepared within laboratory and on real digestate samples. Finally, the absorption kinetics has been verified and the release of ammonium into water has been evaluated. The tests were carried out on the liquid fraction of the digestate as it has the highest concentration of ammonia nitrogen, while characterization tests were carried out on the solid fraction so to allow its use as compost.

However, in wastewater field there are different type of pollutants such as, anions, pesticides/herbicides, and heavy metals. The second part the thesis focused on the synthesis of new materials starch-derived base called nanosponges. Specifically, it was used a commercial maltodextrin (Glucidex 2®) as a raw material. Maltodextrins were chosen as a low cost, water soluble and more sustainable alternative to conventional commercial ion exchange resins or other adsorbent materials. Through the cross-linking process 1,4-butanediol diglycidyl ether (BDE), trimethylolpropane triglycidyl ether (TTE) and neopentyl glycol diglycidyl ether (NGDE) were used in a basic environment, and functionalization with choline chloride, carrageen-k and sultons. In this way, anionic and cationic nanosponges were achieved with positive or negative surface charge depending on the functionalization group chosen. All

nanosponges were characterized by FTIR-ATR analysis, thermogravimetric (TGA) analysis, elemental analysis, ζ-potential, swelling test and scanning electron microscope (SEM). Finally, they were tested to evaluate their removal effectiveness against the following pollutants: Nitrates, phosphates, glyphosate, Cr(VI), As(III), As(V), for anionic nanosponges and Cu, Cd, Cr (III), Pb, Ni, Zn, Al and Mn for cationic nanosponges, at different concentrations (25 - 1000 mg/L).

Last but not least, biochar was also tested for havey metals removal for water treatment purposes. Starting from 12 different wood biomasses, biochar was produced at 550 °C, 800 °C and 1100 °C in classic pyrolysis conditions (using N_2 flow). Biochar was treated with HCl to neutralize its basic nature and abatement tests were performed at different pH condition (pH = 6 and pH= 4). A comparison among these biochar and commercial biochar and active carbon was performed. Cu, Cd, Cr (III), Pb, Ni, Zn, Al and Mn were tested, at different concentrations. All biochar were characterized by FTIR-ATR analysis, elemental analysis, BET analysis, and scanning electron microscope (SEM). Good results were achieved for all material tested and can represent a good and affordable alternative to the traditional and more expensive water treatment methods.

In conclusion it can be said that these three materials could have a chance to be applied in real industrial scale due to their easiness of use and their cost-effectivness.

Index

1. Introduction

Water covers over 70% of the Earth's surface and is a very important resource for people and the environment. Water pollution affects drinking water, rivers, lakes and oceans all over the world. This consequently harms human health and the natural environment. Almost everything humans do, from growing food to manufacturing products to generating electricity, has the potential to release pollution into the environment. Environmental regulatory agencies identify two main categories of pollution: point-source and nonpoint-source pollution. Point-source pollution is easy to identify. As the name suggests, it comes from a single place. Nonpoint-source pollution is harder to identify and harder to address [1]. It is pollution that comes from many places, all at once. The United States Environmental Protection Agency (EPA) defines point source pollution as any contaminant that enters the environment from an easily identified and confined place. Examples include smokestacks, discharge pipes, and drainage ditches. Factories and power plants can be a source of point-source pollution, affecting both air and water. Smokestacks may spew carbon monoxide, heavy metal, sulfur dioxide, nitrogen dioxide, or "particulate matter" (small particles) into the air. Oil refineries, paper mills, and auto plants that use water as part of their manufacturing processes can discharge effluent—wastewater containing harmful chemical pollutants—into rivers, lakes and ocean. Municipal wastewater treatment plants are another common source of point-source pollution. Effluent from a treatment plant can introduce nutrients and harmful microbes into waterways. Nutrients can cause a rampant growth of algae in water. Nonpoint-source pollution is the opposite of point-source pollution, with pollutants released in a wide area. As an example, picture a city street during a thunderstorm. As rainwater flows over asphalt, it washes away drops of oil that leaked from car engines, particles of tire rubber, dog waste, and trash. The runoff goes into a storm sewer and ends up in a nearby river. Runoff is a major cause of nonpoint-source pollution. It is a big problem in cities because of all the hard surfaces, including streets and roofs. The number of pollutants washed from a single city block might be small, but when you add up the miles and miles of pavement in a big city you get a big problem. In rural areas, runoff can wash sediment from the roads in a logged-over forest tract. It can also carry acid from abandoned mines and flush pesticides and fertilizer from farm fields[2]. All this pollution is likely to wind up in streams, rivers, and lakes. Airborne pollutants are major contributors to acid rain. It forms in the atmosphere when sulfur dioxide and nitrogen oxides combine with water. Because acid rain results from the long-range movement of those pollutants from many factories and power plants, it is considered nonpoint-source pollution. In the United States, the Clean Air Act and

the Clean Water Act have helped to limit both point-source and nonpoint-source pollution. Thanks to these two legislative initiatives, in effect for some 50 years now, America's air and water are cleaner today than they were for most of the 20th century [3].

1.1 Water pollution: types of pollution

Water pollution afflicts our rivers, lakes, reservoirs, groundwater, and aquifers – not to mention the seas and oceans which cover most of our planet. However, not all kinds of water pollution come from the same source. Here's a quick rundown of the different types of water pollution currently compromising the quality of H_2O all over the globe.

1.1.1 Chemical pollution:

Industrial and agricultural work involves the use of many different chemicals that can run-off into water and pollute it. Metals and solvents from industrial work can pollute rivers and lakes. These are poisonous to many forms of aquatic life and may slow their development, make them infertile or even result in death. Pesticides are used in farming to control weeds, insects, and fungi. Run-offs of these pesticides can cause water pollution and poison aquatic life. Subsequently, birds, humans and other animals may be poisoned if they eat infected fish. Petroleum is another form of chemical pollutant that usually contaminates water through oil spills when a ship ruptures. Oil spills usually have only a localized have an impact on wildlife but can spread for miles. The oil can cause the death of many fish and stick to the feathers of seabirds causing them to lose the ability to fly. Some pollutants do not dissolve in water as their molecules are too big to mix between the water molecules. This material is called particulate matter and can often be a cause of water pollution. The suspended particles eventually settle and cause a thick silt at the bottom. This is harmful to marine life that lives on the floor of rivers or lakes. Biodegradable substances are often suspended in water and can cause problems by increasing the amount of anaerobic microorganisms present. Toxic chemicals suspended in water can be harmful to the development and survival of aquatic life [2].

1.1.2 Nutrient's pollution

Nutrients are essential for plant growth and development. Many nutrients are found in wastewater and fertilizers, and these can cause excess weed and algae growth if large concentrations end up in water. This can contaminate drinking water and clog filters. This can be damaging to other aquatic organisms as the algae use up the oxygen in the water, leaving none for the surrounding marine life [4].

1.1.3 Microbiological pollution

Unlike most others on this list, microbiological pollution is a naturally occurring form of water contamination. Microorganisms such as bacteria, protozoa and viruses can infiltrate water supplies, causing diseases such as bilharzia and cholera. Humans are most susceptible to this kind of pollution in places where adequate water treatment systems are not yet in place [5].

1.1.4 Oxygen-depletion pollution

Another consequence of algal blooms is their consumption of oxygen supplies. This means that those species which depend upon oxygen to survive are killed off, while anaerobic ones thrive. Some anaerobic microorganisms can produce ammonia, sulfides and other harmful toxins, which can make the water even more dangerous to animals (and humans, too) [6].

1.1.5 Surface water pollution

Referring to all water sources above ground, such as rivers, lakes, seas and oceans, surface water pollution can occur both naturally, accidentally and intentionally. For example, monitoring has an all-important role in natural flood management, which can lead to poor water quality, while accidental oil spills and negligent industries emptying waste into water bodies are also key contributors [2].

1.1.6 Suspended matter

Improperly discarded waste, such as fragments of plastic, rubber or other manmade materials, can find themselves into water sources and persist for a long time. Because they are too robust to dissolve in the water and too big to mix effectively with the molecules, they simply float on its surface and prevent oxygen and sunlight from penetrating below [7].

1.1.7 Groundwater pollution

A lot of the Earth's water is found underground in soil or under rock structures called aquifers. Humans often use aquifers to obtain drinking water and build wells to access it. When this water becomes polluted, it is called groundwater pollution. Groundwater pollution is often caused by pesticide contamination from the soil, this can infect our drinking water and cause huge problems.

1.1.8 Industrial water and water pollution

Industry is a huge source of water pollution; it produces pollutants that are extremely harmful to people and the environment. Many industrial facilities use freshwater to carry away waste from the plant and into rivers, lakes, and oceans. Pollutants from industrial sources include:

- Asbestos – This pollutant is a serious health hazard and cause carcinogenic effects. Asbestos fibers can be inhaled and cause illnesses such as asbestosis, mesothelioma, lung cancer, intestinal cancer, and liver cancer.
- Lead – This is a metallic element and can cause health and environmental problems. It is a non-biodegradable substance so is hard to clean up once the environment is contaminated. Lead is harmful to the health of many animals, including humans, as it can inhibit the action of bodily enzymes.
- Mercury – This is a metallic element and can cause health and environmental problems. It is a non-biodegradable substance so is hard to clean up once the environment is contaminated. Mercury is also harmful to animal health as it can cause illness through mercury poisoning.
- Nitrates – The increased use of fertilizers means that nitrates are more often being washed from the soil and into rivers and lakes. This can cause eutrophication, which can be very problematic to marine environments[8].
- Phosphates – The increased use of fertilizers means that phosphates are more often being washed from the soil and into rivers and lakes. This can cause eutrophication, which can be very problematic to marine environments.
- Sulphur – This is a non-metallic substance that is harmful for marine life.
- Oils – Oil does not dissolve in water, instead it forms a thick layer on the water surface. This can stop marine plants receiving enough light for photosynthesis. It is also harmful for fish and marine birds.
- Petrochemicals – This is formed from gas or petrol and can be toxic to marine life.

1.1.9 Sewage and water pollution

Domestic households, industrial and agricultural practices produce wastewater that can cause pollution of many lakes and rivers. Sewage is the term used for wastewater that often contains feces, urine, and laundry waste. There are billions of people on Earth, so treating sewage is a big priority. Sewage disposal is a major problem in developing countries as many people in these areas don't have access to sanitary conditions and clean water. Untreated sewage water in such areas can contaminate the environment and cause diseases such as diarrhea. Sewage in developed countries is carried away from the home quickly and hygienically through sewage pipes. Sewage is treated in water treatment plants and in the past, waste was often disposed into the sea. Sewage is mainly biodegradable and most of it is broken down in the environment. In developed countries, sewage often causes problems when people flush chemical and

pharmaceutical substances down the toilet. When people are ill, sewage often carries harmful viruses and bacteria into the environment causing health problems [9].

1.2 Other Causes of Water pollution

1.2.1 Eutrophication

Eutrophication is characterized by excessive plant and algal growth due to the increased availability of one or more limiting growth factors needed for photosynthesis, such as sunlight, carbon dioxide, and nutrient fertilizers. Eutrophication occurs naturally over centuries as lakes age and are filled in with sediments [10]. However, human activities have accelerated the rate and extent of eutrophication through both point-source discharges and non-point loadings of limiting nutrients, such as nitrogen and phosphorus, into aquatic ecosystems (i.e., cultural eutrophication) [11], with dramatic consequences for drinking water sources, fisheries, and recreational water sources. For example, aquaculture scientists and pond managers intentionally manage eutrophic waters by adding fertilizers to enhance primary productivity and increase the density and biomass of recreationally and economically important fishes via bottom-up effects on higher trophic levels. However, during the 1960s and 1970s, scientists linked algal blooms to nutrient enrichment resulting from anthropogenic activities such as agriculture, industry, and sewage disposal [9]. The known consequences of cultural eutrophication include blooms of blue-green algae, tainted drinking water supplies, degradation of recreational opportunities, and hypoxia. The estimated cost of damage mediated by eutrophication in the U.S. alone is approximately $2.2 billion annually. The most conspicuous effect of cultural eutrophication is the creation of dense blooms of noxious, foul-smelling phytoplankton that reduce water clarity and harm water quality. Algal blooms limit light penetration, reducing growth and causing die-offs of plants in littoral zones while also lowering the success of predators that need light to pursue and catch prey. Furthermore, high rates of photosynthesis associated with eutrophication can deplete dissolved inorganic carbon and raise pH to extreme levels during the day. Elevated pH can in turn ‘blind' organisms that rely on perception of dissolved chemical cues for their survival by impairing their chemosensory abilities. When these dense algal blooms eventually die, microbial decomposition severely depletes dissolved oxygen, creating a hypoxic or anoxic ‘dead zone' lacking sufficient oxygen to support most organisms. Furthermore, such hypoxic events are particularly common in marine coastal environments surrounding large, nutrient-rich rivers and have been shown to affect more than 245,000 square kilometers in over 400 near-shore systems. Hypoxia and anoxia because of eutrophication continue to threaten lucrative

commercial and recreational fisheries worldwide. Eutrophication is also associated with major changes in aquatic community structure. During cyanobacterial blooms, small-bodied zooplankton tend to dominate plankton communities, and past observational studies have attributed this pattern to anti-herbivore traits of cyanobacteria (e.g., toxicity, morphology, and poor food quality). However, the biomass of planktivorous fish is often positively related to nutrient levels and ecosystem productivity. Piscivorous fishes (e.g., bass, pike) tend to dominate the fish community of nutrient-poor, oligotrophic lakes, while planktivorous fishes (e.g., shad, bream) become increasingly dominant with nutrient enrichment. Thus, an alternative explanation for the lack of zooplankton control of cyanobacterial blooms could include consumption of zooplankton by planktivory's [10], [12].

1.2.2 Global warming and water pollution

Climate change impacts the world's water in complex ways. Consider a water cycle diagram, like the one below; global warming is altering nearly every stage in the diagram. These changes will put pressure on drinking water supplies, food production, property values, and more, in the U.S. and all around the world [13].

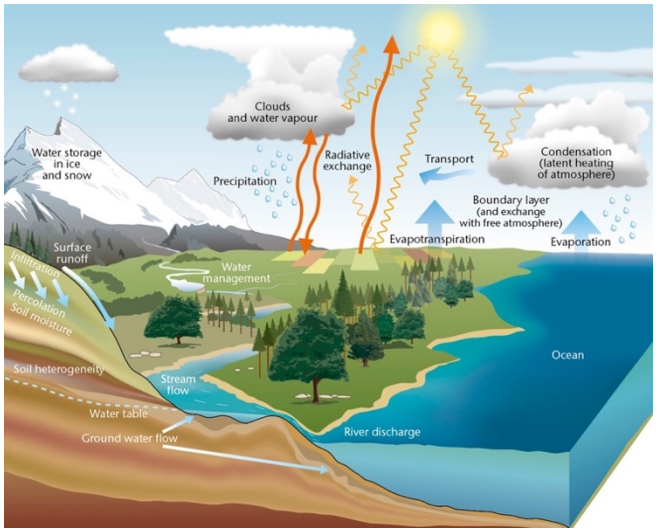

Figure 1: water climate change

By changing air temperatures and circulation patterns, climate change will also change where precipitation falls. Some areas — such as the American West, Southwest, and Southeast — are expected to get drier. Meanwhile, the northern parts of the U.S. and the Midwest are expected to get wetter. These precipitation projections are already becoming reality. The Southwest, southern Great Plains, and Southeast are predicted to see more intense and prolonged droughts, according to the National Climate Assessment. And most of the rest of the country is at risk of experiencing more severe short-term droughts, too. Researchers within the Earth Institute have found that climate change may already have exacerbated past and present droughts, and that drier conditions are making wildfires worse. Changes in precipitation patterns will challenge many farmers, as well as natural ecosystems. Scientists at Columbia University's International Research Institute for Climate and Society are creating tools and strategies to help farmers adapt to these challenges.

Natural ecosystems, however, may not be able to adapt as quickly. Warmer air can hold more moisture than cool air. As a result, in a warmer world, the air will suck up more water from oceans, lakes, soil and plants. The drier conditions this air leaves behind could negatively affect drinking water supplies and agriculture. On the flip side, the warmer, wetter air could also endanger human lives. A study out of Columbia University's Lamont-Doherty Earth Observatory found that higher humidity will make future higher temperatures unbearable in some places, by blocking the cooling effects of our sweat. The heavier bursts of precipitation caused by warmer, wetter air can lead to flooding, which can of course endanger human lives, damage homes, kill crops, and hurt the economy. Heavier rainstorms will also increase surface runoff — the water that flows over the ground after a storm. This moving water may strip nutrients from the soil and pick up pollutants, dirt, and other undesirables, flushing them into nearby water sources. Those contaminants may muck up our water supplies and make it more expensive to clean water to drinking standards. In addition, as runoff dumps sediments and other contaminants into lakes and streams, it could harm fish and other wildlife. Fertilizer runoff can cause algae blooms that ultimately end up suffocating aquatic critters and causing a stinky mess. The problem is compounded by warming water, which can't hold as much of the dissolved oxygen that fish need to survive. These conditions could harm fisheries and make conditions unpleasant for folks who like to use lakes and streams for fishing, swimming, and other recreational activities. Moreover, changing the water cycle, climate change could change how we use water and how much we need. Higher temperatures and evaporation rates could increase the demand for water in many areas [14], [15].

1.2.3 Atmospheric water pollution

Atmospheric deposition is the process, long recognized by scientists, whereby precipitation (rain, snow, fog), particles, aerosols, and gases move from the atmosphere to the earth's surface. Materials reaching the earth in precipitation or as dry deposition originate from a variety of air pollution sources and can be harmful to the environment and public health. Acidic deposition is the most widely acknowledged form of atmospheric deposition, with well-known effects on lakes, streams, and forests. More recently, atmospheric contributions of nutrients have received increasing attention, particularly as a source of excessive nitrogen. In addition to contributing to acidic deposition, nitrogen emissions and subsequent deposition can affect aquatic sources by contributing to their over enrichment with nutrients. Atmospheric deposition is known to be an important source of particulate-bound trace metals (e.g., chromium, lead, tin, and zinc) to oceanic and inland waters including those in the mid-Atlantic region [16]. Emissions from cars,

incinerators, and power plants serve as the primary sources of trace elements and other toxic materials into the atmosphere. One of the dangerous effects on aquatic resources is acidic deposition. Acidic deposition is also associated with both effects on human direct and indirect health such as the exacerbation of respiratory disorders. In addition, degrade many kinds of acidic deposition can building stone and may have substantial adverse effects on historical structures and artworks. Also, nutrient deposition contributes to eutrophication which results in adverse effects such as reduced oxygen levels, nuisance algal blooms, dieback of underwater plants (due to reduced light penetration), and reduced populations of fish and shellfish. The deposition of both trace elements (e.g., arsenic, cadmium, chromium, copper, mercury, molybdenum, nickel, lead, selenium, vanadium, and zinc) and organic contaminants (e.g., PCBs, PAHs, pesticides) can be directly toxic to organisms or pose health risks to humans and other organisms consuming contaminated individuals [17]. Bioaccumulation and biomagnification are important processes that concentrate the number of toxic substances in plants and animals. Bioaccumulation of mercury is one well-studied example that produces direct neurological and secondary effects such as reduced foraging success in fish [18], [19].

1.3 Water pollution analysis in this research project

From this overview of possible pollution sources, this research work has focused on the following main water pollution issues:

- Ammoniacal nitrogen from intensive farming
- Nitric nitrogen form by oxidation of ammoniacal nitrogen and by excessive fertilization
- Phosphates and herbicides such as glyphosate: arising from intensive agricultural activities
- Heavy metals such as Al, As, Cd, Cr(III), Cr(VI), Cu, Mn, Ni, Pb and Zn: arising from different types of human activities.

To solve these issues, the research has been focused on the use of 3 materials such as:

1. **Zeolites**: for the reduction of ammoniacal nitrogen and the reuse in agriculture as a slow-release fertilizer
2. Nanostructured materials called "**Nanosponges**". For the abatement of polluted such as: phosphates, glyphosate, heavy metals such as Al, As(III), As(V), Cd, Cr (III), Cr(VI), Cu, Mn, Ni, Zn.
3. **Biochar**: for the abatement of heavy metals.

Each part of this research work will be divided by the 3 materials used.

2 Intensive Farming

With the progressive increase of human population, food demand has increased, including an increasing of intensive farming. These farming generate huge amount of livestock waste that need to be disposed of. This waste often exceeds the carrying capacity of the agricultural funds available for manure spreading. The use of zootechnical wastewater as fertilizers on cultivated land is a common technique practiced for millennia all over the world.[2] Manure has many interesting properties as it can be used as a natural soil improver to replace industrial fertilizers. It is commonly used for renewable energy production. On the other hand, huge spreading waste determines the distribution of pathogens and pollutants on soils. Consequently, it also produces greenhouse gases and can lead to soil impoverishment in long term. In addition, field spreading promotes water pollution, loss of ammonia (NH_3) by volatilization and the spread of unpleasant odors. The abundance of organic waste each year requires new approach and methods to manage these huge amounts of waste dumped illegally into natural resources.[3] Cattle and pig farming is one of the major sources of livestock effluent production, and one of the main sources of air, soil and groundwater pollution. Developing cattle and pig management manure system that allow useful reuse of this resource is crucial, trying to limit the negative effects as much as possible. Increased environmental awareness of the problems associated with soil and water quality in recent decades has exacerbated the need for management systems capable of using biomass and nutrients in manure without producing unacceptable air pollution, soil, or

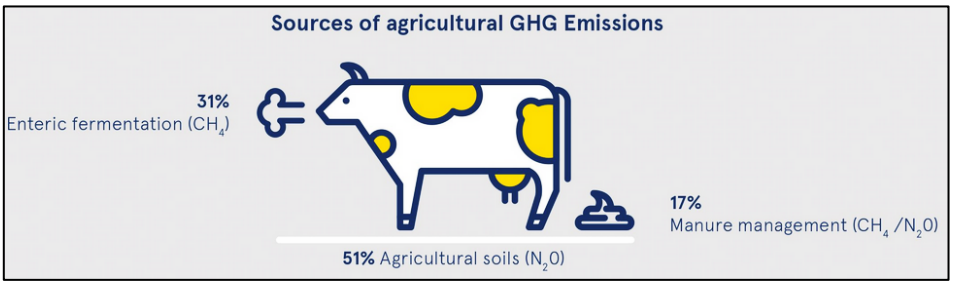

Figure 2: Greenhouse gas emissions from cattle.

water.[4] Especially cattle manure has significant amounts of primary nutrients (N, P and K) as well as other trace elements essential for crops growth development including Ca, S, Mg and Cl. Field application improves soil organic matter, C/N ratio and nutrient content. Methane (CH_4) is one of the main greenhouse gases (GHG, greenhouse gases) produced by intensive livestock farming, with between 5 % and 30 % of global emissions from manure. This compound develops because of the enteric fermentation of cattle and during manure management. The emissions are influenced by the type of livestock, its feed, storage conditions

and temperature.[5] Nitrous oxide (N_2O) is another compound responsible for air pollution by farms. Livestock effluents account about 18 % of the total emissions of this gas, depending on the amount of oxygen in them. The 100-year global warming potential for CH_4 and N_2O is approximately 23 and 310 times that of carbon dioxide (CO_2) on a mass basis respectively [6]. Total GHG emissions from livestock sectors are estimated around 7,1 Gt CO_{2eq}/year and livestock emissions account about 65 % of livestock emissions, equivalent to 4,6 Gt CO_{2eq}. Finally, the farms are responsible for a small amount of CO_2 emissions produced by composting manure. In addition to this compounds, byproducts of uncontrolled decomposition of manure are added, including odorous gases such as amines, amides, mercaptans, sulfides and disulfides. Therefore, the air quality in and around farms is particularly unhealthy because of the odors that develop. The undue spreading of organic waste on cultivated land causes severe water pollution issues. Indeed, the high occurrence of major nutrients such as nitrogen (N) and phosphorus (P), while improving soil fertilization, is responsible for eutrophication on surface waters and groundwater contamination. Nitrate leaching is the main source of groundwater contamination due to an excessive load of easily washed nitrogen in livestock waste. Much of the N and P in farm waste are in their organic form which is not immediately available to the plant. The inorganic forms that represent the lowest percentage, if not fully assimilated by the plants, may become a potential source of environmental contamination and also a threat to human health. Another consequence of manure application to cultivated land is the increase in soil salinity. In fact, in attendance of arid soils where leaching phenomenon is unlikely to happen, Na and K salts can inhibit plant growth, altering the soil structure and reducing the rates of movement of water.[4] Manure has also micronutrients useful for crops development as for previous macronutrients, can accumulate in the soil leading to further pollution. Their bioavailability varies according to metallic species, soil properties and exposure time. Copper (Cu) and zinc (Zn) are easily observable and used in sulphates form to prevent hoof diseases or as food additives in the dairy industry. The transport of Cu and Zn in organometallic complexes form is easier in acid soils, since manure typically has an alkaline pH, leaching of such metals as organic complexes is usually not a significant problem.[7] As intensive livestock farms impose animals a non-natural living conditions, antibiotics, synthetic hormones, growth promoters and antibiotic-resistant bacteria are very often used to be disposed of in manure. These pollutants are called emerging contaminants and are an important factor to consider during field spreading. It is essential to know where the sources of loss of N and P are located to act, minimizing them as much as possible. The highest levels of N loss are due to urea hydrolysis in the urine which turns into NH_3. An important contribution to this assertion

is given by the work of Muck and Steenhuis (Muck, R. E., and T. S. Steenhuis. "Nitrogen losses in free stall dairy barns [Manure as a fertilizer]." (1981)) who observed that when the temperature of the stable is greater than 20 °C, 80 % of urea nitrogen (which is about 40 % of total nitrogen in manure) is lost by volatilization. As far as the loss of P is concerned, it occurs more during the storage period where leaching can occur, for deposition in piles or lagoons. However, there are negligible losses compared to those of the N, and the P can be recovered using collection basins.[4]

The main interest in the treatment and field spreading of livestock manure is the total content in N: this is higher than the total amount of P in manure and is more susceptible to water erosion as it is less likely to bind to soil particles. Typically, manure falling in grazing areas is not considered an environmental problem. However, this depends on the size of the herd, the area, and the proximity of the pasture to water sources and the amount of time the animals spend in the pasture area. An estimated 270 million dairy cows and 677 million pigs are being reared worldwide [8]. Large producers of beef cattle and calves include Brazil (218 million), India (186 million), the USA (94 million), China (83 million), Argentina (53 million) and Australia (26 million) [9]. As far as EU-27 farming is concerned, dairy and meat cattle occupy the highest percentage, followed by pigs and poultry. For example, the United Kingdom has an annual production of cattle and calves of 10 million. Following the introduction of milk quotas in the EU-15 in 1984, the growth of dairy cattle has been halted and decreased by 1 % per year. On the contrary, pig and poultry farming has increased [10]. In Italy cattle rearing on the entire national territory consists of about 5,7 million head, of which about 14,5 % (820 thousand cattle) reared in the Piedmont region alone (data obtained from the National Livestock Register, reference date: 30.06.2021, https://www.vetinfo.it/j6_statistics/#/report-pbi/11).

2.1 Livestock manure

The amount of animal manure produced annually is reported in many studies. These include the work done by Ruiz et al. which have found a total amount of manure produced by pigs and cattle equal to 6500 t/year. Regarding dry weight, 2,7 million tons/year are produced where 76 % is related to cattle farming, followed by equines (10 %), pigs (6 %) and poultry (2 %).[11] A study of North Carolina Agricultural Extension Service (North Carolina Agricultural Extension Service. 1973. Dairy waste management alternatives. North Carolina State University Circular reports a daily production of Holstein cow manure of 34 kg compared to an average weight of 454 kg, where about 70 % is solid and the remaining 30 % is liquid. Arikan et al. [12] observed a production of wet manure of 23 t/year by a dairy cow of 635 kg.

A generation of about 62 kg of manure per day was declared because of the work carried out by Abdallah et al [13]. Carolina Font-Palma reports a daily manure production by farmed cattle in UK of about 5-6 % by weight, with a dry mass of about 5,5 kg, and a slurry production of 7-8 % by weight with a dry mass of 7,3 kg for adult dairy cows. Comparing two countries, the amount of livestock waste in the form of dry mass is 24 billion tons per year for the United States and 35.7 million tons for the United Kingdom [9]. Livestock effluent features depend on many factors, such as: feeding of the herd, type and amount of litter used, environmental conditions and storage. The nutrient content of dairy cattle manure is gradually released to the crops over time. In fact, the rate of release depends on the amount of organic matter, the climate, and the type of soil. This is particularly true for N, while P and K in the effluent are available almost immediately. Cramer et al (Cramer, C.O., J.C. Converse, G.H. Tenpas, and D.A. Schlough. 1971. The design of solid manure storage for dairy herds. American Society of Agricultural Engineers, Paper 71-910) suggest an average manure production for dairy cattle of 50 kg/(day*animal), where the manure is composed of 4100 - 6900 mg/L of total N, 700 - 2500 mg/L of NH_3 and 3800 - 6900 mg/L of P. For the liquid part there are productions between 4,5 and 11 L/(day*animal), with values of total N from 1200 to 2900 mg/L, between 780 and 2200 mg/L for NH_3 emission and 64 to 500 mg/L for P content. Another study by Hill et al [7] suggests a total value of N between 6,8 and 30,7 g/kg manure, a value of P between 2,4 and 9,0 g/kg manure and K between 10,2 and 47,7 g/kg manure. These values were based on dry manure weight. At European level, a survey carried out by the FAOSTAT in 2006 observed that at the beginning of the 1960s a total amount of N was produced from livestock of 7-8 Tg, increased to 11 Tg in the late 1980s and decreased in the following years. The same behavior was noted for the total amount of P, which varied from a value of 1.5 Tg to a maximum of 2.5 Tg/year (FAOSTAT (2006), http://www.fao.org/3/a0800e/a0800e00.htm).

Another work identified, at European level (EU-27), a total excretion of N by livestock of 10400 kt in 2000, like the amount of nitrogen fertilizer used at the same time.[10] A further essential factor to be considered when assessing the pros and cons of the manure application to cultivated land is the pH value. In fact, this parameter is important to establish the availability of nutrients and metals, define the behavior of organic compounds and study its influence on microbial activity. The causes of the pH variation in manure because of aeration are unknown, but some hypotheses have been proposed that consider the complex balance between carbonate and N-species. Husted et al [14] suggest an equilibrium mechanism between two buffer systems:

NH_3 / NH_4^+ and CO_2 / HCO_3^- / CO_3^{2-}

CO_2 is less soluble than NH_3 and volatilizes rapidly, increasing the pH. At the same time, the presence of air causes bicarbonate (HCO_3^-) to degrade to CO_2 and hydroxide ions (OH^-), which cause a sudden increase in the pH value. These reactions justify the pH range typical of fresh manure, which varies between 4,3 and 8,3 pH units. In addition, the HCO_3^- reacts with the NH_3 to give ammonium bicarbonate, $(NH_4)_2CO_3$, which makes the manure almost neutral. The increase in pH could also be attributed to an increase in the rate of degradation of organic matter. In another experiment a change in pH was observed due to a change in the diet: in the case of a low protein content values were recorded between 7,2 and 7,6 pH units, while when nutrition was rich in protein the pH tended to increase from 7,6 to 8,4.[15]

2.2 Zootechnical livestock waste treatment

Livestock wastewater has traditionally been spread on the soil as fertilizers, without further processing. Since, as discussed above, manure is a potential source of environmental pollution, it must be treated to reduce harmful emissions. The decision to pursue manure management in the most optimal way possible is susceptible to several factors, including economic feasibility, government policies, financial incentives, and social acceptance.[16] Certainly, among the most accident conditions that determine the choice of a manure management strategy, there is the profitability of the investment, followed by minimizing of the impact on the environment. Zootechnical wastewater treatment could be divided into two main categories that reflect the primary mechanisms involved in the processes: biological or thermochemical. Sometimes it is possible to observe the integration of management systems to meet different treatment criteria. As far as biological processes are concerned, composting and worm-based composting are used to eliminate pathogens and odors from the fertilizer. Composting, used both in large production systems and in domestic gardens, involves aerobic, thermophilic (self-heating) controlled decomposition of organic matter by microorganisms. During the process, heat develops, and organic matter is oxidized to CO_2 and water. Self-heating is particularly observable in the core of the heap, where there is rapid microbial decomposition of organic matter. The mass of the heap isolates the core and promotes the rise in temperature, preventing it from being homogenized with that environment. As the decomposition process progresses, the available nutrients are depleted and, with time, humification begins. The determining factors of the process include aeration, porosity, nutrients, C:N ratio, humidity, cumulus structure, pH, temperature and time.[2] The compost obtained has an added value because it is useful both in farm and in horticulture field.[4] The time required to get the compost is a few months, during

which it is necessary to stir the heap to reactivate the process. Worms-based composting complements the oxidation of organic material by microorganisms with the contribution of earthworms. In fact, while the former is responsible for biochemical degradation, the worms contribute to aerating, preparing and shredding the substrate for microbial activity.[9] A further biological process that can undergo manure is enzyme fermentation. This technique involves converting the manure fibers (up to 50 % of its composition) into biochemical substances through the hydrolysis of its components (cellulose and hemicellulose) into simple sugars, which can be transformed into fuel ethanol or other chemicals by chemical or biological processes. Pre-treatment with diluted sulfuric acid leading to a total conversion of sugar of approximately 79%. Anaerobic digestion is an increasingly successful biological treatment of animal wastewater. The basic principle on which this technique is based on is the conversion of the organic substance into methane, by specific microorganisms. Working conditions require the absence of oxygen and temperatures ranging between 5 and 70 °C depending on the type of micro-organism involved (psychedelic, mesophilic or thermophilic).

Anaerobic digestion takes place in four phases: hydrolysis, fermentation, acetogenesis and methanogenesis. In addition to the oxidation of organic substances to methane, it can be observed the production of thermal energy and the formation of undigested residue, which it is called digestate. This waste is typically used as agricultural fertilizer while the biogas is sold or used as fuel to produce electricity that is fed into the national grid. In defining the thermochemical processes to which the zootechnical wastewater is treated, it can be included pyrolysis, combustion, gasification, and hydrothermal liquefaction (HTL). Pyrolysis occurs in absence of oxygen and is the prelude for both combustion and gasification. This process depends on the heating speed and the residence time. In the case of a low working temperature, a slow heating rate and a long residence time, the main product that is achieved is biochar. On the other hand, as far as fast pyrolysis is concerned, bio-oil is the compound present in greater amount. Gasification mainly generates a combustion gas consisting of CO, CO_2 and H_2, which is called syngas. The syngas formation reaction occurs in an environment with a lower amount of O_2 than stoichiometric necessary for complete combustion. This gas mixture can be immediately used in heating or in gas turbines and engines or used as a raw material to produce methanol. The latest manure treatment technique mentioned above is hydrothermal liquefaction (HTL), an emerging process of thermal depolymerization of biomass. The methodology involves a direct liquefaction of manure in bio-oil without passing through a drying phase. The working parameters are temperatures between 200 and 350 °C and high pressures between 40 and 200 bar. Following the direct liquefaction of manure bio-oil and

energy are produced. A major problem related to this technique is the concentration of heavy metals in the solid residue following treatment. At European level, the implementation of biomass treatment technologies is limited and geographically dispersed. A value of less than 10 % of the total manure production processed in 2010 in EU-27 is reported in the literature.[17] The large gap in treatment and technology used to solve the problem between one country and another is the result of government policies and perceptions regarding the adoption of a particular disposal technique. Indeed, it can be noted that environmental policies and legislation vary between the EU countries themselves, even though there are Directives aimed at achieving the European objectives that set out the prospectus to which all Member States must comply.

2.3 Air pollutants emissions

Nitrogen certainly plays a key role among the pollutants produced by intensive livestock farming. This element in soil in form of multiple compounds are variously usable by plants. In organic form it is difficult to absorb, only simple organic molecules such as urea and some amino acids can be assimilated, as vegetables prefer nitrogen in the form of nitric and ammoniacal. In the soil, organic compounds undergo the mineralization process that transforms them first into ammoniacal nitrogen (NH_4^+) and then nitric (NO_3^-). Mineralization involves the following reactions [18]:

• AMMONIFICATION: organic substances containing N are transformed by different organisms into ammonium hydrate: $NH_2 \rightarrow NH_4^+$

• NITRIFICATION: the ammonium already formed is oxidized to nitrate:

$$NH_4^+ \rightarrow NH_2OH \rightarrow NOH \rightarrow NO_2^-$$

$$NO_2^- \rightarrow NO_3^-$$

Ammoniacal nitrogen is adsorbed on clays and organic substances surface that make up the soil matrix, in this way stays anchored to such structures that prevent its free circulation. Nitrification results in nitric nitrogen which, being a negatively charged ion (NO_3^-), does not interact with clay in the soil and is completely dissolved in the soil matrix. While this process promotes the uptake of nitric nitrogen by plant roots, it is a potential source of pollution. In fact, the nitrate ion can be leached: the nutrient is removed from the root system of the plants and dispersed into the water beneath the soil. According to a study by Masoni et al.[18], by assessing the amount of N available (nitric nitrogen) for crops in one hectare of soil, less than

1 % of the total content in N is in a plant-absorbable form. Considering an amount of 6500 kg N/ha, there are between 95 and 98 % of nitrogen in organic form (6175-6370 kg/ha), 2-5 % in ammoniacal form (130-325 kg/ha) and about 65 kg/ha as nitric nitrogen. These data indicate that the amount of nitric nitrogen typically occurred into soil is not sufficient to counterbalance the exploitation of soil itself, due to the growing demand for food that follows the trend of the global population. The only crop used to increase the nitric nitrogen content in soil is legume cultivation. This favors the biological fixation of nitrogen thanks to nitrogen-fixing microorganisms, symbionts of legumes, which transform the gaseous nitrogen in the air into compounds useful to plants. Under anaerobic conditions, nitrates and nitrites dissolved in the soil may face the phenomenon of denitrification. This process involves the progressive reduction of nitrates (and nitrites) to gaseous compounds such as molecular nitrogen (N_2) and nitrous oxide (N_2O). The compounds through which nitric nitrogen passes to become gaseous nitrogen are the following:

$$NO_3^- \rightarrow NO_2^- \rightarrow NO \rightarrow N_2O \rightarrow N_2$$

The availability of oxygen in the soil and temperature are the main factors controlling the denitrification reaction.[18] N_2O is a powerful greenhouse gas that has a global warming potential about 300 times higher than CO_2 and is responsible for the degradation of stratospheric ozone. Field manure and N-based fertilizers spread favors N_2O emission.[18] Nitrogen is also an essential element in livestock feed and is present throughout the livestock chain, from fodder to the disposal of livestock waste. The chemical forms in which this element is released, both by the herd and by its excretions, are manifold. Nitrogen is released in gaseous form such as NH_3, N_2, N_2O and NO, in dissolved form as organic and inorganic nitrogen (NH_4^+, NO_3^-) and as particulate matter.[10] Feed proteins in fodder are degraded in cattle's digestive tract by ruminal micro-organisms in peptides, amino acids and NH_3. These compounds are the basis of protein synthesis useful for animals. NH_3 can be absorbed into the bloodstream where it is removed from the liver and transformed into urea.[19] Nitrogen retention in cattle tissues is very low and most (80-90 %) are excreted in urine and feces. 30-50 % is eliminated in the feces and 40-70 % is removed by urine.[19] The amount and form in which N is lost are affected by feed, manure handling processes, type of confinement system and environmental conditions. The greatest losses of N occur by means of urine which contains mainly urea (60-80 % of total urinary nitrogen). The urea is not volatile and is immediately hydrolyzed to the urease enzyme present in the excreta at NH_3 and CO_2. The reactions involving this process are as follows:

$$NH_2(CO)NH_2 + H_2O \rightarrow NH_3 + NH_2(CO)OH$$

$$NH_2(CO)OH \rightarrow NH_3 + CO_2$$

Urea is initially hydrolyzed to NH_3 and carbamic acid but this, which is an unstable compound, spontaneously decomposes to NH_3 and CO_2. Depending on the pH and temperature conditions of the manure, both the NH_3 and its ionic counterpart, ammonium (NH_4^+) may be in solution at the same time. If the temperature is kept stable and the pH is studied, it can be observed that at a low pH value the NH_4^+ is more stable while at high pH values the volatilization of the NH_3 occurs. Thus, if the pH range in manure is between 7 and 10, the volatilization of NH_3 is observed while if the pH value decreases, the volatility of ammoniacal nitrogen is reduced to pH 4,5 where no free NH_3 is present. An increase in temperature corresponds to a greater dissociation of NH_4^+ in NH_3 and therefore greater volatility.[19] It is also possible to observe the mineralization of the organic N when the pH value is about 8. The quantification of the N available in the manure is expressed through TAN (Total Amount of Nitrogen), that is the sum of the ammoniacal and nitric nitrogen present in it: TAN = NH_4^+-N + NH_3-N. From the data of a research by Martins et al.[20] the amount of TAN recorded in bovine manure was 384,4 mg/100 ml. As a result of these considerations, the compound that causes the greatest concern is the NH_3. This molecule is a precursor of inorganic aerosols. By reacting quickly with the nitric and sulfuric acid in the atmosphere, it contributes to the formation of fine particles with a diameter of less than 2,5 μm (PM 2,5), which is responsible for the formation of haze and causes adverse effects on human health. Indeed, it is estimated that at a global level air pollution, also caused by the formation of these particles, causes the premature death of about 2 million people since PM 2,5 may reach peripheral regions of bronchioles and interfere with gaseous exchanges.[19] The way in which these reactions occur is particularly complex and depends on the environmental conditions and the reagents concentration. The amount of NH_3 reaching the troposphere is very low, with concentrations between 1 and 25 ppb. In addition, NH_3 is indirectly responsible for tropospheric ozone formation and may decrease plant productivity. As previously reported, the dispersion of this molecule in the soil involves, because of nitrification, eutrophication of water and acidification of lakes.[21] It is crucial to know where the main losses of NH_3 occur to go and intervene trying to minimize them. In a typical dairy activity, the main sources of emissions are barns and stables, storage systems and field application of manure. At the beginning of the cycle a loss of N is observed in the stables to free housing, where as an example Hristov et al.[19] recorded NH_3 concentrations ranging between 1 and 40 $\mu g/m^3$. The fluctuations in concentration values are due to several factors,

including the sampling site, the height at which it is performed, the temperature and the wind speed. As for the contribution made by temperature, it is important to mention the work done by Muck and Steenhuis (Muck, R. E., and T. S. Steenhuis. "Nitrogen losses in free stall dairy barns [Manure as a fertilizer]." (1981)) indicating that at a stall temperature of more than 20°C there is an 80 % leakage by volatilization of urea nitrogen. Losses of N can be limited by covering the stable floor with straw or other bedding material: this, having a high C/N ratio, will increase the amount of degradable C and will induce the immobilization of mineral N transforming it into organic N and thus decreasing its availability in manure. During manure storage, losses could occurred and can vary between 21 and 77 % of the total N. Martins et al.[20] reported ammoniacal nitrogen losses of between 46,8 % and 77,4 % of TAN over a period of 98 - 114 days. Other literature reports indicate emissions ranging from 0.13 g/m^2 TAN/day in winter to 15 g/m^2 TAN/day in summer. In fact, in an aerobic environment the organic N is oxidized to NH_4^+ which, in aqueous solution and under favorable pH and temperature conditions, can transform into NH_3, increasing even more the pollution related to storage. In addition, the initial C/N ratio in cumulation affects the losses of N during composting. A very tight C/N ratio is responsible for a significant loss of N through the volatilization of NH_3, especially if during storage the manure is mechanically aerated or manually rotated. Additional factors that directly affect N losses are humidity, aeration, and temperature, which within the biomass can reach 70°C. Some methods have been designed to reduce pollutant emissions from manure heaps, for example by acting on the pH value and minimizing the air exposure of the surface of the dung heap. Groot et al.[22] showed that by adding magnesium (Mg) and phosphate (PO_4^{3-}) salts to the composting of zootechnical wastewater, NH_4^+ is precipitated in the form of struvite (ammonium phosphate and Mg, $NH_4MgPO_4 \cdot 6\ H_2O$). Other types of pretreatments concern the use of additives such as acids (sulfuric or nitric acid), alum, calcium chloride ($CaCl_2$), adsorbents or urease inhibitors. However, each of the methods listed above has disadvantages that limit their use in commercial production. In fact, there is an increase in N_2O emissions, an increase in the mass of manure, an increase in P in livestock effluent, a higher sulphate emission, an increase in the Cl content.[19] The combination of several techniques implemented at the same time increases their effectiveness. A solid-liquid physical separation of manure contributes to the reduction of NH_3 emissions to the environment, as most of the ammoniacal nitrogen is in the liquid part that will undergo further treatment before being distributed to the soil. Amon et. al[23] shows a reduction in NH_3 emission following manure separation of 63 %. At the end of maturation period, manure is spread in the field. This can be done in several ways, but it has been observed

that the best method to limit N losses is to inject manure directly under the soil surface, to avoid as much as possible contact with air which would favor organic N decomposition reactions to NH_3. Research study by Lowrance et al. [4] has shown that the loss of N during application to the soil ranges from 1 % to 5 % for spreading manure, from 15 % to 30 % for spreading liquid alone and from 15 % to 40 % for using a sprayer for irrigating liquid alone. Looking at the overall emission values shows that an annual N output around 100 Tg, only 20-40 % is applied to crops.[10] Animal husbandry accounts for around 40 % of global emissions, data on NH_3 and N_2O contributions.[24] The largest global producer of N emissions, ahead of Europe and the United States, is China with values between 4.1-5.1 Tg/year recorded in the period 2000-2008.[21] Considering Europe data, TAN emission values in the summer range from 15 % to 35 % and, of these, about 75 % of NH_3 emitted in the atmosphere is attributable to farms.[15][25]Hou et al. research [24] displayed that the total amount of N produced by animals in the EU-27 was 9,7 Tg/year in the period 2009-2011. Dairy cows contributed 27 % and other cattle 35 %. High N excretion values were recorded by Germany and France, followed by the United Kingdom, Italy, Spain, Poland, and the Netherlands. Considering the amount of N scattered on the ground, the average was 54 kg/ha. Another work resulted in a dispersion of total N into the environment of about 50 %, of which 38 % as NH_3, 7 % in the form of NO, N_2O and N_2 gases and the remaining 4 % through leaching and runoff.[26]

The data also show that implementation of manure treatment technologies in Europe is limited and dispersed at regional level. The main causes are differences in farming systems and environmental conditions in individual geographical areas, followed by the complexity of livestock waste management and nutrient recycling. As discussed above, the amount of major nutrients in livestock wastewater depends on the diet, its digestibility and protein and fiber content, and the age and environment in which livestock lives. Interest in the study of feed components has increased in recent decades, to maintain animal health and vitality, produce as cheaply as possible and reduce the impact on the environment. The key factor behind studies on the feasibility of one diet rather than another is the protein content (PC). It is known that the reduction of the protein content in the feeding of cattle contributes to the decrease of N excreted, especially the urea nitrogen, which is easily converted to NH_3 and volatilizes. Typically, livestock is fed with a higher amount of PC than the protein requirement and, therefore, a decrease will reduce the availability of N in the short term, limiting the possibility of the phenomena of leaching and volatilization.[15] The main source of nutrition in the diet of cows is fodder, which can be obtained from leguminous hay, especially alfalfa and clover, maize and other cereals. Alfalfa is among the richest in protein while maize silage has a high

starch content, useful in reducing enteric emissions.[4], [27] Silage is particularly practical during the winter months, when the herd is forced to feed on dry fodder, thanks to the possibility of using the entire plant. Kulling et al.[6] reports a decrease in the amount of N excreted as a result of low protein diet uptake, which increased from 175 to 125 g/kg PC per day. Testing different PC values, Van Der Stelt et al.[15] shows a significant change in NH_3 amount emitted per head of livestock. Using a low PC diet, the emission range was about 0.13 to 0.21 g of NH_3, while for high PC treatments the values were between 0.93 and 1.41 g of NH_3 emitted. Comparing in terms of volatilized NH_3 per kg of manure, the emission difference between low and high PC diets was 78 %. Of course, low-protein diet introduction can have an impact on the final cost of the feed, and consequently on the cost of farming, because of the different types and quantities of fodder used. According to some studies [21], a less protein-rich diet is cheaper. At European level, feed consumption has been estimated at about 506 Tg per year, consisting mainly of grass, annual fodder (silage maize and legumes) and cereals. Dairy cows account for 6252 kg and other cattle for 2620 kg. Noting the total annual feed intake per head of cattle, for dairy cows it was 144 kg of N while for other cattle it was 58 kg of N.[24] The introduction of a feed regime with a low PC result in a significantly lower release of NH_3 from manure and a possible reduction in the costs incurred by farmers.

2.4 Treatments methods for industrial nitrogen-rich wastewater

Nitrogen anthropogenic sources derive from several activities and have increased proportionately with the increase of the human population, to cause a doubling in the overall cycle of this element. Molecular nitrogen (N_2) accounts for about 80 % of air-forming gases and, as mentioned above, is essential for plant growth but in its reactive forms such as ammonium (NH_4^+), nitrite (NO_2^-) and nitrate (NO_3^-). The main natural sources of reactive nitrogen are lightning (2 %) and biological fixation (98 %). Industrially, with the discovery of the Haber-Bosch process (in 1909) that fixes molecular nitrogen to NH_3, it was possible to produce N-based fertilizers immediately available for crops. Currently, the world consumption of fertilizers is 118 MT [28]. This technique has quadrupled food production capacity but has also influenced the natural cycle of N, damaging the environment and being responsible for potential serious damage to human health. Beckinghausen et al.[29] reports that in 2010 molecular nitrogen fixation through the industrial process was twice as high as natural terrestrial sources of reactive nitrogen. In addition, the Haber-Bosch process is particularly energy-intensive: to produce 1 tons of fertilizer 949 m^3 of natural gas are required (equivalent to 1-2 % of the annual global energy supply) and 1.6 ton of CO_2 is emitted. In addition to the above-mentioned process, there are multiple sources of nitrogen pollution, particularly

ammoniacal. These include municipal wastewater, industrial wastewater, and agricultural wastewater, which facilitate the integration of ammoniacal nitrogen into water effluents. Biological treatment for nitrogen removal from wastewater is responsible for the release into the atmosphere of nitrous oxide (N_2O), a particularly incident greenhouse gas (26 %) on emissions from the entire water chain, although the amount lost is small (3 % of total anthropogenic N_2O emissions)[30]. Wastewater treatment for nitrogenous substances removal is of major interest as it helps to eliminate the high pollutant potential and, at the same time, has the possibility of recovering nutrients, that will be a source of fertilizer and clean water. As a result, the use of fossil fuels to produce synthetic fertilizers will be reduced. The benefits deriving from the collection and reuse of nutrients from wastewater will be environmental, economic and energy, allowing to increase the overall sustainability of the wastewater treatment process [31]. There are still many problems to be addressed to improve the processes efficiency, including energy consumption, secondary pollution, the complexity of equipment and the dependence of biological methods on the activity of microorganisms [32]. In addition, the global water crisis has led countries to develop wastewater treatment techniques and, many of these, are exploring new ways to improve technology and combine urban wastewater treatment with the full use of resources. Conventional wastewater handling methods can be divided into three categories: physical, chemical, and biological. These categories include several distinct treatments according to the technique used. The physical treatments are divided mainly into air stripping, ion exchange, adsorption, and membrane separation. The wastewater treated by chemical purification involves chlorination, struvite precipitation, electrochemical oxidation and photocatalysis. Finally, biological treatment techniques are divided into activated sludge, nitrification and denitrification, anaerobic oxidation of ammonium, treatment with microalgae and photosynthetic bacteria.

1. Physical Treatment

- Air stripping

Air stripping for NH_3 removal from wastewater is a process widely used and low cost. The procedure consists in air flow from the bottom of a stripping tower where water with high ammoniacal nitrogen content is inserted from the top in an alkaline environment (the balance of ammoniacal nitrogen in a basic environment is shifted towards the formation of NH_3); once the NH_3 concentration has reached the gas-liquid balance in the system, the blown air will facilitate the transport of the NH_3, moving it away from the wastewater in gaseous form. The air coming out of the stripping tower will undergo further treatment, being adsorbed by acidic

solutions to form ammonium salts and prevent the removal of NH_3. The solution most used for this purpose is diluted sulfuric acid (H_2SO_4) which, reacting with NH_3, will form ammonium sulphate ($(NH_4)_2SO_4$)[28]. Recent studies to improve stripping technology have focused on improving the mass transfer coefficient per unit volume of liquid and the efficiency of the entire process. This type of treatment requires that the effluent is mainly in liquid form.

- Ionic exchange e adsorption

These two methods are among the most used in the removal of ammoniacal nitrogen because they are efficient, stable, and low-cost. They are reported together as they are often involved in the same removal technique. The ionic exchangers used can have a natural or synthetic origin. Typically, those of natural origin are zeolites that have an absorption of NH_3 between 2.7 and 30.6 mg/g zeolite [33]. Zeolite is a porous mineral based on aluminosilicate and, as such, consists of atoms of Al^{3+} and Si^{4+} arranged in a regular structure of tetrahedral units that form small cavities inside (also called pores, with a diameter of 0,1-2 nm), allowing the entrapment of solid, liquid or gaseous substances [34]. When Si^{4+} atoms replace Al^{3+} atoms, a negative charge forms on the zeolite skeleton that determines the presence of cations (mainly Na^+, K^+, Ca^{2+} and Mg^{2+}) that counterbalance the negative charges that have formed on its surface. Weak electrostatic interactions are involved that allow cations exchange in the solutions with which zeolites come into contact, such as the ammonium ion (NH_4^+). They are materials with a high cation exchange capacity (CEC) and high selectivity. The most used zeolites include clinoptilolite, mordenite, chabazite, eluandite, laumonite, analcite, and etherionite. Following the adsorption process, zeolites can be treated in NaCl or NaOH solutions to be reused as adsorbent materials or, alternatively, they can be applied directly to the soil as sources of ammoniacal nitrogen. Nasir et al.[34] shows removal efficiencies of ammoniacal N from wastewater of natural rubber industry in increase with the amount of zeolite, up to a maximum of 4 g of zeolite which is paid a removal efficiency of 79,4 %. This increase in adsorption can be attributed by increasing the amount of adsorbent, the number of adsorption sites is higher and the surface area of exchange. He also noted that the removal efficiency of ammoniacal N was dependent on pH: at pH values around 9, the efficiency decreased. In fact, at pH 8 the partial dissolution of natural zeolite occurs and the balance of ammoniacal N is shifted towards the production of NH_3. Recent studies have used titanium-based materials obtaining, by hydrolysis, Na titanate (Na_2TiO_3) which has higher adsorption efficiencies than NH_4^+ and is more stable [35]. Furthermore, they are easily regenerable by means of NaOH or NaCl solutions.

- Membrane separation

Membrane separation technology mainly comprises four types: direct osmosis (DO), reverse osmosis (RO), membrane distillation (MD) and electrodialysis (ED). In the case of direct osmosis (DO) natural osmotic pressure is used to force the movement of water molecules from the feeding side to the extraction side. By doing so, the ammonium remains trapped in the feeding side. In reverse osmosis (RO) the working principle is based on the hydraulic pressure, which is against the osmotic pressure and the flow flows through the membrane in contrast to the previous technique. That is, water passes from a solution with a high concentration of solute to a solution with a low concentration. Membrane distillation (MD) involves heating the solution to be treated and, during the passage on the membrane, determines a temperature gradient between the feeding side and the permeate side. In the case of effluents containing ammoniacal nitrogen, the ammonium ions are converted to volatile NH_3 due to the temperatures reached during treatment. The NH_3 is condensed into the permeate side and reacted with acidic solutions (such as HCl), producing ammonium salts. This process is influenced by the temperature of the feed solution, feed rate and pH. Finally, electrodialysis (ED) typically involves the use of a cation exchange membrane (EMC) for the capture of ammonium ions. The method is based on the application of an electric current to a two-chamber system with opposite charge that directs the ammonium ions towards the cathode-ray chamber, determining retention. It's a process that requires a lot of energy. Recent studies have shown that membrane technology can be integrated with the biological process, improving the removal of organic matter and, consequently, reducing the phenomenon of membrane fouling that inevitably occurs during the procedure. This system, which is called bio-electrochemical process (BES), needs some improvements for the sustainable recovery of ammonium [28]. The membranes used for these treatments are based on inorganic materials or substances of high molecular weight, characterized by a selective separative function. Depending on the type of technique used, there are specific membranes with materials and pores of appropriate size. For example, for membrane distillation, the material constituting it must be impermeable to water and allow only water vapor to pass through. Materials are being studied that are highly performing but respond to the need for low costs and minimal environmental impact.

2. *Chemical Treatments*

- Chlorination

Chlorination involves the treatment of wastewater with Cl_2 or NaClO to oxidize NH_3 to gaseous nitrogen. As the amount of Cl_2 required for denitrification is high and generates many toxic and harmful by-products, the technology is currently little used.

- Struvite Precipitation

Struvite precipitation (SP) is used to remove ammonium and phosphorus from wastewater and is then used as a slow-release fertilizer. Struvite is a solid of white orthorhombic crystals formed by precipitation of magnesium (Mg^{2+}), ammonium (NH_4^+) and phosphate (PO_4^{3-}) in weak alkaline conditions, which form the compound ($MgNH_4PO_4 \cdot 6\ H_2O$) [36]. The molar ratios between magnesium ions, ammonium ions and phosphate ions are 1:1:1 but, since the effluents are scarce in magnesium, it is necessary to add magnesium and alkali salts. Sea water or brine is typically added as a source of magnesium to save costs despite being low quality sources. Another possibility is the addition of magnesium oxide (MgO) or magnesium hydroxide ($Mg(OH)_2$) that allow to increase the basicity of the solution avoiding an excessive increase in salinity. In wastewater it is possible to observe alkaline metals that can react easily with ammonia forming complexes and increasing the efficiency of precipitation. Subsequent studies have shown that ammonium can continue to be removed from wastewater by using the breakdown products of struvite pyrolysis. Due pyrolysis process, it could be noticed the formation of $Mg_2P_2O_7$ which is not useful in the removal of ammonium but reduces the recycling times of struvite. The precipitation of the struvite is never complete as it is possible that in solution there are some inorganic ions (Ca^{2+}, K^+, Fe^{3+}, CO_3^{2-} and F^-) that inhibit the formation of crystals, affecting nucleation or competing with NH_4^+ or Mg^{2+} ions for HPO_4^{2-} ions [33]. Experiments on wastewater from a baking yeast industry showed ammonium removal yields of between 80 % and 94 % using struvite [36].

- Electrochemical oxidation e photocatalysis

Wastewater treatment by electrochemical oxidation can take place according to two methods: direct oxidation in the anode or indirect oxidation generating intermediates mediated by oxidation, dependent on electrode materials and solution properties. Some studies indicate that they have been used as cathode of copper electrodes and as anode Ti/IrO_2, to selectively reduce nitrate to nitrogen [33]. Later studies focused on the adoption of graphite anodes to reduce

process costs. The advantages of this treatment method are simple operation, a strong decontamination capacity and no secondary pollution. The process requires electricity to be able to function, significantly affecting the final choice of the type of method to be adopted for wastewater purification. Photocatalysis is based on the photovoltaic effect of semiconductor materials that allow to oxidize the pollutants present in the wastewater thanks to the presence of sunlight. In detail, it can be seen the oxidation of NH_3 only on the surface of photovoltaic materials. Following the formation of NH_3, the removal of NH_3 occurs by the introduction of Cl-ions that spread throughout the solution, generating Cl_2 molecules. NH_3 removal efficiencies were observed in the form of N_2 and NO_3^- equal to 99,9 % [33]. The peculiar characteristics of the technique are the following: it is not selective, is fast and is environmentally sustainable.

3. Biological Treatment

- Active sludge

Activated sludge treatment takes place in an aerobic environment by removing organic matter from sludge-like flakes consisting of aerobic micro-organisms. Aeration is carried out continuously within the mixture of wastewater and activated sludge to promote the oxidation of pollutants and their decomposition. This technique requires large volumes for wastewater treatment and a significant energy consumption to allow constant aeration of the entire mass in the process. In recent decades, new methodologies have been studied that actively involve active sludge as their integration with fixed film, membrane bioreactors, mobile bed biofilm reactors and aerobic granular sludge based on active sludge. Further research has focused on shortening reaction process times, reducing energy consumption, saving costs, and reducing sludge production. An example is the simultaneous nitrification and denitrification (SND) developed to eliminate the need for sludge reflux. The mechanism is still unclear due to the complexity of the metabolic processes involved; the dissolved oxygen gradient develops along the reactor biofilm, determining a separation between the aerobic and anoxic zones and allowing the existence of the two types of micro-organisms simultaneously in the same reactor.

- Nitrification and denitrification

The two-stage process involves an initial nitrification step followed by denitrification and is a typical wastewater treatment method. Nitrification involves the oxidation of NH_3 to NO_2^- and then the oxidation of NO_2^- to NO_3^- under strictly aerobic conditions. Subsequently, the non-reacted NO_2^- and NO_3^- are reduced to molecular nitrogen (N_2) producing NO and N_2O as intermediates in an anaerobic environment. Oxidation and reduction reactions of nitrogenous

compounds are carried out by different types of bacteria. In the first phase, during the oxidation reaction, the bacteria involved use NH_3 or NO_2^- as an energy source, molecular oxygen as an electron acceptor and CO_2 as a carbon source. The overall oxidation reaction is as follows:

$$NH_4^+ + 1{,}83\ O_2 + 1{,}98\ HCO_3^- \rightarrow 0{,}021\ C_5H_7O_2N + 0{,}98\ NO_3^- + 1{,}041\ H_2O + 1{,}88\ H_2CO_3$$

In the denitrification process (that is a heterotrophic bioconversion method under anaerobic conditions) oxidized nitrogen compounds (NO_2^- and NO_3^-) are reduced to N_2 by micro-organisms using nitrites and/or nitrates as electron acceptors instead of oxygen and organic matter as a source of carbon and energy. The main carbon sources used in these processes involve methanol, acetate, glucose, and ethanol. The most widely used compound is methanol (CH_3OH) as it is inexpensive and easily available [37].The process requires considerable energy consumption due to the tank aeration where the aerobic reaction takes place, affecting in a significant way the total cost of management (50 % of total energy and 60 % of total operating cost) [28]. In addition, wastewater treatment with this method produces a high amount of sludge which requires consequent treatment and disposal costs [38].

- Ammonium anaerobic oxidation

The process of anaerobic oxidation of ammonium (Anaerobic AMMonium OXidation, ANAMMOX) is a process of litho-autotrophic biological conversion. This mechanism is responsible for 30-50 % of the nitrogen produced by the oceans [39] and concerns the oxidation of ammonium to N_2, producing as intermediates nitrogen monoxide (NO) and hydrazine (N_2H_4), by means of microorganisms that use NO_2^- as electron acceptor in the absence of O_2 and CO_2 as the only carbon source to produce biomass. Anaerobic oxidation is highly exergonic and is linked to the energy metabolism of the organisms involved. The bacteria involved in the process have always been considered very slow-growing bacteria as their duplication time is 2 weeks. In addition, the complexity of the catabolic reaction that distinguishes them, the difficulties of their cultivation and the autotrophic nature of their metabolism have justified this initial idea. Recently, it has been demonstrated that anammox micro-organisms have daily growth rates of 0,21 d-1 to 30 % under favorable conditions [39]. To date, five genera belonging to the ANAMMOX bacteria involved in ammoniacal nitrogen removal processes have been identified. The absence of aeration and other electron donors in addition to the autotrophic nature of the anammox bacteria, which guarantees a low yield and a lower production of sludge, are the main advantages linked to this type of treatment. These bacteria easily form stable self-aggregated granules that allow to treat systems with high

biomass content and have a conversion rate of up to 5-10 kg N/m^3 per day [38]. Linked to the anammox process is also a lower CO_2 emission in the atmosphere. For the application of the ANAMMOX process, it is important to consider highly complex characteristics of treated wastewater such as pH, salinity, temperature, COD, NO_2-concentration and NH_4^+, heavy metals and antibiotics that could significantly affect the stability of the entire process. There are currently 90 plants that use the ANAMMOX process for the treatment of wastewater characterized by a high concentration of ammoniacal nitrogen such as digested and waste from tanning, food, semiconductors, yeast production, distillery and wine production [39].

- Microalgae treatment

Microalgae are used in wastewater treatment to remove excess nutrients, producing biomass with a high protein, lipid, and natural content. Although these crops feed on nutrients from wastewater, too high ammonia concentration can reduce the yield of biomass by increasing oxidative stress and bringing, in cases where the nutrient content is too high, when algae die. The maximum concentration limit of ammoniacal nitrogen tolerated by algal cultures is 500 mg/L, above which dilution treatments of the influent are necessary before introducing it into the tank containing the microalgae.

- Photosynthetic bacteria

Photosynthetic bacteria are easily observed in nature as they are among the oldest creatures on earth. In occurrence of organic matter these bacteria provide its decomposition in order to get nutrients useful for their survival. This type of bacteria can perform aerobic respiration and photosynthesis. If organic matter is missing, ammoniacal nitrogen, sulphate and other substances may be used for photosynthesis. It is not clear how the ammonia removal mechanism by microorganisms occurs due to their complexity; the known critical parameters are light and oxygen. An advantage of the use of photosynthetic bacteria is that they are an excellent source of biomass energy that can therefore be used as a feed with high protein content and from which you can extract products with high added value.

2.5 Anaerobic Digestion

Farming systems have an impact on the environment which must be reduced by applying more efficient on-farm management methods.[40] In fact, there are many possibilities of pollution from livestock farms that concern the contamination of air, water and soil. Air pollutant emissions include odors, methane emissions (CH_4), nitrous oxide (N_2O) and ammonia (NH_3);

these molecules are responsible for the contribution to the greenhouse effect of the companies in question. As discussed above, CH_4 emissions in dairy farms are directly related to enteric fermentation and manure handling, while nitrogen pollution (N) results in a direct emission of NH_3 and N_2O to the atmosphere and an indirect emission to soil because of nitrate leaching (NO_3^-). In addition, a further contribution to soil pollution may result from contamination due to pathogens, antibiotics and heavy metals potentially contained in animal wastewater. Contributions to total greenhouse gas emissions of 18 % measured as CO_2 equivalent have been recorded for the world animal production sector, of which 37 % concern anthropogenic CH_4. The other main pollutants from livestock farming are N_2O and NH_3, with a contribution to anthropogenic emissions of 65 % and 64 %, respectively [41]. In terms of annual tons of CO_2 equivalent, agricultural activities contribute 405 $MtCO_{2eq}$ per year (10 % of total GHG emissions in Europe) which 210 $MtCO_{2eq}$ are attributable to N_2O emissions, while the remaining 195 $MtCO_{2eq}$ are given by CH_4 emissions.[42] Emissions of CH_4 from untreated slurry management of dairy and suckler cows were reported, resulting in the following values: 34 to 66 kg CH_4/year per dairy cow and 13 to 25 kg CH_4/year per suckler cow, respectively.[40]

2.5.1 Traditional and current zootechnical waste management

Traditionally, the management of pigs and cows waste takes place through its application to the soil, preceded by a possible storage period in which the so-called "ripening" of manure occurs. As a result of the increased demand for dairy products and meat, the number of farms concentrated in a few large farms has increased. As a result, the waste produced by these farms has increased and direct disposal to the ground is no longer sustainable, taking into account certain factors such as nutrient needs of crops, quantity and season, the vulnerability of ecosystems close to farms and the energy cost of manure disposal.[43] At European level, livestock waste production is estimated at around 1.2 billion tons per year, where cattle manure accounts for more than half of the total.[44] To prevent greenhouse gas (GHG) emissions and the leaching of nutrients and organic matter into the environment, by optimally managing the manure produced by the livestock sector and by meeting the Kyoto Agreement targets, increasingly sustainable solutions are required for the management and recycling of animal manure and bio-waste. The non-use, or under-use, of these production scraps not only leads to potential revenues losses, but also leads to increased costs for their disposal. In fact, if managed correctly, these products turn out to be a valuable resource to produce renewable energy as an alternative to the fossil fuel economy and as a source of nourishment for agriculture, reducing

polluting emissions. Anaerobic digestion, in combination with pre- and post-treatment technologies, plays an increasingly important role.

2.5.2 Anaerobic digestion: how it works

Anaerobic digestion is a complex biochemical process of converting animal manure into biogas.[8] This process involves the decomposition of organic matter in the absence of free

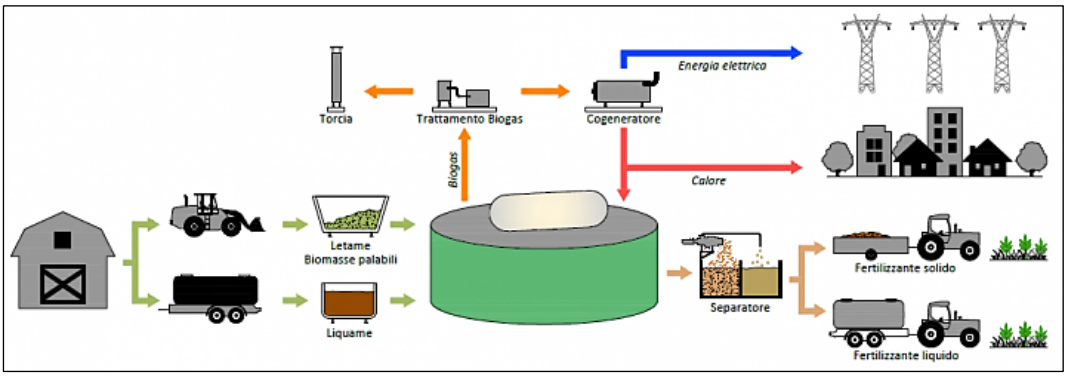

Figure 3: Anaerobic digestion plant scheme.

oxygen and produces a gas mixture, biogas, consisting primarily of CH_4 with a high percentage of CO_2 in addition to NH_3 and traces of other gases and organic acids with low molecular weight.[45] Organic material degradation in the absence of oxygen is a process that occurs naturally and is believed to involve more than 500 species in the anaerobic digester, including microorganisms, enzymes and genes. In addition to the production of biogas, digestate is obtained, that is, undigested matter in the form of a liquid dough containing a solid fraction, and heat. Anaerobic digestion is estimated to reduce the carbon content of manure and dry matter by about 50 %.[23] Biogas is a more versatile renewable energy source than wind, solar or other energy because it is not limited by geographical area or season. Biogas can be used directly for heating, combined heat, and power generation or for transformation into biomethane, which has similar characteristics to natural gas and can therefore be used as motor fuel instead of fossil fuels.[17], [46] For its use as a fuel, it is necessary a treatment for the removal of CO_2, H_2S and other molecules to introduce it into the natural gas network. Instead, to use it as a fuel for electricity generation, the biogas leaving the bio-digestor undergoes a desulphurization treatment followed by dehumidification. At the end of the moisture removal process, the biogas is converted into electricity by means of a cogeneration unit (CHP) with an internal combustion reciprocating engine.[47] The amount and quality of the biogas produced depends on the biodegradability of the digester feed and on other biochemical characteristics, the most important of which is the lignocellulose content. In fact, the higher its content, the more inhibited the production of CH_4 is. The main production inhibitors are derived from the

fibrous materials used in animal litter. The characteristic composition of biomethane is 53-70 % CH_4 and 30-47 % CO_2 and other impurities.[9] A study by Triolo et al. [47] reported a biochemical potential of CH_4 for slurry from cattle and pig farms in the range of 170-400 L CH_4/kg substance. Normak et al.[48] reports an annual potential of CH_4 from cattle manure alone on large farms of 7,3 million m3, with renewable energy potential of 100 TJ of electricity and 130 TJ of thermal energy. In Europe, the great development of biogas production has been strongly influenced by environmental regulations and the European Renewable Energy Directive (EU Directive 2018/2001).[17] One of the EU's policy objectives is to achieve a 40 % reduction in greenhouse gases and to improve renewable energy production capacity by 32 % by 2030.[44] The main EU countries with the largest agricultural biogas plants are Germany, Denmark, Austria and Sweden, to a lesser extent in the Netherlands, France, Spain, Italy, the United Kingdom and Belgium. In the remaining states the technology is being developed and, in some, there is high biomass potential. Germany is the leading European country in the development of anaerobic digestion, with over 8000 operating plants, and a total electricity production from biogas of over 3530 MW.[49] Sweden is the main proponent of the use of biogas as fuel for vehicles, where the market based on this fuel is growing continuously with over 15000 cars running on biomethane.[41] At the Italian level, the production of biogas from animal manure and other agricultural biomass has undergone enormous growth as a result of the support programs for biogas production (introduction of the green certificate and feed-in-tariff, as well as more investment subsidies).[17] Bacenetti et al.[42] reports more than 520 plants in Italy for the production of biogas from agriculture, located in particular in the northern regions of the country, generating 3405 GWh of electricity in 2011. Biogas has earned the nickname "Cinderella Energy" because it is transformed from a by-product of waste treatment into clean, renewable energy. The remaining non-gaseous part that constitutes the waste product of the anaerobic digester is the digestate. This compound consists of a solid and a liquid fraction which can be obtained from a simple physical separation by means of a mechanical separator. The solid fraction can be directly spread on the soil as an organic fertilizer, used in organic small fruit crops, or recycled as litter. The dry matter content is between 25 % and 35 %, the largest fraction being phosphorus, followed by nitrogen (20-25 %) and potassium (10-

Figure 4: Mechanical digestate separator; the digestate enters the upper tube, the liquid part exits in the tubes below and the solid fraction laterally.

15 %).[41] As for the liquid fraction, this contains the highest concentrations of nitrogenous compounds, mostly in the form of ammonia and partly organic, and therefore requires further treatments before it can spread in the field. The heat generated by the anaerobic degradation reaction can be used in situ, for example as process heating of the biogas plant or to heat the milking room or distributed to consumers through a district heating system.

2.5.3 Advantages and disadvantages of anaerobic digestion

The arising of the anaerobic digestion process in livestock and agricultural waste treatment is mainly linked to energy production. Other reasons include the reduction of pollutant emissions from intensive livestock (especially CH_4 from manure deposits in contact with air) and the mitigation of fossil fuel consumption, preferring the use of substances obtained from waste material to reduce the impact on the environment and greenhouse gas emissions of anthropogenic origin. Biogas plants can be fed with energy crops that compete with food production as they occupy the land previously used for cultivation for food purposes. Systems with a power of more than 500 kW require a huge consumption of energy crops. The largest plantations exploited for this purpose are maize, sorghum, and triticale with the highest energy yields.[41] Other issues involving biogas plants concern the long transport distances both from the input side (biomass material) and from the output side (digestate) and the difficulties encountered in the use and valorization of thermal energy. The main advantage of manure is the use of waste instead of energy crop as a renewable energy source, to avoid competition with food production and, at the same time, mitigate greenhouse gas emissions. Secondly, the adoption of anaerobic digestion for manure treatment reduces emissions from the fossil substitute system. In addition, the production of biogas results in renewable electricity and heat, which can be directly used in production plant itself or as thermal energy. The minimization in greenhouse gas emissions because of this method for electricity generation is approximately 1,2 kg CO_{2eq}/kWh.[42] Another advantage of livestock wastewater treatment for biogas generation is the energy produced on demand and can be easily stored. In addition, the existing natural gas infrastructure can be used for its distribution and use in the same applications.

2.5.4 Manure composition

Usually the cattle or pig manure with which a bio-digester is fed is a mixture of soluble and insoluble organic polymeric materials, mainly polysaccharides, lipids, proteins and volatile fatty acids (VFA); the number of inorganic compounds is also high.[50] Other components that form manure are biofibers: these materials are primarily lignocellulosic based: due to its complex structure, lignocellulose is degraded slowly, decreasing the biogas production

potential from manure by about 25 %.[51] In general, the characteristics of manure depend on the protein and fiber content of the feed, the age of the animal and the environment. Analyzing the cattle manure, Nasir et al.[52] noted that the initial total solids (TS) content is between 8 and 20 %, with a volatile solids (VS) content of about 85 %. The degradable fraction consists of hemicellulose (11 %), cellulose (26 to 53 %) and lignin (11 %). Inorganic compounds are mainly based on N, K, Ca and P, with a variable number of heavy metals such as Fe, Mn, Zn and Cu.

2.5.5 Anaerobic digestion steps

It is possible to distinguish four phases in anaerobic digestion:

1. hydrolysis: at this stage, extracellular enzymes transform the dissolved complex material (carbohydrates, proteins and fats) into the corresponding water-soluble monomers (sugars, amino acids and lipids), which will be further degraded by micro-organisms.
2. acidogenesis: at this stage volatile fatty acids (VFA, Volatile Fatty Acids), alcohols, lactic acid, CO_2, H_2, NH_3 and H_2S are produced, as well as new cellular material, starting from simple monomers by dissolved compounds present in the cells of fermentative bacteria.
3. acetogenesis (production of intermediate acids): this phase corresponds to the transformation of digestion products (the highest volatile fatty acids) into acetate, H_2 and CO2, with further production of cellular material.
4. methanogenesis: the last stage involves the conversion of acetate compounds, H_2 plus carbonate, formate or methanol into CH_4, CO_2 and new cellular material.[9]

It has been observed that the hydrolysis phase is the limiting stage of the entire transformation into an anoxic environment. During anaerobic digestion, part of the organic nitrogen is mineralized to ammoniacal nitrogen, increasing the amount of ammonium (NH_4^+) in the digestate. This mechanism ensures that the product leaving the biodigester has 50 % less carbon and there is an increase in pH of 0,5-1 units compared to the untreated slurry. Volatile fatty acids (VFA) are among the compounds responsible for the immobilization of nitrogen in the soil after application of slurry, but these are decomposed during the anaerobic process leading to increased availability of N after digestion.[26] These factors cause NH_3's emission potential to increase, although digestate can be more easily infiltrated into soil by decreasing the risk of loss of such polluting molecule in the atmosphere if application to soil is by direct injection or immediate incorporation of digested manure. There are many factors that influence the

treatment of wastewater in an anoxic environment: the nature of the raw material (composition and nutrients), the presence of toxic or inhibitory substances for microorganisms responsible for anaerobic digestion and the organic load rate. The main parameters that need constant control are pH and temperature, followed by the carbon and nitrogen content required for growth of micro-organisms. The required amount of these two elements is estimated as the ratio between C and N (C/N) and a range between 15:1 and 30:1 has been reported. Higher values limit microbial growth because the N content is more limited and consequently the production of CH_4 decreases as the methanogens for this realization are deactivated. On the other hand, a C/N ratio of less than 15:1 results in a lower C concentration that limits microbial growth by encouraging the synthesis of ammoniacal nitrogen and volatile fatty acids (VFA) in the digester.[9] This causes an increase in the pH: when it reached a value of more than 8,5 pH units, it begins to exert a toxic effect on the methanogenic bacteria.[53] The average C/N ratio in cattle manure is usually 24. As far as temperature is concerned, there are several conditions under which the anaerobic mechanism may occur: thermophilic (50-65 °C) or mesophilic (20-40°C) conditions are the main, although some anaerobic microorganisms work under psychrophilic conditions (<2 °C). The phase in which the temperature is most affected concerns methanogenesis, as the bacteria involved are rather sensitive to temperature changes. The most common mode of large-scale anaerobic digestion is the mesophilic condition with temperature around 35 °C. It has been observed that the mechanism under thermophilic conditions (>50 °C) can increase the solubility of organic compounds, the speed of chemical and biochemical reactions, disable pathogens more easily and reduce odor.[9] On the other hand, such systems are more difficult to control and require additional energy inputs. Rico et al.[43] has carried out tests at different temperatures to establish the influence of temperature on the variation of CH_4 production in anaerobic environment from bovine manure. It turns out that the productivity of the CH_4 to 50 °C is slightly higher than the control executed to 35 °C; in fact, they have obtained values of 19,3 L rm CH_4/kg manure to 50 °C and 17,7 L rm CH_4/kg manure at 35 °C. Data show that at higher temperatures hydrolysis, the limiting phase of anaerobic digestion, is less influential. The optimal pH range for anaerobic digestion is around 6,7 to 7,5 units of the inlet mixture. During the process, large amounts of organic acids develop which decrease the pH; later, the digestion continues transforming the nitrogenous compounds mainly in ammoniacal nitrogen which causes an increase in pH. The pH value stabilizes in the range of 7,2 to 8,2 when biogas synthesis is at full capacity.[53] There are options to adjust the pH within the anaerobic digester in the optimal range and the addition of NaOH is the most used method. The time needed for the reaction to reach completeness is variable and between 12

and 25 days. An equally important parameter is retention time: this is defined as the minimum duration for which organic material and micro-organisms in a digester must remain together to reach the desired degree of degradation. The lower the retention time required, the higher the reactor efficiency.[53] The hydraulic retention time is directly dependent on the digestion temperature and decreases with the same.

2.5.6 Anaerobic digester features plant

Among the main characteristics to be considered in building an anaerobic treatment plant certainly digestion reactor size is a primary design analysis factor. Considering the type of animal reared, it is possible to determine the volume of digester for the treatment of livestock waste. Typically, for a dairy cow the volume is 1 m^3 per animal, comparing the flow rate for a meat pig this is 0,1 m^3 per animal and for a breeding pig it rises to 0,2 m^3 per animal. If you consider the amount of biogas produced, this reaches values between 1,7 and 2,3 m^3 per bovine, for pigs is in the range of 0,085 - 0,396 m^3 per animal.[8] A study by Maranon et al.[40] observed a digester capacity of between 82 m^3 for the smallest farm and 183 m^3 for the largest one. To heat these digesters to right reaction temperature it has been required an amount of CH_4 of 35-55 % produced by the system. Methane generated by biodigesters may be used to heat water in the milking room or as fuel in tractors in crops, as well as for mixing and distribution of feed. Usually, the digesters are fed daily and continuously with different raw materials to achieve a stable biogas production. This means that the engine connected with electrical power plant works at full power, lowering the incidence of pressure losses on the entire system. It is also appropriate to consider that part of the energy (both electric and thermal) is used for the plant operation (pumps, mixers and separators). Typically, electricity consumption is less than 10 % of total energy production.[42] Alternatively, there are anaerobic digestion reactors for the treatment of cattle waste of the batch type, continuous agitated reservoir (CSTR), tubular flow reactors (TFR), plug-flow reactors (PFR), high flow anaerobic sludge (UASB) and current-flow reactors, which vary according to the conditions under which micro-organisms are maintained and to the separation between the acidogenesis and methanogenesis stages.

Figure 5: Example of an anaerobic digestion plant near a livestock farm.

Nielsen et al.[51] performed a study on anaerobic manure digestion by subjecting this zootechnical waste to a pre-incubation period (between 36 and 108 hours) at 68 °C, followed by anaerobic treatment at 55 °C. From the results it could be observed that pre-incubation increased the CH_4 yield between 17 % and 24 %. At the end of the anaerobic transformation, biomass can be transferred into storage tanks, usually covered by a membrane, to recover further biogas that can develop at this stage of the process. Otherwise, the digestate is conveyed, through a pump, to a mechanical separator that divides the solid fraction from the liquid one: the solid fraction is stored in heaps to use it as fertilizer or litter, while the liquid is stored in open storage tanks from which it is taken to be used as fertilizer or soil improver.

2.6 Legislation and Nitrates Directive

The application in field of digestate used as fertilizer must be subject to certain regulations that are intended to protect the environment. In fact, inappropriate handling, storage and application of digestate can cause NH_3 emissions, NO_3^- leaching and aggravate the P load in the soil. European countries have many national laws on the protection of surface water and groundwater, as well as on the treatment and recycling of organic waste and veterinary legislation to control pathogens in the digestate. The objective of the laws issued at European Community level is to promote the biological treatment of organic waste, harmonizing national measures and regulations, preventing possible negative impacts on the environment, and ensuring that bio-waste recycling results in ecological improvement. Community level regulation was established laying down the "health rules for animal by-products not intended for human consumption", outlining the health arrangements and measures to be adopted for animal waste treatment. The most important European legislation concerning the nitrogen load on agricultural land is Directive 91/676/EEC, better known as the Nitrates Directive. This standard aims to protect the environment of surface and groundwater from nitrate pollution from agricultural sources. This law identifies Zones Vulnerable to Nitrates (ZVN), corresponding to the territories that are most subject to potential nitrate pollution or eutrophication of water, in which the annual limit of discharge may not exceed 170 kg N per hectare. To ensure the protection of water, for Member States is mandatory to activate water monitoring plans, with defined deadlines and timing, throughout the national territory. The Nitrates Directive was transposed at Italian level with the Legislative Decree of 3 April 2006 n.152, Article 92, which elects as responsible for the implementation of the obligations of this directive the Italian regions. Each region has identified, within its territory, the Nitrate

Vulnerable Areas, providing to implement the related controls. In the region of Piedmont, there are many areas subject to these restrictions and among these is part of the plain of Cuneo.

3 Natural Zeolite

3.1 Nitrogen compounds issue

Nitrogenous compounds are essential for life and living beings: these are in large number in urban wastewater, in industrial wastewater and in animal wastewater. A high level of nitrogenous substances in the aquatic environment may lead to lakes and rivers eutrophication, where an increased amount of nutrient promotes the growth of algae that lead to the dissolved oxygen depletion in water and the disappearance of the fauna oh that habitat. The most used method for removing nitrogenous compounds, especially ammonium ion (NH_4^+), is through biological treatments. These removing pollutants methods are not particularly efficient, given the strict discharge limits such as those established by the Nitrates Directive. More effective procedures, such as ion exchange and adsorption, are being adopted. The main byproduct of anaerobic digestion is digestate made by a solid and a liquid portion. The ammonium ion is more observable in the liquid portion as it is easily soluble in water. Consequently, the removal of this compound will concentrate in the liquid phase of the digestate, allowing disposal for the most immediate solid portion without further treatments. For agricultural purposes, it is useful to adopt techniques such as NH_4^+adsorption or ion exchange. The difference between the two modes lies in the possible reuse of the withholding material. In fact, if the adsorbent is saturated only once, it can be applied to the fields as a fertilizer. On the other hand, if the ion exchange method is chosen, the exchanger material will be regenerated in column for its subsequent reuse. Regeneration is chemical process and involves the passage of a saline solution trough the exchanger: all sites previously occupied by the retained compound are available again. Focusing on NH_4^+ions, these are easily exchanged by alkaline metal cations (such as Na^+) and at the exit from the regeneration phase there is an effluent flow containing ammonium chloride (NH_4Cl) or ammonium nitrate (NH_4NO_3), depending on the washing solution being used. This effluent may undergo a further stripping process which transforms NH_4^+ ions into NH_3 gas which can be adsorbed to sulfuric acid (H_2SO_4). The time required for proper regeneration depends on the concentration and pH of the washing solution, while the regeneration frequency depends on the amount of heat exchanger used and the loading rate. A cost-effective method for removing the NH_4^+ ion is the use of zeolites as an adsorbent. There are many zeolites of natural origin that can be used as NH_4^+ heat exchangers in wastewater treatment.

3.2 Zeolite origin and classification

Natural zeolites are hydrated aluminosilicate minerals found in sedimentary rocks of volcanic origin and have a porous structure with pores of molecular size that allow the passage (and retention) of molecules below a certain size. The internal surface created by the presence of these channels can reach several hundred square meters per gram of zeolite, making these materials extremely effective exchangers. The internal area is between 400 and 850 m^2/g zeolite. The first reference to these minerals that appears in literature is by the Swedish scientist Axel Fredrik Cronstedt in 1756. This scientist observed that by rapidly heating the mineral large amount of water vapor were formed (previously retained by the mineral) and called the material zeolite, from the Greek “zeo” which means "boil" and “lithos” which means "stone". More than 50 different species of minerals belonging to this group have been discovered, among which the most common are: clinoptilolite, ferrierite, mordenite, phillipsite, erionite and chabazite. 235 types of zeolitic structures were identified and each was assigned a three-letter code by the International Zeolite Association.[54] The formation of natural zeolites occurs at the meeting between volcanic rocks and ash layers that react with alkaline groundwater.[55] The origin of the minerals, given by the variations of the natural processes during their genesis, means that the characteristics of each type of zeolite are different and mineral concentration within the extracted material may vary depending on the deposit from which it derives. It is called “zeolitite” when the content of zeolite in extracted mineral is greater than 50 % by mass. The characteristics due to the origin of the mineral, such as structural imperfections, a variety of exchangeable cations and the presence of clay, can determine the blockage of the pores and a slow rate of diffusion.

The general formula of zeolite is $M_{x/n}[Al_xSi_yO_{2(x+y)}]\cdot pH_2O$, M stands for metal (Na, K, Li, Ca, Mg, Ba, Sr), n stands for cation charge, y/x = 1-6, p-x = 1-4. The basic structure is a tetrahedral form in which Si or Al atom bound with four O atoms at the vertex of the tetrahedron; depending on the way the tetrahedra are bound, there will be different three-dimensional structures, shape and pore size specific to a single configuration. The substitution of Si^{4+} with Al^{3+} creates a negative charge, compensated by monovalent bond or bivalent cations, while water molecules can occupy the voids created by the structure of the mineral or bind to the ions already present. The zeolitic structures, with their electric fields, show different affinities for cations of different types and this is the theory behind the sequence of cationic selectivity. Table 1 shows the chemical formula and structure of the most important natural zeolites.

There are several classifications of zeolites that consider different characteristics such as morphology, crystalline structure, chemical composition, pore diameter, presence in nature.

Among these subdivisions, emerges that the ratio silica: alumina, distinguish the minerals as follows:

- zeolites with a low Si:Al ratio (1,0 to 1,5);
- zeolites with intermediate ratio Si:Al (2 to 5);
- zeolites with a high Si:Al ratio (10 to several thousand).[55]

Zeolite	Chemical formula	Structure type	Symmetry, space group
Clinoptilolite	$(K_2, Na_2, Ca)_3Al_6Si_{30}O_{72}{\cdot}21H_2O$	HEU	Monoclinic, C2/m
Mordenite	$(Na_2, Ca)_4Al_8Si_{40}O_{96}{\cdot}28H_2O$	MOR	Orthorhombic, Cmcm
Chabazite	$(Ca, Na_2,K_2)_2Al_4Si_8O_{24}{\cdot}12H_2O$	CHA	Rhombohedral or triclinic P1
Phillipsite	$K_2(Ca, Na_2)_2Al_8Si_{10}O_{32}{\cdot}12H_2O$	PHI	Monoclinic, $P2_1/m$
Scolecite	$Ca_4Al_8Si_{12}O_{40}{\cdot}12H_2O$	NAT	Monoclinic,Cc
Stilbite	$Na_2Ca_4Al_{10}Si_{26}O_{72}{\cdot}30H_2O$	STI	Monoclinic, C2/m
Analcime	$Na_{16}Al_{16}Si_{32}O_{96}{\cdot}16H_2O$	ANA	Cubic Ia3d
Laumontite	$Ca_4Al_8S_{16}O_{48}{\cdot}16H_2O$	LAU	Monoclinic, C2/m
Erionite	$(Na_2K_2MgCa_{1.5})_4Al_8Si_{28}O_{72}{\cdot}28H_2O$	ERI	Hexagonal $P6_3/mmc$
Ferrierite	$(Na_2, K_2, Ca, Mg)_3Al_6Si_{30}O_{72}{\cdot}20H_2O$	FER	Orthorhombic, Immm Monoclinic, $P2_1/n$

Table 1: Main natural zeolites.

Another classification concerns pore size, classifying the minerals in question as follows:

- small-pore zeolites (8 rings) with free pore diameter of 0,3-0,45 nm;
- medium-pore zeolites (10 rings) with free pore diameter of 0,45-0,6 nm;
- wide-pore zeolites (12 rings) with a free pore diameter of 0,6-0,8 nm;
- extra-wide pore zeolites (14 rings) with free pore diameter of 0,8-1,0 nm.[55]

The rings mentioned above refer to the number of coordinated atoms forming a closed system; for example, an 8-ring system means 8 tetrahedra with Si (or Al) atoms at the center and coordinated with oxygen atoms, in liaison with each other.

3.3 Features and use of zeolites

Zeolites are promising materials in renewable energy fields and environmental improvement, such as biomass conversion, fuel cells, thermal energy storage, the capture and conversion of CO_2 and the remediation of air pollution. The fuel cell allows the conversion of chemical energy into electrical energy following oxidation of the fuel. Zeolite due to its catalytic, adsorption and separation capabilities is an excellent catalyst for efficient fuel production (such as H_2 and CH_3OH) and is used as a material for fuel cell construction (as composite electrolytic membranes) because of its high thermal and mechanical stability.[54] Thermal energy storage provides release of heat energy; hot water heating systems are the current storage systems but are studying techniques that use water and zeolites, where the energy exchanged during the desorption and adsorption of water by these minerals is exploited.[54] Zeolites are widely used as porous materials for CO_2 capture as they are characterized by strong electric fields that allow to retain molecules with large dipole (such as CO_2) while active sites allow to selectively capture such pollutant molecule. They are also used in the abatement of air pollutants from the combustion of fossil fuels, in catalytic reduction of NO_x (mainly NO and NO_2) which are

responsible for acid rain, photochemical smog and cause respiratory problems. In this case zeolites have the task of selectively reducing NO_x to NH_3 and then to N_2 because they are characterized by high activity, easy availability and high stability at high temperature compared to other catalysts used in the past.[54]

Zeolites exhibit several interesting properties such as adsorption, cation exchange, dehydration-rehydration and have a high surface area. Due to their multiple features, they are involved in numerous applications ranging from the use in construction materials, to soil improvement for water retention and nutrients, as food supplements for farm animals and as catalysts. In addition, they are very useful in wastewater treatment and in animal waste management for heavy metals removal and nutrients retention, as well as replacing cat litter clays of creating a compost odorless and rich in nitrogen.

Adsorption is an essential feature in the characterization and use of these minerals and there are many factors that affect this property: the Si:Al ratio, the adsorbed cation, the number, and position of the adsorbent. Adsorption can affect heavy metal ions in industrial wastewater and are responsible for environmental pollution due to their toxicity. The heavy metal ions most observed in polluted water are Hg, Pb, Ag, Cu, Cd, Cr, Zn, Ni, Co and Mn. Many studies have used zeolites as materials that retain these pollutants, focusing on the single metal ion or considering the mixture of potentially present metal ions. In addition, the behavior of these minerals has been studied for the absorption of highly toxic metal cations such as Cr^{3+}, Cr^{6+}, As^{3+} and As^{5+}. Table 2 summarizes the absorption capacity of different metal ions on some natural zeolites. In addition, these minerals have a high affinity for inorganic anions such as

Zeolite	Chemical composition (%)								CEC (meq/g)
	SiO_2	Al_2O_3	Fe_2O_3	CaO	MgO	Na_2O	K_2O	TiO_2	
Turkey clinoptilolite	70.90	12.40	1.21	2.54	0.83	0.28	4.46	0.089	1.6–1.8
Iranian clinoptilolite	70.00	10.46	0.46	0.2	–	2.86	4.92	0.02	–
Cuba clinoptilolite	62.36	13.14	1.63	2.72	1.22	3.99	1.20	–	–
Brazil mordenite	67.82	14.96	0.42	1.87	0.18	0.32	4.47	0.07	2.29
Italy phillipsite + chabazite	56.42	15.8	4.08	2.42	0.86	2.35	8.14	0.004	2.12
Turkey clinoptilolite	69.72	11.74	1.21	2.30	0.31	0.76	4.14	–	1.84
Chinese clinoptilolite	65.52	9.89	1.04	3.17	0.61	2.31	0.88	0.21	1.03
Chilean clinoptilolite + mordenite	67.00	13.00	2.00	3.20	0.69	2.60	0.45	0.20	2.05
Turkey clinoptilolite	69.31	13.11	1.31	2.07	1.13	0.52	2.83	–	–
Croatia clinoptilolite	64.93	13.39	2.07	2.00	1.08	2.40	1.30	–	1.45
Iranian clinoptilolite + mordenite	66.5	11.81	1.3	3.11	0.72	2.01	3.12	0.21	1.20
Turkey clinoptilolite	64.99	9.99	3.99	3.51	1.01	0.18	1.95	–	
Chinese clinoptilolite	68.27	7.48	1.95	2.61	1.87	0.68	1.69	–	–
Turkey clinoptilolite	70.00	14.00	0.75	2.50	1.15	0.20	2.30	0.05	
Chinese clinoptilolite	69.5	11.05	0.08	2.95	0.13	2.95	1.13	0.14	–
Ukrainian clinoptilolite	67.29	12.32	1.26	3.01	0.29	0.66	2.76	0.26	–
Ukrainian mordenite	64.56	12.02	0.95	3.58	0.68	0.94	2.03	0.23	–
Slovakian clinoptilolite	67.16	12.30	2.30	2.91	1.10	0.66	2.28	0.17	–
Croatian clinoptilolite	55.80	13.32	1.30	5.75	0.70	3.90	2.35	–	
Ukraine clinoptilolite	66.7	12.3	1.05	2.10	1.07	2.06	2.96	–	0.64
Australian clinoptilolite	68.26	12.99	1.37	2.09	0.83	0.64	4.11	0.23	1.20

Table 2: Chemical and CEC composition of some natural zeolites.

NO_3^-, SO_4^{2-}, F^-, CN^-, PO_4^{3-}, ClO_4^-, CrO_4^{2-} and $Cr_2O_7^{2-}$, $H_2AsO_4^-$ and $HAsO_4^-$ which are widely present in wastewater. To allow the retention of this species, zeolite should be modified: typically, this happens by means of organic surfactants. Among the most important properties of zeolites, the total cationic exchange capacity (CEC) is the most relevant, defined by the number of fixed charge equivalents per exchanger amount. This parameter indicates the theoretical number of cations that can be housed within the pores of zeolite; however, it does not correspond to the actual CEC which is lower.[56] The ion exchange is linked to many factors including the mineral structure, the size and shape of the ions, the charge density of zeolite, the ionic charge and the concentration of the external electrolytic solution.[57] The ideal CEC range is between 1 and 2,27 m_{eq}/g (or 14-32 mg NH_4-N/g zeolite).

Table 3: Adsorption of heavy metal ions in zeolites.

Material	Metal	Adsorption (meq/g)
Sardinian clinoptilolite	Cu^{2+}	0.34
	Cd^{2+}	0.05–0.19
	Pb^{2+}	0.27–1.2
	Zn^{2+}	0.1
Turkish clinoptilolite	Pb^{2+}	0.299–0.730
	Zn^{2+}	0.108–0.251
	Cu^{2+}	0.022–0.227
	Ni^{2+}	0.017–0.173
Natural phillipsite	Pb^{2+}	0.234–0.345
Natural clinoptilolite	Cr^{3+}	0.237
	Ni^{2+}	0.068
	Zn^{2+}	0.106
	Cu^{2+}	0.186
	Cd^{2+}	0.082
Clinoptilolite	Cd^{2+}	0.12–0.18
Scolecite	Pb^{2+}	0.056
	Cu^{2+}	0.130
	Zn^{2+}	0.064
	Ni^{2+}, Co^{2+}	0.031
	Cd^{2+}	0.0078
		0.0032
Bigadic clinoptilolite	Pb^{2+}	0.222
	Zn^{2+}	0.734
	Cd^{2+}	0.0053
Mexican clinoptilolite	Pb^{2+}	1.4
Ukraine clinoptilolite	Pb^{2+}	0.134
	Cu^{2+}	0.405
	Ni^{2+}	0.222
	Cd^{2+}	0.0375
Turkish clinoptilolite	Co^{2+}	0.448
	Cu^{2+}	0.282
	Zn^{2+}	0.268
	Mn^{2+}	0.153
Brazilian scolecite	Cr^{3+}	5.81
	Ni^{2+}	2.08
	Cd^{2+}	1.78
	Mn^{2+}	4.00

Table 3 shows the chemical composition and cationic exchange capacity of some natural zeolites. The CEC is between 0.6 and 2.3 m_{eq}/g. It is relevant to underline that in the zootechnical wastewater there are also other cations that compete for the exchange sites and follows a lower retention than the theoretical expected. Cation exchange mechanism is controlled by external and internal diffusion. The external diffusion corresponds to the transfer of the affected species by fluid mass to the outer surface of the zeolite, while the internal diffusion takes place in the mineral pores (pores that can take macro, meso and micro dimensions) and involves the transfer of the species to the active sorbent sites.[58] By decreasing the size of zeolite particles (thus increasing the surface area), retention of the species of interest increases. It is also possible to treat zeolites through a chemical modification that increases the content of alkali metals, such that it will have a greater capacity of retention for specific cations.

3.4 Factors affecting zeolite ion exchange capacity

The main factors to consider in zeolites ionic exchange are: granulometry, retention time, ionic strength and pH. Retention experiments have been carried out for different grain sizes (0,5-1,0, 0,3-1,6 and 1,6-4,0 mm) and it has been observed that at a smaller pore size corresponds to a greater cation exchange capacity. When the particle size is greater than 1,0 mm the exchange capacity decreases. However, it must be noticed that with small particle sizes the load losses are greater. The incidence of pH change on cation exchange in zeolites, especially for NH_4^+ ion, has been investigated in a pH range between 4 and 10. It was observed that the highest exchange of NH_4^+occurred at pH 6. At lower pH, NH_4^+ ions compete with H^+ ions for exchange sites while at higher pH NH_3 develops in the form of gas, which moves away.[56] Experiments on temperature-dependent cationic exchange capacity variation have shown that the CEC is independent of the temperature at which the exchange takes place in the range of 10-20 °C. Kithome et al.[59] performed zeolite uptake experiments in the pH range of 4 to 7. At the end of the tests, he observed that increasing pH of the solution there were an increased absorption of NH_4^+ ions, probably due to boost availability of absorption sites and reduced ion competition. Around 3 million tons of natural zeolite are produced worldwide, and the largest producers are: China (2 million tons), South Korea (210000 tons), Japan (150000 tons), Jordan (140000 tons), Turkey (100000 tons), Slovakia (85000 tons), the United States (59000 tons) and Cuba 56500 tons).[60] The wide demand and use of zeolite is given by the great availability at low prices, in competition with other minerals and rocks.

In addition to natural zeolites, there are also synthetic zeolites to improve certain properties (such as ionic exchange power) or by varying specific physical properties. For example, acid/base treatment and impregnation of surfactant by ion exchange are procedures adopted to vary hydrophilic/hydrophobic properties and improve adsorption of certain ions or organic substances.[57] Typically, the acid washing of zeolite is exploited to remove impurities that clog the pores, remove the cations to transform into H-form and lead to dealumination (increasing the hydrophilicity of zeolite). Organic surfactants, such as tetramethylammonium or cetyltrimethylammonium (CTMA), can be used to modify the zeolite surface properties to make it positively charged.

3.5 Clinoptilolite: most abundant and used among natural zeolites

Clinoptilolite is the most widely used natural zeolite in the world with the formula $(Na_3K_3)(Al_6Si_{30}O_{72})\cdot 24H_2O$ [58] and a pore size given by the structure of the crystalline lattice in the range 3-8 Å. This zeolite is rich in silica and has impurities, such as quartz, which reduce the potential of some of its properties. The structure of clinoptilolite is formed by four- and

five-tetrahedron ring channels that create ion sieve channels. The average porosity of this mineral is about 34 %.[56] Its cationic exchange capacity (CEC) is given by the substitution of aluminum (Al^{3+}) with silica (Si^{4+}), which generates an increase in the total negative charge of the crystalline lattice. This negative charge that is formed is offset by the presence of cations such as Na^{+}, Ca^{2+} and K^{+}, which can be exchanged with other cations during the treatments in which the mineral is involved.[61] The CEC of clinoptilolite is about 2,16 m_{eq}/g while the affinity scale for cations is as follows:

$Cs^{+} > Rb^{+} > K^{+} > NH_4^{+} > Ba^{2+} > Sr^{2+} > Na^{+} > Ca^{2+} > Fe^{3+} > Al^{3+} > Mg^{2+} > Li^{+}$.[55], [56]

As can be seen from the affinity sequence, clinoptilolite is particularly selective for the NH_4^{+} ion and very useful in treatment of those wastes with high concentrations of this compound. As mentioned above, the origin of the zeolitic mineral may lead to different results although the same type of zeolite is used. It is possible to make a comparison of the cationic affinity with another type of zeolite such as chabazite, which is characterized by the following affinity scale:

Material	Capacity (mg/g)	Temperature (°C)
New Zealand clinoptilolite	7.1–8.6	–
NaOH–clinoptilolite	7.3–8.4	–
$NaHCO_3$–clinoptilolite	8.1–9.3	–
HCl–clinoptilolite	13.4–16.8	–
New Zealand clinoptilolite	8.5	–
New Zealand mordenite	12.2	–
Croatian clinoptilolite	13.6	–
Croatian clinoptilolite	7.7–17.6	–
Chinese clinoptilolite	2.7–3.2	20
Chinese clinoptilolite	18.5	–
Chinese Ca–clinoptilolite	20.2–26.3	20–60
Chinese clinoptilolite	11.2	–
Chinese Na–clinoptilolite	22.6	–
Chinese clinoptilolite	12.3–12.9	25
Biofilm–clinoptilolite	9.6–13.2	25
Chinese zeolite-microwave	30.6	25
Turkish clinoptilolite	5.2–8.1	25–55
Turkey clinoptilolite	5.7–7.7	30
Turkey clinoptilolite	14.5–15.4	23–70
Canada clinoptilolite	18.4–22.9	20
USA clinoptilolite	18.5	20–21
Na–clinoptilolite	20.5	20–21
Ukraine–clinoptilolite	6.6–21.5	–
Chilean natural zeolite	11.4–14.8	–
Iranian clinoptilolite	17.8	28

Table 4: Ammonium adsorption of some natural zeolites

$Ti^{+} > K^{+} > Ag^{+} > Rb^{+} > NH_4^{+} > Pb2^{+} > Na^{+} = Ba^{2+} > Sr^{2+} > Ca^{2+} > Li+$.[56]

In both zeolites the affinity for K^{+} is particularly high, followed by that for NH_4^{+} and it is possible to separate both cations using these two categories of zeolites. Table 4 shows the absorption capacity of the NH_4^{+} ion by some natural zeolites.

The table shows that the adsorption of the NH_4^{+} ion for a natural zeolite is in the range of 2,7 - 30,6 mg/g zeolite. Clinoptilolites are used as a slow-release nitrogen fertilizer as the NH_4^{+} ion is easily retained by zeolite. The use of zeolites as a fertilizer reduces environmental problems while increasing the efficiency of the same fertilizers. The reason why NH_4^{+} ion is released more slowly is because nitrogen molecules are retained in zeolite channels due to electrostatic attraction forces, which changes the angles of contact and slows down the release of these

compounds. This allows an uptake of ammonium from the roots of the most diluted plant over time, leading to increased production of dry matter from crops. In addition, the size of the clinoptilolite pores prevents the entry to nitrifying bacteria and decreases the probability that ammonium is leached during the passage of water within the cavities of such zeolite. By increasing the content of Ca^{2+} within the pores of zeolite an increase in ion absorption was observed NH_4^+.[58] At the end of use as a retainer, clinoptilolite can be regenerated to be reused later. There are several ways to reconstitute this mineral: the most traditional method is through a chemical treatment that consists in flowing a solution containing a suitable regenerating agent (H_2SO_4, HCl, HNO_3, NaOH, NaCl, NaClO). Another technique involves heating clinoptilolite at different temperatures (between 300 and 600 °C), or biological regeneration by nitrifying bacteria.[62]

3.6 Zeolite in agronomy, horticulture, and aquaculture

The chemical-physical properties of zeolites are fundamental for the applications in agronomy and horticulture fields. For example, in some areas of Japan it is a centuries-old tradition to use natural zeolites, such as clinoptilolite and mordenite, to control pH soil. Most of these applications derive from the zeolite's ability to act as a slow-release agent in the soil and to improve retention of nitrogen compounds and nutrients in general. Zeolites, once added to the soil, release potassium slowly as the plants require it. In this way there are several advantages, including the replacement of traditional fertilizers, generally more expensive than zeolitic materials. Furthermore, due to the slow release, it is possible to avoid over-concentration of fertilizers on the ground, which can favor the pollution of the underlying groundwater.[55]

In many countries, where large semi-desert areas are bordered by deposits of natural zeolites, the latter are thought to be used to restore soil fertility. This is the case, for example, of Argentina, where the extensive arid areas of Patagonia could return to agriculture, using natural zeolites present in the regions of Chubut, San Juan and La Rioja. In recent years a particular application of zeolites in the preparation of artificial soils for crops, called “zeo-ponics”, has aroused great interest, a term used to describe the cultivation of plants in a synthetic soil composed of zeolite and vermiculite, in which nutrients are supplied to plants in necessary amount as for aquaculture, the zeolites have been used with good results to remove the ammonium produced by the fish physiological activity. These, however, cannot survive in environments rich in ammonium, and hence the need to treat these waters to reduce the presence of the cation. In some pilot plants, present in the United States, purification is carried out with a column exchange so that the nursery operating cycle does not suffer any slowdowns. The column, usually made of clinoptilolite tuff, exchanges its cations with the ammonium ion,

thus regenerating the water without it having to be changed continuously, and also with economic advantages.

3.7 Zeolite for digestate treatment

As aforementioned, by-product deriving from anaerobic digestion (which aims to produce biogas) is called digestate and corresponds to 85% by weight of the final digestion mass. The digestate is linked to storage and disposal costs issues, increased by the strict limitations on the amount of nitrogen that can be spread on the fields for the fertigation imposed by the current directive. The separation treatment does not consistently reduce either the ammoniacal nitrogen content or the digestate volume, therefore it cannot be an appropriate solution. The use of zeolites can constitute a solution at least for what concerns the clarified fraction of the digestate, as it contains high values of NH_4^+ ions and ammonia capable of being trapped within the structure of these minerals by exchanging with cations[62]. This process is possible because of compensating cations, such as Na, Mg, Ca, K, Sr, Ba, and others, that are linked to a negatively charged framework of the zeolite minerals by relatively weak ionic bonds. Further weakening by the dielectric field exerted on them by the molecules in strong polar water are replaced by other cations with an equal number of positive charges [56].Zeolites show a "selectivity" toward specific cations depending on their structural features. Generally, the selectivity is related to cations of low solvation energy (K^+, Cs^+, NH_4^+, Pb^{++}, Ba^{++}, Sr^{++}) that can easily get rid of the hydration sphere, so that the ions can enter in zeolite extra-framework sites. The peculiar properties of zeolites make them suitable as adsorbents in liquid digestate separation and purification, and for reuse as plant fertilizers. In fact, they may enhance agroecosystem sustainability by creating a "virtuous" circle between anaerobic digestion and agriculture. The use of natural and enriched zeolites as amendments in agriculture has been studied for its soil characteristic modifications, i.e., reduced N leaching, increased N use efficiency, increased water use efficiency, and improved crop yield. [55]

3.8 Zeolite and Ammonium-rich Zeolite as soil improver fertilizer

Zeolite findings on their ability to release N slowly are well known from literature [63]. Indeed, it was observed an increase in nitrate levels after using natural clinoptilolite enriched by composting with poultry manure. Ammonia or ammonium added to soil is first oxidized into nitrite and then to nitrate by Ammonia Oxidizing Bacteria (AOB) and Ammonia Oxidizing Archaea (AOA). The production of nitrate can promote plant growth, but too much can cause excess nitrification, the release of nitrate into the groundwater, and eventual pollution and eutrophication. Therefore, any evaluation of the potential to use ammonium-enriched zeolite from anaerobic digestate as a slow-release fertilizer must include an assessment of AOA and

AOB. Moreover, the effects of zeolite amendments on the soil microbial biomass (MB) have been mostly unexplored [63]. To test the effectiveness and sustainability of charging zeolite with ammonium from digestate liquid to act as a slow-release fertilizer, we enriched natural zeolite (clinoptilolite) with an ammonium-rich solution that simulated field conditions and assessed its adsorbent properties. To evaluate its potential for use as a fertilizer, ammonium-rich zeolite was applied to a cultivation of strawberries. Plant growth and production parameters during the entire plant cycle, as well as parameters relating to fruit quality, were measured. Strawberry was chosen because it has a short production cycle, and it can be compared to other research on the use of zeolite as substrates in strawberry. Zeolite was chosen as the substrate for NH_4^+ uptake; this choice was made to avoid bringing other nutrients into the system, to stress the model and to verify the benefits of ammonium fully charged zeolite. The application of the enriched zeolites on strawberries was performed in pots. Three different amounts of ammonium-enriched zeolites were administered to vary the N content supplied, and to detect possible nitrogen release differences. Finally, to evaluate the effect on microbial communities and their potential release of nitrate into water, total bacteria (AOB) and archaea (AOA), as well as nitrogen forms, were measured in the plant substrates.

3.9 Nitrogen role in plant

In plants, nitrogen is part of the composition of many compounds, including proteins, enzymes, nucleic acids, chlorophyll and some vitamins, essential elements for the performance of biological functions. Nitrogen in plants makes up about 1-3% of the dry matter of mature tissues and up to 5-6% of that of young tissues. However, there are some differences between the different botanical families, and within them between the different species, depending on the stage of development and the organ of the plant (roots, leaves, stems). Nitrogen is a nutrient with a plastic action (this means that it is a nutrient that provides a substance necessary for the growth of the plant) and occupies a position of fundamental importance among the nutrients. It is an element that is absorbed throughout the biological cycle of plants, with the highest need at times of maximum growth. Furthermore, after being absorbed, it is partly used in roots and partly transported towards the aerial part (stem, leaves). The chemical forms used for the transfer are the amino acids (glutamic acid and aspartic acid in particular) and their amides (glutamine and asparagine). Nitrogen being one of the most important factors of agricultural production, the application of nitrogen fertilizers causes a marked increase in plant growth, a more intense green coloring of leaves and stems, greater vegetative growth, and a substantial increase in biomass production. Nitrogen, however, must be dosed in soil in an appropriate manner since excessive use of nitrogen fertilizers results a substantial increase of cultivation

costs and it can cause serious environmental damage (water pollution by nitrates). Nitrogen deficiency in the plant can determines:

1. low production of chlorophyll, resulting in a reduction in photosynthesis, which is manifested by a light green or yellow leaf color (the discoloration starts from the basal part of the plant and goes up to the apical zones, the first leaves to yellowing are therefore the older ones and, only after the chlorosis has reached an advanced stage, it spreads to the younger leaves);
2. weak growth of small plants at level; [64]
3. radical, with little deepened and little ramified roots, both at the level of the aerial part, with small leaves and thin stems;
4. reduction of the biological cycle length and an early maturation;
5. reduced production and, in some cases, a reduction in its quality.

On the other hand, the excess of nitrogen has the following effects slows down the development of plants, causing the lengthening of the biological cycle;

- increasing water consumption;
- reduces resistance to climatic and parasitic adversities;
- reduction of flowering;

reduces the resistance of the stems, encouraging breakage and causing appeasement.

Plants roots, as previously explained, can absorb nitrogen in nitric form, ammoniacal form and in the form of very simple organic molecules, such as urea and some amino acids. It is necessary that the forms of nitrogen listed in root surface to be absorbed by the plant. The ammoniacal nitrogen is adsorbed in soil and retained on the surfaces of the clays and organic substance (such as zeolite), thus being in the solution circulating in the soil in very small quantities and for very short times. Nitric nitrogen is almost completely dissolved in the solution and in soil, within which it moves by mass flow and can easily reach the root surface and easily be absorbed. The absorption of nitrogen by vegetation occurs almost exclusively at the expense of the nitric form alone. Then, after being absorbed by the roots, nitrates are reduced in the chloroplasts of the leaves and in the roots. This process is carried out in two successive phases:

- passage of nitrate to nitrite, catalyzed reaction by the enzyme nitrate-reductase;
- transformation of nitrite into ammonium, reaction catalyzed by the enzyme nitrite-reductase [65]

Nitrogen organic forms occur in soil in higher amount than inorganic ones and, on average, represent more than 95% of the total nitrogen. The amount of inorganic nitrogen in the soil

depends largely on the evolution over time of mineralization processes and microbial immobilization. The total nitrogen content of soils, consisting of all organic and inorganic forms, varies according to their organic matter content of all intrinsic and extrinsic conditions of soil. Sandy soils with high macro-porosity characterize of high aeration, high mineralization of organic matter, high leaching of salts can be distinguished: this type of soils always have a humus content (ie the process of microbial humification or humification that is deepened later) and nitrogen is more reduced than those of medium-textured soils and those tending to clay, in which the macro-porosity is much smaller. In soil ammonium ions are divided into three different types according to their link with the different soil components:

1. fixed ammonium ions: these are in spaces between the layers of some phylloalates (especially vermiculites and micas);
2. exchangeable ammonium ions are those adsorbed by the soil exchange complex (clay and organic matter or zeolite);
3. dissolved ammonium ions are those dissolved in the soil solution.

In soil there is a balance between fixed ammonium ions, ammonium ions in solution and exchangeable ammonium ions: the speed of exchange ammonium ions from the interstate spaces of the phyllosilicates to the circulating solution takes place with difficulty and slowness. On the other hand, adsorbed ions from the exchange complex and the circulating solution is easy and very fast. The possible destinies of ammoniacal nitrogen are as follows:

1. uptake by plants (assimilation);
2. absorption by soil organisms (immobilization);
3. oxidation to nitrate (nitrification). This transformation is carried out by autotrophic organisms, which derive energy through chemosynthesis of inorganic compounds;
4. transformation into ammonia.

The nitrate ion (NO_3^-), instead, comes from the complete dissociation of nitric acid (HNO_3) or nitrates dissolved in water or oxidation of NH_4^+. The nitrate ion is easily soluble in water and is not retained by the absorbing substances: clay minerals surfaces and organic matter also have electronegative charges and cannot adsorb NO_3^-. Thanks to this property, nitric ions are extremely mobile in the soil (they have a faster speed of movement than water). The nitric nitrogen present in the soil can be absorbed by plants (assimilation), through two different mechanisms:

- the first, passive penetration, occurs when the nitrate concentration of the circulating soil solution exceeds that of the free root space; second, active penetration, also occurs when the concentration of nitrates within the radical cells is higher than the external concentration;

- absorbed by soil organisms (immobilization);
- transported by percolation water to the deepest strata of the soil and in groundwater (leaching); converted into molecular nitrogen (denitrification).

4 Nitrogen and Phosphorus pollution

Since the second half of the twentieth century, radical change in habits and use of land and resources has had a significant impact on biogeochemical balances. One of the most significant effects was the mobilization of nitrogen and phosphorus because of fertilization activities, discharge of wastewater from animal farming and the application of household and industrial cleaning products. As a result of these activities, surface, and groundwater in different parts of the planet have developed, since the mid-twentieth century, high concentrations of these nutrients compared to those found earlier. Below are some evidence documented in the literature. In a work by J.E. Cloern, nitrogen and phosphorus concentration values were reported in different marine environmental compartments [66]:
As for the enrichment of nitrogen and phosphorus in rivers, one of the consequences was the transport of these elements to coastal areas. Jaworski et al. (1997) [67] estimated an increase in nitrogen flows in these areas from five to fourteen times the natural velocities in some areas north-east of the United States. Phosphorus concentrations follow similar trends: Conley (2000) [68] identified increases in phosphorus loads in several estuaries in the same geographical area by two to six times those present at the beginning of the '900. Eutrophication resulting from the presence of nitrogen and phosphorus and toxicity associated with nitrates are the main cause of degradation of rivers, lakes and marine compartments across the planet. While point sources of pollution are easy to monitor and control, as they are attributable to the release of contaminants at a single point in a geographical area, the non-point sources are of specific concern, associated with activities not always well identified or not foreseeable such as the occurrence of rainfall over an extensive cultivated and fertilized region [69]. Even, in 1978 Gakstatter et al. estimated that to have water in standard requirement values about 72-82% of the eutrophicate lakes would require a control on all non-punctual sources, even if emissions from all point sources were reduced to zero [70]. For most temperate estuaries, nitrogen is the main limiting element of primary production and therefore the most important responsible for eutrophication. On the other hand, phosphorus is an essential element present in limiting quantities in almost all aquatic compartments and therefore plays a leading role in the context of eutrophication [69]. The following pages will describe in more detail the main

consequences associated with nitrogen and phosphorus pollution, the reference legislation and the relevant removal methods carried out over the years, with reference to those technologies that have seen effective implementation on an industrial scale.

4.1 Nitrates

4.1.1 Nitrogen role in agriculture

As described above, plant growth is sustained by a constant supply of essential macro and microelements provided by the soil. Among the various macro-elements, the most important nutrient with a plastic action is nitrogen, which is naturally found in the soil thanks to nitrogen-fix processes. The main form of nitrogen in the soil is organic (conventionally referred to as - NH_2) and on average represents more than 95% of the total nitrogen present in the soil. However, the organic nitrogen is not directly usable by the plant, in fact it is necessary a mineralization process able to convert it into inorganic nitrogen. On the other hand, is represented by nitrites, nitrates and ammonium ions, the quantities of which largely depend on the evolution over time of the processes of mineralization and microbial immobilization. The plants can absorb nitrogen from the soil mainly in nitric form and, to a lesser extent, ammoniacal [71]. The nitrogen naturally in the soil is not sufficient to meet the needs required by the rhythms of modern agriculture, which requires an increasing use of nitrogen fertilizers. If after spreading into the soil the nitrogen supplied exceeds that absorbed, nitrates can easily be washed away by rain and transported to the percolation water. In this case, the nitrates undergo leaching, which involves the movement of soluble nitrogen along the soil profile up to groundwater, where a progressive accumulation occurs over time [71]. In recent decades, nitrate concentrations in surface water and groundwater in agricultural areas, especially in areas with intensive activities, have increased significantly. The agricultural system is one of the most demanding hydro productive sectors and with the use of fertilizers and plant protection products determines a significant impact on the territory and on water resources. Furthermore, nitrates are often the main cause of poor groundwater quality, which, it should be recalled, is by far the primary source of drinking water production.

4.1.2 Nitrates effects on human health

Nitrate is characterized by low and negligible toxicity, there were no concerns about the amount introduced into the human body until 1945, when the first report on childhood methemoglobinemia associated with nitrate-rich water and food consumption was published [72]. The ability of certain bacterial enzymes to reduce nitrate to nitrite under easily verifiable conditions, such as medium to long shelf-life and heat, is the main risk factor for human health. When it meets the organism, nitrite ion oxidizes the iron atom of the heme group of

hemoglobin. This forms methemoglobin, which is no longer able to transport oxygen to the tissues. The result is a state of cyanosis, which is a consequence of cell death, then of tissues and finally of the subject, when 60% of hemoglobin has been converted into methemoglobin. In adults the presence of an acidic environment at the level of the gastric mucosa limits the formation of nitrite by the bacteria of the digestive tract. In children, especially in the first weeks of life, there is no acid barrier to prevent the colonization of different bacterial strains along the digestive tract. This results in a rapid conversion of the catalyzed introduced nitrates of the enzyme nitrate reductase [73]. A further concern regarding nitrates is the possibility of forming N-nitroso compounds, which are believed to be carcinogenic. When the nitrite ion is in an acidic environment, it is protonated to give nitrous acid which can eliminate a water molecule and form the nitrous ion. The nitrous ion with its electrophilic features is easily attacked by a secondary amine to form N-nitrosamine. Many nitrosamines can cause genetic mutations by DNA alkylation. There is no longer any doubt as to the danger of nitrate in water intended for human consumption, and legislative measures have been taken over the years to minimize the risks.

4.1.3 Nitrates Legislation

In addition to the Nitrates Directive already mentioned in the previous chapters, nitrates have been regulated since 1980, by setting classical limits of 25 mg/L as a guide value and 50 mg/L as a limit value for nitrate concentration in water for human consumption [74]. After exceeding this limit value, the water is classified as "polluted" according to what established by the European Commission about the four quality classes for the assessment of groundwater: 0-24 mg/l (good quality water, which can be monitored more frequently); 25-39 mg/l and 40-50 mg/l (water at risk of exceeding the limit values); values greater than 50 mg/l (polluted water) [75]. The Report 50/2005 of the APAT (Agency for the Protection of the Environment and Technical Services), with a monitoring carried out in the two-year period 2001-2 through more than 2000 dedicated stations, shows the following national picture: nitrate concentration < 25 mg/L (66%); 25-39 mg/L (16%); 40-50 mg/L (6%); > 50 mg/L (12%). The study found that most groundwater is with acceptable quality, but a considerable proportion is not suitable for direct use as a drinking water source. The State of the Environment Report (RSA 2001) submitted by the Ministry of Environment to the Parliament reports on the use of more than 4,600,000 tons of fertilizers containing N, P and K corresponding to about 890,000 tons of nitrogen with an average use around 53 kg of nitrogen per hectare. The geographical distribution of these nutrients is very diversified, reaching in some provinces of the Po Valley a general surplus of more than 200 kg/hectare (unused nitrogen and therefore washed away).

In addition to these inputs, livestock farming, and civil and industrial settlements are being provided through a persistent purification deficit or inadequate operation of the existing purification plants, despite major investments in the sector [75]. For all these reasons, methodologies have been developed to reduce too high concentrations of nitrates in water.

4.1.4 Traditional methods for nitrates in water treatment

The removal of nitrates from water is an extensive and developing area of research. There have been several technological developments in this area, but further process optimizations are required. Among the various possible processing processes, three are those that have been carried on a large scale [76]:

1. Ion exchange
2. Reverse osmosis
3. Biological denitrification

There are other methods, but they have limited potential for large-scale application.

- Chemical denitrification
- Electrodialysis
- Catalytic denitrification
- Electrocatalytic reduction
- Denitrification using membrane bioreactors (MBR)
- Ion exchange combined with membrane bioreactor
- Nanofiltration

1. Ion exchange

The ion exchange process involves the passage of the water to be treated on an anionic exchange resin on which the exchange of chloride or bicarbonate with nitrate takes place, until the resin is exhausted. When the resin is exhausted, it is regenerated with a concentrated solution of sodium chloride or sodium bicarbonate. The efficiency of this process depends on various factors such as initial nitrate concentration, regeneration, resin type and number of dissolved salts, especially sulphates [77]. Efficiencies up to 99,8% are reported (for initial nitrate concentrations of 25 mg/L and total dissolved salt concentration of 400 mg/L), which fall to 45-60% if the initial nitrate concentration is 18-25 mg/L and 530 mg/L of dissolved salts of which 43 mg/L of sulphates [76]. The ion exchange process has been estimated five times cheaper than the reverse osmosis process [76].

2. *Reverse osmosis*

The osmosis process is reversed using high pressures (directly linked to feed concentrations). The species to be felled are retained by a membrane that allows only the passage of water molecules. The reverse osmosis can simultaneously remove many pollutants, since only water molecules can pass over the semipermeable membrane [78]. In the area of nitrate removal, pressure between 20 and 100 bar and membranes made of cellulose acetate, polyamides and composite materials are used [76].The efficiency of the process depends on both the type of membrane and the initial concentration of nitrate. The best efficiency obtained is 93%. Increasing the initial concentration from 25 to 200 mg/L causes a decrease in removal efficiency from 93.5 to 82.5% [77]. However, there are several problems associated with the reverse osmosis process. The main ones concern the phenomenon of the pollution (fouling) of the membranes, as well as their deterioration in time following the deposition of organic material, colloidal particles, and suspended material. For this reason, the process of reverse osmosis requires a pretreatment of the diet.

3. *Biological denitrification*

Many bacteria belonging to different strains can grow anaerobically optionally by reducing different oxidized forms of nitrogen to give gaseous products:

$$NO_3^- \rightarrow NO_2^- \rightarrow NO \rightarrow N_2O \rightarrow N_2$$

Each step is catalyzed by enzymes involved in biochemical reactions by such bacteria.

In this context, nitrites and nitrates can play the role of electron acceptors in biochemical processes of ATP generation [79]. This allows, in addition to denitrification, to maintain cell biomass within operating levels. In the field of biological denitrification, a distinction is made between two types of process:

• Heterotrophic denitrification

• Autotrophic denitrification

The difference lies in the way microorganisms procure energy [80]. In heterotrophic denitrification bacteria obtain energy from the oxidation of organic substances such as methanol, ethanol, methane, and acetic acid. In autotrophic denitrification, bacteria of the genus Paracoccus, Thiobacillus and Thiosphaera can carry on denitrification by inorganic substances such as hydrogen or several reduced forms of sulfur such as S, S^{2-}, $S_2O_3^{2-}$, $S_4O_2^{2-}$, o SO_3^{2-}. There are other genera such as Ferrobacillus, Gallionella, Leptothrix and Sphaerotillus that can use the Fe^{2+} ion as a reducing agent for energy generation and electron transport to nitrite and nitrate ions. When the reducing agent is hydrogen, it is called "hydrogen denitrification", as in the case of the DENITROPUR process [81]. The efficiency of biological

denitrification processes depends not only on all operating parameters but also on the carbon/nitrogen ratio (C/N) and can reach 86-89%[77].

Despite being widely used; such methods still see some difficulties not yet overcome. In particular:

- Removal of nitrates by ion exchange is not suitable for high water in TDS (total dissolved solids) [82], which, as seen above, results in a drastic decrease in the efficiency of the process, especially in the presence of sulphates. In addition, during the regeneration of the resin, there are large quantities of nitrates in aqueous solution to be disposed of.
- The removal by reverse osmosis is affected by the phenomenon of fouling and deterioration of the membranes. In addition, it is a costly process as it requires large amounts of energy to apply the high pressures required. In addition, even in this case, concentrated nitrate water must be disposed of.
- Biological denitrification is a system that even in its simplest form is complex. The number of aspects to be monitored is high, the sensitivity to operating conditions is high and so is the risk of formation of nitrites following incomplete denitrification [83][84].
- As regards other methods of denitrification of water, large-scale application is currently limited. Electrodialysis can be used and is characterized by good efficiencies (almost the same as the reverse osmosis process [85]), but the complexity of the system, the maintenance difficulties and the high costs associated with it [83][84] does not put it in the foreground in the context of nitrate removal processes from water.

4.2 Phosphates

Phosphorus is an essential component of nucleic acids and multiple intermediate phosphorylated metabolites. It is a factor of growth and maintenance for different forms of life. Except for low phosphine emissions from volcanoes, phosphorus in nature is found primarily in pentavalent phosphorus form, especially in aquatic systems, where it may occur as an ion orthophosphate, pyrophosphate, polyphosphate (inorganic forms) or as esters of phosphoric acid called organophosphate and organic phosphonates (organic forms). Whatever the chemical form in which phosphorus occurs in an aquatic system, it is rapidly hydrolyzed by enzyme-catalyzed reactions to orthophosphate: the only form that can be assimilated by bacteria, algae and plant species. The efficiency of transforming and assimilating phosphorus by all these organisms makes them particularly sensitive to pollution by excessive amounts of

phosphorus. The various protonated or not protonated forms of the orthophosphate ion are the most common phosphorus-based fertilizers and household products (in which phosphorus is used as a complexing agent to soften water in the application of detergents). These forms, besides being the most bioavailable, are also the most soluble. However, the concentrations naturally present in water bodies are very low (averagely 10 to 25 μg/L; 70-72 μg/L in the oceans.) [86]. For this reason, phosphorus is a limiting nutrient. Consequently, once orthophosphates are carried by water flows in the different aquatic compartments, they are quickly assimilated by numerous micro-organisms. Phosphorus role in pollution does not concern a direct toxicity to humans, but the problem of eutrophication and it can however achieve an indirect toxicity. Eutrophication occurs because of over-enrichment of nutrients in an environment which would normally not have such amount. G enerally, this phenomenon is found due to nitrates and phosphates resulting from the application of fertilizers and the discharge of wastewater of urban or industrial origin. In the context of a normal system, identified as "oligotrophic", deep water remains oxygenated throughout the phosphate introduction and consumption cycle. During this regime the introduction of an essential limiting element, such as phosphorus, blocks the growth within levels of containment of eutrophication. In fact, while nitrogen and carbon can be supplied by different biogeochemical routes, phosphorus in aquatic compartments is naturally present in quantities that can be defined as the essential limiting nutrient. Human activities can provide large amounts of phosphorus and generally do so by releasing important streams of phosphorylated species into aquatic systems. When an external input of phosphorus-based chemical species higher than normal occurs, the new system is called "eutrophic". In this system, deep and even surface waters are in anoxic conditions during the growing season. This mechanism is summarized in Figure 6 [87]. It can also be seen that the biodiversity curve tends to fall, which can be explained by the inhospitable conditions generated by algal blooms. In fact, the limitation of the gaseous exchanges between the water and the atmosphere affects the death of other living species, which encounter putrefaction and fermentation processes that release ammonia and hydrogen sulfide. Then there is the possible affirmation of toxic algae with danger of damage both on the species

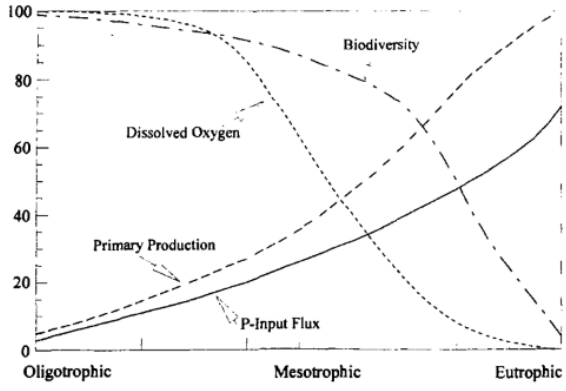

Figure 6: Graphic representation of the three oligotrophic, mesotrophic and eutrophic systems that can be established depending on the environmental conditions of a water compartment. The following curves are represented: biodiversity, amount of dissolved oxygen.

living in the aquatic compartment, and on the population that is drinking the waters concerned [88]. Another aspect not negligible, concerns damage of an economic nature. The degradation of aquatic environmental resources, both in terms of aesthetics (decrease of the transparency of the water column and change of color), and in terms of expendability of recreational services results in a tax damage not negligible [89].

4.2.1 Phosphates Legislation

Eutrophication is a serious problem, so much so that the European Union has issued a series of directives aimed at containing it. Eutrophication issue is one of the eleven descriptors of Directive 2008/56/EC [90] for which the "good environmental status" or GES (good environmental status) shall be achieved. The Directive requires that eutrophication of human origin, especially its negative effects such as loss of biodiversity, degradation of the ecosystem, harmful algal blooms, and lack of oxygen in the background water, be minimized. The legislation indicates how the assessment of eutrophication in marine waters should consider the assessment of coastal and transitional waters under Directive 2000/60/EC [91]. The assessment of GES requires the consideration of certain criteria for the various descriptors. The criteria for assessing GES are: 1) nutrient concentration in the water column; 2) chlorophyll concentration in the water column as a direct effect of nutrient enrichment; 3) dissolved oxygen with a threshold value of 3 mg/L or less in the background water, changes due to increased organic matter decomposition and the extent of the affected area as an indirect effect of nutrient enrichment. About emission limit values, these are regulated by D. Lgs. 152/06 [92]. Legislative Decree 152 of 2006 (Part Three, Annex 5, Table 3) sets emission limit values for surface water and sewerage. For total phosphorus (as P) the limit value of 10 mg/L has been set for both surface water discharge and sewage discharge.

4.2.2 Phosphorus sources

Phosphorus is now essential to produce food required by the growing world demand. Indeed, plant growth is highly dependent on this element and, like nitrogen and potassium, is not substitutable in the application of fertilizers in modern agriculture. 90% of global demand for phosphorus is required for food production [93]. It is an amount of phosphorus corresponding to about 148 million tons of phosphate rock per year. This scenario introduces the issues of the limit of phosphorus resource, in addition to pollution problems. Over the years, to meet the ever-higher demand for this essential element, the use of organic and natural forms such as guano, animal and human manure to inorganic forms such as those found through the extraction of phosphatic rocks, said "phosphorite", the deposits of which are scattered in a heterogeneous way on the earth’s crust (see pie chart) and do not represent a renewable or unlimited resource

[86]. The following graph shows how from the second half of the '900 we have passed from the use of organic forms to inorganic. Overall, it is also noted that, from the same years, the production of phosphorus for use as a fertilizer has followed an exponential increase [93]:

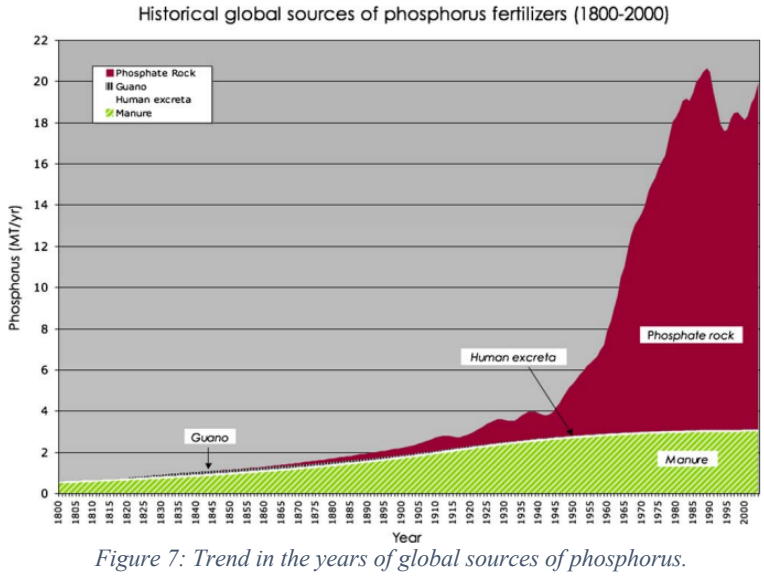

Figure 7: Trend in the years of global sources of phosphorus.

The need for the systematic and repeated use over time of such relevant amount of phosphorus to meet world food demand cannot be dissociated from an equally important focus on the removal of this element introduced in environment system. According to the SOER 2010 [94], agricultural emissions of phosphorus into fresh water exceed 0,1 kg phosphorus/ha/year in many parts of Europe, but at some critical points they exceed 1,0 kg P/ha/year. For this reason, methodologies have been developed to remove phosphorus from water, to avoid the occurrence of the above-described eutrophication phenomena.

4.2.3 Phosphorus removal methods and technologies in water treatment

The development of phosphorus removal technologies began around 1950 in response to the above-mentioned problem of eutrophication and the need to reduce phosphate levels in surface water [95]. The first removal method developed was chemical precipitation. Later, biological removal was introduced, which was developed on a large scale; followed by crystallization technology, also this on a commercial scale. Generally, phosphorus removal methodologies from water are classified into three macro areas: physical (and chemical-physical) removal, chemical and biological [86].

1. ***Physical and physical-chemical removal***

Physical methods allow the removal of particulates from wastewater containing both inorganic and organic phosphorus, using membrane technologies. These processes exploit as adsorption, ion exchange processes and artificial aeration processes. These methods are simple and capable of removing other types of solid particulates simultaneously. They are mainly used in the early stages of high particulate water treatment. If a semi-permeable membrane is used, the reverse osmosis process can be carried out, which can also be used in the purification of waters rich in nitrates, as well as in phosphorus. The use of membrane bioreactors, already mentioned

regarding nitrate removal methods, can also be a strategy to combine phosphate removal with nitrate removal at a single stage of the process. As for processes that exploit adsorption (identifiable as chemical-physical processes), they consist in adding flying ash or alumina to adsorb phosphates. In ion exchange processes, two types of ion exchange resins are used: one to remove ammonium ions and one for phosphate ions. In the regeneration phase of the two resins will then be released adsorbed ions, which will be precipitated as struvite after stoichiometric correction by adding appropriate amounts of magnesium and/or phosphate [95]. There are other methods such as artificial aeration that can prevent eutrophication but see poor application in lakes not very deep.

2. Biological removal

The development of this type of process is based on research carried out in the late 1950s, which showed that, under certain conditions, activated sludges can capture phosphorus in excess by normal biomass growth[95]. This phenomenon has been called "luxury uptake" and is the basis of many applications. In the area of phosphorus removal. This method has the advantage of avoiding the use of large amount of chemicals and avoiding the production of huge sludge. On the other hand, it requires installations in complex configurations, as well as a non-trivial monitoring of different operational aspects. The efficiencies of this process can reach up to 80-90%. However, acceptable phosphate concentration values are achieved by coupling a simultaneous chemical precipitation.

3. Phosphorus removal by algae treatment

Generally, phosphorus in living organisms is used by cells for phospholipids formation, ATP and nucleic acids. By optimizing growth conditions of some microalgae, it is possible to induce the assimilation of high amounts of phosphorus, the accumulation of which occurs beyond the functions. By appropriately dosing carbon dioxide and bicarbonate into the system, photosynthesis by these organisms is promoted. Within a pH range of 7 to 9, the following stoichiometry of the process can be encouraged (which also becomes a method for simultaneously removing nitrate) [96]:

$$106\ HCO_3^- + 16\ NO_3^- + HPO_4^{2-} + 16\ H_2O + 12\ H^+ \rightarrow C_{106}H_{263}O_{110}N_{16}P + 138\ O_2$$

4. Chemical removal

Phosphorus chemical removal from wastewater was developed in Switzerland during the 1950s in response to the growing problem of eutrophication. Such technology has now established itself in numerous countries around the world. It is a process involving the addition of a salt of a trivalent metal to the wastewater to obtain the precipitation of an insoluble metallic

phosphate. This is removed after sedimentation. The most useful metal ions in this type of process are iron and aluminum, added as chlorides or sulfates. Lime is also used, which can precipitate phosphate as calcium phosphate. Coagulation and flocculation can be achieved by using flocculant agents such as aluminum or acrylamide-derived polymers or crystallization processes. The chemical precipitation process is flexible and can be applied at different stages of the wastewater treatment process. These are primary, secondary, and tertiary precipitations, which lead to increasingly poor water in phosphates, but with an increasing trend in the costs associated with them (in addition to the formation of additional amounts of sludge). The lack of opportunities to reuse the precipitate in agriculture and thus to give it added value, has helped to increase the focus on technologies that led to a recyclable product in agriculture and industry.

5. Crystallization technologies

The development of crystallization technologies has occurred in response to increasingly restrictive demands for the removal of phosphorus from water. No less important was the growing desire to obtain more commercially appealing end-products. This type of process has been carried on industrial scale and to date there are numerous operating plants in the Netherlands [97]. One of the best known is the DHV Crystalactor ® process. It is based on the crystallization of calcium phosphate on a granular support (called "seed material") used to trigger heterogeneous nucleation, typically sand. Process conditions are optimized to promote the crystallization of calcium phosphate by the addition of soda or lime milk.

The great advantage of this process is that the crystallization speed allows for low retention times. Consequently, it is possible to operate small, fully automated reactors. In addition, the Crystalactor® can be retrofitted for different types of wastewater treatment. Another important advantage is the shape of the final by-product. This is not presented as a sludge as in the previous cases, but as a solid pellet without water consisting mainly of calcium phosphate (40-50%) and granular material used as a nucleating agent for crystallization (30-40%) [95]. Consequently, it can be recycled by phosphorus industry. There are also other technologies based on crystallization, which are simply a different version of the Crystalactor technology. They differ in some variations but have the same principle of nucleation and growth used in this technique. By way of example, in the literature you can find many works in which various seeding materials are used to produce struvite ($MgNH_4PO_4$ $6H_2O$) or hydroxyapatite in granular forms, with the aim of reusing the final product as fertilizer. Struvite in particular aroused interest due to its slow-release properties [98]. This type of product represents a turning point in research into the reuse of phosphorus. On this environmental issue, legislation has not yet been expressed. Although Article 5 of the Urban Wastewater Treatment Directive [99]

requires the elimination of phosphorus from wastewater, does not require the extraction of phosphorus in usable form. For example, the Directive allows phosphorus to be flocculated by precipitation using iron, but it produces an insoluble compound from which phosphorus is not easily extracted for commercial purposes and which is unlikely to be assimilated by plants. Alternative techniques for the extraction of phosphorus that do not cause this problem are for example precisely the removal of phosphorus from wastewater in the form of struvite. The conditions under which struvite and other phosphorus minerals can be generated have been well investigated in the literature and reviewed by a review published in 2019 [86].

5 Glyphosate

N-(phosphonomethyl)glycine commercially known as Glyphosate is a systemic, non-selective, broad-spectrum herbicide used on a global scale due to its extreme versatility, effectiveness, and cost-effectiveness. It was introduced by Monsanto in early 1970 in the wording Roundup®. In 2001, the year in which the production patent expired, it became free to produce. Since then, agriculture has evolved significantly and is now used in the form of various other commercial formulations. The best known are: Abundit Extra; Credit; Xtreme; Glifonox; Glyphogan; Ground-Up; Rodeo; Touchdown; Tragli; Wipe Out; Yerbimat. All these products are designated as glyphosate-based herbicides (Gbhs, glyphosate-based herbicides) and the active substances, together with their metabolites, can now be found in soil, surface water, groundwater, as well as in many food products and even in the human body [100].
In the original formulation Roundup®, glyphosate is present as the salt of isopropyl amine, but today the various formulations on the market also use it as ammonium or sodium salt. In general, the application of GBHs pesticides has stronger effects than with glyphosate used individually, due to the addition of other components such as surfactants, phosphoric acids and sulfuric acids in the formulation, in addition to the salified form of glyphosate, which improve the uptake of the active substance from plants [101]. Broad spectrum efficacy is due to the mechanism of action, which involves the inhibition of the enzyme 5-enolpiruvilshikimate-3-phosphate synthase (EPSPS). The result is an accumulation of shikimato-3-phosphate and the blocking of the production of aromatic amino acids and therefore of the biosynthesis of the proteins necessary for the normal vital functions of the plant. The fact that the EPSPS enzyme is the only target enzyme of glyphosate makes glyphosate highly selective to all species that possess the shikimate pathway, that is to certain plants and microorganisms [102].

5.1 Agriculture use

In agriculture, glyphosate is used to combat grassing. It acts as an herbicide against more than one hundred species of weeds and more than sixty species of perennial herbs. It can also be used, at low doses, as a regulator of plant growth and to promote dissection [55]. Recent developments in agricultural practices and the development of glyphosate resistance by many plant species, involving adaptive genetic mutations, have helped to promote an increasing use of GBHs. The total amount of glyphosate used increased from 3200 tons per year in 1974 to 825,000 tons per year in 2014 in over 140 countries[101]. The trend is in increase and is assumed that in the next few years the figure will go up to a million tons per year [103].

5.2 Glyphosate effect on human health

The numerous evidence that glyphosate residues were found in some food products increased the focus on its effects and that of its metabolites on human health. These consequences have been widely investigated in literature. For example, in October 2012 the UK-Food Standard Agency carried out tests on bread samples and detected glyphosate residues equal to or greater than 0,2 mg/kg in 27 of the 109 samples analyzed. Other tests performed by the US Department of Agriculture in 2011 found glyphosate residues in 90.3% of the 300 samples of soya and amino methyl phosphonic acid (AMPA, the main product of glyphosate degradation) in 95,7% of cases in concentrations of 1,9 and 2,3 mg/kg respectively [104]. In more recent years, other laboratories have detected much higher amounts in other food products derived from agriculture [105]. In 2015, the International Agency for Research on Cancer (IARC) undertook an assessment of the oncogenic potential of glyphosate. An IARC working group, which met in March 2015 at the IARC in Lyon, France, published online 29 July 2015 the complete IARC monograph (Volume 112) [106]. IARC concluded that glyphosate is "likely to be carcinogenic to humans (group 2A) on the basis of limited human evidence and sufficient experimental animal evidence; it was also concluded that there is strong evidence of genotoxicity and oxidative stress". The IARC review links glyphosate to the increased dependent dose of malignant tumors at many anatomical sites in experimental animals and to the increased incidence of non-Hodgkin lymphoma in exposed humans. This assessment is supported by several epidemiological studies on humans and pets. Such studies suggest associations between exposure to GBHs and adverse health outcomes. For example, congenital malformations have been reported in young pigs fed with soya contaminated with GBHs residues. This suggests that GBHs could be at least a contributing factor to similar birth defects observed in human populations that meet such products[107][108].

However, the issue is controversial and conflicting studies appear in the literature. Already a year after the evaluation by the IARC, reviews appeared in which independent studies were compared to conduct a detailed critique of the tests in light of the above assessment. The effects of neoplasms in biotests on animals were not associated with exposure to glyphosate on the basis that they lacked statistical strength. Therefore, in those studies it was concluded that glyphosate is unlikely to pose a carcinogenic risk to humans[109]. In 2015, the European Food Safety Authority (EFSA) revealed another technical assessment[110], that "glyphosate is unlikely to constitute a carcinogenic hazard to humans". In any case, EFSA has established "new levels of safety which will make the monitoring of glyphosate residues in food more stringent" as a precautionary measure. A year later, the World Health Organization and the United Nations Food and Agriculture Organization classified glyphosate as "unlikely to pose a cancer risk to humans as a result of dietary exposure"[111]. The question has not yet been resolved. The absence of an intrinsic glyphosate hazard cannot be stated from all the studies carried out. If, however, the risk associated with it exists, it may be brought to very low levels by taking appropriate measures to reduce it.

5.3 Glyphosate legislation

Even if the judgment on the potential dangerousness is uncertain, the EU commission has adopted the implementing regulation 2016/1313, that it establishes the conditions of approval of the substance[112]. In addition, several countries have long taken precautionary measures to reduce the inappropriate use of glyphosate products, for example:

- In the Netherlands, selling to private households was banned in 2014.
- In France, the Minister of Ecology asked in 2015 to nurseries and gardening shops not to expose glyphosate on shelves accessible to the public, which remains free for sale.
- In Italy, a decree of the Ministry of Health[113] established that herbicide will no longer be used in areas "frequented by the population or vulnerable groups such as parks, gardens, sports and recreation areas, children's play areas, courtyards and green areas inside schools and health facilities". The same Decree also established that products containing amines of polyoxylated tallow coupled to glyphosate, a combination which according to the EFSA report could be responsible for the toxic effects on humans, were withdrawn from trade in November 2016 and their use by the end-user was prohibited from the end of February 2017.

As regards the legal limits for drinking water, Directive 98/83/EC set as a minimum standard limit for each individual pesticide the value of 0,1 μg/L and the value of 0,5 μg/L for the total

of all pesticides present [114]. This is a very restrictive value when compared with the relative maximum permitted levels in waters imposed by the United States and Canada (respectively 700 and 280 µg/L[115]).

5.4 Glyphosate removal methods and technologies

Given the restrictive limits, several methods for glyphosate removal in contaminated water have been developed and proposed in the literature. These can take advantage of degradation by oxidation or biodegradation of the pesticide or removal by membrane or adsorption processes.

1. *Oxidation methods*

These methods are described in the literature as advanced oxidation processes (AOPS: advanced oxidation processes) and seem to represent potential options for the reduction of organic contaminants to acceptable levels according to the limits imposed. As regards glyphosate degradation, advanced oxidation processes mainly include photocatalysis with TiO_2, H_2O_2/UV and Fe(III)/H_2O_2/UV. There are also electrochemical oxidation methods of glyphosate, which are however characterized by low efficiencies due to competition with the oxygen present (efficiencies of 32% after four hours of electrolysis)[116]. Finally, methods of removal of glyphosate and AMPA have been reported using aqueous suspensions of birnessite (a manganese oxide common in many soils), able to achieve an advanced oxidation process that can also be implemented electrochemically.

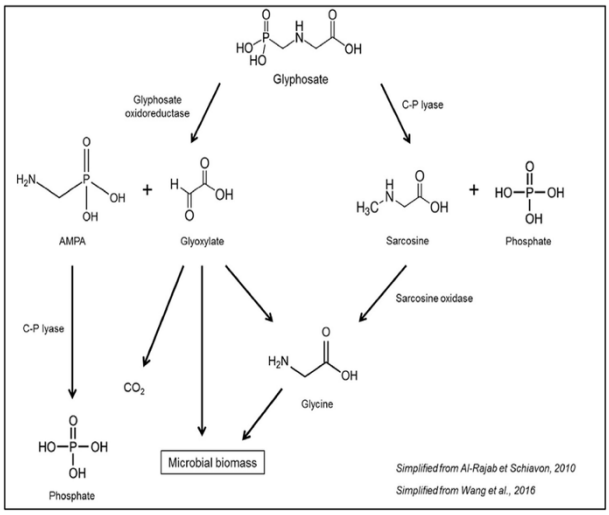

Figure 8: Simplified scheme of metabolic pathways for microbial degradation of glyphosate.

2. *Biodegradation methods*

They are based on the enzymatic degradation of glyphosate by micro-organisms. There are two pathways for microbial degradation of glyphosate: the splitting of the carbon-phosphorus bond, to give sarcosine and phosphoric acid; and the splitting of the carbon-nitrogen bond, to give glyoxylate and aminomethylphosphonic acid (known as AMPA). Each substance subsequently sees a well-defined metabolic fate, simplified in the following scheme[117] (figure 8). The micro-organisms responsible for the degradation of glyphosate are mainly bacteria belonging to

different strains. These are often genetically modified by techniques such as ultraviolet light irradiation[118], to obtain strains with increasingly high glyphosate degradation yields.

3. ***Membrane filtration technologies***

These technologies exploit reverse osmosis, nanofiltration or electrodialysis with bipolar membranes (BMED). They have been used for the removal of glyphosate to recover it from concentrated discharges, but the very high costs of the membranes, combined with the problem of their low lifetime, have not allowed a development on industrial scale[119].

4. ***Adsorption methods***

Multiple materials have been proposed for this technique: activated carbon; iron oxide/SBA-15; MOFs; zeolite 4A, biopolymers, nonabsorbent (nanotechnology). Each of these brings its advantages and disadvantages, but they are generally not yet applicable on a large scale, due to low capacities or kinetic lenses. In 2019 it was proposed the use of a functionalized dendrimer that presented excellent performance in terms of rapid removal and high efficiencies (over 95%). However, these are still small laboratory realities, but in a constant development with promising potentiality for industrial realities.[120]

6 Nanotechnologies: an overview

Nanotechnology is a field of science focused on the design, synthesis, characterization of materials and devices with nanometric dimensions.[121] They can be divided into two categories:

- nanostructured as polymeric nanomaterials,
- nanocrystalline, non-polymeric materials such as carbon nanotubes and metallic or silica-based nanoparticles.

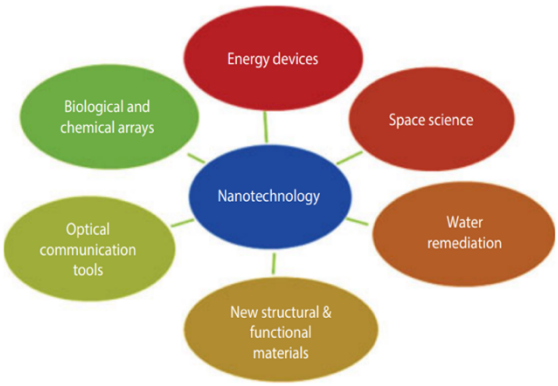

Figure 9: Nanotechnology applications

They can be presented in atoms clusters form (aggregates of atoms) such as quantum dots, nanodots, inorganic macromolecules or in the form of grains, fibers, and films smaller than 100 nm. Nanotechnology affects every single area of our lives; in fact, it is applied in various fields as shown in Figure 9.[122]

In recent years water sanitation, using nanotechnologies, (called "water nano remediation"), has become the main objective of scientific research. In fact this technology has great potential

in purification of contaminated water sites and the protection of the environment from pollution.[122] The use of nanotechnology for pollutant removal has become a very cost-effective and efficient alternative to other conventional techniques. Indeed, they allow in-situ contaminated water treatment, minimizing the use of additional chemicals. In addition, because of their nanometric size, they have a very high and reactive surface compared to the volume of the bulk itself. These materials can also be modified to achieve the desired features and exceeding the application limits resulting from the complexities of the environmental matrices to be treated. Their high mobility in aquatic environments maximizes their potential for treating large volumes of contaminated fractions. According to the website "Project of Environmental Nanotechnology" and the "United States Environmental Protection Agency" (USEPA), over the past decade, nearly 70 sites have been successfully treated around the world on an industrial scale, using nanotechnologies.[123] These new approaches have significantly reduced time (days instead of months) and operating costs (up to 80%) compared to conventional methods and this could be a winning solution given that in Europe there are estimated to be more than 2.5 million potentially polluted sites, that need to be remedied and 350,000 contaminated sites could pose a potential risk to humans and the environment.[124]

Despite these promising expectations, the environmental and human risk assessment associated with the use of nanotechnologies is still being debated today and it is seen as emerging technologies; in Europe they are still little applied, probably for emerging social concerns about them and the lack of adequate regulatory and legislative support. In addition to their expected benefits in terms of the removal or degradation of contaminants, environmental behavior of these materials raises questions, especially about their potential environmental impact after release into water. The additional costs associated with their possible recovery and/or removal from the purified site must also be considered. In fact, nanomaterials such as iron, titanium and zinc metal oxides and carbon nanotubes are considered potentially hazardous to aquatic organisms, if not removed at the end of application.[124] To address these limitations, many researchers have turned their attention to emerging materials based nano compounds, with the aim of combining the benefits of nanotechnology with the use of renewable, more sustainable, and environmentally friendly sources, requirements for polysaccharides.[124]

6.1 Polysaccharides

Polysaccharides and their derivatives are versatile polymeric materials to produce nanometric systems.[125] They are biopolymers composed of at least more than ten monosaccharides (monomer units) joined together by glycosidic bonds. The number of monomer units refers to

the degree of polymerization, which for polymers such as cellulose and starch is quite high. For example, for cellulose is in a range of 7000-15000.[126]

Polysaccharides can be obtained from natural sources and often from by-products of the food industry, through low-cost processes. The main raw materials are:[127]

- plants from which starch, cellulose, lignin, pectin, β-glucan, guar gum are derived;
- animals, from which chitin and chitosan are derived;
- algae, from which alginate, agar and carrageenan are derived;
- microorganisms from which dextran, pullulan, xanthan gum and bacterial cellulose are derived.

The different properties of these macromolecules depend on their different molecular weight, chemical composition, and reactive functional groups, which allow numerous chemical transformations to meet specific requirements for end use. Most important characteristics of polysaccharides are good stability, semi-crystallinity, nontoxicity, biodegradability and biocompatibility.[127] The physical and chemical features of polysaccharide-based nanomaterials depend on their composition and the functional groups present. In addition, electrostatic interactions, influenced by intrinsic charges on polysaccharide chains, are essential during the formation of nanometric systems. Polysaccharides can also be classified as:[127]

- neutrals such as amylose, amylopectin, cellulose and guar gum,
- anionic as alginate, carrageenan, gellan, gum Arabic and xanthan gum,
- cationic like chitosan.

They may also be distinguished according to their function:[122]

- reserve polysaccharides, such as starch, which have the task of storing energy;
- structural polysaccharides, such as cellulose, which protect the cell wall.

Among plant polysaccharides, the use of starch and its derivatives, such as cyclodextrins and maltodextrins, has aroused much interest in the scientific field for the removal of heavy metals.

6.2 Starch

Starch, the natural homopolymer of D-glucose, is a type of polysaccharide composed of glucopyranose units, joined by glycosidic bonds, which has the function of storing energy in plants.[122][128] It is presented in the form of small granules, each of which is composed mainly of two types of α -glucan, amylose and amylopectin, which make up 98-99% of the net weight of starch. Amylose has a linear structure, consisting of 1% bonds α(1-6) and 99% bonds

α(1-4) glycosidic while amylopectin has an extremely branched structure with 5% bonds α(1-6) and 95% bonds α(1-4). In addition, starch also has small amounts of protein and lipids.[129] The main source of starch is corn, including other types of cereals such as wheat, rice, oats, and barley, which contain 60%-80%, but is also present in legumes such as chickpeas, beans and peas from 25% to 50%, in tubers such as potatoes, Maranta starch, cassava and cocoyam from 60% to 90% and in some fruits such as bananas and mango, around 70%.[122]

Starch is considered an excellent alternative to activated carbon and other synthetic polymers as an adsorbent on heavy metals and dyes, as it is abundant, biodegradable and environmentally safe. Starch has interesting properties such as stability and high chemical reactivity, thanks to hydroxyl groups in its polymer chains. However, natural starch, (that is unmodified starch), cannot be used directly as adsorbent due to its insolubility in water at room temperature, easy retrogradation, gel instability and lack of properties such as controlled particle size, wear resistance, hardness and porosity.[122][130] Therefore, the functionality of starch can be varied through chemical transformations and the introduction of several functional and chelating groups such as: carboxylic, acetyl, hydroxypropyl, amine, amide groups and many others. For example, di-thiocarbamate starch (DTCS), porous starch citrate (PSC), porous starch xanthate (PSX) and esterified maize starch containing maleic acid and itaconic acid were used for the adsorption of heavy metals into water. These modified starches are supposed to form chelating and ionic interactions with these metal ions.[130]

Many hydroxyl groups in starch provides many reactive sites for chemical transformation. There are several methods to induce starch functions such as: grafting, cross-linking, etherification, and esterification reactions.[130]

6.3 Cyclodextrin

Cyclodextrins (CDs) are cyclic oligomers obtained from enzymatic starch glycosyltransferase (CGTase). They may contain six, seven or eight glucose units, respectively called α-, β- e γ-cyclodextrins and bound, to form a ring, by α-(1-4) glycosidic bond (Figure 10).[127][128] This cyclic structure has an empty cavity that is relatively hydrophobic in nature, because hydrogen atoms and glycosidic oxygen atoms are directed inwards. While, the outer part is hydrophilic, as there are hydroxyl polar groups.[128] The lipophilic nature of the cavity allows suitable size molecules to be complexed through hydrophobic interactions. The hydrophilic outer part, on the other hand, increases the solubility of cyclodextrins in water and other polar solvents.[127] The three types of cyclodextrins differ by the diameter of the cavity which depends on the number of glucose units.[128] In any case, the β-cyclodextrin is the most widely

used due to its low cost, its average cavity size, diameter 0,70 nm, the stability of its crystalline structure and the predisposition to the formation of intramolecular hydrogen bonds, through which it can generate complexes and aggregates.[128][131][132]

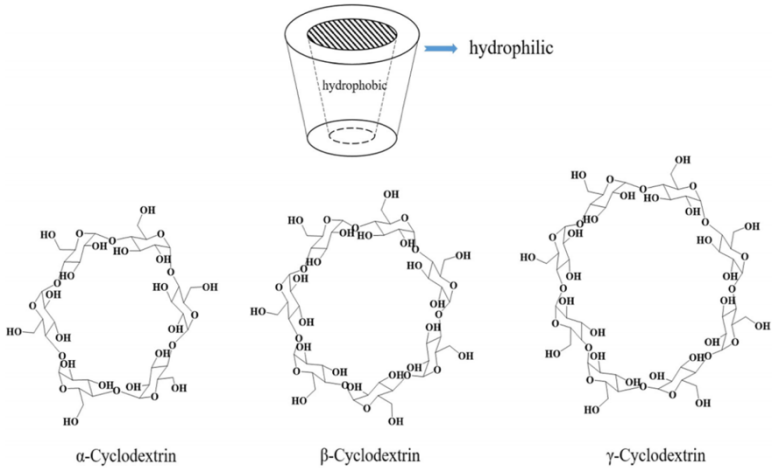

Figure 10: Cyclodextrin structure.

These excellent properties make you an excellent candidate in the environmental field.[133] The main chemical and physical properties of the three types of cyclodextrins are summarized in Table 5.[134]

Cyclo-dextrin	Number of glucose units	Molecular weight (anhydrous)	Volume of cavity, Å³ (approx.)	$[\alpha]_D^{25}$ (approx.)	Crystal forms (from water)	pK_a (25°C)	Solubility in water g/100 mL at 25°C	Crystal water wt.%	Diffusion constant at 40°C	C1′-O4-C4 angle°	O4-O4′ distance Å	O2-O3 distance Å
Alpha	6	972	174	+150.5±0.5	hexagonal plates	12.33	14.5	10.2	3.443	119	4.23	3.00
Beta	7	1135	262	+162.0±0.5	monoclinic parallelo-grams	12.20	1.85	13.2–14.5	3.223	117.7	4.39	2.86
Gamma	8	1297	427	+177.4±0.5	quadratic prisms	12.08	23.2	8.13–17.7	3.000	112.6	4.48	2.81

Table 5: Cyclodextrin features.

Since natural cyclodextrins have properties which limit their application, especially in the purification of wastewater, such as their high solubility in water, they can be transformed by appropriate methods such as admixture, esterification, etherification, and many others. In the modification process the hydroxyl group in position 6 is the most active.[133]

Thanks to the presence of the cavity, cyclodextrins can form inclusion complexes, that is, chemical species consisting of two or more molecules, in which one of them, the host molecule, can admit another within its cavity, forming a stable complex without the presence of covalent bonds. This way it can interact with inorganic, organic and ionic compounds.[135] Inclusion complex formation can protect complexed host molecules from degradation caused by external conditions such as pH, heat or light. Cyclodextrins are versatile to solubilize food dyes and vitamins and mask unwanted smells and flavors, allowing controlled release of bioactive compounds.[127] In addition, as they are not toxic, they can also be used as food additives.[128] Thanks to their complexing properties, they are now widely used in the pharmaceutical, biomedical, food, cosmetic, water treatment and catalysis fields.[128][136] In addition, they have aroused a great deal of interest in different areas of research as shown in

Figure 11.[137] In the pharmaceutical field they are used to improve the controlled release of drugs, to increase the solubility and bioavailability of lipophilic ones and to improve their transport in the body. In the cosmetic field they are used to trap and prolong the release of molecules in essential oils. Another interesting application is in cosmetics for oral hygiene, improving the release of volatile molecules, and thus increasing the feeling of freshness. In agriculture in the controlled release of fertilizers. They are also used in the transport of various types of gases such as carbon dioxide, oxygen and 1-methylcyclopropene.[138]

6.4 Maltodextrin

Maltodextrins are derived from advanced starch hydrolysis through acids or enzymes.

They are classified according to the length of their chain, which is expressed through dextrose equivalents (DE), defined as the number of reduced sugars present in dextrose and calculated as the percentage of total dry matter. Maltodextrins are a type of dextrin with a DE < 20: with a low DE value, have a high molecular weight and are not hygroscopic, on the contrary, with a high DE value, have a low molecular weight and a high-water solubility.[128]

Maltodextrins are D-glucose polymers with bonding properties α-(1,4) e α-(1,6) glycosidic bond (Figure 11), derived from the degradation of amylose and amylopectin.[139] They can be produced using two enzymes:

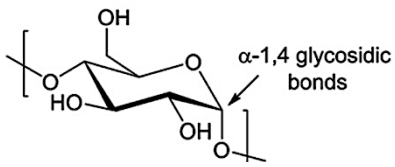

Figure 11: Maltodextrin structure.

- the α-amylase enzyme, which randomly hydrolyses the (1-4) glycoside bond to reduce the viscosity of the suspension;
- the pullulanase enzyme, which is specific to (1-6) glycosidic binding and acts as a de-ramifying enzyme, producing short linear chains (1,4).

The application of these two enzymes allows to produce maltodextrins with high yields.[128] Maltodextrins are highly soluble in water, forming a solution of low viscosity.[127] Their composition reflects the physic-chemical characteristics of the type of starch from which they derive, the amylose/amylopectin ratio is important. In fact, a maltodextrin with an DE of 12 shows retrogradation in solution, causing turbidity. While maltodextrins derived, for example, from gluten corn to the same DE, do not show retrogradation, due to the high level of α-(1-6) ramifications. As DE decreases, differences become more pronounced.

A variety of maltodextrins with disparate functional properties, such as the possibility of forming gels, can be obtained from different starch-based raw materials. Maltodextrins with different molecular weights can be plasticized with water, thus decreasing their glass transition temperature.[128]

To improve peculiar properties such as bioactive retention, controlled release, reduction of oxygen permeability of the cell wall matrix and emulsifier characteristics, maltodextrins are mixed with other materials such as rubbers, pectin, alginate, and whey protein.[127]

Maltodextrins are widely used for the encapsulation of food components, for the protection of nutrients, odors, antioxidants, and bioactive components from thermal and oxidative degradation, during storage and drying. In addition, they are low cost, widely available and compatible with different materials.[127][140]

6.5 Nanosponges

As previously stated, both cyclodextrins and maltodextrins are optimal materials for wastewater treatment. Unfortunately, due to their hydrophilic characteristics and good solubility in water, their use is limited in these applications, where polymers with certain mechanical properties are required, and need to be chemically modified.[141][142][143][144] In addition, various functional groups can be added on their surface such as amino, alkyl, alkoxides, phosphates, sulfates, tosylates, imidazole's and ammonium groups. The systems that came out could be in various forms such as powder, gel, resins or particles.[135]

Nowadays, insoluble polymers of cyclodextrins as well as maltodextrins [142] are usually called "nanosponges" (NS). They have a spongy structure, which has a high porosity and ability to trap various types of molecules in the matrix.[137] They have the advantage of being able to form complexes both with organic molecules and with metallic cations and in addition they can be easily separated from the aqueous medium by filtration.[141]

To make these polymers insoluble, several synthesis methods have been studied to allow the removal of various pollutants from aqueous solutions. They can be divided into three categories:[143]

- reactions of immobilization,
- reactions of self-assembly,
- cross-linking (cross-linking) reactions.

Immobilization refers to blocking, for example cyclodextrins, on a solid substrate, by chemical or physical methods. Supports can be magnetic materials, such as iron oxides, graphene oxide, or organic and inorganic fibers. For example, CD-based fibers immobilized on carbon nanoparticles (CNPs) prepared by electrospinning have a much higher specific surface area and a very porous structure with a much larger total pore volume than normal carbon fibers. While introducing CDs, through chemical interactions, in natural fibers such as cotton, you have the possibility to improve the adsorption capacity of dyes.[143] Self-assembly concerns cyclodextrins by their cavities. This is a process of transition from a disordered system to an

ordered one, with local interactions between the components, which usually occurs in nature and in the body. Cross-linking is a reaction in which molecules are bound together by means of a cross-linking agent to form a more stable structure.[143]

6.5.1 Nanosponges synthesis: general features

It is mainly the cross-linking reactions that are most used for the synthesis of nanosponges.[143] Cross-linking agents interconnect molecules, increasing their molecular weight and generally provide more mechanical properties and better stability in the aqueous environment.[145]. Dextrins are chemically modified by the addition of acid functional groups. In fact, the hydroxyl groups in the polymer react with suitable bi- or polyfunctional monomers, carrying free acid groups, which could undergo deprotonation in aqueous media, thus obtaining insoluble polymers with negative charge.[141] A rather studied reticulating agent is epichlorohydrin (EPI), much used since about 50 years. The β-CDs-EPI system has been considered for practical applications due to its easy preparation and low cost. Glutaraldehyde, with two aldehyde groups capable of reacting with hydroxyl dextrin groups, has also been used to create adsorbents with a three-dimensional structure. While the use of rigid aromatic groups gives a high surface area to the adsorbent system.[143] However, cross-linking agents such as EPI and glutaraldehyde are harmful to humans and the ecosystem;[143] for example, glutaraldehyde is considered cytotoxic if used above 8%.[146] Whereas, in cross-linking reactions with rigid aromatic groups, organic toxic solvents are used.[143]

Due to the limitations of previous cross-linking agents, many researchers have focused on the use of greener alternatives such as citric acid, a tricarboxylic acid, which has very effective groups, which allow to achieve high adsorption efficiency. It can simultaneously connect the CDs and introduce carboxylic groups, allowing selective adsorption, adjusting the pH.[143] Citric acid is a very good chance as a crosslinker, as it has low cost, is environmentally friendly and can be used in mild conditions.[147] Another alternative for the introduction of carboxylic groups was studied by Zhang et al.[148] They have cross-linked β-CD with thimalic acid, which in addition to containing -COOH groups, also has a thiol group (-SH). Another option is EDTA, which is widely used due to its chelating properties with heavy metals. The adsorbent, formed after cross-linking, also can interact simultaneously with both organic pollutants and dyes, thanks to its porous structure. Compared to EPI, cross-linking with EDTA gives the adsorbent excellent performance for the removal of cationic dyes.[143] Zhao et al.[149] found that unlike the adsorbent system EPI-β-CD, in the EDTA β-CD, the EDTA groups do not only act as interlockers, but also chelating sites for metal ions and in addition they are able to make the hydrophobic cavities of cyclodextrin much more polar, allowing the

formation of inclusion complexes with dye molecules. Another possibility are water-soluble diglycyl ethers, which have been recognized as excellent functional molecules for grafting reactions and hydrogel formation from hyaluronic acid, chitosan, and β-cyclodextrins.[142]
In their research work, Rodriguez-Tenreiroet et al,[150] used ethylene glycol diglycyl ether (EGDE) as a cross linking agent, containing two epoxy groups in its structure, both with the same reactivity and able to react simultaneously with the hydroxyl groups of cyclodextrin used. EDGE has been shown to be an excellent cross-linking agent for polysaccharides thanks to its low toxicity, which allows it to be used in preparation of protective coatings inside cans for food and drinks. Cross-linking process greatly affects the swelling of these adsorbents. Increasing cross-linkers amount, the stability of the nanosponge is improved.[133] This leads to a polymer that tends to swell less and more ideal for water treatments. In addition, they can also be applied in filtering devices, such as cartridges, as they undergo only moderate changes in volume during the various cycles of humidification and drying.[141]
As regards synthesis methodologies, they can be get by different methods such as: the fusion method, solvent synthesis (such as dimethyl formaldehyde, DMF, or dimethyl sulfoxide, DMSO) and ultrasonic or microwave synthesis.[138] However, research is moving towards increasingly green methodologies, to minimize environmental impact, using not too drastic conditions and environmentally friendly reagents, as previously mentioned. Generally, aqueous environment and in a temperature range of around 80-100°C is preferably chosen.[141][142][143][148][151] For instance, Yu et al,[152] for the synthesis of the P-CDEC adsorbent system, they used 2-methyltetrahydrofuran (MeTHF), which is considered much greener than tetrahydrofuran (THF), as it is produced from renewable resources through the catalytic reduction of furfural derived from the dehydration of pentose sugars in biomass.

6.5.2 Parameter that influences nanosponges adsorption process

Some of the main parameters that affect the behavior of nanosponges towards contaminants that must be adsorbed are the initial pH, the contact time and the presence of other contaminants. It is well known that the adsorption process and the adsorbent capacities of the systems considered are different at various pH values, due to the change of the adsorbent surface charge, the ionization of the functional groups and the shape of the ion in solution.[133][148] As previously mentioned, polysaccharide-based adsorbents may be anionic, cationic or amphoteric, depending on the charge on their surface and on the ion to be adsorbed.

Taking into consideration several works from the literature; it is possible to evaluate the effect of pH on the adsorption capacity of the contaminant considered.

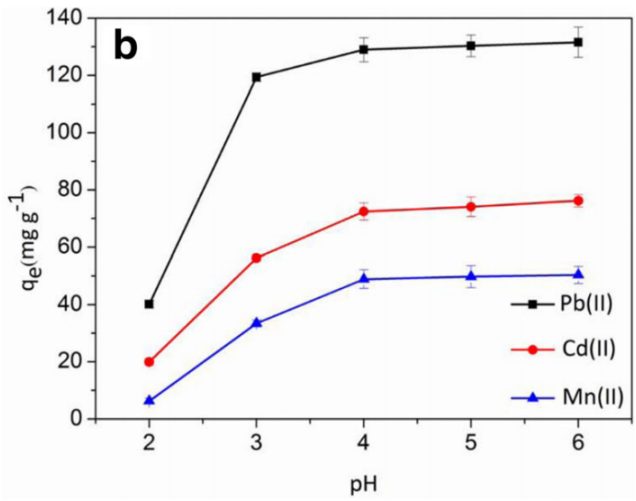

Figure 12: Effect of pH on a cationic adsorbent.

In general, for the removal of cations, such as heavy metals, an alkaline environment promotes adsorption phenomena. In fact, when the pH of the solution is lower than the pH value at the zero-charging point, the number of adsorbed pollutants is unsatisfactory. Usually, as the pH of the contaminant solution is increased, the adsorbent can remove more and more of it.[133] At lower pH the functional groups are protonated, thus creating a positively charged site that would generate a repulsive force towards the metal cations and therefore a decrease in adsorption.

The same thing happens, in the opposite situation dealing with an anionic contaminant, whose interaction with the adsorbent surface is facilitated in a more acidic environment. [141][148][153][154][151][155]

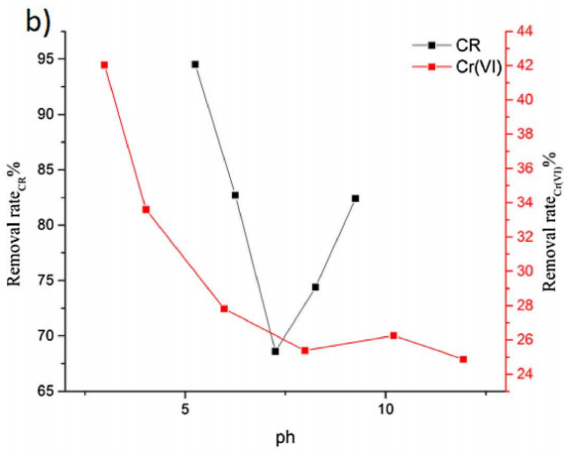

Figure 13: Effect of pH on an anionic adsorbent.

Zhang et al. [148] have synthesized a new adsorbent system based on β-cyclodextrin, PVA-TA-β-CD, for the removal of heavy metals such as lead, cadmium and manganese. The adsorption capacity increased from pH 3 to pH 6, thanks to the enhanced deprotonation effect, as shown in Figure 12. Cai et al. [156] assessed the effect of pH on the adsorption of anions as $Cr_2O_7^{2-}$ and anionic dye CR (congo red), using a quaternary ammonium multilayer magnetic adsorbent and β-cyclodextrin, conjugated with magnetic iron particles. They found that at relatively low pH, the surface of the adsorbent was protonated and then the iron nanoparticles, the carboxylic group, and the quaternary ammonium ions in the following forms: Fe-OH_2^+, -$COOH_2^+$ and -$N^+(CH_3)_3$. In this way the coordination affinity with the anions is enhanced as shown in Figure 13. Contact time between adsorbent and pollutant is different depending on the type of substrate used. Generally, with the increase of the contact time, there

is an increase of the adsorption speed, until the equilibrium is reached. Indeed, when more active sites on the adsorbent surface are occupied and we are close to saturation, the removal efficiency tends to decrease with time.[154] In fact, for example using the P-CDEC system, based on β-cyclodextrin and chitosan, the maximum amount of pollutants removed is reached after one minute [154], while with the β-cyclodextrin and maltodextrin nanosponges, the maximum adsorption for the removal of the Cu^{2+} ion from an initial concentration of 500 mg/L was obtained after 24 h.[141][153] In general, the adsorption rate depends on the number of unoccupied sites and the adsorption curve tends to reach a plateau, indicating its saturation (example shown in Figure 14).[156]

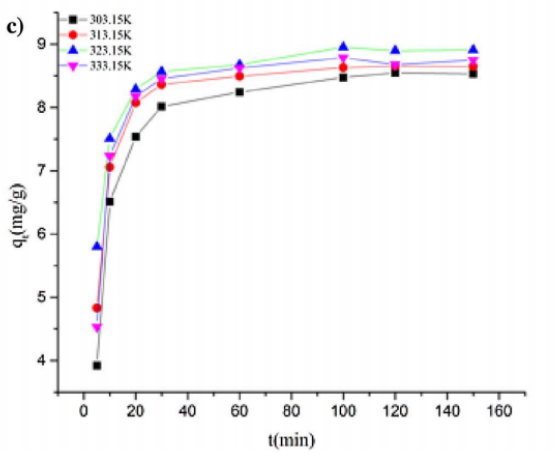

Figure 14: Adsorption process of Cr (VI) ions on a multilayer cationic magnetic polymer at different temperatures.

Other polluting species may influence adsorption. Some ions of similar value have a competitive effect, particularly in industrial waste water containing a variety of metal ions such as Mg(II), Zn(II), Co(II), Ni(II), Mn(II) and others.[133] The competitive effect is evaluated by calculating the ratio between the amount of metal within the mono-component system and that in the multi-component system and tendentially smaller ratios of one are synonymous with competition between the ions, inhibiting adsorption. [148][154][156]. Zhang et al.[148] have assessed the adsorption competition in a multi-component system, including copper, lead and manganese ions, noting that the ratios were lower than one and therefore the removal capacity decreased. In fact, metals with great affinity for the adsorbent system considered can inhibit interaction with those that had minor affinities. Yu et al. [154] have, on the other hand, established that the adsorption capacity of P-CDEC (β-cyclodextrin, chitosan and EDTA) was not particularly affected by the presence of different contaminants in solution, as the active adsorption sites were different. In fact, for nickel ions the main culprits were the groups of the EDTA crosslinking agent, while for bisphenol A the culprits of cyclodextrin were.

7 Heavy metal: general overview

Another current issue arising from human activities, but also from contamination of natural origin, is heavy metals contamination. Heavy metals are elements having an atomic weight between 65,5 and 200,6 g/mol[157] and a density greater than 5 g/cm^3.[158] Today with the term "heavy metal" we mean species that are toxic for the environment and for man.[159] The most common heavy metals are: titanium, vanadium, chromium, manganese, iron, cobalt, nickel, copper, zinc, arsenic, molybdenum, silver, cadmium, tin, platinum, gold, mercury and lead.[159] Some of them called micronutrients, are considered essential elements for living organisms at low concentrations, such as copper (Cu), zinc (Zn), iron (Fe), manganese (Mn), cobalt (Co), molybdenum (Mo), chromium (Cr^{3+}) and selenium (Se).[160] Zinc, for example, is important as a constituent of enzymes, while iron is essential for hemoglobin.[159] Copper, on the other hand, is an essential element for humans, as it plays an important role in the activation of hemoglobin in red blood cells, is found in enzymes responsible for oxygen transport and helps to strengthen tendons and cartilage.[161] However, at high concentrations, they can induce toxic effects, adversely affecting the growth of organisms, metabolism and reproduction, with effects on the food chain, and consequently on humans. Other elements, such as lead (Pb), cadmium (Cd), nickel (Ni), arsenic (As) and mercury (Hg), are defined as non-essential and even at very low concentrations have toxic effects on organisms.[162] The main features that make these elements particularly dangerous are:[157][162]

- toxicity;
- bioaccumulation;
- biomagnification in the food chain,
- non-biodegradability.

Heavy metals are one of the water pollution main sources. In fact, once introduced into the aquatic environment, they redistribute and accumulate in sediment or are consumed by plant and animal organisms. Due to metal desorption and remobilization processes, precipitates are a long-term source of contamination for the food chain. In addition, metal residues in contaminated habitats can bioaccumulate in the aquatic ecosystem, and in turn enter the food chain, and have effects on human health.[162]

An interesting aspect for environmental pollution study is the bioavailability of heavy metals, defined as the fraction of the total concentration of metal that has the potential to accumulate in the body.[162] An estimate of their bioavailability in polluted marine sediments is important

from an eco-toxicological point of view, as a fraction of these pollutants can be adsorbed and accumulated by marine organisms, causing adverse effects in them.[163] Factors affecting their bioavailability may be of a type:[162][164]

- physical, such as temperature, phase association and adsorption;
- chemical, such as thermodynamic equilibrium, complexation kinetics, pH, lipid solubility, ionic force and octanol/water partition coefficient;
- biological, such as species characteristics, trophic interactions, chemical/physiological adaptation, feeding strategy, reproductive phase, metal assimilation efficiency;
- geochemical, such as sediment, suspended matter and metal speciation.

Heavy metals toxicity is proportional as the dose to which an individual is exposed. It is influenced by multiple factors such as:[165]

- chemical speciation of metals in the aquatic environment, as a metal can be either in the form of an ion or as an organometallic molecule, and be transported in dissolved or particulate form;
- other metals or pollutants, which may reduce or increase the toxicity of each element;
- environmental conditions: temperature, pH, salinity and dissolved oxygen are parameters that affect the physiological activity and metabolism of aquatic organisms, making them more or less susceptible to the effects of contaminants;
- characteristics and conditions of the organisms;
- adaptation of the organism to the absorption of metals.

7.1 Primary heavy metal sources

Heavy metals can result from both natural and anthropogenic processes (Figure 15).[166]

They can be emitted naturally by volcanic eruptions, forest fires, rock erosion, biogenic sources, wind-borne particulate matter.[167] Natural disasters, such as floods, also play an important role in the transport of heavy metals. In fact, they contribute to an acceleration of the circulation of metals in river valleys, compared to the non-flooded soils.[168] Floods can also be responsible for changing the chemistry of river water. In acidic waters, such as those

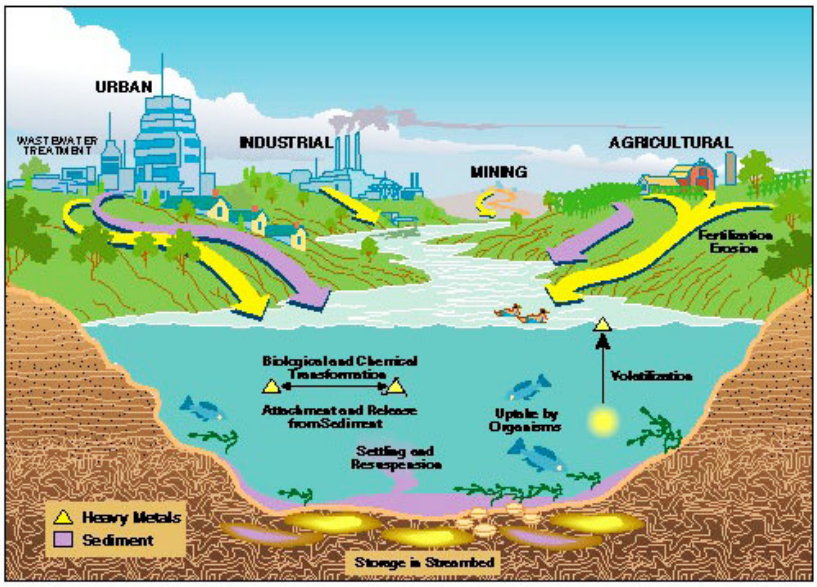

Figure 15: Heavy metal sources.

containing acid mine drainage, the increase in rainwater can promote, for example, the hydrolysis of ions such as Fe^{3+}, followed by the precipitation of iron oxides. Particulate matter can settle in water basins for a long time and precisely during floods, due to the reductive conditions that arise, metals such as Fe, Mn, As, Cd, Cr, Mo, Ni, and Zn can be released from the solid phase.[169]

However, the major causes of contamination of water bodies by heavy metals arise from anthropogenic activities: industrial, urban and mining discharges.[167] The main culprits are the galvanic industries and metal surface treatment processes, which generate a significant amount of effluent containing heavy metals such as cadmium, zinc, lead, chromium, nickel, copper, vanadium, platinum, silver and titanium; the wood processing industry, which uses arsenic and hexavalent chromium salts for the treatment of wood, releases arsenic into waste water; the production of inorganic pigments causes the release of chromium and cadmium compounds; oil refining generating catalytic converters contaminated with nickel, vanadium and chromium.[170] Effluent irrigation by industries such as paper or fertilizers is also a possible source of heavy metal contamination in soil. Traffic emissions, on the other hand, can release lead, cadmium and arsenic.[171]

As a result, there are several studies in literature on the correlation between heavy metal pollution and proximity to industrial activities and urban areas. For example, Mingkhwan et al. [172] focused on the study of an industrial zone near Bangkok, and its impact on the environment and man. Analyses were carried out both on water samples and on various types of fish in the area. They found high levels of concentrations of metals such as copper, manganese, nickel and lead on surface water samples, and manganese in a fish species, compared to normal. Saha et al.[173] assessed the impact on man both for the proximity of the industrial area and the residential area. They detected concentrations of metals such as Mn, Fe and Pb above the limits established in drinking water. In addition, the assessment of the heavy

metal pollution index showed that more than 50% of the sampled areas were polluted, indicating an impact on the health of the population through exposure to water bodies, by oral.

7.2 Chromium and Arsenic: sources and application

In aqueous solution hexavalent chromium is present in different forms depending on the pH of the solution in which it is found. At pH between 2 and 6 the species is observed $HCrO_4^-$ and $Cr_2O_7^{2-}$ only the CrO_4^{2-} anion for pH values above 8. When the pH decreases, it can be observed the phenomenon of chromium polymerization, which determines the formation of tri- and tetra-anions (polyoxometallates) $Cr_3O_{10}^{2-}$ e $Cr_4O_{13}^{2-}$. [174] Chromium is generally extracted from the mineral Chromite, $FeCr_2O_4$. Chromium is produced in two commercial forms, ferrochromium, and metallic chromium. Ferrochromium is an alloy obtained by chromite reduction with coking carbon in an electric arc. It is used in the metallurgical industry to produce stainless steels. Metallic chromium is obtained by reducing Cr_2O_3. The process involves the initial oxidation of chromite in molten alkalis, giving sodium chromate Na_2CrO_4, which is leached with water, precipitated, and oxidized to Cr (III) oxide with coal. The oxide is then reduced to metallic Cr in the presence of silicon. [175] Since 2013, the largest chrome extractor and producer is South Africa (where there are 96% of known reserves). Industrial applications are very diverse; more than 80% of the chrome produced each year is used for metallurgical application: the excellent anti-corrosion and antioxidant properties make it the main additive element in ferrous alloys. Electroplating is the second industrial application of chromium. The process involves the adhesion of a thin layer of metallic chromium on the surface of everyday objects for decorative or functional reasons (corrosion/oxidation protection). The technique involves immersing the artifact in a hexavalent chromium bath or, alternatively, in a trivalent chromium bath. Chromium is also used in the textile industry for leather tanning. It is estimated that 90% of the leather produced worldwide is chrome tanned. The process typically uses a Cr (III) compound as reagent, capable of forming complexes with collagen carboxylic groups. Finally, among the various industrial applications of Chromium, it is also used in formulations of enamels and paints.

All the industrial processes described above produce effluents containing higher or lower concentrations of Cr, which are easily released into the environment. [176]

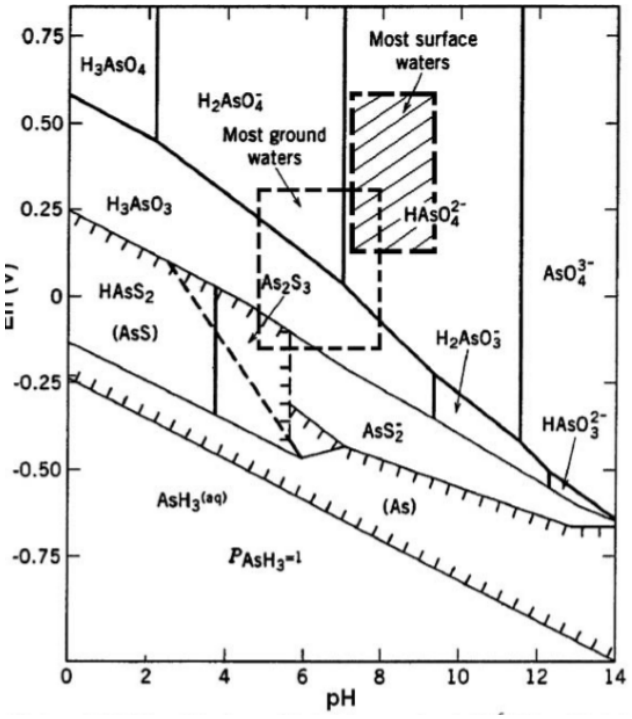

Figure 16: Arsenic Pourbaix diagram.

On the other hand, arsenic is a common semi-metal in nature. The oxidation states in which it may be present are: As^{3+}, As^{5+} and As^{3-}, but in nature the forms +3 and +5 are more available in nature. Arsenic occurs naturally in soil and water at low concentrations. It is estimated to be the 20th most abundant element on the Earth's crust, with an average concentration of 1.8 ppm. There are more than 200 minerals containing arsenic impurities. The most important are realgar (As_4S_4), orpimento (As_2S_3), arsenolite (As_2O_3) and arsenopirite (Feass). Since arsenic is often found in precious metal mines such as Cu, Au and Ag, it is likely to contaminate the groundwater in the surrounding area. Arsenic is also found in geothermal sources, where its concentration can reach 1 mg/L. The presence of arsenic in the environment is also attributable to anthropogenic activities related to agriculture (fertilizers) and generally industry.[177] In aqueous phase it is found in the form of different anionic species, depending on the pH and redox potential. The presence of arsenic acid is detectable only at pH<2. In the pH range between 2 and 11 is replaced by species such as H_2AsO^{3-} and $HAsO_3^{2-}$. Arsenious acid is observed in moderately reducing environments at low pH; by increasing the pH the species H_2AsO^{3-} is observed and subsequently for pH greater than 12 the species $HAsO_3^{2-}$ is detectable. Under extremely reducing conditions it is possible to observe the formation of compounds such as AsH_3 and its derivatives. The figure 16 illustrates a diagram of Pourbaix in which it is possible to appreciate all the forms of arsenic in the aqueous phase to the variation of redox potential and pH. In aerobic surface waters, arsenic can be found in the form of arsenate anion, while for anaerobic groundwater it is detected as arsenious acid. The reactivity of arsenic anions depends on the oxidation state: As^{3+} forms bonds with sulfur and sulfidic groups such as cysteine, dithiols, proteins and enzymes, while it does not react with amino groups, or with organic groups containing nitrogen. The opposite is the case of arsenic (V), which has a propensity to react with amino and nitrogenous groups, while it is inert towards sulfur and sulfide groups. Both species react with carbon to give organo-arsenical compounds [178], [179]. Arsenic was used in ancient times as a poison to

commit murder (especially in the upper classes, for this reason it was nicknamed the Venom of Kings), used for this purpose until the invention of the Marsh Test, an assay capable of detecting traces of arsenic. Elemental arsenic is obtained on an industrial scale by the fusion of minerals such as $FeAs_2$ and FeAsS at 650-700 °C in the absence of air condensing the sublimated element.

$$FeAsS \rightarrow FeS + As_{(g)} \rightarrow As_{(s)}$$

Residual arsenic trapped in sulfides can be released by a process of roasting in air, with subsequent storage of sublimated As_2O_3. Arsenic (III) oxide can be obtained in large quantities as a residual powder from the fusion of Cu and Pb minerals (it is the main industrial source from which it is derived). The oxide can be used as it is or reduced with coal at 700-800 °C to elemental arsenic. Commercially arsenic is mainly used in alloy with lead and copper (for example in ammunition, where the addition of a % between 0.5 and 2 improves the sphericity of projectiles). It has also been used as an insecticide in the compound $Pb_3(AsO_4)_2$. Lead was then replaced with calcium, until the complete abandonment of these types of pesticides due to the great potential contaminant. Other recent applications concern the semiconductor and electrical industry in general: intermetallic compounds between arsenic, gallium and indium are the main components for LED, laser and diode tunnel applications. In the preservative industry, $AsO(OH)_3$ is used in wood impregnation formulations.

7.3 Heavy metal impact on environment and human health

Environmental risks are associated with contaminated effluents release. Even heavy metals traces can cause serious problems to flora and fauna. Indeed, adverse physiological effects have been found for heavy metals such as cadmium, copper, nickel, lead, and mercury compounds in mammals, birds, reptiles, amphibians, crustaceans, and fish. In addition, they can also cause disturbances in seed germination, plant metabolism and growth, oxidative stress in algae and induce a decrease in chlorophyll concentration in plants.[180]

Heavy metals release may cause changes in the physical conditions of aquatic systems. In fact, pH changes in water, the organic content of the substrate and particles size in water can occur. Consequently, flora reacts to these imbalances with a decrease in species diversity, density and composition.[161] Heavy metals accumulation in aquatic organisms results in their transfer to the food chain, leading to potential risks due to the intake of contaminated fish.[162] In fish the metals absorption generally occurs through ingestion of food or particulate matter are then transported into cells through biological membranes and ion channels.[162] In addition heavy metals can cause serious health problems,[181] especially concentrations greater than the critical values.[161]

Heavy metals toxicity can negatively affect central nervous system activities, damage the lungs, liver, kidneys, blood composition and other key organs. Prolonged exposure can cause muscular dystrophy, Alzheimer's disease, different forms of cancer and multiple sclerosis.[161] They can also cause problems in growth and development and generate disorders to bioregulatory systems, responsible for functional and psychosomatic disorders such as chronic fatigue.[181] Heavy metals exposure is observed through three preferential routes: oral ingestion, inhalation, and skin exposure. They depend on the specific characteristics of the metal.[161] The adverse effects on hu man beings is described as follow.

- *Copper (Cu)* is considered an essential element for living beings and can be taken through the food chain, residues and water.[161] The free Cu^{2+} ion (cupric ion) is one of the most dangerous and toxic copper species. Use of water or food contaminated with copper-based compounds in high concentrations can cause nausea and severe gastric problems.[161]
- *Zinc (Zn)* is a basic micronutrient and is one of the least dangerous metals. However, high consumption, through respiration of vapors and intake of contaminated water and food, may cause growth and proliferation dysfunction, but also acute symptoms such as liver problems and kidney failure, blood in the urine, abdominal and stomach cramps, nausea and vomiting and chronic symptoms such as pancreatic damage and anemia.[161]
- *Cadmium (Cd)* is one of the most dangerous metals. It can accumulate in the human body and cause irreversible damage even at low concentrations. It meets humans easily by inhalation and by oral route, through tobacco intake and the food chain. In fact, it is available in some types of fish, mussels and clams, present in contaminated bathing regions.[161][159] The kidneys and liver are the organs with the highest concentration of cadmium and together with the bones are the first to be damaged. This metal is also known as powerful carcinogen, affecting kidneys, lungs, pancreas and prostate and is also responsible for apoptosis and DNA damage.[159]
- The toxicity of *chromium (Cr),* however, varies greatly depending on the chemical form (oxidation number, ion type, oxide, hydroxide). For example, hexavalent chromium (Cr^{6+}) is much more toxic than trivalent chromium (Cr^{3+}).[181] Cr (III) is considered an essential micronutrient for humans and animals and is naturally found in many foods such as vegetables, fruit, meat and wheat and in drinking water. Instead, Cr (VI) is corrosive to skin and mucous membranes; if inhaled it causes asthma, swelling of the larynx and bronchi, pneumonia and sensitization. It is a suspected teratogen and is

classified by the International Agency for Cancer Research (IARC) as a type 1 carcinogen by inhalation, for most living organisms. Unlike Cr (III), which is absorbed at the cell level in a slightly marked manner (simple diffusion mechanism), Cr (VI) enters cells by facilitated diffusion as a chromate ion, where it is progressively reduced to Cr (V), Cr (IV) and Cr (III) from reducing systems such as glutathione, ascorbate, cysteine and enzymatic activities such as cytochrome P-450. Unstable forms Cr (IV) and Cr (V) cause changes in DNA and cell cycle, oxidative stress (formation of OH radicals responsible for DNA mutations and degradation of phospholipids in the cell membrane) and induction of genes responsible for cellular apoptosis. [182], [183] [184]

- Exposure to lead (Pb) occurs mainly through inhalation and ingestion of contaminated particles or aerosols and food, water and plants respectively. In the human body a high percentage of lead is found in the kidneys, liver, heart and brain, while in the bones there is the highest fraction. The nervous system is the most vulnerable target of lead poisoning, which causes clumsiness, irritability, attention problems and memory loss. In addition, it also affects organs such as kidneys, liver, the hematopoietic system, the endocrine and reproductive system and is considered a possible carcinogenic species for humans by the International Agency for Research on Cancer (IARC).[164]
- *Aluminum (Al)* can affect organs such as lungs, the central nervous system (causing diseases such as Alzheimer's and encephalopathy [185]) and bones (causing osteomalacia).[159] High amounts of aluminum can also cause renal excretion, especially for patients with kidney failure, because they are unable to expel excess aluminum.[186]
- Although *nickel (Ni)* is one of the lightest heavy metals, its prolonged contact with the skin and mucous membranes can cause itching and allergies. In fact, dermatitis is the most frequent effect for nickel exposure. In addition, ingestion of nickel salts can cause intestinal disorders, while chronic inhalation can lead to cases of asthma and tubular dysfunction.[181]
- *Manganese (Mn)* is an indispensable element for the human body for the proper functioning of physiological processes, such as for the immune system. However, exposure to high amounts of Mn can be neurotoxic. In fact, it can cause cognitive disorders, Parkinson's and memory problems. While, by intake of highly contaminated drinking water, serious health risks may arise due to rapid absorption of Mn in the intestine and blood cells.[187]

- The toxicity of *arsenic* compounds increases progressively as follows: organic compounds < Arsenic (V)<Arsenic (III)<AsH_3. Arsenic (III) toxicity is 70 times higher than organic arsenic, and 10 times higher than arsenic (V). The increased toxicity of As (III) compounds is due to its ability to bind to sulfide groups, leading to some influence on metabolic activities such as cell glucose uptake, gluconeogenesis, the oxidation of fatty acids and the production of glutathione. As for arsenic (V), its similarity to the phosphate anion allows its substitution in reactions and vital compounds. In general, arsenic toxicity can deactivate more than 200 enzymes (most of which are involved in cellular energy pathways); interaction with DNA is indirect, since it is able to change its gene expression by interrupting the methylation process, inhibit its shelter and promote oxidative stress (formation of ROS radicals). [188] The majority of cases of acute Arsenic poisoning occur because of accidental ingestion of pesticides and insecticides or contaminated water. The minimum lethal dose of As in acute intoxication is around 1 mg/kg. Clinically, symptoms such as colic, nausea and vomiting are observed following ingestion of these amounts.

7.4 Heavy metal legislation

Given the serious consequences that heavy metals can have for man and the environment, limits have been placed on their concentration within the water. For example, according to the United States Environmental Protection Agency (US-EPA) and the World Health Organization (WHO), the concentration limits for heavy metals range from 0.01 to 0.05 mg/L.[181] In Europe, reference is made to Directive 2008/105/EC on environmental quality standards (EQS). In Italy, on the other hand, reference is made to the “Testo Unico Ambientale” (TUA), i.e. Legislative Decree no., 152/2006. Table 2 summarizes the limit concentration values for certain heavy metals.

Table 6: Heavy metal law limits in water.

Metal	***Limit (EPA)** for drinking water **mg/L**[159]*	***Limit (WHO)** for drinking water **mg/L**[159]*	***Limit** for drinking water **(98/83/EC) mg/L***	***Limits** for emissions in surface water **(TUA) mg/L***	***Limit** for **emissions** in sewerage **(TUA) mg/L***
Cu	1,3	/	2,0	≤0,1	≤1
Zn	/	/	/	≤0,5	≤4
Al	0,05–0,2	≤0,1	0,2	≤1	≤2,0
Pb	0,015	0,01	0,01	≤0,2	≤0,3
Cr (total)	0,1	0,05	0,05	≤2	≤4
Cr(VI)	0,015	0,01	0,01	≤0,2	≤0,2
Mn	0,3	0,4	0,5	≤2	≤4
Cd	0,005	0,0003	0,005	≤0,02	≤0,02
Ni	0,1	0,02	0,02	≤2	≤4
As	0,015	0,01	0,01	≤0,5	≤0,5

*TUA: Testo unico ambientale, (https://www.bosettiegatti.eu/info/norme/statali/2006_0152_allegati.htm#P_3).

*98/83/EC, https://eurlex.europa.eu/LexUriServ/LexUriServ.do?uri=CONSLEG:1998L0083:20090807:IT:PF.

The removal of heavy metals from water and effluents is a very important issue, as they are toxic and dangerous to human health, living organisms and the environment.[161] It is therefore essential that research be carried out into the development of effective methods of waste water treatment in order to improve their quality for reuse, but also for two main reasons: preventing the transmission of diseases and preserving the aquatic environment.[189]

7.5 Wastewater treatment for heavy metal removal

Water pollution is becoming an increasingly vital issue worldwide and this is also highlighted by the vast number of articles, reviews and books published, on wastewater treatment. Since 2000s, scientific publications concerning solutions for the abatement of heavy metals in effluents are increased, both with conventional treatments, now consolidated for a long time, that with innovative processes.

7.5.1 Heavy metal traditional treatment

Among the main conventional processes for the treatment of inorganic effluents there are:[190]

- chemical precipitation,
- ion exchange,
- electrochemical processes (electrocoagulation, electrodeposition, electro-flotation),

- adsorption processes (on conventional solid materials such as activated carbon, carbon nanotubes).

1. *Chemical precipitation*

Chemical precipitation is one of the most efficient methods and by far the most widely used in industrial processes, thanks to its relative ease of use and cost-effectiveness.[191] The process consists of reacting chemicals (precipitators) with metal ions to form insoluble precipitates. The latter may subsequently be separated from the water by sedimentation and filtration.[192] pH is a fundamental parameter to consider. In fact, basic conditions are preferred to improve the removal of heavy metals.[190] The most appropriate pH range ranges from 8 to 11.[161] The effectiveness of chemical precipitation is also influenced by the type and concentration of the heavy metal, the precipitating material used, the reaction conditions and the presence of other compounds that could inhibit the reaction itself.[193] The most common precipitators are alum, lime, iron salts and organic polymers.[184][194] The current processes are: precipitation of hydroxides and sulphide precipitation.[157] Heavy metals can be precipitated as hydroxides, using an alkaline precipitator.[194] The metal ion removal mechanism is as follows:

$$M^{2+} + 2(OH)^- \leftrightarrow M(OH)_2,$$

where M^{2+} and OH^- represent the dissolved metal ion and the precipitator respectively, while $M(OH)_2$ is insoluble metal hydroxide.[194] It is the most widely used chemical precipitation technique, thanks to its simplicity, low cost and easy pH control (8-11).[192]

The most commonly used precipitators are oxides, hydroxides and calcium and sodium carbonates.[194] Among all, lime is preferred in the industrial sector, thanks to its availability, low cost and effective treatment of inorganic effluents with concentrations of metals higher than 1000 mg/L.[195] The addition of coagulants such as alum, iron salts and organic polymers help to improve their removal.[192] The efficiency of the process depends on several factors such as:[184]

- ease of hydrolysis of the metal ion,
- nature of the oxidation state,
- pH value,
- formation of complexing ions,
- degree of agitation,
- weather,
- characteristics of the precipitate.

The sulphuration process is like the previous one and consists in the precipitation of metal by means of sulfides, as precipitating agents. The mechanism is as follows:

$$Na_2S + MSO_4 \leftrightarrow MS + Na_2SO_4,$$

where MS is the precipitate.[194] This is another very efficient technique for removing heavy metals. In fact, one of its first advantages over the previous technique is that the solubility of the precipitated metal sulfides is much lower than metallic hydroxides (Table 7) and is not amphoteric, High levels of heavy metal abatement can be achieved in a wide pH range. In addition, the sludge produced shows better characteristics: in particular, it is easier to thicken and dehydrate than that obtained during the precipitation of hydroxides.[194]

Table 7: Theoretical solubility of hydroxides and sulfides of heavy metals in pure water.

Metal	Solubility of metal ion (mg/L)	
	As hydroxide	As sulfide
Cadmium (Cd^{2+})	$2.3 \cdot 10^{-5}$	$6.7 \cdot 10^{-10}$
Chrome (Cr^{3+})	$8.4 \cdot 10^{-4}$	No precipitate
Cobalt (Co^{2+})	$2.2 \cdot 10^{-1}$	$1.0 \cdot 10^{-8}$
Copper (Cu^{2+})	$2.2 \cdot 10^{-2}$	$5.8 \cdot 10^{-13}$
Iron (Fe^{2+})	$8.9 \cdot 10^{-1}$	$3.4 \cdot 10^{-5}$
Lead (Pb^{2+})	2.1	$3.8 \cdot 10^{-9}$
Magnesium (Mn^{2+})	1.2	$2.1 \cdot 10^{-3}$
Mercury (Hg^{2+})	$3.9 \cdot 10^{-4}$	$9.0 \cdot 10^{-2}$
Nickel (Ni^{2+})	$6.9 \cdot 10^{-3}$	$6.9 \cdot 10^{-8}$
Silver (Ag^{+})	13.3	$7.4 \cdot 10^{-12}$
Tin (Sn^{2+})	$1.1 \cdot 10^{-4}$	$3.8 \cdot 10^{-9}$
Zinc (Zn^{2+})	1.1	$2.3 \cdot 10^{-7}$

The main precipitators used in this process are sodium sulfide, sulfide, sodium thiosulfate, calcium sulfide, barium sulfide, iron sulfide and ammonium sulfide.[194]

The main factors influencing this technique are pH and the source of sulfides. Other parameters to be considered are the type and initial concentration of metal, the precipitating agent used and the concentration ratio of the two components.[194] One of the most dangerous limits, compared to precipitation of hydroxides, is that heavy metals in the form of ions are generally found in an acidic environment and under these conditions precipitated sulfides can lead to the formation of toxic fumes of hydrogen sulfide. It is essential that precipitation takes place in a neutral or basic environment. In addition, colloidal precipitates may form which cause separation problems in sedimentation and filtration processes.[192]

Over the years, especially with precipitation of hydroxides technique, excellent results have been achieved. In fact, as reported by one of their studies carried out by Benalia et al.,[196] good results have been gotten in the abatement of copper (99%) and zinc (97%) in industrial effluents, using as precipitating agents' lime and soda at the maximum dose (400 mg/L), at an optimal pH of 9. Also, Oncel et al.,[197] in one of their articles, they reported very good abatement rates of over 99% for heavy metals such as iron, aluminum, zinc, lead and chromium present in the acid drainage wastewater of coal mines. Although chemical precipitation is already a well-established method, it has many disadvantages including:[198][199]

- requires large amounts of precipitation to treat high volumes of wastewater;
- low concentration metal removal inefficiency,
- requires an oxidation step if the metals are complexed, to prevent them from inhibiting the precipitation of metallic hydroxide.
- some metal hydroxides have amphoteric properties, which can create a problem in the use of this technique, because the ideal pH for one metal may not be ideal for the other, which would lead to the remission of the latter in solution,
- management problems for large volumes of sludge produced, especially disposal costs.[199] However one solution, could be to use as precipitating Na_2CO_3. Indeed, in their study, Benalia et al. [200] have tried to precipitate copper and zinc metals with sodium carbonate to a lower volume of sludge produced when compared to calcium and sodium hydroxides, this is because the precipitates formed using sodium carbonate have a higher crystallinity and their recovery by decanting is much simpler and faster.

2. *Ion exchange*

Ion exchange is a technique extensively used in heavy metals removal from effluents, due to its excellent abatement efficiency, high treatment capacity and fast kinetics.[192] In this process, cations or anions in solution are replaced by the same type of ions in the insoluble material, called ionic exchange resin. The contaminated water thus enters the ionic exchange column from one end and, throughout it, is purified. Once the column is saturated, a counter-washing process is carried out to remove the deposited heavy metals and it is regenerated.[161] The resins are made of a cross-linked polymer matrix, in which a functional group is attached through a covalent bond. The spaces in the structure allow the ions to be transferred appropriately.[157] Ion exchange resins can be both synthetic and natural, but the former is preferred because they are more effective.[161] Among the natural ones, zeolites play an important role, crystalline species formed by aluminum and silicon atoms, connected through oxygen bridges [157]. Many researchers have demonstrated their efficiency in removing heavy

metals from the effluent. Clinoptilolite, one of the most studied zeolites, has received great attention thanks to its high selectivity towards heavy metals. In addition, the purified water could be reused for human consumption or agricultural use. Unfortunately, one of the limitations is that their application has been studied only experimentally and not on a large scale for the industrial field.[192] Cationic resins are the most widely used in the removal of heavy metals from wastewater. They may present as strongly acidic resins, containing sulphonic groups or weak acids consisting of carboxylic groups. The presence of hydrogen ions in resin acid groups allows the exchange with cationic forms of metal ions in solution.[161] The mechanism is:[190]

$$nRSO_3^- - H^+ + M^{n+} \leftrightarrow nRSO^{3-}\text{-}M^{n+} + nH^+,$$

where "n" indicates a constant of the reaction species, relative to the oxidation number of the metal. Factors affecting the ion exchange process can be pH, anions, temperature, initial adsorbent and adsorbed concentration and contact time.[190]

In some studies, many researchers have reached good abatement results by ion exchange resins. Hussain et al.,[201] in one of their laboratory experiments, have used bentonite as an ion exchange resin for the removal of lead and copper, resulting in 89% and 87.7% abatement respectively, with an initial concentration of the two heavy metals of 10 mg/L, with a contact time of 60 minutes. They also estimated that an increase in the amount of bentonite used led to an improvement in adsorption due to increased accessibility to a larger surface, which contains more active sites for ion exchange. Alyüz et al.,[202] instead, using as a commercial resin the Dowex HCR S/S, always a cation exchange resin, they evaluated its removal efficiency for nickel and zinc, obtaining abatement rates of around 99% from an initial metal concentration of 100 mg/L. In addition, they noted a dependence of the process on pH, the optimal value of which to have a good removal had to be in the range of 4-6, in how much in strongly base atmosphere the two metals precipitated like hydroxides, carrying to a decrease in the percentage of abatement (Figure 17). Excellent results were also obtained in a study on the abatement of heavy metals present in wastewater of different industries in Iran (ceramic, polyethylene and coal industry), using as commercial cationic resin the Dowex 50WX8 for the removal of metals such as Cd (II), Cu (II), Zn (II), Pb (II) and Ni (II), obtaining good abatement rates higher than 70%.[203]

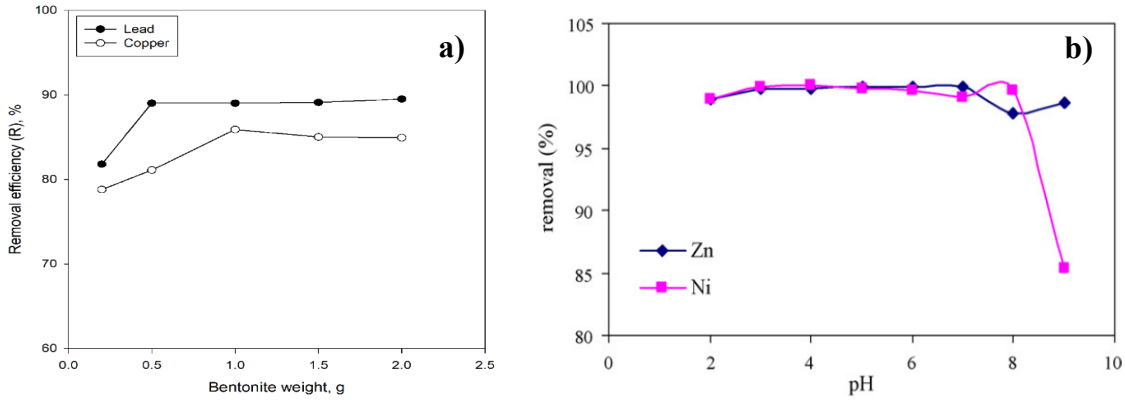

Figure 17: a) Effect of resin amount on metal removal percentage, b) effect of pH on metal removal percentage.

Although it is a widely used technique, it has some disadvantages such as the high costs of both resin and maintenance [198], because it requires large amounts of resin to treat large volumes of wastewater;[161] concentrated solutions of metals cannot be retained, as the matrix is easily soiled by the presence of organic substances and other solids in wastewater. In addition, this technique is not selective and is very sensitive to the pH of the solution.[195]

3. *Electrochemical treatment*

These processes are known for their extreme effectiveness in the treatment of wastewater, for the abatement of heavy metals.[161] They consist in the recovery of heavy metals in their elemental state, through oxide-reduction reactions in an electrochemical cell.[161]

Unfortunately, they did not receive much attention initially, due to the need for large capital investments and the expensive supply of electricity.[190] However, due to strict environmental rules and regulations for the discharge of effluents into the environment, these treatments have aroused interest in many researchers [161], thanks also to advantages such as: their versatility, do not release secondary products,[157] the use of few reagents, the generation of low volumes of sludge and the maximum removal of metal ions.[161] Treatment efficiency depends on the electrode material and cell parameters such as: mass transport, current density, water composition.[157] The main electrochemical treatments are: electrocoagulation, electro flotation and electrodeposition.[161]

4. *Adsorption*

Today, the adsorption process is considered as an efficient and highly valued method compared to other technologies for heavy metal removal.[157] It is a very flexible treatment from an operational and design point of view.[161] The mechanism consists of the transfer of solid/liquid mass, in which the heavy metal (adsorbed) migrates from the effluent to the surface of the solid, called adsorbent, and binds to it through chemical or physical adsorption. Physical adsorption occurs by weak van der Waals interaction, while chemical adsorption occurs by strong covalent bonds (Figure 18) [161],[204]. The main stages of the process are as follows:[190]

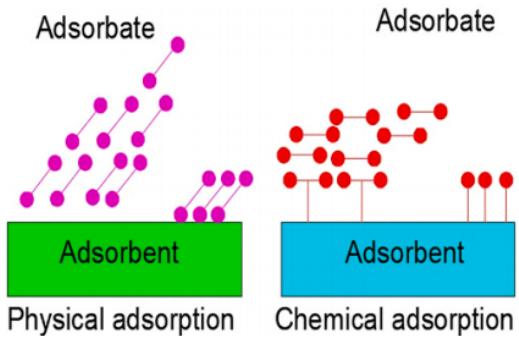

Figure 18: Diagram of the main adsorption mechanisms.

1. the penetration of the contaminant from the bulk of the solution to the surface of the adsorbent solid;
2. the adsorption of the contaminant on the adsorbent surface;
3. penetration into the adsorbent structure.

A positive aspect is that the process can be reversible, and the adsorbent can be regenerated through desorption.[190] Process efficiency is influenced by parameters such as: high surface area, pore size distribution, functional groups and adsorbent polarity.[157]

Some of the conventional adsorbents widely studied and used are activated carbon (AC) and carbon nanotubes (CNTs).[190] Activated carbon (AC) is undoubtedly the most popular and widely used adsorbent in the world for waste water treatment,[184] especially in the felling of heavy metals, thanks to its high surface area and its great affinity towards these toxic species.[161] Activated carbon is prepared by three processes:[184]

1. dehydration of raw organic materials such as biomass, lignite, coal (the most widely used);[157]
2. carbonization, which converts organic materials to primary coal, a mixture of ash, tar, amorphous carbon and crystalline carbon;
3. Acid or basic activation at 500 °C.

Activated carbon can occur in four different forms: as powder (PAC), granules (GAC), fibers (ACF) or tissue (ACT).[205] The main surface properties to be considered for the removal of heavy metals are surface area, functional groups, surface charge and pore size (micropores and

mesopores).[161] In a work reported by Karnib et al.,[206] The use of activated carbon has led to excellent results of abatement of metals such as nickel, cadmium, zinc, lead and chromium, whose percentages reached were respectively 90%, 86%, 83.6% and 50.6%. In addition, they also analyzed the efficiency of the silica/activated carbon substrate (2:3 ratio) in the reduction of nickel starting from an initial concentration of 30 mg/L and 200 mg/L, with excellent results of 92.1% and 87.6% respectively. In a study carried out by Rashed et al.,[207] the removal capacity of the Cd^{2+} ion has been demonstrated using the TiO_2/ASS (activated carbon from sewage sludge ASS) system, suitable for the removal of water contaminated by multiple types of pollutants, because the presence of titanium oxide is useful for the degradation of substances such as dyes. The abatement efficiency has been assessed for both a solution containing only metal, and one containing both metal and a dye. The results obtained, in the case of metal removal, after irradiating the system for four hours with UV light were as follows: 95% in the solution with metal alone and 92.97% of cadmium removed in the solution with both contaminants. Among the parameters evaluated, the most influential one is the pH of the solution; in fact, in a very basic environment (pH = 9) there was an increase in the percentage of removal, as the H_3O^+ ions are less, and there are more sites available for adsorption on the substrate. In addition, they established that the main sites responsible for adsorption of the Cd^{2+} ion were silica (SiO_2) present in the ASS and TiO_2 compounds, according to the following mechanism:

$$2(\equiv SiO^-) + Cd^{2+} \rightarrow (\equiv Si\text{-}O)_2Cd.$$

Despite its excellent properties, activated charcoal has the disadvantage of being too expensive and the limit of having problems in regeneration [161], as it results in a decrease in adsorption capacity, as well as an increase in costs.[208] The cost limits of the materials used for its preparation can be contained by obtaining activated carbon from natural materials or agricultural by-products.[161][157][208] Carbon nanotubes (CNTs) are excellent adsorbents widely studied, thanks to their excellent properties and above all they have been considered potential candidates for the adsorption of heavy metals such as cadmium, copper, chromium and lead from waste water.[192] They consist of cylindrical graphite sheets folded into a tubular structure and are classified into two categories: single-walled (SWCNTs), which consists of a single graphite sheet or multiple-walled (MWCNTs), containing several graphite sheets.[157]

The mechanism of interaction between metal ions and carbon nanotubes is rather complicated and would appear to be attributed to electrostatic attraction, sortation-precipitation, ion exchange or chemical interaction.[192] Characteristics that make them promising adsorbents

are excellent mechanical, magnetic properties and high thermal and chemical stability. In addition, modifications have been made to best disperse carbon nanotubes, such as acid treatments, addition of functional groups and impregnation with metals, to increase adsorption efficiency. In fact, in a study it was found that MWCNTs acidified as adsorbents play an important role in the removal of Pb (II), obtaining good percentages of abatement around 75%.[157] Excessive use of these materials could cause them to be dispersed in the aquatic environment, causing undesirable effects on human health. To overcome this problem, researchers have experimented a system consisting of carbon nanotubes immobilized by calcium alginate, reaching a reduction of 83.3% Cu (II), compared to 74.8% using only as adsorbent CNTs.[190][192]

7.5.2 Heavy metal innovative treatment

The conventional treatments described above have several inadequacies. Chemical precipitation, although a simple and economical technology, produces large amounts of toxic sludge, which requires treatment and thus increases the running costs. Conventional adsorbent materials, such as activated charcoal, however, have good abatement capabilities, with almost total removal of heavy metals, however, the main disadvantage is to have high cost and regeneration problems. Ion exchange resins, while being cheap and effective, have as disadvantage the occlusion of the medium of exchange by contaminants, and the recovery of metals becomes difficult after washing. Finally, electrochemical treatments, despite their high selectivity, speed and good operational control, and their high removal efficiency have the limit of high investment costs and sacrificial electrode.[209] Among the innovative methods, which have recently become increasingly important for heavy metals treatment, will be discussed: adsorption on unconventional materials such as biomaterials, nanomaterials, MOFs (metallic organic frameworks) and membrane filtration processes.

7.6 Nanosponges: heavy metal removal

Generally, heavy metals can be removed by electrostatic interactions, complexation or ion exchange and the removal mechanism depends on the adsorbent system preparation method and operating conditions.[143] In this context, cyclodextrins and maltodextrins nanosponges, have been studied and used for the abatement of heavy metals.

As regards complexation, using β-cyclodextrin cross-linked with EDTA with metal ions led to abatement results for Cu (II) and Cd (II) of 79,4 mg/g and 124,3 mg/g respectively. Complexation of amino groups with metal ions is the main removal mechanism of Cr (VI), using an adsorbent system of β-cyclodextrin-chitosan modified with biochar, and the adsorption capacity was 206 mg/g at pH 2. Through the study of second-order kinetics and the

Freundlich model to describe the adsorption mechanism, it was found that it was likely to be related to the concentration of both metal ions and adsorbent, and in addition, it was demonstrated that the chemisorption of metal ions was the determining step in the adsorption rate, which promoted the mechanism of complexion.[143]

A biodegradable β-CD gel showed excellent performance for adsorption of Cd (II), Pb (II) and Cu (II), 98.9 mg/g, 210.6 mg/g and 116.4 mg/g, respectively, by ion exchange. It depends mainly on the concentration of active sites on the adsorbent surface.[143]

Cross-linked systems can also remove metal ions through electrostatic forces. During this adsorption mechanism, the main constraint is to reach a very negatively charged surface. Metal cations such as lead, copper and cadmium can be adsorbed in concentrations greater than 100 mg/g due to the presence of rigid aromatic groups that make the polymer β-CD negatively charged, increasing gradually the pH. Magnetic nanoparticles based on β-CD (CD-Fe_3S_4) also showed good adsorbent properties against Pb (II) at pH 6, equal to 256 mg/g. As previously mentioned, adsorption is facilitated by the increase in pH, as the concentration of H_3O^+ ions become low.[143] In addition, adsorption can also be given by the combination of multiple interactions. For example, in the removal of ions Pb^{2+}, Cd^{2+} and Ni^{2+}, by means of a carboxymethyl-β-CD adsorbent modified with iron oxide nanoparticles (Fe_3O_4), it has been shown that metal ions were captured by the formation of chelating complexes, after being attracted by the electrostatic forces of carboxylate ions.[143] From some works taken from the literature, with the use of these types of adsorbents have obtained promising results.

In a study carried out by Yu et al.,[154] using the adsorbent system P-CDEC, based on β-cyclodextrin and chitosan and EDTA, as a cross linking agent, the abatement of metallic cations Pb (II), Ni (II) and Cu (II) reached 98.7%, 98.2% and 97.4% at an optimal pH of 3, because most of the pollutants made of heavy metals were acidic. This trend is attributed to the deprotonation of EDTA carboxylic groups. They also estimated the adsorption kinetics, which showed a good abatement result corresponding to 98.6%, 90.7% and 93.3% for Pb (II), Ni (II) and Cu (II) respectively, reaching equilibrium after two minutes. While limiting the study of copper abatement in a multi-component solution with bisphenol A (BPA), to assess its competitiveness, the results achieved were 93% for Cu (II) and 98.7% for BPA.

In a recent work by Zhang et al.,[148] instead, using the adsorbent system PVA-TA-βCD, with thimalic acid as a cross linking agent, they obtained adsorptions of 199,11 mg/g for Pb (II), 116,52 mg/g for Cu (II) and 90,28 mg/g for Mn (II). While in binary solutions, Pb-Cd, Pb-Mn and Cd-Mn, and ternary Pb-Cd-Mn, the removal capabilities were lower than in the single-component system. In the Cd-Mn solution the adsorption relative to the two metals decreased

significantly, reaching the following values: 58,20 mg/g for Cd (II) and 27,06 mg/g for Mn (II). While in both binary and ternary solutions, adsorption of Pb was reduced slightly, as it did not compete with the other two metal ions. The selective adsorption of the three metals on the adsorbent system was very dependent on their properties. Considering electronegativity, it is much higher in the case of lead than copper and manganese. Electrostatic interaction with counterions increases as electronegativity increases, so this property indicates that lead is much more likely to adsorb to PVA-TA-βCD. The ability to interact with the Pb^{2+} ion was given by the fact that the adsorbent system, due to the cross-linking with thimalic acid, in addition to owning the carboxylic group ($-COO^-$), also had thilico group (-SH), which forms a stable complex with lead ion. This was also demonstrated by the analysis of polymer morphology at SEM. They assessed that the surface of the PVA-TA-βCD before adsorption was mostly uneven and filled with holes, due to the bubbles produced during thermal cross-linking. On the contrary, adsorption became smoother, as the pores were occupied by metal ions complexed by the thiol group. [148]

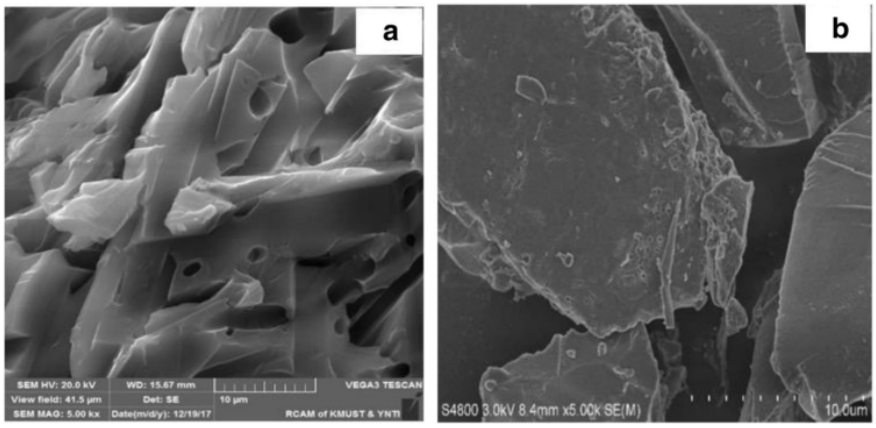

Figure 19: SEM images of the PVA-TA-βCD surface before (a) and after (b) the adsorption of metal ions Pb (II), Cd (II) and Mn (II).

In another recent study, four β-CD and linecaps (LC) nanosponges were synthesized, a maltodextrin derived from pea starch, cross-linked with two different cross-linking agent's pyro methyl dianhydride (PMDA) and citric acid respectively: β-PMDA, β-CITR, LC-PMDA and LC-CITR. By evaluating the adsorption capacity of these types of nanosponges for the removal of the following metal cations Cu^{2+}, Zn^{2+}, Pb^{2+}, Cd^{2+} and Fe^{3+}, the reductions reached ranged from 25% to 95%, starting from an initial concentration of pollutant of 500 mg/L. The ones reticulated with PMDA have gotten the best results for ion Pb^{2+} abatement: the nanosponge possessed two carboxylic groups for every unit of cross-linked, while those reticulated with citric acid had one. However, at low concentrations of 5, 1 and 0.1 mg/L, citric nanosponges showed 90% reduction in the removal of the Cu^{2+} ion, much higher than those

with PMDA. In addition, the performance of the four nanosponges was evaluated for selective adsorption of Cu^{2+} and Zn^{2+} ions in artificial seawater. Unlike the previous case in ultrapure water, citric nanosponges showed a better adsorption capacity, compared to those with PMDA, reaching 80-84% abatement for copper ions and 60% for zinc ions. That's because the second reticulating agent was being interfered with by other salts in the water.[141]

Adsorption performances for the EDTA-β-CD system were studied by Zhao et al.[151] They estimated, through the analysis of adsorption isotherms, that the active sites occupied by the adsorbent corresponded to 85% by Cu (II) and 75.5% by Cd (II). By analyzing the adsorption capacity in a binary solution containing copper ion and a cationic dye, they found that the presence of the dye improved the adsorption of Cu (II). On the other hand, the metal ion did not facilitate interaction with the former. This is due to the metal-EDTA divalent mechanism, as the metal ions are surrounded by the groups present on the EDTA, forming octahedral complexes and thus the presence of copper ions on the adsorbent surface, did not allow further interaction with dye molecules.

The simultaneous interaction mechanism is described in Figure 20. In addition, they also evaluated the application of this adsorbent system in practice, for the simultaneous removal of Cu(II) and methylene blue dye in effluent from a textile industry. They used an adsorbent dose of 2 g/L reaching a reduction of 96.06% of copper ions, but only 37.91% of the dye. However, by increasing the dose of EDTA-β-CD to 5 g/L, they found an improvement in the removal of the two pollutants: 96.87% copper and 91.82% dye [151]. The adsorption capacity of methylene blue was lower than in single-component and binary solutions due to dissolved organic nitrogen in the industrial effluent. They also assessed the regenerative capacity of the adsorbent, which could be reused without a significant decrease in efficiency, thus demonstrating that the EDTA-β-system CD is qualified for practical applications in complementary treatments for toxic pollutants removal. Morin-Crini et al. [210] have assessed the abatement of a series of heavy metals, such as Cd, Co, Cu, Mn, Ni, and Zn in various effluents, previously treated with physiochemical methods, through an adsorbent system based on hemp modified with maltodextrin and cross-linked with 1,2,3,4- butantetracarboxylic acid. The modification of this raw material imparted in it many carboxylic groups on its surface. The concentration of the heavy metals present was reduced significantly: in 30 minutes, using 1 g of adsorbent. It was able to break down 16.3 mg of heavy metals contained in a liter of effluent, starting from an initial concentration of 19.6 mg of total metals. In these removal pollutants, play an important role the carboxylic groups in the structure, which are responsible for the bond with metal ions through electrostatic interactions and ion exchange. Also in another recent

study, a modified maltodextrin was used by grafting 2-acrylamide-2-methyl-1-propansulfonic acid, for the abatement of Ni (II), Fe (III) and Cd (II) ions in the aqueous environment. The percentages of abatement at pH 8 reached are 90%, 97.80% and 71.74% of nickel, iron and cadmium ions respectively. In addition, the assessment of the contact time showed that the abatement efficiency increased until equilibrium was reached after 30 minutes.[211]

7.6.1 Regeneration and reuse

From an economic and environmental point of view, a good adsorbent should have good reproducibility especially for current operations.[148] Stability and reuse are two fundamental properties of these adsorbents.[154] Cationic adsorbents tend to be regenerated using acid solutions of HNO_3, HCl or Na_2EDTA,[148][153][154] while anionic ones with basic solutions such as NaOH.[156] From the articles in the literature examined, the adsorbent systems used have been shown to have good reproducible properties. For example, the P-CDEC,[154] considers even more than 90% of contaminants after five cycles of reuse, as well as CD/CA-G-PDMAEMA;[153] EDTA-B-CD,[151] Instead, it shows a regeneration efficiency of over 95% for the first four cycles. The PVA-TA-βCD system has also demonstrated good reusability for four adsorption-desorption cycles, although with a slight decrease in removal when the number of cycles increases (from 131.25 to 122.08 mg/g for Pb (II), from 75.3 to 70.8 mg/g for Cd (II) and 53.88 to 45.78 mg/g for Mn (II)). In addition, it has been shown that desorption efficiency using EDTA for adsorbent regeneration is much higher when compared to eluents such as HNO_3 and HCl, as it forms stable complexes with metal ions. The percentage results obtained after re-use are: Pb (II) (98.52%), Cd (II) (95.86%) and Mn (II) (94.28%).[148]

7.6.2 Advantages and disadvantages of nanosponges

In conclusion it can be said that polysaccharide-based adsorbents and their derivatives, for the removal of pollutants, such as heavy metals in wastewater, are promising thanks to their following advantages:[122]

- are low cost and are obtained naturally;
- are biocompatible;
- their use is cost-effective. Crosslinked materials are easy to prepare with, even, the use of cheap reagents;
- the amount of adsorbent used is generally reduced compared to conventional ones, as polysaccharides are very efficient.
- These materials are versatile, because they can be used in different forms, such as insoluble particles, gels, nanosponges, capsules, films, membranes and fibers. In

addition, they have the advantage of being applied in a wide variety of processes and can be reused for multiple cycles;

- have high capacity and adsorption rate;
- cyclodextrin-based adsorbent materials have excellent and unique properties such as high surface area, good mechanical strength and high porosity.[133]

Unfortunately, still many of their applications are just on laboratory scale.[133]

7.7 Biochar: material and application

Among the potential materials of recent interest in water treatment, one of the most interesting is biochar. Biochar is a carbonaceous and porous material, very stable, deriving from pyrolysis, that is heating under nitrogen flow and non-oxidizing atmosphere, of biomass of plant and/or animal origin that finds applications in agriculture and in environment protection. Depending on the starting biomass and the temperature at which the pyrolysis is performed, biochar will be characterized by peculiar properties and potential for application in agriculture. From the environmental sustainability point of view, there are many remarkable aspects. The first one is the starting raw material that often corresponds to buy-products typically waste resulting from pruning. This means an application of a circular economy model. Biochar is also produced by heating biomasses at high temperatures, but in a very low oxygen atmosphere: this entails a negligible amount of CO_2 developed during its production. In addition, syngas a flammable gas and bio-oil, also a good fuel, are also produced. Biochar is a sustainable and environmentally friendly solution for the following reasons and applications:

- The increasing use of agricultural and forestry residues as a raw material for biochar production is due to their abundance and low cost. The total annual production of agricultural residues is estimated at 500 million tons, the conversion of this biomass into high value-added products can reduce the operating costs associated with the disposal of these abundant agricultural and forestry materials.
- increasing soil fertility by burying the biochar and thus reducing the use of synthetic fertilizers, with lower expenditure for farmers, lower impact on the environment, lower consumption of resources and energy; the agricultural biochar is used as a soil improver, not as manure;
- improve soil properties and fertility, decrease nutrient leaching and increase yields from many agricultural crops;
- managing agricultural crop residues, often considered more of a problem than a resource, avoiding their elimination by burning;

- underground biochar is different from burying simple carbonaceous residues resulting from the combustion of pruning waste, they in fact oxidize in the soil generate significant CO_2 emissions, vice versa by burying the biochar can subtract high amounts of this gas, it is estimated that by putting one ton of this material into the ground, 3 tons of CO_2 are subtracted from the atmosphere (since each ton of biochar is generated by an amount of atmospheric carbon dioxide equal to about three times its weight);
- the possibility of producing energy from renewable sources;
- recover degraded and fertility-free land and help reduce deforestation by improving energy efficiency;

Biochar can be used as an adsorbent of organic and inorganic contaminants, heavy metals and pesticides in soils, reducing percolation in groundwater and availability to uptake by plants. In recent years, studies about biochar, are focusing especially on the determination of its adsorbent capacities towards heavy metals, whether they are dissolved in solid matrices (soils) or aqueous. As far as our study is concerned, it aims to determine whether it is possible to obtain drinking water, from samples of water polluted by heavy metals, through the permanence of the aqueous sample, artificially contaminated, with a certain amount of biochar.[212]

7.7.1 Soil fertility increase by biochar

The introduction of carbon residues as ash rain deposits from frequent volcanic eruptions has shown a correlation with soil fertility. Analyses of this type of soil have revealed characteristics such as alkalinity, leaching resistance and high nutrient concentration, high presence of carbonaceous material, and based on crop studies, these soils were found to be much more fertile than the surrounding ones. The use of biochar in agriculture influences the porosity of the soil, the ability to retain water, density and resistance to penetration. According to numerous studies, therefore, the addition of biochar to the soil is an added value for the same, because it generates an increase in soil composition, better water retention, the growth of the percentage of nutrients in the soil and thus an increase in soil productivity. Studies in fields with biochar additions show significantly higher plant growth than untreated control media. Depending on the type of biomass used and the pyrolysis conditions, the biochar is found to have different concentrations of fertilizers (N, P and K); the biochar deriving from manure and sewage is particularly rich. It is not possible to use the biochar as a fertilizer, which is normally added to the soil annually, but can be understood as a reserve with a slow release of nutrients, that is, a soil improver. However, this phenomenon of land yields improvement by biochar is

still unclear and is still being studied. As regards its agricultural use, in Italy, Italian farmers, who will have to choose whether to use the biochar as a soil improver, must be aware that:

- there is no single type of biochar, but that the product is different depending on which biomass is used and the process used to obtain it;
- the legislation sets limits to any pollutants present within the biochar. It will then be the care of those who sell or produce their own biochar issue the certificates of analysis.

The body "char" has carefully analyzed the scientific literature produced so far on the subject, and states that the increase in agricultural production resulting from the use of biochar is estimated on average around 10%, percentage which may also be much higher for specific situations and crops [229].

7.7.2 Climate change mitigation

Another interesting use of the biochar is the stability of carbon within it. As explained above, the growth, felling and pyrolysis of biomass are steps that generate a decrease in atmospheric CO_2, then going to bury the biochar thus produced has a negative CO_2 balance: if added to the soil, it stores carbon in a stable way, so it reduces carbon dioxide emissions to the atmosphere. The plants absorb CO_2 to grow; once their life cycle is over, it returns to the atmosphere relatively quickly. Any form of organic matter that is decomposed or released into the soil is rapidly degraded, producing high CO_2 emissions which contributes to increasing the greenhouse effect. Biochar produced by the thermochemical process of pyrolysis plays a fundamental role: it transforms organic matter into a very stable form, more difficult to degrade, which can make a decisive contribution to reducing emissions. This technique is sustainable only if biomass is used to produce biochar that would otherwise have undergone decomposition or combustion, such as pruning, crop residues and municipal wet waste. Woolf et al. (2010) reports that the production and storage of biochar in soil can lead to a reduction of up to 12% of anthropogenic CO_2. To date, the UNFCCC, the United Nations Framework Convention on Climate Change Conference, notes that the average residence time of carbon stored in soil, through the biochar, is about 2,000 years, welcomed the inclusion of the biochar in the "Enhanced Action on Mitigation" section (June 2009, Bonn, Germany) as a new technology for climate mitigation and admitted the inclusion of the biochar in the Clean Development Mechanism (CDM) [230].

7.7.3 Energy use

One of the major benefits of biochar is the high energy density and specific weight, in addition to its hygroscopicity, which make it an easily transportable product. Its energy density is comparable to that of coal and can replace it 100% in the production of electricity or heat, with

simple plant adaptations. The EU is the world's largest consumer of pellets with 18.8 Mtons consumed in 2014 (+3% compared to 2013), of which 1/3 imported. Italy in turn is the strongest consumer in the EU. If it is not conceivable to replace directly imported pellets with residues (it would be like replacing 10-12% with water), according to EUBIA their carbonization would offer an interesting alternative [230].

7.7.4 Contaminants removal from soil and water

Biochar can be used as an adsorbent of organic and inorganic contaminants such as heavy metals and pesticides in soils, reducing percolation in groundwater and availability to uptake by plants. The high pH, the large surface area, the anionic and cationic exchange capacity, the hydrophobicity, and the negative surface charge are the properties that make this material a good adsorbent. These properties depend on the pyrolysis temperatures in biochar production, for example biochar produce at high temperatures are better for the absorption of organic contaminants. The ability to absorb pollutants is excellent for the treatment of contaminated soils because it avoids the spread of pollution, however it must be carefully evaluated its use because it can interfere and neutralize certain types of pesticides. It follows that, heavy metal pollution has become one of the most serious and serious environmental problems. A solution which could be very useful would be to find systems capable of breaking down such substances directly on site, for example by immobilizing them in materials capable of permanently adsorbing or binding such metals, without harming plants and their consumers. Biochar could be suitable for this purpose and as regards aqueous matrices, could be used for the treatment of wastewater and sludge. To date, studies performed on biochar from woody biomass are many, for example, in the book "Biochar for Environmental Management: Science and Technology (Lehmann, 2012)" are described production techniques, stability, physical and biological properties and different applications. Among the applications of the material in the environmental field, it is possible to find in literature excellent reviews about its ability to immobilize contaminants present in the soil, such as organic substances and metals, but some aspects such as the kinetics and thermodynamics of the phenomenon are still little known and complex to determine with precision, since multiple[231].

7.8 Biochar Features

The biochar's chemical-physical properties significantly influence its ability to absorb metals. Before exploring the mechanisms regulating the removal of metal from the biochar, its properties must be well characterized, including surface area, porosity, pH, surface charge, functional group and mineral content[232].

7.8.1 Surface area and porosity

Surface and porosity are the main physical properties that influence the absorption capacity of metals in the biochar. When biomass is transformed into biochar by pyrolysis, micropores are formed for water loss (dehydration process) [229]. Biochar pore size is very variable and includes nano- (<0.9 nm), micro- (<2 nm) and macro-holes (> 50 nm). The size of the pores is important for the absorption of metals, for example biochar with small pores cannot trap large ions, regardless of their charge or polarity[233]. Porosity and surface of biochar vary considerably with pyrolysis temperature. Studies show that a high temperature generally leads to larger pore sizes and thus to a larger surface area. As the temperature has risen from 500 to 900 °C, biochar porosity has increased from 0,056 to 0,099 cm^3/g, while the surface has increased from 25,4 to 67,6 m^2/g [234]. However, it should be noted that in some cases, at high temperature, the porous structure of biochar can be destroyed or blocked by tar, resulting in a reduction in surface area [232]. Lignin-rich biomass (such as bamboo and coconut) generally develops a biochar with a macro-porous structure, while cellulose-rich biomass (e.g. shells) produces a biochar with a predominantly microporous structure [235].

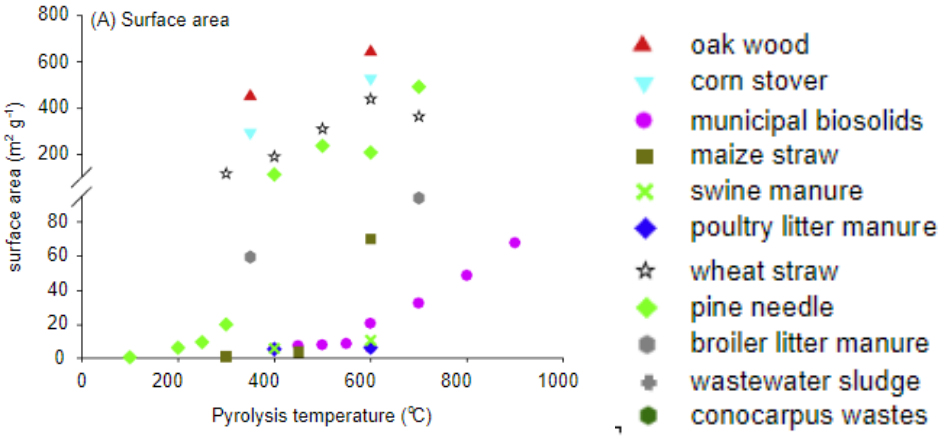

Figure 20: Surface area of different types of biochar, depending on the pyrolysis temperature.

7.8.2 Carbon and graphitic structure of biochar

One aspect to focus on is the appearance of graphitic structures partially ordered and containing sp^2 hybridized carbon atoms that occurs in some pyrolyzed woods over 900 °C. From literature data [236], a calculation of the sp^2 carbon content is reported: it is noted that it varies with the variation of the carbonization temperature with which different biochar samples were produced. In particular, the calculated sp^2 hybridized carbon content increases from 58.0 to 77.6 moles% when the carbonization temperature increases from 300 to 1000 °C and it can be noted two obvious transitions. The first transition occurs at 350 °C, an increase of 4,7 moles in the sp^2 carbon content caused by the degradation of carbohydrates, leading to an increase in

atomic and fixed carbon [237]. The second transition is between 400 and 500 °C, where the sp^2 carbon content increases by 4.2 moles. In this range, other biomass components are further degraded and the carbon fraction in the biochar increases [238].

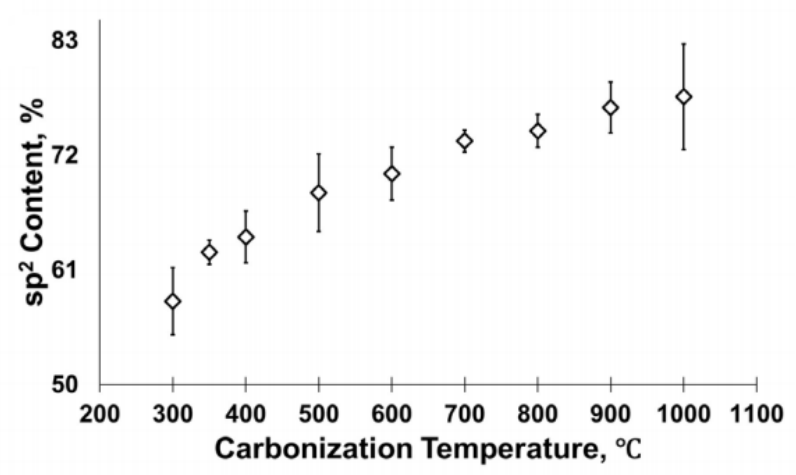

Figure 21: Content % of sp2 carbon in the biochar as a function of pyrolysis temperature.

Biochar crystalline structure has been studied by X-ray diffraction, EELS spectroscopy [239], EDS and XPS [240] [241] [242] SEM and TEM microscopy [243]; this has allowed to characterize quantitatively the behavior of the structure and chemical-physical characteristics of biochar during carbonization at different temperatures, to propose a schematic model about the material structural development [236]. This model is described in figure 23, where appear the different biochar phases that occur at pyrolysis temperatures between 350 and 1000 °C related to chemical and morphological changes during biomass carbonization at different temperatures. The nomenclature of the different phases derives from the model hypothesized by Keiluweit et al. [237] and the transition from one phase to the next is indicated by the increase in carbon content sp^2.

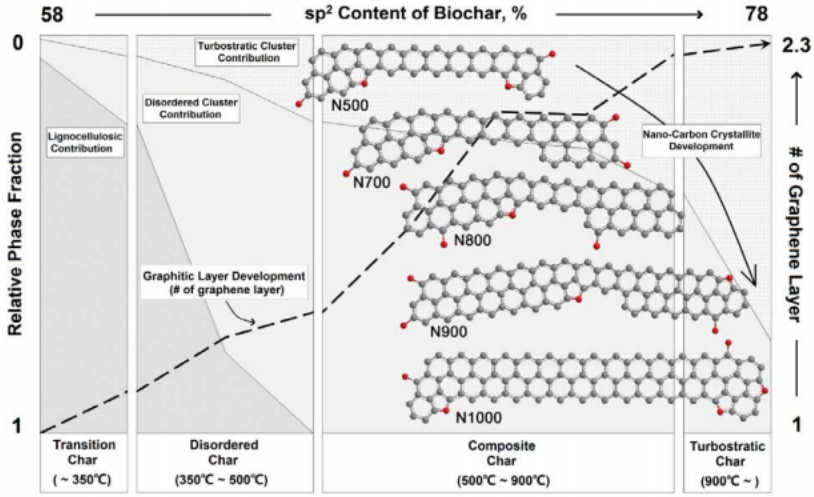

Figure 22: Appearance of phases with different structures and sp2 carbon content % in the biochar as a function of pyrolysis temperature.

Loblolly pine biochar at temperatures of about 350 °C biochar is called "Transition Char" and is composed of a high fraction of hydrogen, oxygen and volatile substances, crystalline structure consisting of cellulose, absence of graphite layers and little developed porosity. After 350 °C and up to 500 °C there is the "Disordered Char", that is a carbonaceous material with a disordered structure, with greater presence of micropores and sp^2 carbon content. Small carbon crystals begin to develop longitudinally. Between 500 and 900 °C is the phase of "Composite Char", in which the crystallites grow and the volume of the micropores reaches the maximum, and then decrease over 600 °C. The sp^2carbon content and the number of graphene layers increase. Finally, beyond the 900 °C is in the presence of the "Turbostratic char", characterized by a primitive graphic structure, not completely ordered, and absence of micropores. Finally, some images by STEM HAADF (High Angle Annular Dark Field) microscopy are shown, all with a magnification of 500 nm, on samples produced by pyrolysis at different temperatures (a-f: 300, 400, 500, 700, 800 and 900 °C) [236].

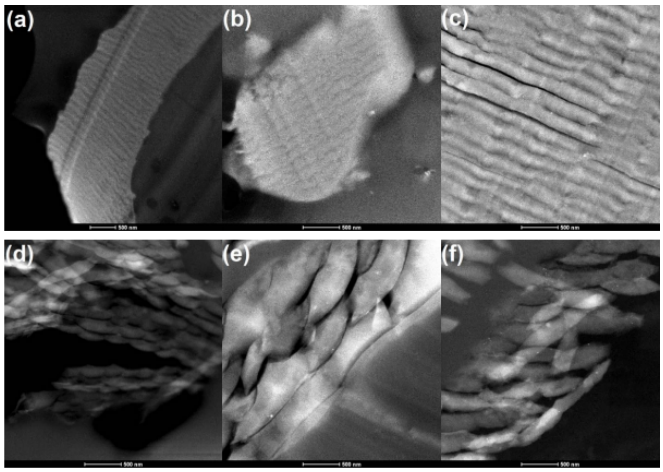

Figure 23: Pictures STEM HAADF biochar produced at different temperatures.

Samples at 300 and 400 °C (a and b) show a dense structure with parallel and repetitive lines consistent with the dense morphology from the original wood; the image (c), relating to the 500 °C pyrolyzed sample, shows the cleavage of the dense structure and the initial formation of primitive fibril-like structures, which appear clearly separated in the sample produced at 700 °C (d). In the last two images (e, f) the fibrils are clearly separated, small and show torsion. The presence of fibril-like structures suggests longitudinal growth of carbon crystallites [244], [245].

7.8.3 pH and surface charge

Like the surface area and porosity, the pH of biochar varies with the pyrolysis temperature and the raw material with which biochar is produced. Generally, biochar is alkaline, with some exceptions depending on the starting biomass, e.g., biochar produced from oak wood at 350 and 600 °C is acid. In any case, biochar's pH typically increases as the pyrolysis temperature increases; the rise in temperature leads to a higher ash content, which positively correlates with the biochar's pH, suggesting that the ashes are a factor that contributes to having a high pH biochar [232].

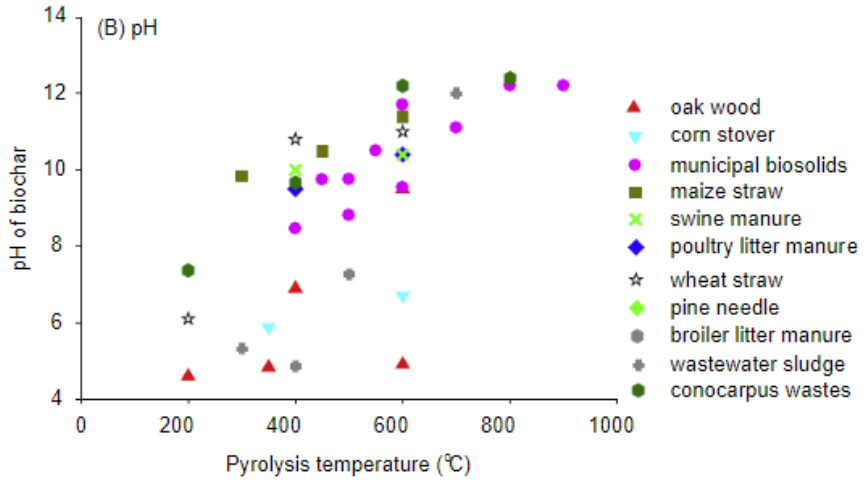

Figure 24: pH measured on different types of biochar, depending on the pyrolysis temperature.

As the temperature rises from 300 to 700 °C, the total cation and carbonate content in biochar is increased, resulting in an increase in pH [246]. In addition, the disappearance of acid functional groups such as carboxylic groups -COOH, at high temperature is another contribution. For example, with the increase in temperature from 200 to 800 °C, the basic functional groups on the surface of biochar produced by vegetable waste increased from 0.05 to 3.55 mm/g, while the acid functional groups decreased from 4,17 to 0,22 mm/g, in line with the pH increase from 7.37 to 12.4[247]. Another important feature that influences the absorption of metal by biochar is its surface charge. When biochar is applied for the removal of dissolved metals in water, the pH of the solution strongly influences its surface charge. Biochar's zero charge point (pHPZC) corresponds to the pH of the solution at which its net surface charge is zero. When the pH of the solution is greater than pHPZC, biochar is negatively charged and binds to metal cations such as Cd^{2+}, Pb^{2+} and Hg^{2+}. When the pH of the solution is lower than pHPZC, biochar is positively charged and binds metal anions such as $HAsO_4^{2-}$ and $HCrO_4^{-}$. As the temperature rises from 500 to 900 °C, biochar pHPZC is increased from 8,58 to 10,2 [234]. Some authors determined the zeta potential of biochar produced by rape, corn, soya, and peanut shells at 300, 500, and 700 °C. In solution at pH between 3 and 7, all biochar were found to be negatively charged. However, compared to the biochar produced at 300 and 500 °C, those produced at 700 °C are charged less negatively, implying an increase in pHPZC as the pyrolysis temperature increases [246]. Thus, at higher pyrolysis temperatures, the amounts of functional groups negatively charged on biochar (e.g. -COO-, -COH and -OH) are reduced, resulting in less negative surface charges and increased pHPZC[232].

7.8.4 Functional groups

Functional groups such as carboxylic, amine and hydroxyl groups play an important role in collection of metals. The pyrolysis temperature and biochar starting raw material are the two key factors that control the amounts of functional groups on its surface. However, unlike the surface area, porosity, pH, and pHPZC, the abundance of functional groups in biochar decreases as the temperature rises, mainly due to a higher degree of carbonization. As the temperature increases, the atomic ratios of H/C, O/C and N/C decrease, suggesting a decrease in the presence of hydroxyl, carboxylic and amino groups. Fourier Transform Infrared Spectroscopy (FTIR) spectra have been widely used to characterize functional groups on biochar surfaces. Biochar spectra, produced at different temperatures, are distinctly different. The FTIR spectrum of the grass biochar changes when the pyrolysis temperature is increased from 100 to 700 °C [237]. Compared to raw material biomass, no significant difference was observed in low-temperature FTIR spectra, ranging between 100 and 200 ºC, suggesting that there are no changes in functional groups. The dehydration of the cellulosic and ligneous components in biochar begins at 300 °C (3500-3200 cm^{-1}) while the transformation products derived from lignin and cellulose appears at 400°C in the form of multiple peaks at 1600-700 cm^{-1}. An increasing degree of condensation was observed at carbonization temperature >=500 °C (intensity loss at 1650-1500 cm^{-1} correlated to that at 885-752 cm^{-1}) [237]. During pyrolysis at increasing temperature, most functional groups of lignocellulosic materials are lost. Using FTIR spectroscopy, Yuan et al. [246] observed a reduced intensity of the peaks corresponding to carboxyl (-COOH) and hydroxyl (-OH) groups when the temperature increased from 300 to 700 °C in the rape biochar, corn, soy and peanut shells. In addition to the use of FTIR spectra, nuclear magnetic resonance (NMR) spectra were also used to characterize the functional groups of several biochar. Li et al. [232] studied the development of functional groups in straw biochar and rice bran produced at 100 and 800 °C using 2D NMR spectroscopy 13C.

The biochar of straw and rice bran has been subjected to processes of dihydroxylation/dehydrogenation and aromatization. In general, as the temperature increased, abnormal O-alkylated and O-C-O groups occurred before the production of aromatic structures. Biochar produced at temperature < 300 °C, had predominantly O-alkylated and aliphatic carbon atoms, which are generally lost in the biochar produced at temperatures > 300 °C, where they dominate aromatic structures. Similarly, based on NMR spectroscopy, Zhang et al.[234] observed a decrease in the contribution of O-alkyl carbon from 20-54% to 6,9 and 13% for wheat straw.

7.8.5 Mineral content

The mineral components including potassium (K), calcium (Ca), magnesium (Mg) and phosphorus (P) in biochar are also responsible for the absorption of metals from the water. They can exchange or precipitate together with heavy metals and thus reduce their availability. Cao et al. (2009) concluded that Pb phosphate precipitation was the main mechanism controlling the biochar's absorption of Pb from manure. It was then demonstrated that during the absorption of metal cations such as Cd^{2+}, Cu^{2+}, Ni^{2+} and Pb^{2+} through biochar obtained from guano, cations such as Ca^{2+}, Mg^{2+}, Na^{+} and K^{+} were released by biochar into the solution due to cation exchange phenomenon [248]. Temperature and biomass at which biochar was produced, control the amounts of mineral components in biochar itself. The total concentrations of K, Ca, Mg and P increase with the increased pyrolysis temperature in biochar generated by [249], manure [250], vegetable waste [251] and oak wood [252]. However, the water-soluble amounts of mineral components behave differently from their total concentrations. Generally, during the production of biochar, the amounts soluble in water of K, Ca, Mg and P increase if the heating is at 200 °C but decrease for higher temperatures. This is probably due to increased crystallization as demonstrated by whitlockite formation [$(Ca,Mg)_3(PO_4)_2$] or incorporation into the structure. In addition to temperature, starting raw material is also an important factor influencing the amounts of mineral components in biochar. For example, phosphorus in oak wood is very low [252], while biochar obtained from poultry guano and pig manure is generally rich in potassium[251].

Biochar features vary considerably, mainly of pyrolysis temperature and starting raw material. However, temperature may have opposite effects on biochar properties, leading to opposite effects on metal absorption. For example, high pyrolysis generally results in greater surface area, providing more sites for metal absorption. However, it reduces the number of functional groups, which can lead to a reduction in the absorption of metals. In addition, the impacts of biochar properties on metal absorption depend on the nature of the metal itself since different metals are absorbed through different mechanisms.

7.8.6 Heavy metal removal mechanism

Several mechanisms can play a role in controlling heavy metals removal from aqueous solutions by biochar, including precipitation, complexion, ion exchange, electrostatic interactions (chemisorption) and physisorption (Figure 26). Like active carbon, different biochar can have a high ability to abate metallic contaminants due to their surface heterogeneity, in addition, many biochar have been reported to have a high surface area with a well-distributed network of pores, including micropores (area < 2 nm), mesopores (2-50 nm) and macropores (>50 nm). Biochar with a high surface area and high pore volumes have a high affinity for metals because metal ions can be physically absorbed on the surface of the char and kept within the pores [231]. Many biochar have negatively charged surfaces and can interact positively with metals through electrostatic interactions. Functional groups with complexing action on the biochar can also interact with various metals to form complexes or precipitates, forming solid mineral phases. Figure 26 summarizes the mechanisms of immobilization of aqueous metallic species by various biochar [231].

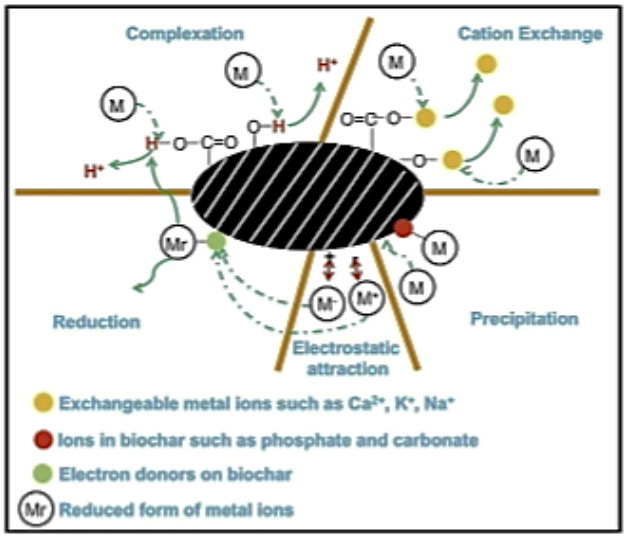

Figure 25: Abatement mechanism of biochar.

The mechanisms involved in the killing of metals are explained and described in more detail.

1. ***Physisorption***

Physical or surface absorption describes heavy metals removal by the diffusion of metal ions in pores without the formation of chemical bonds. For animal and plant biochar, the rise in carbonization temperatures (from 300 °C and above) will favor high surface areas and pore volumes. For example, pine wood biochar pyrolyzed around 700 °C can effectively remove aqueous uranium (U) and copper (Cu^{2+}) through a diffusive abatement process. Biochar produced at high pyrolysis temperatures tend to break down metal ions mainly through a physical abatement mechanism [231].

2. ***Ion exchange***

The removal of heavy metals through the exchange of protons/cations on the surface of biochar is another possible mechanism. The efficiency of the ion exchange process in retaining contaminants is closely related to the size of the metallic contaminant and the chemistry of the

surface functional group of the biochar. The ion exchange on biochar is happened by selective replacement of the cations on biochar surface with the metallic cations in solution as contaminants. Following the geochemical classification of Goldschmidt, most of the metallic species within groups 1-3 on the periodic table (e.g., Na, K, Ca, Li, Mg, Be and Sc) are more likely to be replaced or exchanged with other metallic elements within this group having similarities about their ionic rays, charge differences and bond characteristics. Several transition elements may also have a strong binding capacity for these trading sites. As for plant materials, cation exchange capacity (CEC) is mainly controlled by surface functional groups, so biochar with high CEC will have a good removal of heavy metals. In general, non-woody and grassy biochar with high oxygen content and acidic surface sites have higher CEC than biochar from woody plants with low oxygen content. The highest CEC levels were observed in plant biochar produced at 300 or 350 °C due to the higher carboxylic acid content on the surface. In contrast, low CEC values were observed at relatively high temperatures (>350 °C). Biochar from bones rich in these functional groups can also remove heavy metals such as cobalt (Co) from aqueous solutions through ion exchange mechanism. In conclusion, the removal of metal cations through an ion exchange mechanism is favored when biochar has been obtained by pyrolysis at low temperatures, since the carbonization temperature increases the number of active functional groups, as carboxylic, hydroxyl and amine groups present on biochar surface decreases. This phenomenon can be observed by comparing biochar FTIR spectra by pyrolysis at different temperatures. Cationic exchange and precipitation are the most implicated mechanisms in the abatement of metals such as lead and cadmium [231].

3. Electrostatic interaction

Electrostatic interaction between surface-loaded biochar and metal ions is another mechanism for immobilizing heavy metals. The prevalence of this mechanism in the biochar-metal absorption process depends on the pH of the solution and the zero-charge point (PZC) of biochar. The high temperatures (>400 °C) of carbonization also promote the formation of graphene-like structures within biochar that favor the abatement. A high retention of Pb in the grain and rice biochar was reported due to the attraction between positively charged Pb and negatively charged biochar. Electrostatic attractions were also reported for Cr(VI) and negatively charged biochar surfaces [231].

4. Complexation

Complexation involves the formation of multi-atomic (i.e., complex) structures with specific metal-binding interactions. This binding mechanism is important for metals, such as transition metals, with partially filled orbitals, which therefore show a high affinity for binders. It has

been shown that functional groups containing oxygen (carboxylic, phenolic and lactonic groups) present in biochar at low pyrolysis temperature, can bind effectively with heavy metals. It has also been demonstrated that the oxygen content in biochar significantly increases the phenomenon, probably due to the oxidation of its surface and the formation of carboxylic groups [253].The removal of contaminants by their complexation is more common among biochar of plant origin compared to biochar of animal origin. Plant char origin are easily bound with different heavy metals, as Cd^{2+}, Cu^{2+}, Ni^{2+} and Pb^{2+} by precipitation of phenolic and carboxylic metal complexes on biochar.

5. Precipitation

Precipitation is the formation of solids, in solution or on a surface and can occur during abatement processes. Precipitation has been commonly cited as one of the main mechanisms responsible for the immobilization of heavy metals by biochar. Metals and elements with an intermediate ionization potential between 2,5 and 9,5 (e.g., Cu, Zn, Ni, Pb) are more likely to precipitate on biochar surfaces than other elements. The thermal degradation of cellulose and hemicellulose in plant biomass at relatively high temperatures (>300 °C) often produces alkaline biochar [254]. When it's in solution, biochar can trigger the precipitation of metallic species. For example, a previous study showed that biochar with a pH of 10,93 was able to precipitate Pb by the formation of the compound [$(Pb_3(CO_3)_2(OH)_2$] on its surface [255]. In addition to biochar high pH, heavy metal precipitation can result from the reaction between metal ions and various mineral phases in both plant and animal raw materials. Animal and plant biochar produced at high temperatures have a high content of mineral substances with significant levels of calcium, magnesium, iron, copper and silicon. This is particularly true for biochar from animal waste, such as pollen biochar (45% mineral matter) [256]; and bone biochar (84% mineral matter) [257]. These mineral phases including, KCl, quartz (SiO_2), amorphous silica, calcite ($CaCO_3$), hydroxyapatite ($Ca_{10}PO_4)_6(OH)_2$) and calcium anhydrite ($CaSO_4$) exist in free forms or are intercalated within biochar carbon matrix. The soluble forms of these phases also exist in low-temperature biochar (200 °C) and may react directly with heavy metal species in solution to form insoluble metal precipitates such as pyrolite [$Pb_5(PO_4)_3Cl$]. Less soluble forms of these mineral phases exist at higher temperatures (350-600 °C), and they are more likely to be released slowly during the abatement reactions of heavy metals to form precipitates on the surfaces of biochar [255].

8 Aim of research

In view of direct and indirect environmental issue associated with pollutants, these substances in environmental and industrial field must be removed or treated. However, in most cases these are expensive methods or characterized by the inability to overcome the problem of subsequent disposal. Adsorption methods, which are particularly promising from the point of view of the efficiencies achieved and applicable in the context of all the pollutants mentioned, adsorbent material (usually a polymeric resin) even if regenerated, leads to high amounts accumulation of removed substance concentrates. These wastes should be disposed appropriately, which adds up to a positive contribution to costs. Even considering other more advanced, efficient methods, no one seems to have a large-scale implementation potential with acceptable costs. Given the general picture of the current state of water pollution, it is essential to find new opportunities for wastewater treatment that could be sustainable, but also low-cost.

Therefore, the aim of this research project is to assess the retention effectiveness of new adsorbent materials for water treatment that have low cost and could easily applied and re-use in industrial scale. This project shall be split in different section, each one dedicates to peculiar adsorbent material: *zeolite, anionic and cationic nanosponges and biochar*.

- ***Zeolite:*** the first part of the research aimed to assess the retention of ammonium ion (NH_4^+) in natural zeolite and the competition between NH_4^+ and other cations, mainly the potassium ion (K^+) ubiquitous in plant matter, to reduce the number of nitrogenous substances in the digestate and to comply with the limits imposed by Directive 91/676/EEC (also known as the Nitrates Directive). Knowing the composition of the digestate, the objective is to define the amount of zeolite to have a reduction of NH_4^+ ion of at least 60 %, which is within the regulatory parameters and allows the spreading of more digestate in the field. The digestate samples studied come from two cows' farms in the Cuneo area and two pig digestate supplied by a farm in Piacenza area, both areas known as the Nitrate Vulnerable Zone (ZVN), to have a greater representativeness of the realities on the studied territory. Pig digestate was tested specially to evaluate the potentiality of zeolite and its use in industrial scale. On the other hand, the company in Cuneo area processes the manure in an anaerobic digester; at the end of the anaerobic reaction the product is taken and spread on the fields, partly distributed to neighboring companies that have previously supplied the digester with waste material. The second farm, however, provides for the inclusion of animal manure in a first anaerobic digester in which it undergoes an initial digestion treatment. The partially digested product

passes into a second anaerobic reactor that further processes the company waste, to produce the maximum amount of methane (CH_4). At the exit from the second biodigester, there is a mechanical separator that divides the digestate into the solid and liquid fractions. The solid part is used as litter for animals while the liquid component is kept in a large tank from which it will be taken to be spread over the fields as fertilizer. Initially tests were carried out to study the competition of ammonium and potassium ions for the active sites of zeolites, varying the ratio of the two cations in solution. Subsequently, digestates were analyzed to define the composition and estimate the ammoniacal nitrogen content present. The effectiveness of ammonium culling has been assessed both on synthetic samples prepared in the laboratory and on real digestate samples. Finally, the kinetics of absorption of this cation on zeolite was verified and the release of ammonium in water was evaluated for both synthetic and real samples. The digestate tests were carried out on the liquid fraction as it has the highest concentration of ammoniacal nitrogen (about 2000-40000 mg/L), while on the solid part characterization tests were carried out with the aim of using it as compost. Subsequently, zeolite enriched with ammonium were reused in agriculture as slow-release fertilizers. To achieve this goal, enriched zeolite has been tested on the soilless cultivation of strawberries. The study compared different treatments (differentiated contributions of zeolites) with an untreated control thesis. On the plants belonging to the different theses, growth and production parameters have been detected, as well as parameters relating to the strawberries plant and fruit quality.

- ***Nanosponges:*** The second part of the research work carried out focused mainly on achieving new polymer-based nano-adsorbent materials (anionic and cationic nano-adsorbent), known as nanosponges, for the abatement of nitrates, phosphate, glyphosate, and heavy metals in wastewater, through green and environmentally friendly synthesis methods for a future scaling up. In this framework, a commercial maltodextrin, deriving from the partial hydrolysis of corn starch, (Glucidex 2®), crosslinked with 1,4-butyldimethyl ether (BDE, considered non-toxic), in a basic or simply aqueous environment, was used as raw material. Other crosslinker for anionic nanospongese were used, such as TTE e NGDE. Maltodextrins were chosen as low cost, water-soluble and more sustainable alternatives than conventional raw materials used in commercial ion exchange resins or other adsorbent materials. To make the adsorption capacity of pollutants more efficient, maltodextrin has been functionalized to obtain two types of nanosponges:

- anionic nanosponges: functionalize with DABCO and Choline Chloride for the introduction of ammonium quaternary group,
- cationic nanosponges: carrageenan-K or sultons (1,3-propylsutone and 1,4-butylsulton) for the inclusion of sulphate or sulphonic groups

  The nanosponges, thus obtained, were characterized by FTIR-ATR, TGA, potential-ζ, elemental analysis (CHNS), swelling tests and SEM. Subsequently, nanosponges were tested to assess their abatement effectiveness with nitrates, phosphate, glyphosate, heavy metals: Cr(VI), As(V), As(III) Cu, Cd, Cr (III), Pb, Ni, Zn, Al and Mn, evaluating their removal performance from solutions of 10 to 1000 mg/L.
- ***Biochar:*** The third part of this research work concerns the use of biochar obtained from residual biomass, for the abatement of heavy metals in wastewater. Biochar was produced in the laboratory from different wood waste matrices (spruce, corn cob, poplar sawdust mixed, hazelnut shells, cherry tree, acacia, elder, hazelnut wood, jube, plum, fig, walnut.) at different pyrolysis temperature (550 °C, 800 °C e 1100 °C). They were also two commercial samples such as commercial biochar and activated carbon. Then characterize FTIR-ATR, TGA, Elemental Analysis (CHNS), SEM, porosity and surface area using the BET isotherm. Biochar was tested to assess their abatement effectiveness with heavy metals: Cu, Cd, Cr (III), Pb, Ni, Zn, Al and Mn, evaluating their removal performance from solutions of 0,1 to 2 mg/L at different pH. The choice to change the pH between 1 and 6 was made to simulate different pH conditions of contaminated water. In addition, moving towards basic pH metals in solutions could precipitate, compromising the effectiveness of biochar. The results allowed to identify which essences and best pyrolysis conditions will get the most performing biochar for metal abatement.

9 Material and Methods

9.1 Zeolite

9.1.1 Screening and evaluation tests with standard solutions

There are different types of zeolites that can potentially be used for the absorption of nitrogen in ammoniacal form. Screening tests were performed to understand which zeolite will have the greatest efficiency and most suitable features. After all these tests, the best type of zeolite was chosen. It was also evaluated, as an alternative to the batch, a continuous system to have an efficiency comparison between them. Therefore, abatement tests were carried out by placing the zeolite in a column and making it pass through the solution to be purified from the high ammonium amount. The purpose of this method is to:

1. Determine the zeolite abatement capacity
2. Evaluate the possibility of using zeolites as a continuous system to apply in industrial scale.

A column with 10 g of zeolite and a 1000 mg/l standard solution of ammonium nitrate were used, keeping the tap always open. To understand the adsorption of ammoniacal nitrogen by zeolite, kinetic on both column and in batch system was performed. To settle the problem of column clogging that drastically reduces the flow and much longer abatement times, a percolation system was tried. Adopting a system with percolation involves a recycling of the solution on the fixed zeolite bed. In this way the problem the system is energetically less expensive. A ring support supports a strainer capable of retaining 20 grams of zeolite and the solution is taken from the capsule by a peristaltic pump and poured onto the fixed zeolite bed and back into the capsule. Finally, a conductometer was also used to get an indication of adsorption range, as the zeolite releases sodium ions to incorporate ammonium ions and the conductivity of the solution inevitably undergoes a change. Given the good functioning of the percolation system, to evaluate the exchange capacity the zeolite is brought to exhaustion continuing to renew the

Figure 26: Lab percolation system.

solution with which it comes into contact. In this way it is possible to determine the maximum amount of ammonium retained by the zeolite.

9.1.2 Matrices tested

To assess the real zeolite holding capacity, digestate samples were tested. Initially, to evaluate the potentiality of zeolite and how it can be used for research purposes, tests were carried out on two samples of pig digestate from the same holding in Piacenza area. The sample will then be defined as "Digestate 0". This digestate has a very important liquid fraction (80% liquid fraction, 20% solid fraction). The digestate has been obtained by inserting into the digester about 70% pig manure and 30% by inserting maize silage and agricultural waste of various kinds. The Digestate 0 was sampled at the mouth of the first digester tank. On "Digestate 0" sample subsequent tests were conducted for the industrial scale plant. The digestate was sampled by taking it directly from the reactor outlet tank, following mixing, and was placed in a closed 20 L plastic tank, transported to the laboratory, and maintained at room temperature. The digestates on which the abatement tests and competitions with other ions in solution were carried out come from two farms located in Cuneo area. The sample subsequently defined as "Digestate 1" comes from a herd of Piedmonts beef cows and was obtained by inserting into the digester about 70 % maize silage and about 30 % manure, with small amounts of poultry manure. This sample is presented as a mixture of liquid substance within the solid substance is clearly observed, consisting mainly of the unprocessed matter from anaerobic bacteria. The digestate was sampled by taking it directly from the reactor outlet tank, following mixing, and was placed in a closed 5 L plastic tank, transported to the laboratory, and maintained at room temperature. The samples hereinafter referred to as "Digestate 2.0", "Digestate 2.1" and "Digestate 2 solid" come from a dairy herd. The anaerobic digester from which these samples arrived was fed with maize silage, alfalfa silage, triticale, and manure, in varying proportions depending on the season. The distinction in the name of the samples is due to the stage of the process in which they were taken: "Digestate 2.0" was sampled at the passage of the digestate from the first digestion tank to the second and is presented as a liquid with a high percentage of solid substance. The samples "Digestate 2.1" and "Digestate 2 solid", were taken at the exit of the second anaerobic digester at the end of which there is a physical separator that divides the solid part (which will be used as litter in the barn or fertilizer for organic small fruit crops) from the liquid part (which will be spread in the fields as fertilizer). "Digestate 2.1" corresponds to the liquid fraction while the "Digestate 2 dry" is the solid part. The sample called "Digestate 2.0" was taken through a tap placed at the passage of the semi-treated product leaving the first

biodigester and at the entrance of the second, inserted in a 5 L plastic container and kept at room temperature in the laboratory. As for the "Digestate 2.1" this was sampled from the outlet of the mechanical separator, inserted in a plastic tank of 5 L and kept at room temperature. The sample "Digestate 2 solid" was taken at the exit from the separator and placed in a plastic bag, stored at room temperature.

9.1.3 Reagents

The analytical grade reagents used in the analyses are listed below:

Table 8: Reagents for zeolite experiments.

Substance	Brand
Ammonium Chloride (NH_4Cl)	Sigma-Aldrich
Ammonium Carbonate ($(NH_4)_2CO_3$)	Sigma-Aldrich
Sodium Hydroxide (NaOH) in tablets	Sigma-Aldrich
Sulfuric Acid (H_2SO_4) 0,1 N	Merck
Sulfuric Acid (H_2SO_4) 2 N	Merck
Boric Acid (H_3BO_3)	Merck
Potassium Chloride (KCl)	Sigma-Aldrich
Sodium Chloride (NaCl)	Sigma-Aldrich
Calcium Nitrate tetrahydrate ($Ca(NO_3)_2 \cdot 4\ H_2O$)	Sigma-Aldrich
Nitric Acid (HNO_3) 69 %	Merck
Sodium Nitroprussiate ($Na_2Fe(CN)_5NO{\cdot}2H_2O$)	Sigma-Aldrich
Sodium Salicylate (HOC_6H_4COONa)	Merck
Sodium Dichloroisocyanate ($C_3Cl_2N_3NaO_3$)	Sigma-Aldrich
Trisodium Citrate dihydrate ($Na_3C_6H_5O_7{\cdot}2H_2O$)	Sigma-Aldrich

Devarda alloy, a metal alloy consisting of 50 % copper (Cu), 45 % aluminum (Al) and 5 % zinc (Zn) was used as reagent.

9.1.4 Zeolite used

Different types of zeolites were tested initializing and the composition varies from zeolite to zeolite (chabasite, clinoptilolite and philpsite). A zeolitite from the Campania region (around the slopes of Vesuvius) was also tested. The zeolite with the best characteristics and used in this work is from a mine located in Bulgaria.

The composition of the mineral is mainly clinoptilolite, with small percentages of cristobalite and tridimite as can be seen from the Table 9:

Table 9: Zeolite features.

Clinoptilolite	Cristobalite	Tridimite	Chemical formula	CAS Number
90-95%	0-5%	0-5%	(Ca_2, K_2, Na_2, Mg)4Al8Si40O96·24 H2O	12173-10-3

Chemical composition %		Physical features			
SiO_2	**65-72 %**	**Oil Absorption Capacity**	57 %	**Microporous Area**	11 m2/g
Al_2O_3	**10-12 %**	**Water Absorption Capacity**	42-50 %	**Mesoporous Area**	29 m2/g
CaO	**2.4-3.7 %**	**Pore Effective Diameter**	87	**Softening point**	1150 °C
K_2O	**2.5-3.8 %**	**Solubility**	4 Å	**Fusion point**	1300°C
Fe_2O_3	**0.7-1.9 %**	**Abrasion**	None	**Apparent density**	0.6-0.8 g/cm3
MgO	**0.9-1.2 %**	**Plasticity**	Minor	**Real density**	2.2-2.4 g/cm3
Na_2O	**0.1-0.5 %**	**Plasticity**	Minor	**Real density**	2.2-2.4 g/cm3
MnO	**0-0.008 %**				
Cr_2O_3	**0-0.01 %**				
P_2O_5	**0.02-0.03 %**				
SiO_2/Al_2O_3	**5.4-7.2 %**				

Minerals have been washed with deionized water at least twice to remove any powdery residues before use. After several testes, the size of zeolite chose for the experiments was between 2 and 3 mm.

9.1.5 Apparatus used:

1. Kjeldahl distillation apparatus

- 250 ml round-bottomed flask with three-way coupling;
- The flowmeter for the bubbling of N_2 in the solution;
- Dripper funnel for the introduction of NaOH solution;
- Refrigerant tube;
- Hot plate (Falc brand);
- Becher;
- Burette class A.

2. Apparatus used for retention and release of NH_4^+

- Autoclavable borosilicate glass bottles with screw cap by Schott (100-1000 ml);
- Horizontal stirrer VDRL mod. 711.
- Roller stirrer.

3. *Digestate composition determination apparatus*

- Falc hot plate.
- Memmert 854 stove.
- Muffle (Cavallero).
- Ceramic and graphite crucibles.
- Perkin Elmer's ICP-OES Optima 7000 DV.

4. *Apparatus for the adsorption and release kinetics*

- Autoclavable borosilicate glass bottles with screw cap by Schott (100-1000 ml).
- 1-5 ml graduated pipettes.
- 20-1000 µl micropipettes
- Jasco V-550 UV-visible spectrophotometer.
- peristaltic pump.

5. *Apparatus for digestate pre-treatment*

Figure 27: Hermler Z380 centrifuge.

Initially the digests were filtered on filter paper to obtain the liquid phase to be analyzed later. Since the separation time is very long and the quantity obtained is small, the digesters have been subjected to centrifugation to separate the two phases. Four falcon tubes (50 ml) were filled and centrifugated at a rate of 3600 rpm for at least two cycles for at least two minutes to ensure complete phase separation. The centrifuge used is a Hermler Z 380.

6. *Kjeldahl Distillation*

Figure 28: Kjeldahl apparatus.

The distillation of Kjeldahl is carried out to determine the ammoniacal nitrogen in samples by distillation in a basic environment. The principle is based on the displacement of NH_3 by an excess of NaOH, followed by distillation and fixation of NH_3 in a known volume of H_3BO_3, subsequently titrated with H_2SO_4 at a known concentration. The diagram of how the Kjeldahl distillation apparatus is mounted is shown in Figure 28.

Within the flask, a known volume of the test sample is inserted, and deionized water is added for a final volume of about 100 ml. Water will be needed during boiling of the solution to prevent it from going dry. At the outlet of the refrigerant, a known volume of H_3BO_3 solution with mixed indicator methyl red - bromocresol green is introduced into the beaker, which has a red coloration. Ensure that the lower end of the coolant outlet is below the surface of the solution to prevent possible NH_3 leakage. The distillation apparatus is set up, a known volume of 30 % NaOH is introduced into the flask (needed to have the sample analyzed in an alkaline medium and then the ammoniacal nitrogen balance shifted to NH_3), N_2 is flushed into the flask to maintain the right pressure and the warm-up begins. Once the boiling has started, approximately 35-40 minutes are calculated for the whole NH_3 to be released. The formation of the NH_3 is visible from the change of color of the solution placed at the end of the refrigerant that assumes a blue-green color. After the distillation, it is washed with some deionized water inside and the end at the outlet from the coolant that has remained in contact with the solution of the beaker. Titrate this solution with H_2SO_4 at a known concentration, observing a green to grey to pink change, indicative of reaching the equivalent point. The titration reaction involved is as follows:

$$2\ (NH_4)H_2BO_3 + H_2SO_4 \rightarrow (NH_4)_2SO_4 + 2\ H_3BO_3$$

The distillation of Kjeldahl is also useful for determining the total nitrogen content in the sample (ammoniacal, nitrite and nitrate). The latter is subjected to a preliminary reduction of nitrite and nitrate to ammonia. The reduction is achieved by adding the Devarda alloy to the sample before distillation. At the end of the reduction reaction, Kjeldahl distillation is carried out as described above and subsequently titrated with H_2SO_4.

9.1.6 Study of ammonium competition with major competitors in zeolite uptake

Initially, tests were carried out to study the competition for zeolite cavities by the cations potentially present in the digestates.

Since the main competitor of NH_4^+ is K^+, solutions with a fixed concentration (0.1 N) of $(NH_4)_2CO_3$ and a variable concentration of KCl are produced. Concentration of KCl in solution is progressively increased from 0 to 100 % in concentration compared to the carbonate content. These solutions are put in contact with about 5 g of zeolite in autoclavable glass bottles with screw cap, placed on a horizontal stirrer and left to agitate for 24 h. Then, Kjeldahl is distilled in duplicate for each sample titrated with H_2SO_4 0,1 N.

Further investigations were carried out to verify the incidence of other cations on the adsorption of NH_4^+ by zeolite. Mixtures of salts of NH_4^+, K^+, Na^+ and Ca^{2+} have been made at known concentrations and put in contact with about 5 g of zeolite each. The samples were subjected to the same procedure as described above. ICP-OES analysis of samples containing different concentrations of K^+ and fixed NH_4^+ was performed to assess the retention of K^+ in zeolite and to determine the maximum free volume per gram of zeolite. Zeolite KCl-Treated and $(NH_4)_2CO_3$ solutions on which ICP-OES analysis is carried out were mineralized prior to analysis. The mineralization takes place by placing these solutions in the beaker on a hot plate and adding a few drops of concentrated HNO_3; then the solutions obtained are diluted.

9.1.7 Digestate composition determination

The pH, the ammoniacal nitrogen content and the amount of alkali and alkaline earth metals were determined for each digestate. The pH has been identified using litmus paper and pHmeter. For the determination of ammoniacal nitrogen distillation of Kjeldahl was used while the remaining cations were observed following mineralization and ICP-OES analysis of the liquid part of the digestates.

9.1.8 NH_4^+ abatement by zeolite in digestate samples

Tests were carried out to reduce the ammoniacal nitrogen contained in the liquid phase of the digestate using zeolites. The re-adoption of the same three system (batch, column and percolation) to the liquid fraction of the digestate instead of the standard ammonium nitrate solution was performed. Initially a known volume of sample was contact with 5 g zeolite to observe the maximum amount of NH_4^+ retained by the mineral. As a result of the results obtained, the amount of zeolite was increased, leaving unchanged the volume of digestate taken, to increase the percentage of ammoniacal nitrogen retained to a target of 60 %.

The digestate samples were brought into contact with the zeolites and placed in autoclavable glass bottles with a screw cap on a horizontal stirrer and placed under constant agitation for 24 h. Subsequently the distillation of Kjeldahl was carried out to verify the amount of ammoniacal nitrogen remaining in solution. After those tests, the percolation system was reused and has shown greater results than other system. Therefore, design a pilot plant was required to treat more digestate volume. To this end two 20-liter tanks were used containing a fixed bed consisting of zeolite in a mesh basket (with meshes enough fine to hold it). The reactor was equipped with an outlet hole, located in the lower part, connected to a pump by a rubber tube. The pump extracts the solution from the reactor and recirculates making it fall back from the top into the tank. In this way, the solution was forced to cross the zeolite bed in the basket several times, carrying out a continuous process. The focus is to make zeolite interact with the digestate solution at maximum ammonium concentration. Only after reaching the optimum abatement equilibrium the digestate will be transferred into the second reactor to complete the ammonium detention.

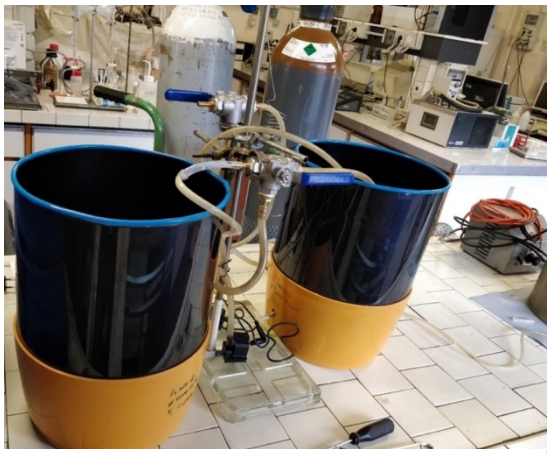

Figure 29: Lab pilot plant for digestate treatment.

During the entire process, regular analytical controls were carried out by sampling at regular intervals and monitoring the NH_4^+ concentration according to the Kjeldahl distillation method.

9.1.9 Detection of alkali and alkaline earth metals in solid matter

The solid part was gotten by digestates 1 and 2.1 centrifugation, to separate the solid part from the liquid one. The elimination of the remaining liquid part was done by evaporation in the oven at 120 °C for 2 h. In addition, the sample "Digestate 2 solid" was analyzed: a certain amount of known material has been taken and transferred to the stove at 120 ºC for one night to ensure complete removal of moisture. A quantitative transfer of the dry matter of each sample was carried out into the crucible, previously brought to constancy of weight, and the crucibles were introduced into the muffle at 550 °C for one night. The ash obtained was diluted with deionized water and treated with concentrated HNO_3 to ensure complete separation of carbonates, with the addition of further deionized and filtered water on quantitative filter paper (produced by Schleicher & Schüll, pore diameter 110 mm). The filtered part was analyzed at the ICP-OES to detect the presence of the Na, K, Ca and Mg cations. The bottom body retained by the filter, together with the filter, was introduced into the crucible and placed in the stove at

120 ºC throughout the night. Subsequently, the crucibles containing the ash were weighed and the amount of $LiBO_2$ needed for melting was assessed based on the estimated mass of the SiO_2 present. Inside the graphite crucibles $LiBO_2$ was transferred and above it was placed the ashes obtained previously. The samples were placed in a muffle preheated to 900 °C for half an hour during which the 5 % HNO_3 solution was prepared. At the end, the pearl formed was transferred to the 5 % HNO_3 acid solution, agitated and filtered on filter paper. The filtrate is made up to the volume with deionized water in the flask and analyzed at the ICP-OES for Fe and Si.

9.1.10 Adsorption kinetics

Figure 30: Ammonium standards at different concentrations.

The method used to establish absorption kinetics is the indophenol spectrophotometric method. This procedure is based on the reaction of ammonia with sodium salicylate and chlorine in a basic environment that forms a derivative of indophenol, easily observable by adding sodium nitro prussiate which acts as a catalyst coloring the blue-green solution. The wavelength corresponding to the formed compound can be measured at 690 nm.

The analysis initially involves building a calibration line. This is achieved by using NH_4Cl solutions as a reference standard at known concentrations, varying between 0 and 2 ppm, defined by the initial ammonium concentration data in digestate samples. After adding the necessary reagents, it is necessary to wait 4 h before carrying out the absorbance measurements, keeping the standards at a temperature of 20-22 ºC, and it is possible to carry out the measurements within 24 h. The absorbance is read by setting a wavelength range between 600 and 700 nm. For the retention tests of NH_4^+ in zeolite, an initial test is carried out using a solution of $(NH_4)_2CO_3$ 0,1 N. The percolation method is used for this purpose: a known volume of the solution is introduced into a porcelain capsule, placed on top of it a strainer containing 5 g of zeolite and plastic tubes suction the solution from the porcelain capsule and make it fall on the zeolite thanks to the presence of a peristaltic pump. The time and volume of the samples to be taken are determined. The volumes taken shall be added to the reagents of the and the absorbance shall be measured at 690 nm after waiting for a minimum of 4 h. Color variations in the samples determined by the different concentration shall be clearly observed with the naked eye the indophenol derivative in solution. In Figure 30, the color variations corresponding to different concentrations of NH_4^+ in solution can be appreciated. Analysis of

the uptake kinetics was carried out on the "Digestate 1" and "Digestate 2.1" samples, which are spread over the soil and are therefore of greater interest for the determination of retention. The samples were treated as described in the previous process, each previously undergoing a centrifugation at 3600 rpm for 10 minutes for 2 times to work only on the liquid part of the digestate. Known volumes were taken at defined times and the uptake kinetics curve was build.

9.1.11 Water release content and nitrate content

For the release tests, 100 g of zeolite was introduced into a 1 L borosilicate glass bottle, to which 500 ml of NH_4Cl 1000 mg/L solution was added. The bottle was placed on a horizontal shaker and left shaking for one day. The liquid fraction was then separated from zeolite by filtration. The liquid part was analyzed by Kjeldahl distillation to verify the amount of NH_4^+ remaining in solution, while zeolite was added an additional 500 ml volume of NH_4Cl 1000 mg/L solution and re-stirred in a glass bottle for one day. At the end, filtration of the solution and distillation of Kjeldahl was carried out with the same objective described above. At 50 g of NH_4Cl-treated zeolite, 500 ml of deionized water were added, placed in a 1 L borosilicate glass bottle and placed on a horizontal stirrer. Samples were taken at predetermined intervals to be analyzed with the Ammonium Test 2.0-150 mg/L NH_4-N kit (Merck) to verify the release kinetics of the NH_4^+ ion by zeolite. For this analysis it is appropriate to construct a calibration line which has been obtained with standards at known concentration of NH_4Cl with concentrations between 5 and 100 mg/L.

The test involves introducing into a glass tube 5 ml of "reagent 1", 0,1 ml of the standard (or sample) and shaking, adding a spatula tip of "reagent 2" and shaking again. After a waiting time of 15 minutes for the completion of the reaction, the spectrophotometer analysis was carried out at a wavelength of 690 nm, corresponding to the maximum absorption of the formed compound. The water release kinetics of the NH_4^+ ion has also been evaluated for other zeolites previously ammonium enriched.

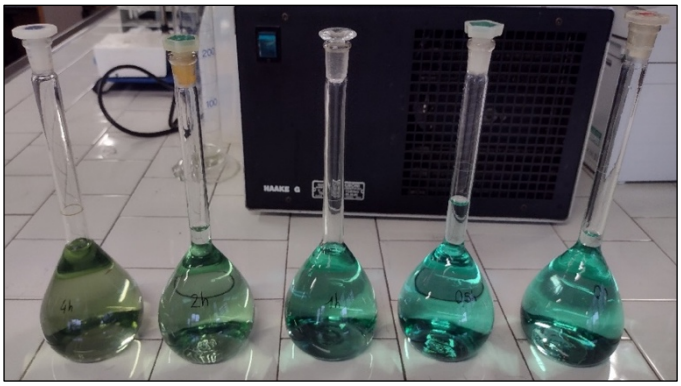

Figure 31: Digestate samples for spectrophotometric analysis.

Table 10: Zeolite sample amount for NH4+ analysis.

SAMPLE	ZEOLITE
NH_4Cl	50 g
Digestate 1.0	10 g
Digestate 2.1	15 g
Digestate 2.1	20 g
K:NH_4 = 1:5	5 g
K:NH_4 = 1:9	5 g

The ammonium-rich zeolite samples were placed in borosilicate glass bottles and placed in contact with known volumes of distilled water on a horizontal stirrer. Aliquots were taken at defined times to assess the kinetics of NH_4^+ ion release to water. Tests were also carried out to verify the possible formation of nitrates in solution. For this purpose, it is necessary to build a calibration line using standards with a known concentration between 1 and 20 mg/L of KNO_3. The test used for nitrate testing is the Merck Nitrate Test Kit 109713 0.10-25.0 mg/L NO_3-N. The analysis involves introducing into a glass tube 4 ml of "reagent 1", 0,50 ml of standard (or sample), 0,50 ml of "reagent 2" and shaking at the end of the operations by holding the tube from above since the reaction is exothermic. At the end of the 10-minute wait for completion of the reaction, spectrophotometric analysis shall be performed in a wavelength range of 300 to 400 nm, at 345 nm the absorption peak being detected. The kinetics of NO_3^- ion release into water has also been evaluated.

Table 11: Zeolite samples amount for NO3- analysis.

SAMPLE	ZEOLITE
NH_4Cl	50 g
Digestate 1.0	10 g
Digestate 2.1	15 g
Digestate 2.1	20 g

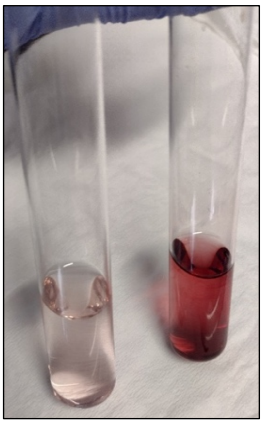

Figure 32: Samples for nitrates analysis.

Enriched zeolite samples were placed in borosilicate glass bottles and placed in contact with known volumes of distilled water on a horizontal stirrer. Aliquots were taken at defined times to assess the water release kinetics of the ion NO_3^-. A sample portion of "Digestate 1.0" and "Digestate 2.1" was treated to quantify the total nitrogen content present. For each sample 5 ml were taken and placed in a round-bottomed flask with three-way coupling of the Kjeldahl distillation system, with about 70 ml of distilled water, ¼ Devarda alloy spatula, about 30 ml of NaOH at 30 % and 5 ml of 96 % ethanol. The ethanol introduced serves to limit

the foaming and the passage of this foam to the coolant placed at the end of the system. The apparatus is closed, and it is expected that the reduction of NO_3^- to NH_4^+ at room temperature by the Devarda alloy will take place. During the reaction the formation of a grey foam and the development of bubbles in the beaker at the end of the coolant due to the formation of NH_3 is observed thanks to the presence of the Zn that produces H which is responsible for the reduction reaction. At the end the flask is heated and Kjeldahl is distilled as described above. A Kjeldahl distillation of the samples "Distillate 1.0" and "Distillate 2.1" was carried out several months after sampling to verify the amount of NH_4^+ still present in solution. In addition, the pH of the two digested was verified.

Table 12: pH values of digestate samples.

SAMPLE	pH
Digestate 0	8,5
Digestate 1.0	7
Digestate 2.1	8

For samples "K:NH_4 = 1:5" and "K:NH_4 = 1:9" the release of K^+ over time has been evaluated. The previously charged zeolites were placed in borosilicate glass bottles and placed in contact with known volumes of deionized water. The container has been inserted on a horizontal stirrer and at predefined intervals the samples have been taken. Subsequently, the samples were diluted and analyzed at the ICP-OES for release kinetics.

9.2 Culture Substrate for strawberries growing

The chosen culture substrate was a commercial horticultural compost mix (Domotorf). The substrate was a mix of fine blond, brown peat and bark humus, enriched with fulvic acids and organic substances that improve the soil structure. The chemical–physical features are as follows: Total organic carbon: 30% peat = 50% w/w, Humic + fulvic acids: 7% w/w, total N: 13% w/w, Cu (ppm) = 150, Zn (ppm) = 500; pH (in H_2O) = 6.5–7.5, Electric conductivity (dS/m) = 0.4, apparent dry density (Kg/m^3) = 180, total porosity = (% v/v) = 87.

9.3 Strawberry Planting and Treatments

The study was conducted on a commercial variety of strawberry plants (cv Clery). Each plant was transplanted into a 10 L volume plastic pot containing the different cultural substrate. A total of four treatments (9 pots each) were evaluated:

1. **zeolite**: cultural substrate (600 g) + 280 g of enriched zeolite
2. **zeolite + 30%:** cultural substrate (600 g) + 360 g of enriched zeolite

3. **zeolite − 30%:** cultural substrate (600 g) + 200 g of enriched zeolite
4. **control**: cultural substrate (600 g), not fertilized (no zeolites were added).

The nitric and ammonium nitrogen content of the compost was measured at the start of the trial. Charged zeolites, enriched with 4% ammonium, were introduced into the pots and mixed with the cultural substrate. The zeolite amounts were chosen based on previous work and set to optimal N concentration in the growth medium for strawberry [213]. After the transplant, water was supplied with a drop-by-drop automatic system (0.5 L/day) until the plants were well-developed. Thereafter, water was supplied by drip irrigation (one dripper per pot) at a frequency adapted to the climatic demand (approximately 0.5 L four times a week). All the pots were placed in an open field under shade cloth. The cultivation cycle was of 8 weeks. No fertilizers or pesticides were added.

9.4 Analyses of Strawberry Plants

Several parameters related to plant growth were measured and recorded as follows:

(i) plant weight, at the beginning and end of the production cycle (g),
(ii) flower count per plant,
(iii) leaf length (cm)
(iv) leaf count per plant
(v) stolon count per plant,
(vi) fruit count per plant,
(vii) fruit weight (g),
(viii) leaf chlorophyll content (SPAD content),
(ix) upper side leaf color (L*, C*).

At the end of the production cycle, the strawberry plants were removed with a shovel to prevent damage to the root system. Any substrate stuck to the roots was carefully removed. The plants were transferred to the laboratory, where they were washed and dried. Leaf chlorophyll content (SPAD index) was measured nondestructively with a portable SPAD-500 chlorophyll meter (Konica Minolta Sensing Inc., Osaka, Japan). Relative values displayed by the instrument were positively correlated with chlorophyll concentration. The SPAD-values were recorded from five leaves on each plant. Leaf color was measured with a colorimeter (Model CR-400, Minolta, Osaka, Japan) and expressed according to the CIELAB scale (L* a* b*). The L*, a*, and b* values indicate lightness (dark to light), index of redness (green (−) to red (+)) and index of yellowness (blue (−) to yellow (+)), respectively. The dimensions of color Chroma (C = (a*2 + b*2)1/2) were calculated from the numerical values of a* and b*v[214]. Chroma shows the

radial component of the cylindrical coordinate of the L*a*b* color system and represents color intensity. All the parameters, except plant weight, were evaluated weekly for the first three weeks, and then again at the end of the cycle (after 60 days).

9.5 Analyses of Fruit

All the strawberries from each treatment plot were picked when about 90% of their surface was red. All the strawberries were hand-picked during the cycle. The first red strawberries were picked after 2 weeks, the last after 8 weeks. A daily log of the number of strawberries picked was made. Freshly picked, strawberries were weighed, put in a closing envelope, immediately frozen and then transported to the lab. Later, analyses were performed in the lab after defrosting the strawberries. Three chemical parameters were measured: total soluble solids content (TSS), titratable acidity (TA), and total polyphenols. TSS (◦Brix) was measured with a digital refractometer (ATAGO Co., Ltd., Tokyo Japan). TA was determined by titrating 0.1 NaOH to a pH 8.1 with an automatic titrator (Compact 44–00; Crison Instruments, Barcelona, Spain); the results were expressed as milliequivalents of 0.1 mol NaOH per liter [215]. Finally, the total concentration of phenols was estimated by a slightly modified Folin-Ciocalteu method [216], [217]. In a vessel, five g of the pulp was extracted with MeOH after 30 min in an ultrasonic bath and filtered. Then, 0.05 mL of the extract and 0.45 mL distilled water were mixed with 2.5 mL of Folin–Ciocalteu's phenol reagent (1:10 diluted), followed by 2 mL of 7.5% (w/v) sodium carbonate. After 5 min at 50 ◦C, absorbance was measured at 760 nm using a U-5100 Spectrophotometer (Hitachi, Tokyo, Japan). The total phenolic content was estimated from a standard curve of gallic acid, and the results were expressed as mg gallic acid equivalents (GAE)/100 g fresh weight. The measurements were taken in triplicate and mean values were calculated.

9.6 Microbial Analysis

This analysis was performed in collaboration of DISAFA Department – University of Turin. DNA was extracted from the cultivation substrate using the FastDNA® Spin kit for soil (MP Biomedicals, Solon, OH, USA), according to the manufacturer's instructions. Three replicate samples of DNA extraction were performed. The quantity and purity of the DNA was measured spectrophotometrically with a NanoDrop ND-1000 (NanoDrop Technologies, Wilmington, DE, USA). Total bacteria and archaea (16S rRNA genes), aerobic ammonia-oxidizing bacteria (bacterial amoA gene—AOB) and archaea (archaeal amoA gene—AOA) standards and samples were analyzed using specific primers described in Mania et al. [218]. The qPCRs were conducted with a 2 µL 1:10 DNA dilution. The 20 µL reaction mix contained 10 µL

SsoAdvanced Universal SYBR Green Supermix (Bio Rad Laboratories, Munich, Germany) and 0.3 µM of forward and reverse primers. The optimal dilution of the DNA extracts was previously tested to compensate for any reaction inhibition (data not shown). The qPCR reactions were done on a Chromo 4TM Continuous Fluorescence Detector, associated with a PTC-200 thermocycler (MJ Waltham, MA, USA), using appropriate target gene-specific amplification cycles. Data acquisition and analysis were conducted with Opticon Monitor 3.1.32 software (Bio-Rad Laboratories). To eliminate artefacts and specific amplification, melting curves were verified and amplicon size checked by electrophoresis.

9.7 Chemical Analyses of Zeolite at the Beginning of the Experiment

The sorption kinetics of NH_4^+ by zeolite was evaluated. All the withdrawals taken during kinetics were analyzed following the ammonium official distillation method using a Kjeldahl apparatus [219]. The zeolite removal efficiency was due to the pH of the solution, which affects the zeolite ion exchange mechanism [220]. For this reason, we chose to evaluate the influence of pH on removal efficiency. Under the same conditions, 20 g of zeolite was put into the percolation system with 200 mL of NH_4^+ buffered solution at pH between 5 and 9. All buffer solutions had the same concentration (about 1000 mg/L). Thereafter, a test with a sample of real digestate was conducted in the percolation system, this time using 40 g of zeolite and 200 mL of digestate at about 3700 mg/L and pH 8.5. Characterization by the Kjeldahl method detected the ammonia nitrogen content after the real digestate was in contact with the zeolite.

9.8 Chemical Analyses of the Substrate at the End of the Strawberry Growing Cycle

At the end of the growing cycle, the substrates were analyzed to determine the amount of N in them and what was still available to the plant. To evaluate the amount of N adsorbed into zeolite frameworks at the end of each growing cycle, 20 g of fully charged zeolite was put in contact with 200 mL KCl 2 M and stirred for 1 h at 20 °C. After that step, it was centrifuged for 10 min at 3000 RPM and filtered using Whatman n◦4 paper. The filtered solution was analyzed following the official distillation method using a Kjeldahl apparatus [219]. At room temperature, potassium removes the ammonium ions bound to the soil exchangers, while the nitrogen fraction (comprised of nitrates and nitrites) is brought into solution by the dipolar effect of water. To analyze the zeolite-treated solutions, the distillation method to determine ammonium was followed. Nitrogen run-off was not evaluated; it was assumed that all the nutrients were sequestered by the plant. In addition, it was supposed that the drip irrigation system had eliminated of any feasible leaching during the strawberry growing cycle.

9.9 NANOSPONGES: Synthesis material

9.9.1 Maltodextrins

Glucidex 2® (GLU2): a commercial maltodextrin with dextrose equivalent to 2 and average molecular weight 314000 Da, resulting from partial hydrolysis from corn starch. At room temperature it is presented as white powder and being hygroscopic is dried in the oven at 75 ° C to keep the weight constant before use. It is provided by Roquette Italia SPA.

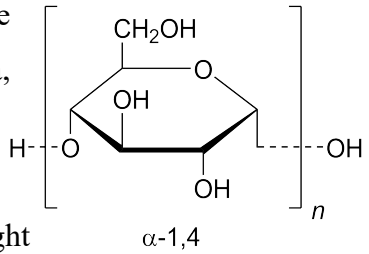

Figure 33: Maltodextrin (Glucidex 2®).

9.9.2 Cross-linkers

1,4-Butanediol diglycidyl ether (BDE) ≥95%, is the basic cross-linking agent used, provided by Sigma-Aldrich (Darmstadt, Germany). It has low toxicity, good water solubility and biocompatibility.

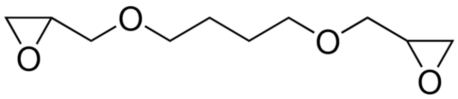

Figure 34: BDE.

Other cross-linkers have been used in this study including:

- TTE: trimethylolpropane triglycydil ether ≥95% Sigma-Aldrich (Darmstadt, Germany)

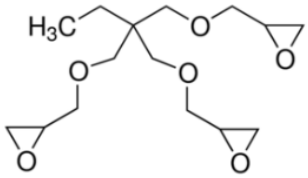

Figure 35: TTE.

- NGDE: neopentyl glycol diglyl ether ≥95% Sigma-Aldrich (Darmstadt, Germany)

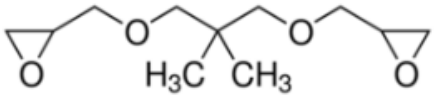

Figure 36: NGDE.

9.9.3 Solvent

As solvent was used:

- Deionized water
- Basic solution composed of NaOH 97%, in pellet form, supplied by ACS reagent.

9.9.4 Functionalizing agents

All reagents were supplied by ≥95% Sigma-Aldrich (Darmstadt, Germany.

- Choline chloride (CHO)

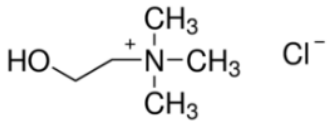

Figure 37: Choline chloride.

- DABCO: 1,4-Diazabicycle [2.2.2] octane

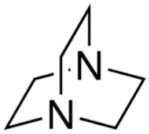

Figure 38: DABCO.

- Carrageenan-K supplied by Gioia Group S.R.L. Comes in the form of white powder at room temperature. Carrageenan-K is extracted from Irish musk (Chondrus Crispus), a red alga and consists of salts or sulphate esters with a ratio of sulphate unit to exposes close to one. Its structure is composed of 1,3 glycosidic bonds of galactose-4-sulfate unit and 1,4 glycosidic bonds of anhydrous 3,6-D-galactose unit. Carrageenan can form thermally reversible gels whose resistance and freezing temperature are dependent on potassium and ammonium cations. It is often used in combination with starch. The two compounds form complexes that have useful properties in food.[128]

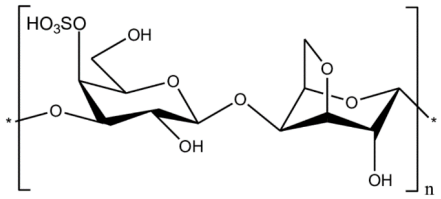

Figure 39: Carrageenan-K.

- 1,3-propylsulton. At room temperature it is in solid form.

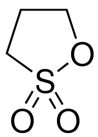

Figure 40: 1,3-propylsulton.

- 1,4-butylsulton. At room temperature it occurs in liquid form.

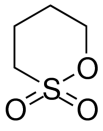

Figure 41: 1,4-butylsulton.

9.9.5 Reagents

1. *Reagents for nitrates, phosphates, and glyphosate solution preparation*

All reagents were supplied by ≥99% Sigma-Aldrich (Darmstadt, Germany.

- Ultrapure water
- Potassium nitrate
- Sodium sulphate
- Sodium orthophosphate
- Sodium monohydrogen phosphate
- Sodium dihydrogen phosphate
- Glyphosate: N-(phosphonomethyl)glycine

2. *Reagents for heavy metals solution preparation*

All reagents were supplied by ≥99% Sigma-Aldrich (Darmstadt, Germany.

- Ultrapure water
- copper (II) sulfate pentahydrate ($CuSO_4$ $5H_2O$)
- zinc (II) sulfate heptahydrate ($ZnSO_4$ $7H_2O$)
- aluminum nitrate ($Al(NO_3)_3$ $9H_2O$)
- chromium nitrate nonohydrate (III) ($Cr(NO_3)_3$ $9H_2O$)
- cadmium nitrate ($Cd(NO_3)_2$)
- nickel nitrate ($Ni(NO_3)_2$)
- manganese (II) sulfate monohydrate ($MnSO_4$ H_2O)
- lead nitrate ($Pb(NO_3)_2$) supplied by ACS
- Sodium chromate, Na_2CrO_4
- Arsenic trioxide, As_2O_3
- H_2O_2 solution
- Sulfuric acid 98%, H_2SO_4
- Acetic acid, CH_3COOH

3. *Reagents for nanosponge-metal interaction mechanism determination*

- EDTA, ethylenediaminetetraacetic acid, ($(HO_2CCH_2)_2NCH_2CH_2N(CH_2CO_2H)_2$) (anhydrous, Bio-Ultra ≥ 99% titration);
- Calcium chloride dihydrate ($CaCl_2$ $2H_2O$) (ACS reagent, ≥ 99%).

9.10 Nanosponge synthesis

9.10.1 Base synthesis: GLU2_BDE.

20 ml of 0,2 M NaOH solution shall be taken and placed in a 100 ml flask with a magnetic stirrer, heating to 60 °C, using a magnetic heating plate equipped with a digital thermoregulator and hemispherical metal support to obtain a homogeneous heating of the flask (Figure 42). Add 7 g of GLU2 slowly, avoiding the formation of lumps. A complete solubilization and continuing to stir, 2 ml of BDE grating is added, and the synthesis is started by raising the temperature up to 75 °C. The mixture begins to become very viscous and after about 15 minutes should occur the reticulation reaction with the formation of a gel. At this point leave for 90 minutes, after which you get a brown gel as the final product.

Figure 42: base synthesis of GLU2_BDE.

9.10.2 Anionic Nanosponges Synthesis

To synthetize an anionic nanosponge, a commercial maize-derived maltodextrin (Glucidex 2®) was used. It has been used as building-block, 1,4 Butanediol diglycidyl ether (BDE) or Trimethylolpropane triglycidyl ether (TTE) or Neopentyl glycol diglycidyl ether (NGDE) as cross-linker, while 1,4-Diazabicyclo [2.2.2] (DABCO) was initially used as reaction catalyst to get the amine-mediated epoxy ring-opening reaction.

The synthesis of the polymer was carried out by dissolving in a round-bottom flask 1.75 g of Glucidex2® in 5 mL of 0.2M NaOH sodium hydroxide distilled water solution. Afterwards, while keeping the solution under stirring the amine (DABCO) was added at certain molar ratio (1:2, 1:4, and 1:8 mol:mol) in respect of epoxide. 0.35 mL of BDE/TTE/NGDE were added, and the temperature was increased at 70 °C, using a hotplate stirrer equipped with thermoregulation and a metal hemispheric bowl to get a homogeneous heating of the flask. The reaction was allowed to occur and after 90 minutes a bulky gel as product was attained. Later, the product was recovered from the flask with a spatula and subsequently purified with distilled water, to remove any non-reacted reagents. At the end of the purification step, the product was dried in oven at 70 °C to constant weight and grinded in a mortar, obtaining a powder. The syntheses were carried out with and without the choline chloride, to investigate the presence of other mechanisms of abatement of polluting anions. The effect of choline, as well as the possibility that the abatement of the polluting anions concerned other mechanisms besides ion

exchange, were evaluated by performing the synthesis with and without choline chloride. In this way 6 different anionic nanosponges are synthetize and called as follow.

GLUTTE GLUCHOTTE GLUBDE GLUCHOBDE GLUNGDE GLUCHONGDE

The following table shows reagents amount used. The products were tested during the abatement tests of nitrates, sulphates, phosphates and glyphosate, hexavalent chromium and arsenic (V) and arsenic (III).

Table 13: Reagents amount for anionic nanosponges synthesis.

	GLUTTE	**GLUCHOTTE**	**GLUBDE**	**GLUCHOBDE**	**GLUNGDE**	**GLUCHONGDE**
NaOH 0,2M	200 ml	200 ml	200 ml	200 ml	200 ml	200 ml
Glucidex 2	70 g	70g	70 g	70 g	70 g	70 g
Choline chloride		10,8 g		10,8 g		10,8 g
DABCO	5 g	5 g	5 g	5 g	5 g	5 g
TTE	27 g	27 g				
BDE			15,73 g	15,73 g		
NGDE					16,82 g	16,82 g

9.11 Cationic nanosponge synthesis

9.11.1 Nanosponge synthesis with carrageenan K

a) *Basic environment synthesis*

20 ml of 0,2 M NaOH solution shall be taken and placed in a 100 ml flask with a magnetic stirrer, heating to 60 °C, using a magnetic heating plate equipped with a digital thermoregulator and hemispherical metal support to obtain a homogeneous heating of the flask. Add 500 mg carrageenan-K (10% compared to GLU2), stirring until completely dissolved. Add 5 g of GLU2 slowly to avoid the formation of lumps, continuing to mix. At complete dissolution, 2 ml of BDE is added, and the synthesis is started by raising the temperature to 75 °C. The mixture begins to become very viscous and after about 15 minutes should occur the reticulation reaction with the formation of a gel and at this point leave for 90 minutes, obtaining at the end a brown gel as the final product. The final product was named as follows: *GLU2_BDE_CARK10%.*

b) *Water environment synthesis*

20 ml of deionized water is taken and placed in a 100 ml flask with a magnetic stirrer, heating to 100 °C using a magnetic heating plate equipped with digital thermoregulator and hemispherical metal support to obtain a homogeneous heating of the flask. Carrageenan K was added to different percentages by weight compared to the grams of maltodextrin (10% and 15%), continuing to mix until completely soluble. Then add 5 g of GLU2 slowly to avoid the formation of lumps, continuing to mix. The color of the mixture is lighter, as there is no NaOH. After complete dissolution, add 5 ml of BDE. The mixture begins to become very viscous and after about 1-3 hours should occur the reticulation reaction with the formation of a gel and at this point it is left for 90 minutes, obtaining at the end a sand-colored gel as the final product. The final products were named as follows: *GLU2_BDE_CARK10%_H2O and GLU2_BDE_CARK15%_H2O.*

9.11.2 Nanosponge synthesis with sulton

a) One step synthesis

20 ml of 0,2 M NaOH solution shall be taken and placed in a 100 ml flask with a magnetic stirrer, heating to 60 °C, using a magnetic heating plate equipped with a digital thermoregulator and hemispherical metal support to obtain a homogeneous heating of the flask. Add 7 g of GLU2 slowly, avoiding the formation of lumps. At complete solubilization 1,3-propylsulton or 1,4-butylsulton (d = 1,331g/ml) are added 10% in moles compared to maltodextrin: 0,47 g and 0,39 ml respectively. Finally, add 2 ml of BDE grating and start the synthesis by raising the temperature up to 75 °C. Synthesis with 1,3-propylsulton does not generate the solid gel; therefore, the temperature has been brought to 100 °C, however not obtaining the desired product. On the contrary, the one with the 1,4-butylsultone, only after increasing the temperature up to 85 °C, generated a gel after 15 minutes. At this point, it is left for 90 minutes, after which a brown gel is obtained as the final product. The final product was named as follows: *GLU2_BDE_1,4BUTS10%.*

a) *Bi-step synthesis*

Place 10 ml of a 0,2 M NaOH solution in a 40 ml vial with magnetic stirrer, heating to 80°C in an oil bath, using a magnetic heating plate equipped with a digital thermoregulator. Add 500 mg of the basic nanosponge, GLU2_BDE, previously prepared. Leave under constant agitation for 30 minutes. Subsequently, 1,3-propylsultone is added in the following percentages in weight to 10%, 20% and 30% compared to the grams of nanosponge used or 1,4-butylsultone in the following percentages in weight to 20% and 30%. The synthesis is then started for 90 minutes, finally obtaining a heterogeneous mixture as a product. The final products were named as follows: *PROPS10%_POSTSYNTH, PROPS20%_POSTSYNTH, PROPS30%_POSTSYNTH, BUTS20%_POSTSYNTH and BUTS30%_ POSTSYNTH.*

9.11.3 Recovery and purification of nanosponge synthetize

The final products obtained were allowed to cool for 24 hours and then recovered from the flask by breaking and crushing the block of friable solid gel obtained with a spatula, reducing it to smaller pieces. The products are then placed in 1 L beakers and purified by 3-4 washes with deionized water. Then proceed with filtration with funnel Buchner on a filter paper disc, for three more times washing with deionized water, to remove any reagents that are not

Figure 43: Example of post synthesis and purification of nanosponge.

chemically bound. Whereas about bi-step synthesis with sultons, the purification of the product was performed by filtering directly the heterogeneous mixture obtained with a funnel Büchner on a disc of filter paper, washing with deionized water for three times. Finally, the product is left to dry in the oven at 70 ° C to keep the weight constant. The dry product obtained from the mass balance is weighed and finely ground in a mortar with a pestle to obtain fine grains, as shown in Figure 43.

9.12 Nanosponge characterization

9.12.1 FTIR-ATR analysis

Infrared spectroscopy (IR) is an analytical technique based on the interaction between electromagnetic radiation and matter. The wavelength range, which includes infrared radiation, ranges from 700 nm to 1 mm, between visible and microwave regions. The energy released by the IR radiation, which invests a molecule at a certain frequency "ν" (expressed as a wave number, $1/\lambda$ in cm^{-1}), is converted into rotational and vibrational energy, causing variations in bond vibrations. This phenomenon occurs only if the frequency of the radiation has a value equal to or multiple of that of the bond and if the vibrations induce a variation of the dipole moment of the bond. The technique used for the characterization of nanosponges is FTIR-ATR, which is based on the principle of total attenuated reflectance (ATR), because one is interested in the analysis of the surface of a substance, specifically for signals related to functional groups. The IR radiation passes through a particular crystal, transparent to the IR, (Zn, Se or Ge), which allows it to be reflected within it many times. During the test the sample is fixed on the surface of the crystal, then the radiation enters the crystal, is reflected through it and penetrates within the sample for some fraction of a micron, being in small part absorbed (or attenuated). At some point, the attenuation of the IR beam intensity is sufficient to be detected by the spectrophotometer, giving a full attenuated reflectance FT-IR spectrum. For FTIR-ATR analysis we used the Perkin-Elmer Spectrum 100 FT-IR spectrometer with universal ATR sampling accessory (Waltham, MA, USA) as an instrument. All spectra were taken in a wavelength range of 650-4000 cm^{-1}, at room temperature, with a resolution of 4 cm^{-1} and 8 scans per spectrum. For each sample, an aliquot was taken, which was finely ground, of which a spatula tip was placed directly on the crystal, for ATR analysis.

9.12.2 Thermogravimetric analysis (TGA)

Thermogravimetric analysis (TGA) consists of recording the variation in the mass of a sample, in a controlled atmosphere, as a function of time or temperature. The result of the analysis is usually expressed with a thermogram (or TG curve) that shows the temperature or time in abscissa and the mass change as absolute value or percentage in ordinate. Often the derived curve (or DTG curve) is also reported, which allows to better highlight the weight variations of the sample. The heart of the instrument is a thermobalance that consists of an extremely precise balance, with two arms, with one of the two (the one in which the sample is inserted) located inside the furnace, that can gradually vary the temperature from that environment to over 1000°C, with programmable temperature ramps and controlled gas flow, which can be both inert as nitrogen or argon that reactive as oxygen or air. The resulting thermogram depends mainly on the analytical conditions set as sample weight and shape, temperature scanning rate, gas type and flow, and system pressure conditions. In particular, the degradation temperature of the polymer, defined as the onset initial temperature, can be determined from the TG curve ($T_{onset\text{-}i}$), but also the temperature of maximum degradation rate (T_{vmax}), determined as the minimum point of the derived curve DTG and corresponding to the inflection point of the curve TG. Thermogravimetric analyses were carried out using Q500 TGA from TA Instruments (New Castle, DE, USA), from 25 °C to 700 °C, under nitrogen or air flow, with a heating rate of 10 °C/min, to assess the thermal stability of citric nanosponges, with sodium alginate, carrageenan-K and 1,4-butylsulton. The experimental conditions are summarized in Table 14.

Table 14: TGA working parameters.

	Working parameters	
Atmosphere	N_2	air
Temperature	25-700 °C	
Test time	70 min	
Heating rate	10 °C/min	
Equilibrate T	200 °C	

9.12.3 Potential-ζ

The determination of the ζ potential is carried out to assess the stability of dispersions. In fact, most of the nanoparticles dispersed in water present a superficial charge, generated by ionization phenomena or absorption of charged species. When they move in solution, the particles move along with a double ionic layer and the ζ-potential turns out to be the potential

at the level of this double layer. It is, therefore, the main force of particle interactions and is very sensitive to the composition of the species charged in the dispersion.

A high value of potential-ζ causes nanoparticles to stay away from each other by repelling themselves enough to eliminate the possibility of agglomeration, aggregation and/or flocculation. A Malvern Zetasizer Nano-ZS (United Kingdom) was used as an instrument for the determination of the ζ-potential of synthesized nanosponges, as shown in Figure 29. The samples were prepared as follows: take an aliquot of nanosponge and grind it finely. Then a spatula tip is placed in a 5 ml Eppendorf tube with a magnetic anchor inside and then two ml of deionized water are added. The sample, thus prepared, is placed under agitation at room temperature on a magnetic plate for ten minutes. With a 1 ml syringe, an aliquot is taken, which is inserted inside a capillary cell equipped with electrodes: a difference in potential is applied, generating an electric field in the suspension. Charged particles, because of electrophoresis, move with a certain speed towards the electrode which presents opposite charge. The instrument performs three measurements for each sample and returns the mediated value. To verify the replicability of the tests and to obtain accurate average values, each test was repeated a second time while maintaining the operating conditions.

9.12.4 Elemental analysis (CHNS)

The following analysis was carried out to assess the percentage of sulfur present in the following sulphonic nanosponges. The chemical compositions of the samples were studied using a combustion analyzer from the Thermo Fisher Flashea 1112 Series (Waltham, MA, USA). The weight of the sample measured in the microbalance varies from 245 mg to 255 mg.

9.12.5 Swelling test

Swelling tests (swelling) were carried out by weighing 200 mg of nanosponge, to which 15 ml of deionized water is added. Centrifuge tubes, 15 ml Falcon, are used. The samples have been prepared in triplicate and have been allowed to swell for 24 hours. Then, each sample was centrifuged for 15 minutes at maximum power, so that the swollen nanosponges were stratified well at the bottom of the test tube. At this point, the liquid phase is removed, and samples are repeated. The swelling percentage is calculated by the following formula:

$$\%\, swelling = \left(\frac{g_{(\,swelled\ polymer)} - g_{(dry\ polymer)}}{g_{(dry\ polymer)}}\right) \times 100.$$

9.12.6 Scanning electron microscope analysis (SEM)

The scanning electron microscope (SEM) is a type of microscope that uses an electron beam as a radiation source, rather than light as in the case of optical microscopes. This is because the

electrons have a shorter wavelength than the photons that make up the light, and since the resolution power of a microscope is inversely proportional to the wavelength of the radiation used, with the electrons the resolution reached is higher. This instrument, following the emission of an electron beam, makes it possible to analyze the various signals produced by the interaction of the electrons in the beam with the sample under examination, such as retro diffuse electrons (BSE), secondary electrons (SE) and X-rays. The main information that can be obtained from an SEM analysis can be morphological, compositional, and structural. The parameters on which you work are those related to the sample such as: its positioning, its distance from the beam output, (called working distance), the position of the detector, its focusing and the choice of the magnification to be used. You can also act on the electron beam by configuring it according to the type of analysis to be performed, for example going to act on the acceleration, modifying the difference in potential (from a few hundred volts to 30 kV) and on the final diameter or spot-size that can vary from about a micron to some microns. Through the SEM analysis, the morphology of the nanosponges based on sodium alginate, carrageenan-K and 1,4-butylsulton was assessed. The samples were prepared as follows: a layer of adhesive graphite was placed on a sample holder (stub) to make the sample conductive. Then, you take a sample (as fine as possible and in case the grains were too big, you grind) and you have it on a sheet of aluminum. The stub is placed on top of the sample to attach the fine nanosponge grains, to form a monolayer on the surface of the support. A VEGA scanning electron microscope produced by TESCAN was used as an instrument for morphological analysis. Working parameters are summarized in Table 15.

Table 15: SEM working parameters.

Magnification	500 x, 2.00 kx
Field of view (FoV)	1,86 mm, 558 µm, 140 µm
Working distance	15 mm
Power	10 pA
Segnals	Secondary electrons (SE)
Energy	5 keV

9.13 Abatement tests

9.13.1 Mother/Stock solution preparation

All the stock solutions of all the compounds we started from had a concentration of 1000 mg/L. For the preparation of each solution, it was started from the salt of the compound of interest

(nitrates, phosphates, glyphosate, or salts of heavy metals) the quantity in grams has been calculated according to the concentration to be obtained. It is then dissolved in deionized water at room temperature in a 100 ml flask.

9.13.2 Testing solution preparation for nanosponge abatement tests

To evaluate the performance of nanosponges, we have prepared solutions at different concentrations to test on different types of nanosponges.

Anionic nanosponges have been tested by putting it in contact with standard solutions of nitrate anion with the following concentrations: 100, 200, 300, 500 and 1000 mg/L. For phosphates, four phosphate solutions at different pH values have been prepared from: sodium orthophosphate, sodium monohydrogen phosphate, sodium dihydrogen phosphate. The prepared solutions are summarized in the following Table 16:

Table 16: Phosphate buffer solutions at different pH values.

Phosphate	**g weight**	**pH**	**P concentration (mg/L)**
Na_3PO_4	0,3999	11,88	32,58
Na_2HPO_4	0,1854	8,49	32,24
NaH_2PO_4	0,1423	5,25	31,93
Na_2HPO_4 + NaH_2PO_4	0,1127 + 0,0558	7,04	32,12

Anionic nanosponges were tested on all solutions to observe the effect of pH on the percentage of abatement. The following concentrations with 100 mg/l,10 mg/L and 1 mg/l of glyphosate were used for glyphosate. Cationic nanosponges have been tested on different heavy metals at various concentrations of 10, 25, 50, 100, 400 and 1000 mg/L from 1000 mg/L stock solutions.

9.13.3 Abatement test method

Each abatement test consists of inserting one gram of nanosponge and 100 ml of solution at known concentration of the species to be killed in a 100 ml vial.

Each nanosponge was ground manually by means of a mortar to homogenize the grain size of the material. The system is agitated for 24 hours at room temperature in an orbital shaker.

After this time, the solution in contact with the nanosponge is separated by filtration on a pleated filter. For each abatement test three replicates were carried out. For cationic nanosponges some preliminary tests were performed to verify their adsorption capacity. To this end initially test on copper solution at 25 mg/L were carried

Figure 44: Batch abatement test.

out. Nitrates were analyzed using both colorimetric kit and ion chromatography, while glyphosate and heavy metals were analyzed using ICP-OES.

9.13.4 Release test

For the water release tests we used the nanosponges left on the filter after the abatement tests and dried in the oven at 70°C. They are placed inside vials or Falcon tubes and diluted with deionized water of the same amount used for the tests felling. The samples are left in the shaker for 24 hours and then filtered on filter paper into 50- or 100-ml flasks based on the amount in the vial. The filtrate was analyzed.

9.13.5 Nanosponge-metal interaction mechanism determination

The purpose of the following method is to verify whether nanosponge - metal cation interaction mechanism occurs by ion exchange or complexion. For this purpose, two solutions have been prepared, one of EDTA 0,01 M and one of $CaCl_2$ 0,01 M. Using the first, the mechanism that is determined is that of complexation, as the metal will tend to bind more easily to EDTA, because it is a stronger complexing agent than carboxylic or sulfonic groups. While, using the second solution, what occurs is the ion exchange, since the active sites of the nanosponge release the metal, and bind to the calcium cation.

Those saturated with 1000 mg/L of copper solution were used as nanosponges following the abatement tests. Then at 100 mg of loaded nanosponge, add 25 ml of EDTA or $CaCl_2$ solution. The samples thus prepared were left on the shaker for about one hour and then filtered on filter paper into 50 ml flasks and analyzed at ICP-OES.

9.13.6 Apparatus for analysis

- *pH meter:* The pH determination of phosphate solutions was carried out using the pH meter AMEL 338.
- *Ionic chromatograph*: Analysis of nitrates and residual sulphates in solutions in contact with nanosponges were carried out by ionic chromatography using the instrument "CI 883 plus - MetrOhm".
- *ICP-OES*: The analysis of the total residual phosphorus in the solutions that have been in contact with the nanosponges, both in the case of phosphate abatement tests and in the case of glyphosate tests, were conducted using the Perkin-Elmer Optima 7000 DV instrument. The analyses were carried out under the following conditions: 1,5 L/min auxiliary argon flow, 0,5 L/min argon flow and 0,6 L/min argon flow nebulizer. The instrument provides answers directly in concentration, thanks to the use of calibration curves obtained with multi-elementary standards.

9.14 BIOCHAR: Materials

9.14.1 Woody biomasses

Biochar from residual woody biomass were tested, such as pruning waste, hazelnut shells, corn cobs, all renewable raw materials and highly produced in Italy. It might be interesting to apply the same study to biomass commonly produced in developing countries. The essences used to produce biochar are the following:

1. Spruce
2. Corn cob
3. Mixed sawdust of poplar (or mixed sawdust)
4. Hazelnut shells
5. Cherry tree
6. Acacia
7. Elderberry
8. Walnut wood
9. Jube
10. Plum
11. Fig
12. Hazelnut tree
13. Commercial biochar (supplied by NeraBiochar srl)
14. Commercial activated carbon.

The biomass used have different characteristics in terms of lightness, porosity, and hardness, have been studied precisely because these characteristics can positively influence the adsorbent capacity of biomass. The results obtained about the abatement of heavy metals are, in fact, different depending on the biomass used. The prune, the walnut, the cherry, the jube are hard woods, we therefore expect that they have a similar behavior; the spruce is instead a conifer, while all and hazelnut shells are matrices extremely different from those just listed, Finally, the fig and elder wood are light woods, not very valuable because they have poor mechanical properties and low calorific value.

9.14.2 Reagents and apparatus

Apparatus	**Reagents**
ICP-OES OPTIMA 7000 DV Perkin Elmer equipped with cyclonic nebulization chamber in Argon flow; KNIFE MILL SM 300, Verder Scientific; Horizontal opening tube furnace Est 12-450, Carbolite; Mortar with ceramic pestle; Tubes of polypropylene type Falcon; Sartorius analytical scale; Orbital agitator 711, Asal; Centrifuge Z 380, Hermle; Filter paper, Whatman No 3 and 4; Glassware of class A; FTIR coupled with ATR Perkinelmer UATR Two;	HNO_3 69% Ultratrace, ppb-trace analysis grade, Scharlau; Hydrochloric acid, Merck; Acetic acid, Merck; Multielemental standard for ICP, solution IV Certipur 1000 mg/l, Merck Millipore; Ultrapure water, Milliq; Sodium hydroxide, Sigma-Aldrich; Sodium acetate, Sigma-Aldrich; Cadmium nitrate, Carlo Erba; Nickel nitrate, Merck; and Lead nitrate, Merck; and Copper nitrate, Carlo Erba; Aluminum nitrate, Merck; Chromium nitrate, Carlo Erba; Zinc acetate, Carlo Erba; Manganese acetate, Merck Vanadium pentoxide, Thermo-scientific

9.15 Methods

9.15.1 Biochar pyrolysis

For biochar preparation, it was started from wood waste of medium size: it was necessary to make samples homogeneous and representative by grinding them in a knife mil. In this way the sample could be easily used for laboratory purposes. The milling process was followed by sieving to achieve sawdust of the size of the millimeter. For pyrolysis, a tubular furnace with a sample-carrying carrycot about 50 cm long was used. During heating, the furnace was continuously flushed with nitrogen to make the environment oxygen-free, until the biochar was completely cooled. To obtain about 20 grams of biochar per heating cycle, about 50-60 g of

ground wood sample were weighed in the spacecraft. The heating cycles were carried out at three different temperatures: 550 °C, 800 °C and 1100 °C, so a total number of biochar samples of 36 were gotten. The heating process at each temperature was performed with a temperature ramp of 10°C per minute and maintenance of the final temperature for 3 h. The biochar was extracted from the furnace only after cooling to room temperature.

9.15.2 Stock solution preparation

To assess the adsorbent capacity of biochar, a solution containing metal mix cations was prepared. For this purpose, metal salts were weighted: all the elements were in the only form of nitrates or acetates to avoid precipitation or complexation phenomena. The final concentration was 1g/L for each cation. The solution was prepared using the previously dried salts in oven. The salts were placed in a 1000 ml flask and made up to the volume with deionized water. The pH of this solution was 3,7. This solution was used to prepare more dilute solutions, at 2 and 1 mg/l, used to evaluate the metals removal by biochar. To perform the abatement tests, they were placed in contact with 1g of biochar with 50 ml of standard solution, in a 50 ml Falcon plastic tube.

9.15.3 Biochar acid treatment post pyrolysis

One of the problems initially met during the abatement tests is the pH increase of the solution containing metals in contact with biochar. This phenomenon is caused by the fact that biochar is basic, due to carbonates and oxides of alkaline and alkaline earth metals. The solution reached a pH of about 10-12. In this way at alkaline pH, most metal cations precipitate and this can distort the abatement values. Before each analysis pH was checked and brought to the desired value using a buffer. Following several buffered tests, it was preferred not to introduce large amounts of buffered salts, but to perform an acid treatment on all biochar samples by washing with 0,1M hydrochloric acid. A 0,1 M solution of HCl was used (8,3 ml of HCl 37% to 1 liter volume) and approximately 3 g of each biochar sample was inserted into 200 ml flasks together with 100 ml of HCl 0,1M. The flasks were introduced for a few minutes in an ultrasonic bath and rested for one night. The following morning the samples were washed several times with water, neutralized with a very dilute solution of ammonia, washed again with deionized water several times using a vacuum filter flask, until the washing water had neutral pH. Finally, biochar been dried in oven at 80 °C and further heated to 550 °C for 1 hour in the tubular oven to completely remove any traces of reagents used. As a result of this treatment, there were no major increases in pH caused by the calcination of the biochar. To

work at pH 6 (conditions use in this research work) it was often necessary to dab the solution slightly with 10% acetic acid and 5% or 10% sodium acetate to avoid any pH increases.

9.15.4 Metal release from non-treated biochar

Before determining the biochar's abatement capabilities, it was necessary to know the metal content that could be released into the water from each sample and whether the release could interfere with the abatement yields. The release tests were performed in water in 0,01 M acetic acid buffer solution (pH=4) and in 0,1 M hydrochloric acid solution (pH=1). Falcon-type test pieces were used, in which 0,5 g of biochar has been inserted together with 25 ml of each solution. Each sample was sonicated for about 10 minutes and then agitated for 72 hours on an orbital shaker. The samples were then centrifuged, filtered through a pleated filter and the aqueous solutions were analyzed at the ICP-OES. Before filtration, for tests carried out at pH=4 it was necessary to check the pH of each sample did not change, since a significant variation in pH affected the release and abatement phenomena. To restore the pH to this original value, a few drops of 1:1 concentrated solution of acetic acid were introduced with Pasteur pipette. Metals such as calcium, magnesium, potassium, and sodium are described in literature as the main phenomenon promoting abatement by ion exchange and precipitation. Therefore, it is possible to say that the higher their content in the biochar the greater will be its crushing capabilities.

9.15.5 Abatement tests

Biochar abatement tests were performed: the tests measured the corresponding metal amount each type of biochar can absorb, according to characteristics (biochar-solution ratio, volume involved, concentration) of the solution in which the sample is placed. These tests were carried out initially by contacting about 0,5 g of biochar which had previously undergone acid treatment, with 25 ml of solution containing cadmium, lead, aluminum, nickel, chromium, manganese, zinc and copper. All biochar samples were gotten from various wood essences at three temperatures. 36 samples have been tested to performed abatement test on the solution at pH= 6 at a concentration of 2 mg/l for each of the metals listed above. 50 ml or 25 ml of 2 mg/l solution were introduced into Falcon-type plastic tubes containing 1 g or 0,5 g of biochar, weighed on an analytical balance, sonicate for 5 minutes, and finally shake on the orbital stirrer for 24, 48, 72 hours. After that, samples were centrifuged for 5 minutes, pH checked, filtered and on the filtrate, acidified with a few drops of nitric, the analysis was performed using ICP-OES. From the results, it was possible to select which essences provided a biochar with better abatement performances. Other abatement tests at pH 2 and 4 were performed only on best

performing samples. These abatement tests were carried out using the same procedure with solution of 1 and 0,1 mg/l at pH=6.

9.15.6 Metal release tests

To verify the effectiveness of metals retention on the best samples, after the abatement tests several tests have been carried out to release the retained metals, to understand whether the retention phenomenon was reversible or not. Knowing whether a biochar sample can permanently retain the metal ions removed from the solution is a very important aspect, because it allows to understand if the abatement can fail to vary environmental conditions such as pH or leaching.

10 Results and Discussion

10.1 Zeolite

10.1.1 Choose of the best zeolite: preliminary screening tests

In the tables below, the results of the tests for the reduction of ammoniacal nitrogen by the various types of zeolites available are shown, classified according to the size of the granules that compose them. Approximately 10 g zeolite was used with 100 ml of ammonium standard solution at 10 mg/l.

Table 17: Zeolite screening tests.

Weight (g) zeolite 0,5-1 mm	**$[NH_4^+]$ (mg/l)**	**Abatement NH_4^+ %**	**mg NH_4^+ retained/gr zeolite**
10,2794	0,426	95,7	0,996
10,2585	0,368	96,3	0,996
10,1986	0,631	93,6	0,994
	Average	**95,2**	**0,99**
	Dev. Std	**1,4**	
	Dev. Std %	**1,5**	
	Error Std	**0,8**	
Weight (g) zeolitite	**$[NH_4^+]$ (mg/l)**	**Abatement NH_4^+ %**	**mg NH_4^+ retained/gr zeolite**
10,1215	1,315	86,85	0,987
10,1166	1,668	83,32	0,984
10,026	3,667	63,33	0,963
	Average	**77,83**	**0,978**
	Dev. Std	**12,7**	
	Dev. Std%	**16,3**	
	Error Std	**7,3**	

Weight (g) zeolitite	$[NH_4^+]$ (mg/l)	Abatement NH_4^+ %	mg NH_4^+ retained/gr zeolite
10,1352	0	100	1,00
10,0579	0	100	1,00
10,0889	0,100	99,00	0,999
	Average	**99,66**	**0,999**
	Dev. Std	**1,4**	
	Dev. Std%	**1,4**	
	Error Std	**0,8**	
Weight (g) Zeolite Fr 1-3 mm	$[NH_4^+]$ (mg/l)	Abatement NH_4^+ %	mg NH_4^+ retained/gr zeolite
10,0097	1,368	86,32	0,986
10,0033	3,047	69,53	0,970
10,0054	0,856	91,44	0,991
	Average	**82,43**	**0,982**
	Dev. Std	**11,5**	
	Dev. Std%	**13,9**	
	Error Std	**6,6**	
Weight (g) zeolite 0-0.3 mm	$[NH_4^+]$ (mg/l)	Abatement NH_4^+ %	mg NH_4^+ retained/gr zeolite
10,0165	1,478	85,22	0,985
10,0803	1,066	89,34	0,989
10,1785	2,062	79,38	0,980
	Average	**84,65**	**0,985**
	Dev. Std	**5,0**	
	Dev. Std%	**5.9**	
	Error Std	**2,9**	
Weight (g) Zeolite Fr 0.3-0.5 mm	$[NH_4^+]$ (mg/l)	Abatement NH_4^+ %	mg NH_4^+ retained/gr zeolite
10,0088	0,885	91,15	0,991
10,0013	2,442	75,58	0,976
10,005	1,732	82,68	0,983
	Average	**83,14**	**0,983**
	Dev. Std	**7,8**	
	Dev. Std%	**9,4**	
	Error Std	**4,5**	
Weight (g) zeolite Energom	$[NH_4^+]$ (mg/l)	Abatement NH_4^+ %	mg NH_4^+ retained/gr zeolite
10,0911	2,153	78,47	0,979
10,0568	1,350	86,50	0,987
10,0535	2,200	78,00	0,978
	Average	**80,9**	**0,981**
	Dev. Std	**4,8**	
	Dev. Std%	**5,9**	
	Error Std	**2,8**	

Of all the types of zeolites tested, the one with the best abatement performances was composed mostly of clinoptilolite. 10 g of zeolite was used with 100 ml of standard ammonium solution at 10 mg/l. The results showed ammonium reductions between 75 and 95%. This range is due to the size of the zeolite: the finer the zeolite (granulometry 0.1-0.3 mm) the greater was the surface area and, consequently, the abatement. However, the particle size leads to problems with the use of the zeolite itself on industrial scale. In addition, some problems of mechanical strength occurred. For these reasons, the zeolite with the best tradeoff between mechanical and abatement properties was chosen (80% of ammonium abatement). As an alternative to zeolite, zeolitite, the waste of mineral processing, was tested. Zeolitite performances were lower than zeolite (60-70% ammonium abatement), but it is less expensive than zeolite. The best zeolite chosen was tested with digestate during time and the graph above shows the abatement trend:

Table 18: Best resulting zeolite.

Weight (g) zeolite	$[NH_4^+]$ (mg/l)	Abatement NH_4^+ %	mg NH_4^+ retained/gr zeolite
10,1196	316	68,4	6,76
10,2783	288	71,2	6,93
	Average	69,8	
	Dev. Std	1,9	
	Dev. Std%	2,7	
	Error Std	1,1	

10.1.2 Preliminary tests: kinetics in batch system

Table 19: kinetics in batch system.

Time sampling (min)	Absorbance Sample N°			Average $[NH_4^+]$ in the solution (mg/l)	Average Abatement %	Standard deviation
	1	2	3			
5	2,717	2,556	2,747	892,2	10,77	0,10
15	2,703	2,899	2,460	875,5	12,44	0,21
30	2,845	2,244	3,108	868,4	13,15	0,44
45	2,764	3,074	2,676	811,7	18,82	0,20
60	2,0051	2,572	2,824	784,2	21,57	0,41
90	2,743	2,61	2,128	793,4	20,65	0,32
120	2,676	2,912	2,356	757,4	24,25	0,27
180	2,455	2,506	2,214	760,4	23,95	0,15
240	2,347	2,553	2,334	747,5	25,24	0,12
1300	1,892	2,069	2,056	638,2	36,17	0,09

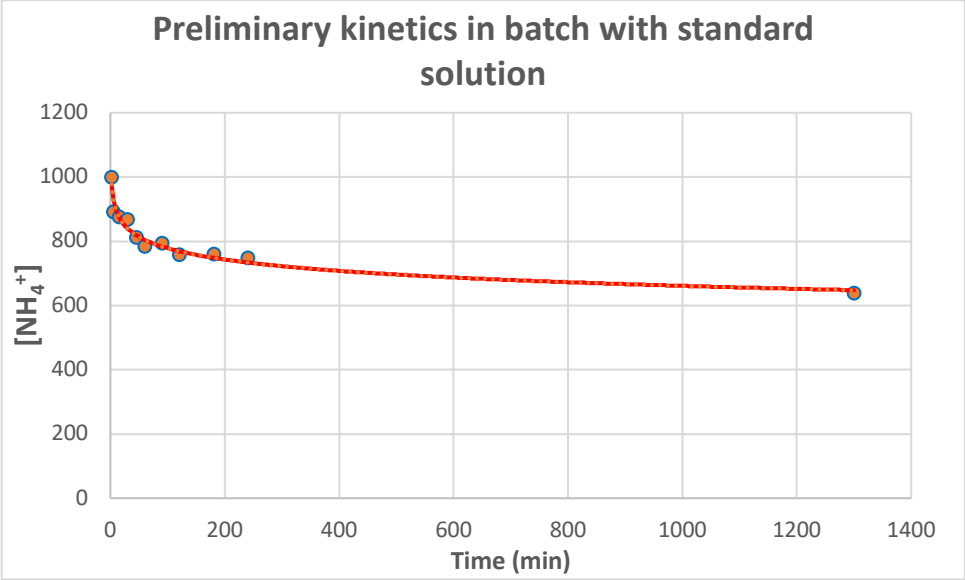

Figure 45: Graph of kinetics batch tests.

The kinetics were performed in triple, using 10g of zeolite in each container and a solution of 1000 mg/L of ammonium. The analysis was performed using the indophenol method with spectrophotometer. In the trend found in the chart above, there is a maximum abatement of about 35% and very long times connected to a very slow kinetics that reaches the equilibrium of exchange at high times. These tests confirm the results of the previous tests carried out on the column.

10.1.3 Preliminary tests: column test

After batch tests, a column system was performed. 10 g of zeolite and a 1000 mg/l standard solution of ammonium nitrate were used, keeping the tap always open. It is possible to see a logarithmic trend that tends to a saturation plateau in the graph below:

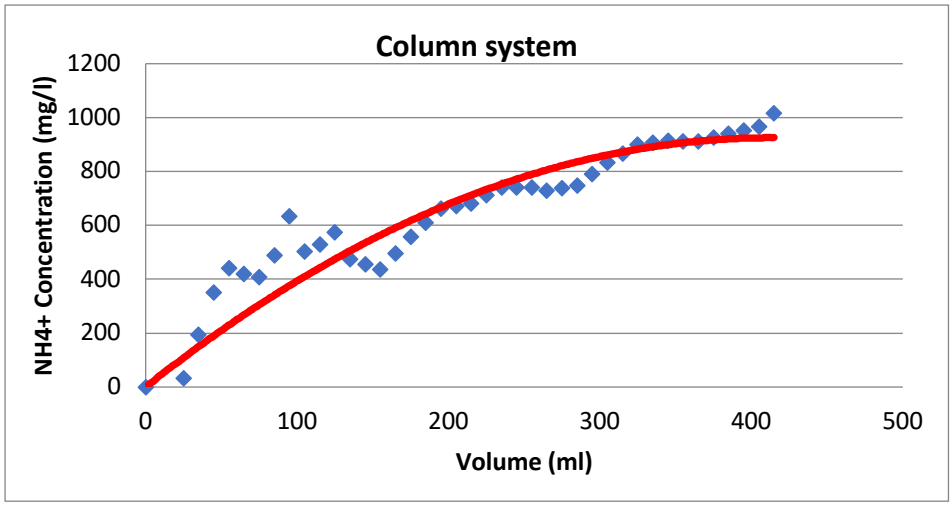

Figure 46: Column tests graph.

Even though the column system is more powerful than the batch system, showing best abatement value, a fluctuating trend occurs. Therefore, it is hypothesized that the liquid introduced into the column has a maximum level, the flow is faster than the optimal flow for the absorption and consequently the zeolite has less time to adsorb the NH_4^+. When the door leaf decreases the flow slows down and there is an increase in adsorption. The continuous system does not constitute best working condition since the solution flows too quickly through the zeolite and the contact time is not enough to guarantee a significant adsorption. Moreover, after a certain volume dispensed, the problem of clogging that drastically reduces the flow and abatement times is found. The column system was tested also on digestate. From the trend of the underlying curve, there is an excellent interpolation between the logarithmic curve and the experimental points. The breakthrough is also reached around 80/100 ml of digestate. Having been confirmed the kinetics both in batch and column, it has performed the kinetics with the percolation system.

10.1.4 Preliminary tests: percolation test

The system was made of a porcelain capsule in which 200 ml of standard NH_4NO_3 solution with ammonium concentration equal to 1000 mg/l are introduced. Using this method, it was possible to evaluate the kinetic aspect of the adsorption by performing an analytical check on aliquots of samples taken every half hour:

Table 20: Percolation test results.

Time (min)	$[NH_4^+]$ during time (mg/l)	Abatement %
0	1000	0
1	940	6
5	786	21,4
10	676	32,4
15	694	30,6
20	638	36,2
25	616	38,4
30	596	40,4
35	580	42
40	564	43,6
45	524	47,6
50	536	46,4
55	516	48,4
60	536	46,4
90	452	54,8
120	412	58,8
150	408	59,2
180	390	61
210	382	61,8
240	348	65,2
270	334	66,6
300	346	65,4
330	320	68
1320	270	73
1440	292	70,8

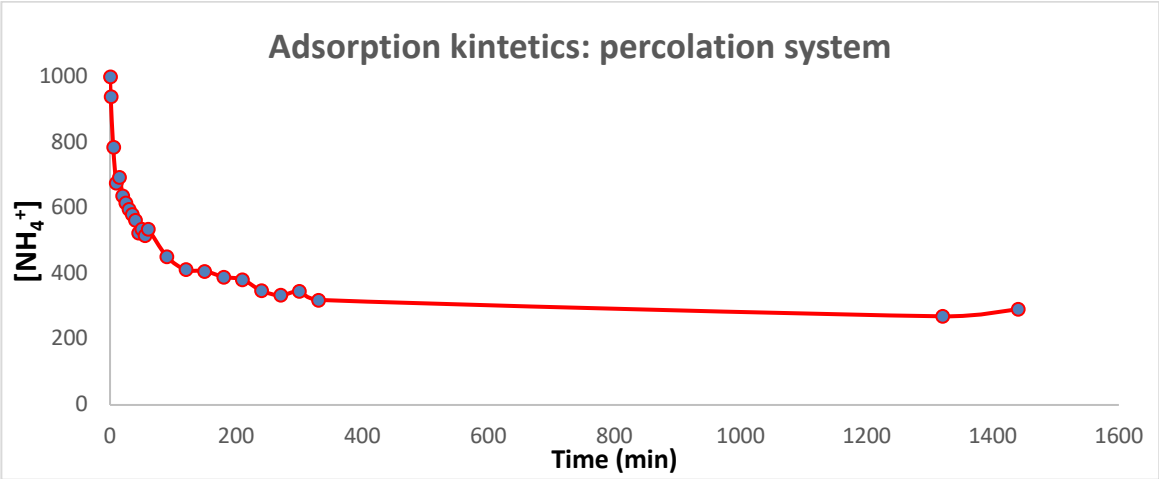

Figure 47: Percolation test graph.

From the graph above we note that kinetics is mostly in the first hour, so we proceed with another experience by scheduling sampling in more restricted times. At the end of the test the concentration of NH_4^+ is very low and a reduction of over 80% is detected.

10.1.5 Parameters variation as function of NH_4^+ adsorption

The tests carried out to assess which parameters (absolute NH_4^+ amount, $[NH_4^+]$ and volume) are the most determining factors for the reduction of ammonium with zeolite in the leachate system. The results of the tests carried out were as follows.

1. *Absolute amount of NH_4^+ constant*

Table 21: Absolute amount of NH4+ constant.

Absolute amount of NH_4^+ 100 mg				
Volume (ml)	**$[NH_4^+]$ starting (mg/l)**	**$[NH_4^+]$ final (mg/l)**	**Abatement %**	**Abatement (mg/g)**
100	1000	348	65,2	6,52
1000	100	44,4	55,6	5,56
10000	10	5,18	48,2	4,82

2. *Concentration constant*

Table 22: Concentration constant.

Concentration constant 1000 mg/L				
Volume (ml)	**$[NH_4^+]$ starting (mg/l)**	**$[NH_4^+]$ final (mg/l)**	**Abatement %**	**Abatement (mg/g)**
50	1000	166	83,4	4,17
100	1000	348	65,2	6,52
200	1000	586	41,4	8,28
300	1000	630	37	11,1

3. *Volume constant*

Table 23: Volume constant.

Volume constant 100 ml				
Volume (ml)	**$[NH_4^+]$ starting (mg/l)**	**$[NH_4^+]$ final (mg/l)**	**Abatement %**	**Abatement (mg/g)**
100	1000	348	65,2	6,52
100	100	7,2	92,8	0,92
100	10	0,1	99	0,09

From the above data it can be noted that having high absolute amount of ammonium, low volumes and high concentrations has the maximum abatement. This phenomenon can be explained by the fact that as concentration increases the gradient promotes the passage of ammonium in zeolite. Therefore, for the maximum exploitation of the mineral it is good to put the same with solutions at high concentrations of ammonium. One last test was performed: on the same zeolite using each time100 ml of standard solution was used with increasing the ammonium concentration, the following results:

Table 24: Volume constant vs Increasing of concentrations.

Volume 100 ml			
[NH_4^+] starting (mg/l)	**[NH_4^+] final (mg/l)**	**Abatement %**	**Abatement (mg/g)**
2000	575	71,25	7,12
3000	1205	59,83	8,97
4000	2180	45,5	9,1
5000	2910	41,8	10,45
Total ammonium retained by zeolite			**35,64**

It is known that the abatement increases as the concentration of the solution increases, but it is also true that by continuing to increase the concentration the saturation of zeolite is reached. Obviously, considering the amount of adsorbed ammonium per gram of zeolite it is possible to notice how these increases, if only slightly, with the increase of the concentration. This result further confirms that as the gradient increases between the solution and zeolite (increased by the concentration) the amount of ammonium that passes into zeolite itself increases. As a result, as the concentration increases, the amount of ammonium remaining in solution increases by further charging zeolite with ammonium. However, if the latter is used for the purification of water, it is necessary to consider that there is a limit to the concentration of the inlet solutions in relation to the amount of zeolite used. It will therefore be necessary to work in several stages so that the zeolite of the first stage receives a higher concentration of ammonium while the subsequent stages will deal with the further abatement to bring the ammonium content under the legal limits.

10.1.6 Percolation system: pig digestate

Having checked all process parameters, the test on the real pig digestate sample was carried out with the percolation system, using 20 g zeolite and 200 ml digestate. The Kjeldahl characterization detects the ammoniacal nitrogen content on the digestate in contact with zeolite. The values are given in the following table.

Table 25: Percolation test with pig digestate.

Sample	**Average starting [NH_4^+]**	**Average Zeolite (g)**	**Average pH**	**Average Abatement %**
Digestate 0	3710	40	8,5	99
Digestate 0	3715	50	8,5	82

After the 6-hour abatement test, the concentration of NH_4^+ is very regained and between 80% and 90% abatement is detected,

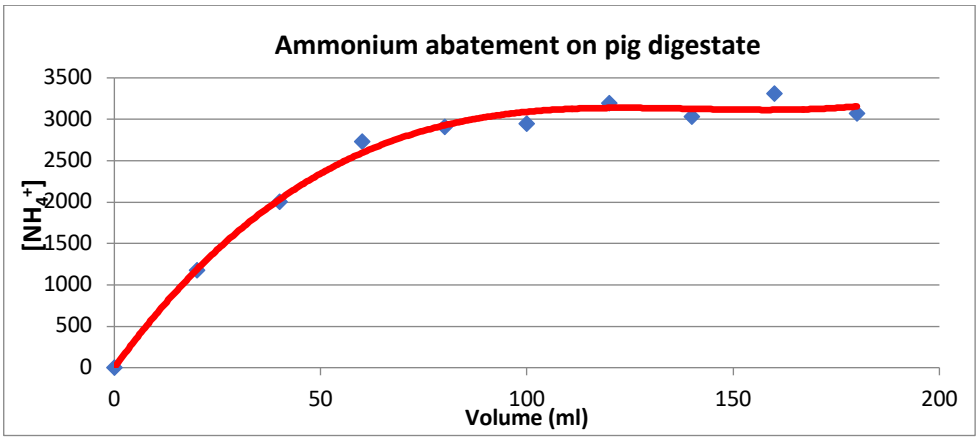

Figure 48: Ammonium abatement on pig digestate.

It is possible to see a better correlation between the experimental points and the theoretical curve, with the digestate rather than with the standard solution. A possible explanation could depend on the type of matrix and the high pH value of the digestate.

1. pH influence

The influence of pH on the abatement process has been assessed by several tests. The pH was changed, but the mean concentration of the standard solution stayed unchanged at 1000 mg/L. The results shown in the following table are obtained from the analyzes performed according to the methods described in the previously. For each test three replications were performed.

Table 26: pH influence results.

pH	Average [NH_4^+] (mg/l)	Average Abatement %	g zeolite	Average Abatement (mg/g)
5,5	1004,3	65,0	10,0653	6,5
7	1005,7	70,6	10,0940	7,0
8	1061,5	70,8	10,0621	7,4
9	1472,0	48,7	10,0439	7,1

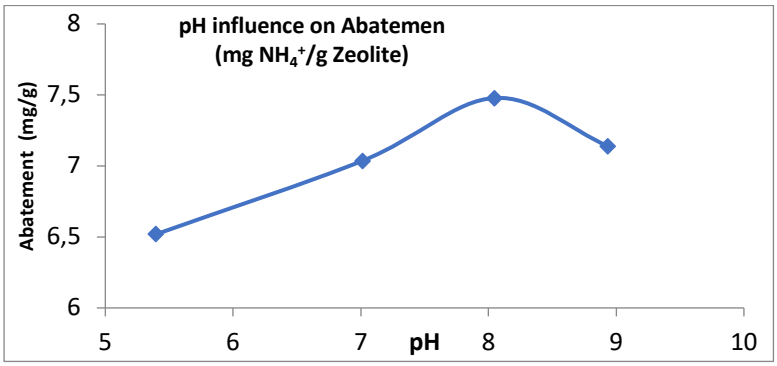

Figure 49: pH influence on ammonium abatement graph.

From this graph it is possible to notice how the abatement of ammonium by the zeolite depends strongly on the pH value of the solution used. There is a trend that reaches the maximum at a pH of around 8, which is very positive since the liquid fraction of the digestate to be treated is characterized by a pH of about 8.5 thus facilitating the adsorption mechanism.

10.1.7 Percolation system: scale-up percolation system for industrial purposes

After having performed all the tests and understood the fundamental parameters for a more performing zeolite ammonium retention in digestate, in collaboration with TEA Sistemi & Tecnologie srl, a pilot plant was set up for digestate treatment. The schematic representation of pilot plant for the abatement of ammonium in different standard solution is shown in figure 50:

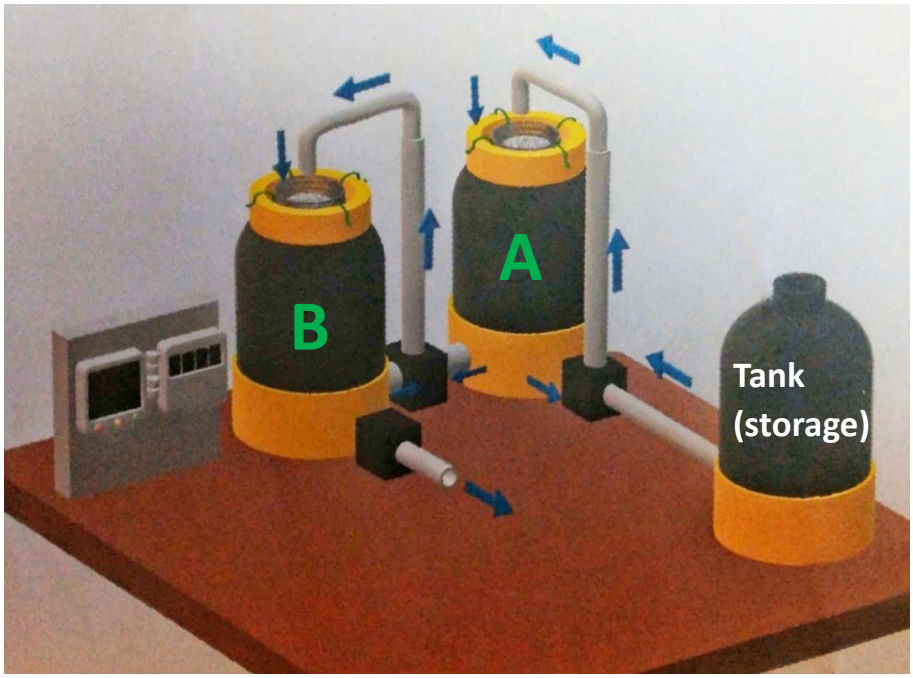

Figure 50: Pilot plant for digestate treatment.

The pilot plant is made of a storage tank in which the solution or digestate is stored and ready to be pumped into the plant. The solution throughout a pump and a three-way valve is pumped in tank A. In this Tank 1kg filter of zeolite was previously placed. The solution is recirculated on the zeolite in tank A for 3h. After this time, the solution is pumped into tank B where 200 grams of zeolite was placed. The solution is recirculated in tank B for 5 h. This process is carried out 3 times with 3 different solutions: 5L of ammonium carbonate at pH of 8,5 with different concentrations. The first two solutions had an ammonium content of 5000 mg/L, while the last solution had an ammonium content of 8000 mg/L. These high ammonium concentrations were chosen to verify the zeolite saturation in the stacked prototype. The following Table 27 showed the data result:

Table 27: Results of pilot plant: standard solution.

Standard solution: 5L NH_4CO_3					
[NH_4^+] (mg/L) IN Tank A	**[NH_4^+] (mg/L) OUT Tank A**	**mg NH_4^+ / g zeolite Tank A**	**[NH_4^+] (mg/L) IN Tank B**	**[NH_4^+] (mg/L) OUT Tank B**	**g NH_4^+ / g zeolite Tank B**
5000	1173	19,14	1173	523	6,24
5000	2615	11,92	2615	2155	11,50
8052	6927	5,98	6927	6603	6,31
	Total (mg/g)	**37,04**		Total (mg/g)	**34,05**

As it can be seen from the table, zeolite saturates as the ammonium concentration increases. It is possible to notice that in the tank A the first solution in output has a concentration slightly above 1000 mg/l, which indicates an ammonium reduction of 77%. The same solution pumped into tank B is further reduced by 50% and with this second step an overall reduction of 90% is reached. Subsequently, the tank A still breaks down about 50% of the ammonium in the new incoming solution, while the same exiting solution into the tank B is reduced by only 28%, indicating the saturation of zeolite active site. The third solution, at a concentration of 8000 mg/l, comes out of the Tank A with a very high ammonium content: the abatement occurred for about 14%. In tank B, instead, ammonium was adsorbed by a low 4%. Zeolite in tank B has practically exhausted its retention function, while the tank A, despite the three steps, still have a partial retention activity. The best performance was achieved in the first step: the abatement was almost total. A slight reduction in the nitrogen content coming out of these stages will allow the zeolite to be completely saturated and ammonium rich. This is a great feature to consider for a further use as a fertilizer in agriculture. After testing the prototype with the standard solution, pig digestate previously tested into the lab percolation system, was used into the plant. For this test, the same conditions and previous procedure for ammonium carbonate were applied:

- 5 L pig digestate: 3710 mg/L NH_4^+, pH 8,5
- Tank A: 1 kg zeolite
- Tank B: 200 g zeolite

The following table shows the results:

Table 28: Pilot plant results: pig digestate.

Pig digestate: 5L					
$[NH_4^+]$ (mg/L) IN Tank A	**$[NH_4^+]$ (mg/L) OUT Tank A**	**mg NH_4^+ / g zeolite Tank A**	**$[NH_4^+]$ (mg/L) IN Tank B**	**$[NH_4^+]$ (mg/L) OUT Tank B**	**mg NH_4^+ / g zeolite Tank B**
3710	371,5	16,69	371,5	0	18,55
3710	556,5	15,76	556,5	1589	11,13
	Total (mg/g)	**32,45**		Total (mg/g)	**29,68**

It can be noted that the zeolite ammonium absorption capacity is very efficient: in the first step in tank A, after a recirculation of 3h, the ammonium is cut off 90%. Moving to tank B, the ammonium is kept by zeolite. These results are fully consistent with the laboratory test carried out with the percolation system. In the second step with a new digestate solution at 3710 mg/L of ammonium, it can be seen the beginning of zeolite saturation: in tank A ammonium abatement is 85%, while the abatement in tank B is about 70%. Although ammonium concentrations were different in these experiments, it can also be noted that the NH_4^+ mg retained per g of zeolite are comparable with the mg NH_4^+ /g zeolite retained in the test with standard solutions:

Table 29: Pilot plant results comparison: standard solution vs real sample.

Sample	mg NH_4^+ / g zeolite Tank A	mg NH_4^+ / g zeolite Tank B
Standard solution NH_4CO_3	**37,04**	**34,05**
Pig Digestate	**32,45**	**29,68**

In both cases great results were achieved. For these reasons ammonium enriched zeolite can be considered as a fertilizer in agriculture for a further use. Thanks to these results of this study, TEA Sistemi & Tecnologie srl has been able to design and scale up the prototype plant. This plant is still building and is being applied at the company that supplied the sample of pig digestate in Piacenza area. Since large amount of digestate must be treated, the plant consists of several tanks as illustrated by the following figure 51-52:

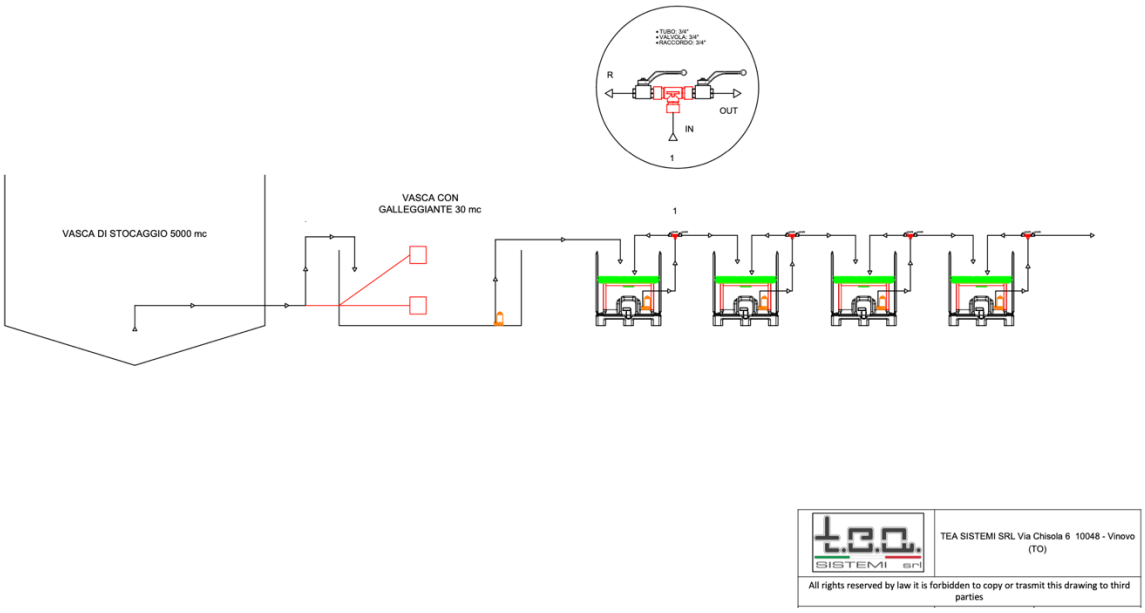

Figure 51: Scale-up pilot plant - industrial scheme by TEA Sistemi & Tecnologie srl.

From the storage tank, pig digestate goes to the settler. From there, digestate is pumped into the first tank containing the zeolite filter. Each tank has a volume of 1 m^3 and has about 200 kg of zeolite in it. The digestate is recirculated with a pumps system for about 3h, then it is pumped to the next tank. Doing more steps, pig digestate decreases gradually the ammonium content and at the end it can be used for fertigation. Once the zeolite of the first tank is completely exhausted, it will be removed and used or sold as a slow-release fertilizer. The digestate will be pumped to the second tank and the process will continue. The exhausted zeolite will be replaced, and the tank will be queued at the trial. TEA Sistemi & Tecnolgie srl is planning to implement a plant automation system to program zeolite replacement and make the process easier and more practical for users. The installation and start-up of the plant has suffered severe delays due to the COVID-19 pandemic situation and is only resumed in the last period of 2021. For this reason, reliable analytical tests on the installation have not yet been carried out. During 2020, spot analyses were carried out to verify the operation of the plant. These analyses confirmed the reductions recorded in the tests carried out with the laboratory prototype plant.

Figure 52: Scale-up industrial plant realization.

10.1.8 Study of ammonium competition with major competitors in zeolite uptake

Changing the type of digestate and feeding of digester, the composition of the digestate varies accordingly. By increasing the plant and vegetable content compared to the organic waste content of livestock, sodium and potassium salts content in the digestate increases as a consequence. However, the main competitor of ammonium in zeolite uptake is K^+, as can be seen from the following affinity scale:

$$Cs^+ > K^+ > NH_4^+ > Ba^{2+} > Na^+ > Ca^{2+} > Fe^{3+} > Al^{3+} > Mg^{2+}[56]$$

Potassium is in all plant material used, both as animal feed and as an energy source in the anaerobic digester. Since K^+ is before the NH_4^+ion in the cation affinity scale, it is necessary to define what affects the retention of NH_4^+itself within zeolite. Preliminary tests have been carried out to define the incidence of K^+ in the retention of the NH_4^+ ion, keeping the concentration of the latter constant and varying the amount of competitor in solution, defining a fixed mass of zeolite. Table 30 shows the solutions analyzed and the results:

Table 30: Synthesized solutions to study the competition between NH4+ and K+ in zeolite.

$(NH_4)_2CO_3$		KCl	ZEOLITE	NH_4^+ retained	m NH_4^+/ m ZEOLITE
N	**mL**	**N**	**g**	**%**	**mg/g**
0,10	50	/	5,1176	80,25	12,42
		0,01	5,1813	72,84	11,13
		0,02	5,0529	66,19	10,37
		0,03	5,1957	62,01	9,45
		0,04	5,0265	56,70	8,93
		0,05	5,1193	51,14	7,91
		0,06	5,1575	51,00	7,83
		0,07	5,0550	46,63	7,30
		0,08	5,0264	43,02	6,78
		0,09	5,0000	41,12	6,51
		0,10	5,0000	38,27	6,06

In Figure 53, the incidence of K^+ in the retention of NH_4^+ in natural zeolite can be assessed with data from the analyses carried out. From the data it can be observed that an increase in the concentration of K^+ corresponds a decrease almost specular and inverse in the withholding of the NH_4^+ by zeolite.

Figure 53: K+ incidence of NH4+ retention in zeolite.

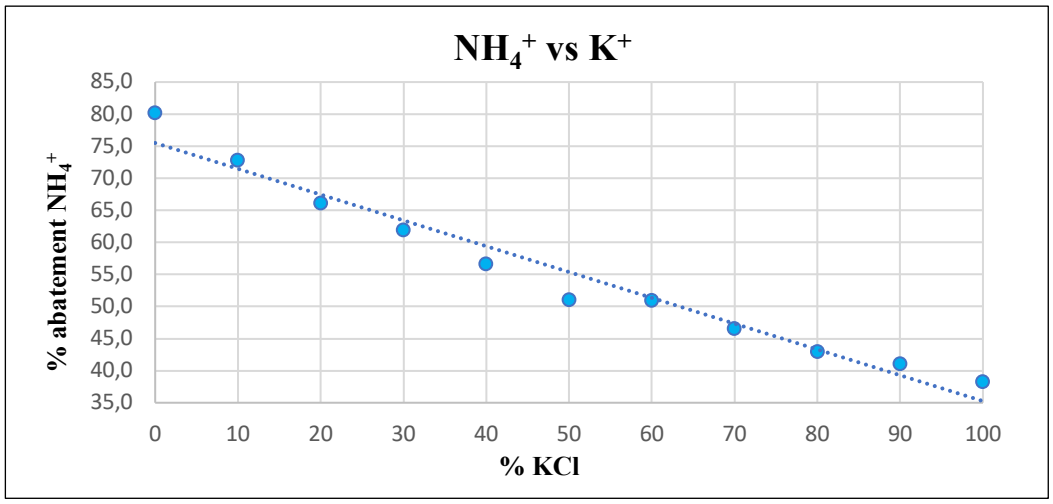

This behavior is in line with what was stated in previous works [55], [57], confirming a greater affinity of zeolite for K^+. Subsequently, the amount of zeolite was increased, and tests were carried out on solutions of $(NH_4)_2CO_3$ 0,1 N and KCl at concentrations of 0,09 and 0,1 N, as summarized in Table 31.

Table 31: Solutions analyzed with a higher zeolite content.

$(NH_4)_2CO_3$		KCl	ZEOLITE	NH_4^+ retained	m NH_4^+/ m ZEOLITE
N	mL	N	g	%	mg/g
0,10	50	0,09	16,3770	84,24	4,07
		0,10	14,3006	79,68	4,41

Although the reduction of the ammoniacal ion has increased because of a greater amount of zeolite, it is possible to see that at an increase in the concentration of K^+, the retention of the cation of interest is not particularly affected. As further confirmation, two tests were carried out keeping the concentration of K^+ fixed and varying the concentrations of NH_4^+, with a fixed amount of zeolite of 5 g. The data can be viewed in Table 32.

Table 32: Tests with fixed K+ and variable NH4+ concentrations.

KCl	$(NH_4)_2CO_3$	ZEOLITE	NH_4^+ retained	m NH_4^+/ m ZEOLITE
N	**N**	**g**	**%**	**mg/g**
1,0	0,4	5,0302	15,58	11,84
	0,8	5,0370	16,45	24,96

The results show that an increase in NH_4^+ concentration corresponds to a greater retention of the same ion by zeolite, although the percentage retention variation is very small. On the other hand, mg NH_4^+ /g zeolite is doubled for the highest concentration of $(NH_4)_2CO_3$. This result is justifiable considering that increasing the NH_4^+ concentration increases the possibility that this cation occupies inner space of zeolite, thus concurring with the K+ for zeolite cavities. Subsequently, some tests were carried out introducing in solution other cations which can easily be found both in the zootechnical wastewater and in the silage, to observe their relevance on ammonium abatement. The solution included an equal concentration, 0.1 N of the following cations: NH_4^+, K^+, Na^+ and Ca^{2+} in contact with 5 g of zeolite; the analysis was carried out in duplicate. The data for this test are presented in Table 33.

Table 33: Tests with equal concentrations of cations.

TRIAL	$(NH_4)_2CO_3$	KCl	NaCl	$Ca(NO_3)_2 \cdot 4\ H_2O$	ZEOLITE	NH_4^+ retained
/	N	N	N	N	g	%
1	0,10	0,10	0,10	0,10	5,0053	27,39
2					5,0668	29,36

Comparison with data from tests carried out on solutions containing exclusively NH4+ and K+ ions in equal quantities shows a further decrease in the ammonium retention by zeolite. Presumably the occurrence of other cations decreased the probability of ammonium adsorption, although the values of the two tests do not differ too much between them. Further analysis predicted a change in the concentration of the Na^+ and Ca^{2+} cations. Specifically, the concentration of all cations was kept constant except for Na^+ (or alternatively Ca^{2+}), the concentration of which was 25 % and 50 % relative to the other ions in solution. Data show

that a change (a decrease) in the concentration of Na^+ (or Ca^{2+}) does not have a specific effect on ammonium retention. The results can be seen in Table 34.

Table 34: Tests with varying concentrations of Na+ and Ca2+ cations.

TRIAL	$(NH_4)_2CO_3$	KCl	NaCl	$Ca(NO_3)_2 \cdot 4\ H_2O$	ZEOLITE	NH_4^+ retained
/	N	N	N	N	g	%
Ca 50 %	0,10	0,10	0,10	0,050	5,0979	28,87
Ca 25 %				0,025	5,0478	30,74
Na 50 %			0,050	0,10	5,0342	29,56
Na 25 %			0,025		5,0138	30,54

Analyses at ICP-OES identified the K^+ content remaining in solution after treatment with zeolite and are useful for estimating the overall area contained in a certain mass of natural zeolite. In fact, knowing the initial and final amount of NH_4^+ and K^+ ions it is possible to define the internal volume of zeolites. Samples with respective dilution and retention percentages are presented in Table 35. The results indicate an average of 74 % retention of the K^+ ion, a figure in line with previous considerations that establish the high affinity of this cation for zeolite cavities.

Table 35: K+ variable concentration solutions analyzed at ICP-OES.

NH_4^+	K^+	ZEOLITE	K^+ retained
N	N	g	%
0,10	0,02	5,0342	75,0 ± 3
	0,04	5,0375	79,2 ± 3
	0,06	5,1575	73,8 ± 3
	0,07	5,0550	74,1 ± 3
	0,08	5,0264	71,2 ± 3
	0,09	5,000	73,1 ± 3
	0,10	5,000	71,1 ± 3
/	0,10	5,0795	77,6 ± 3

The percentage of K^+ ion abatement is almost constant for all concentrations analyzed; values variation is justified by the difficulty of analysis, which requires many dilution steps with consequent cumulative errors. For low concentrations of K^+, the retention value does not vary a lot, and this behavior is justifiable by the high concentration of NH_4^+ ions in solution that have greater possibilities to occupy the empty spaces defined by the crystalline grid of zeolites. The following graph compares the percentages of retention of NH_4^+ and K^+ ions in natural zeolite by varying the concentration of K^+ in solution.

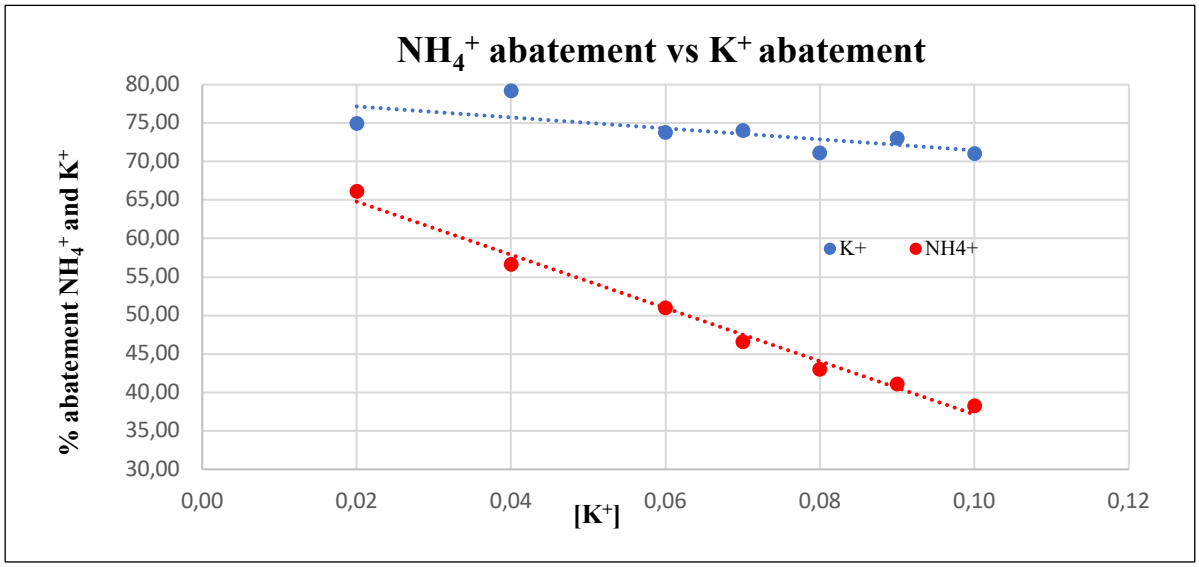

Figure 54: NH_4+ abatement vs K+ abatement graph.

The above graph shows the different affinity of the two cations for the clinoptilolite cavities used. It denotes that an increase in K^+ concentration corresponds to a decrease in the retention of the NH_4^+ ion, a result that confirms the theory of the greater affinity of K^+ for the ore pores. At the same time, an increase in K^+ concentration is almost irrelevant to the amount of this cation retained by zeolite. This demonstrates that the concentration of K^+ in solution does not affect the adsorption capacity of that ion up to the maximum concentration of 0,10 N.

10.1.9 Determination of cow digestate composition

The pH values of the samples are around 8 pH units, a typical value of digested considering the high amount of ammoniacal ions in solution and the presence of CO_2 released by anaerobic microorganisms during digestion. In the work done by the team of Normak et al.[48] Digestate pH values like those got in the laboratory can be appreciated. As a result of Kjeldahl distillation, NH_4^+ concentrations are found at around 0,1 N for all samples analyzed. The data of each digestate sample can be viewed in Table 36.

Table 36: Starting concentration of ammonium in real samples.

SAMPLE	**[NH_4^+]**	**NH_4**
/	N (eq/L)	mg/L
Digestate 1.0	0,0957	1726
Digestate 2.0	0,1015	1827
Digestate 2.1	0,1103	1990

The data in the table shows that the majority of ammoniacal nitrogen content is in the sample called "Digestate 2.1", followed by "Digestate 2.0" and by "Digestate 1.0". The increased of NH_4^+ ion in the last sample is a given in line with what is expected as ammoniacal nitrogen is soluble in aqueous compounds and, consequently, will be found in greater quantity in the liquid

fraction of the digestate. Analysis at ICP-OES investigated the presence of K^+, Ca^{2+}, Mg^{2+} and Na^+ cations within digestates. A very high concentration of K^+ is observed in all the samples analyzed, which can be justified by its large presence in plant compounds, which thus become both a food for the anaerobic digester and a nutrient source for livestock. Then follow Ca^{2+}, Na^+ and Mg^{2+} which have varying concentrations in the samples but very similar to each other and in any case much lower than those of K^+. The results of ICP-OES analyses of digestate samples are presented in Table 37.

Table 37: Concentration of the main cations in digestate samples.

ELEMENT	Digestate 1.0	Digestate 2.0	Digestate 2.1
/	mg/L	mg/L	mg/L
K	2165	2575	1708
Ca	203	370	460
Mg	83	508	210
Na	270	338	251

A survey of heavy metals was carried out in the sample "Digestate 2.1" which showed a high concentration of Cu^{2+} ions. The non-negligible amount of this metal can be justified by a possible treatment of livestock hooves with $CuSO_4$. In fact, cows raised in stables with concrete floors are subject to abrasion of the hoof, as this is soft in the inner part. A further hypothesis is that the crops from which the forage given to the animals derives come from cultivations on soils previously occupied by vineyards (the crops were treated with verdigris that has dissolved in the soil). This is followed by a high concentration of Zn^{2+}, with Mg^{2+}, $Al3^+$ and Pb^{2+}, which have very low concentration data. The results of the analysis are presented in Table 38.

Table 38: Concentrations of the main metals present in the digestate 2.1.

ELEMENT	CONCENTRATION
/	µg/L
Al	2256
Cu	20520
Fe (intensity)	92884
Mn	3736
Pb	912
Zn	10360

Heavy metals such as Cu, Zn and Pb are essential for bacterial growth in very small amounts, but higher amounts have a toxic effect.[53] Some data comparable to those obtained during research and relating to the presence and quantity of cations contained in the digestate are present in the work carried out by Normak et al.[48] and Yu Li et al.[44].

10.1.10 Abatement of ammoniacal nitrogen by zeolite in cow digestate samples

Tests were carried out to reduce the ammoniacal nitrogen in digestate samples using zeolites as retainers. The aim is to achieve an abatement rate of 60 % to lower the ammonia content and to allow farmers to increase the amount of digestate to be spread on the fields in compliance with current legislation. The tests were carried out on previously centrifuged digesters and a known volume of sample was first put in contact with 5 g zeolite. Only "Digestate 2.0" reached (and exceeded) the target of interest while the other samples had lower values of 60 % abatement. The zeolite mass was increased by another 5 g and at this point the "Digestate 1" produced an average abatement of 97,7 %, well above the target, while the "Digestate 2.1" has much lower values. Once the target for "Digestate 1" has been reached, the tests are continued only on "Digestate 2.1" increasing from time to time the amount of zeolite placed in contact with a fixed volume of sample. In addition, the way in which sample was agitated varied: it was observed that the horizontal agitation alone prevented total contact with zeolite, forming a compact bottom body at the base of the autoclavable glass bottle used as container. The cause is probably the organic fraction in the digestate which, during agitation, settles by the action of gravity on the surface of zeolite and blocks the free movement of the mineral. In addition, it should also be considered the size of the tank in which the sample is introduced: as the larger the surface area of the base of the vessel, the more contact between solution and zeolite will be facilitated. For the test involving the use of 20 g of zeolite, an oscillating roller agitator was used which allowed the contents to be shaken horizontally and obliquely by placing the autoclavable bottle horizontally. The results obtained correspond to an average abatement of 89 %, exceeding the specified abatement target. The tests carried out with the relevant results are shown in Table 39.

Table 39: NH_4^+ abatement data of different digestates varying zeolite amount.

SAMPLE	ZEOLITE	NH_4^+ retained	m NH_4^+/ m ZEOLITE
/	g	%	mg/g
Digestate 1.0	5,0352	44,25	7,59
	10,0688	97,74	8,38
Digestate 2.0	5,0348	71,93	13,08
Digestate 2.1	5,0195	40,64	8,06
	10,0258	49,00	4,39
	15,0655	60,80	3,62
	20,0604	89,13	3,94

The graph shows a linear pattern between the increase in zeolite mass and the percentage of ammonium ion retention.

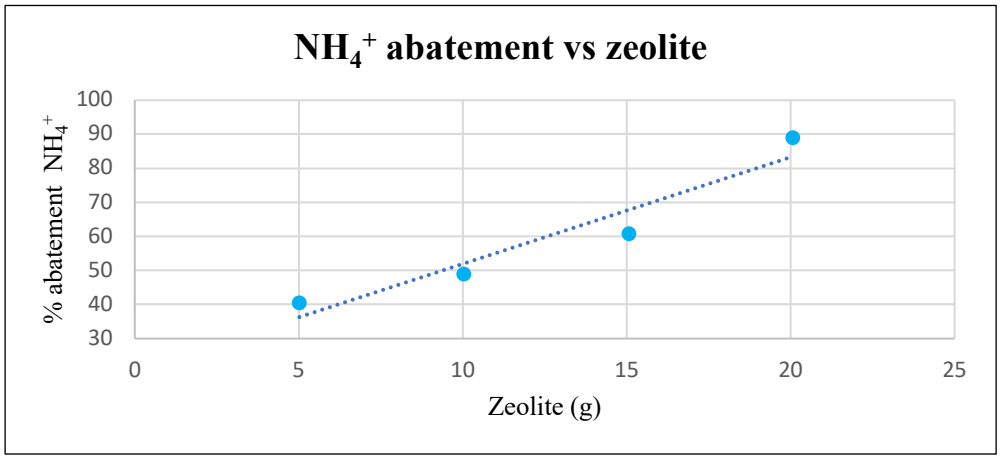

Figure 55: Trend NH_4^+ abatement vs zeolite.

A comparison between digesters can be made by observing that the composition of the anaerobic digester's feed greatly influences the reduction of the ammoniacal nitrogen in the digestate. In addition, the amount of organic matter and other insoluble residue reduces the cationic exchange capacity of zeolite, manifesting itself as a dark precipitate on the mineral mass that blocks NH_4^+ ion accesses to the zeolite internal cavities. There is no doubt that the mode of agitation has been quite effective in achieving the results, and the possibilities of detention have varied considerably. In fact, greater agitation has resulted in greater contact between zeolite and digestate. From the obtained results it is evident that in the "Digestate 1" there is a minor content of such substances while in the "Digestate 2.1" the composition contributes in more important way.

10.1.11 Detection of alkali and alkaline earth metals in the cow solid fraction

Initially, the residual ash content of the samples was defined as "Digestate 1", "Digestate 2.1" and "Digestate 2 solid". Immediately the samples were taken to dry in stove at 120 ºC to work only on the dry fraction of digested. As a result of the melting in the muffle at 550 °C, the ashes of the samples were achieved and stored in the dryer to avoid contact with atmospheric humidity. The samples ashes "Digestate 1" and "Digestate 2 dry" assumed a reddish coloration indicative of the presence of iron oxides, while the last sample had ash with gray-white hues given by silica and, in the darker part, residues of magnesium oxide. In Table 40 the ash data from the samples are presented.

Table 40: Amount of ash from each digestate sample.

SAMPLE	BEGINNING	AFTER MELTING	ASHES
/	g	g	%
Digestate 1.0	2,9836	0,7975	26,73
Digestate 2.1	1,8767	0,6553	34,92
Digestate 2 solid	1,8944	0,2175	11,48

Compared to a very similar initial mass samples "Digestate 2.1" and "Digestate 2 solid", more ashes in the first sample were observed. Considering in proportion ash amount derived from "Digestate 1" it has been noted a smaller percentage of ash than the "Digestate 2.1". These results indicate that most of mineral component remains in solution in the liquid fraction at the exit from the second anaerobic digester regarding the "Digestate 2". As for "Digestate 1" it can be observed that this is less rich in mineral compounds than the other samples. As a result of mineralization and transfer to quantitative filter paper, the ICP-OES analysis of the liquid fraction was carried out to investigate the content of alkali metals present in solution. In Table 41 it is possible to see the results.

Table 41: Data on ICP-OES analysis of digestate ash.

ELEMENT	DIGESTATE 1.0	DIGESTATE 2	DIGESTATE 2.1	DIGESTATE 2 SOLID
/	mg/L	mg/L	mg/L	mg/L
K	1087	1056	944	112
Ca	910	833	584	249
Mg	245	324	226	98
Na	120	158	148	10

A comparison of the "Digestate 1" data and the results of the other samples shows a high content of K^+ in both digestates, followed by a high value in Ca^{2+}, while Mg^{2+} and Na^+ are in smaller quantities. These results are in line with what is expected as K+ is among the most present alkaline metals in vegetation (one of the three macro-elements, along with N and P) used as a nutrient and Ca^{2+} (one of the meso-elements, along with Mg and S) plays an important role in the mechanical strength of plants. The lower amount of Mg^{2+} is attributable to the high concentration of the elements described above that act as antagonists in the absorption of this meso-element. The low amount of Na+ is justifiable by the high content of K^+ which can perform the same functions. The quantitative filter paper, together with the trapped precipitate, consisting largely of silicates, was placed in the crucible, and left in the oven at 120 °C for one night. Inside graphite crucibles has been inserted the $LiBO_2$ that works as flux, in the ratio of 1:4 between SiO_2 and $LIBO_2$, and above have been placed the ashes of digested. At the end of the melting process in a 900 °C muffle, dissolution of the pearl formed in the 5% HNO_3 solution and filtration, was analyzed at the ICP-OES the filtrate of each sample (previously brought to

volume in a flask) for the search of Si and Fe. The analysis should be performed in the same day as the precipitation of silicic acid is observed in an acidic medium. Data are shown in Table 42.

Table 42: ICP-OES analysis data for Fe and Si.

ELEMENT	DIGESTATE 1	DIGESTATE 2	DIGESTATE 2.1	DIGESTATE 2 SOLID
/	mg/L	mg/L	mg/L	mg/L
Fe	112	99	34	65
Si	1150	1770	1240	530

Comparing the results of "Digestate 1" with the results of "Digestate 2" results in a high Si content in both samples. The Si^{2+} (considered one of the essential microelements for the growth of the plants) is absorbed by the plants with the function of physical and biological barrier because, being in the cuticle of the leaves, goes to thicken the cell walls and decreases the sites of attack by pathogens. Consequently, the high Si content in "Digestate 2" may be an indication of a higher plant matter content in the biodigester than "Digestate 1". The content of Fe in both samples is significantly lower than Si: this is partly since this element in nature is hardly available for plants and the occurrence of other elements that prevent its absorption. Studying the results of the samples "Digestate 2.1" and "Digestate 2 solid" denotes a higher Si content in the liquid fraction of the digestate than the solid one. The silicon compounds were probably dissolved in the form of colloidal substances, observable as a thin layer over the zeolites during the ammonium ion abatement tests. More Fe is in "Digestate 2 solid".

10.1.12 Adsorption kinetics: comparison with cow digestate

The tests were carried out using the indophenol method, which involves the use of many reagents, including sodium dichlorocyanate solution ($C_3Cl_2N_3NaO_3$) which is decisive in the success of the analysis. In fact, the free chlorine that forms during the reaction is important for the realization of the derivative of indophenol, without which the reaction of NH_3 does not take place and, consequently, a variation in the coloration of the solution is not observed. After constructing the calibration curve using NH_4Cl as standard, an ammoniacal nitrogen retention test was made in zeolite using $(NH_4)_2CO_3$ 0,1N as the ammonium ion source. The time interval at which the samples were taken and the volumes to be taken was decided, considering a maximum adsorption time of 24 h (time interval during agitation for the preceding abatement tests). This verification is necessary to go to evaluate on which kinetics of absorption the system is based. In Table 43 it is possible to observe the times and the amount of NH_4^+ remaining corresponding, while in figure 56 it is possible to appreciate the absorption kinetics.

Table 43: Unabsorbed NH4+ during time.

Time	NH_4^+ in solution
h	mg/L
0	245,8
0,5	218,7
1	197,5
2	138,3
4	75,5
6	60,7
8	52,7
24	24,0

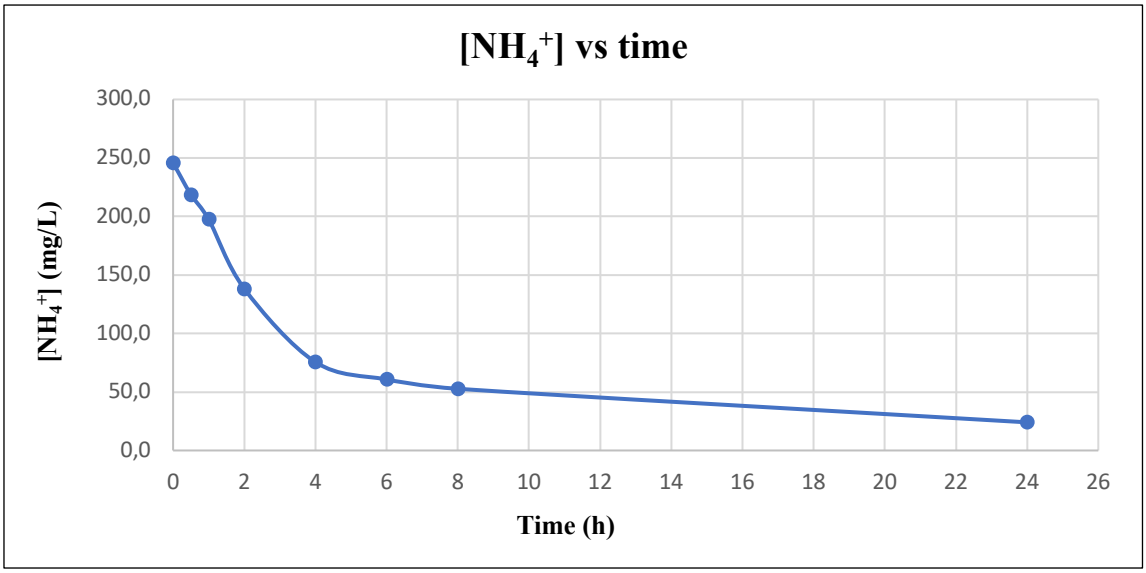

Figure 56: NH_4^+ uptake kinetics in clinoptilolite.

The graph shows that the concentrations of NH_4^+ in solution decrease over time with a pseudo-second order kinetics as described by the work carried out by Aydin et al.[221] In fact, it is observed that, after a certain interval of time, the rate of abatement decreases up to the complete occupation of the available sites of zeolites. The analysis of the kinetics of the samples "Digestate 1" and "Digestate 2.1" show an identical trend both between them and with respect to the test carried out with $(NH_4)_2CO_3$. The data of the absorption kinetics of the two samples are presented in Table 44.

Table 44: Unabsorbed NH4+ vs time in digestate samples.

Time	NH_4^+ Digestate 1	NH_4^+ Digestate 2.1
h	mg/L	mg/L
0	337,6	597,7
0,5	323,6	542,0
1	193,6	370,8
2	86,9	243,0
4	51,8	124,6
6	48,6	98,1
8	47,3	68,1
24	42,9	42,9

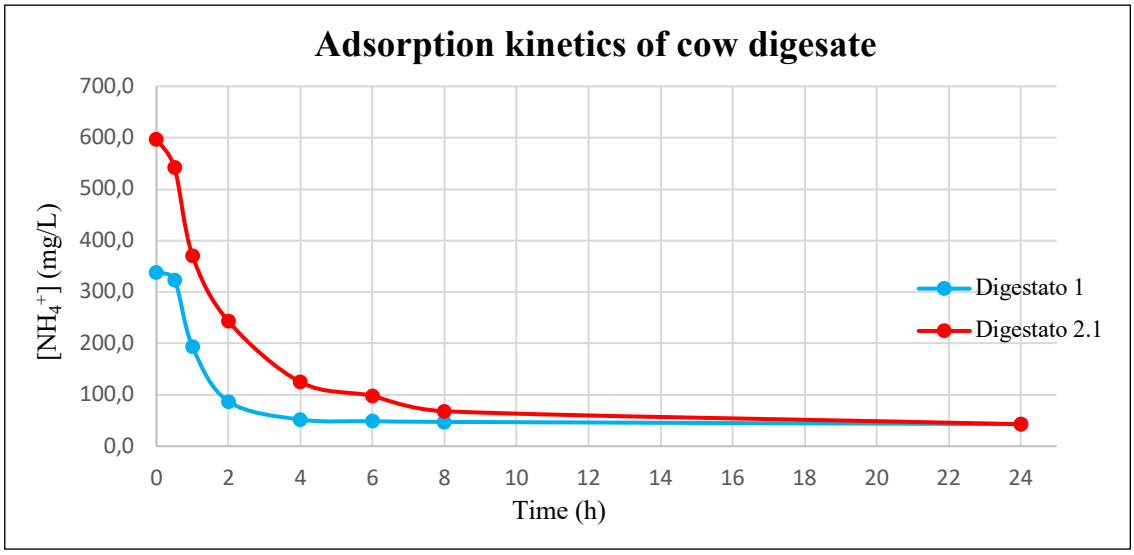

Figure 57: Adsorption kinetics of cow digestate.

Analyzing the behavior over time, it can be observed that the kinetics of both digestate samples are the same, only the initial concentrations of NH_4^+ vary. After a certain amount of time, the concentration of NH_4^+ absorbed tends to stabilize, behaving asymptotically, but never reaching

Figure 58: Comparison between ammonium abatement in digestate samples.

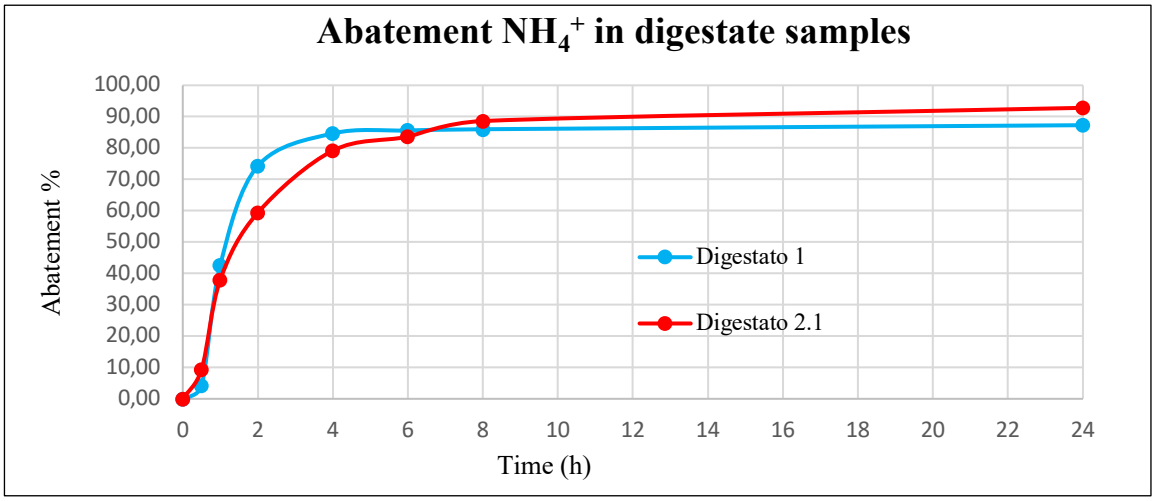

a total absorption of the cation concerned because it comes first to saturation of the pores of zeolite. From Figure 58 it is possible to see that the achievement of the 60 % abatement target takes less than 2 hours for the "Digestate 1" and a little more than 2 hours for the "Digestate 2.1". Retention of the NH_4^+ ion is greater than 80 % in both analyzed samples after six hours from the start of digestate recirculation on zeolite. These results are in line with previous tests, demonstrating once again that the presence of organic compounds is decisive in the cationic exchange of zeolite. In both samples it is observed that the kinetics reach a maximum after 1 hour from the start of the test to slow down successively, first slowly and then faster, without ever reaching 100 % abatement.

10.1.13 Water release tests and nitrate content

Kjeldahl distillations of NH_4Cl solutions 1000 mg/L treated with zeolite for one day produced the results presented in Table 45.

Table 45: ammonium adsorption by zeolite during time.

DAY	NH_4^+ in solution	NH_4^+ retained
/	mg/L	%
1	81	91,9
2	198	80,2

Data show that the amount of NH_4^+ remaining in solution on the second day is double that of the first day. This behavior suggests that the cations initially occupy the most available cavities on the zeolite surface while, afterwards, they cover the innermost concavity. The retention values are very high and demonstrate the high affinity of clinoptilolite for the NH_4^+ ion. The kinetics of ammoniacal nitrogen release into water were evaluated: known volumes were taken at defined times of the zeolite previously charged with the 1000 mg/L NH_4Cl solution and the release was verified through spectrophotometric analysis. The table 46 shows the obtained values and in Figure 60 it is possible to appreciate the release trend.

Table 46: Times and amount of NH4+ released by zeolite.

Time	NH_4^+ release
h	mg/L
6	15,19
24	18,72
48	21,72
72	24,11
168	22,38
432	11,67

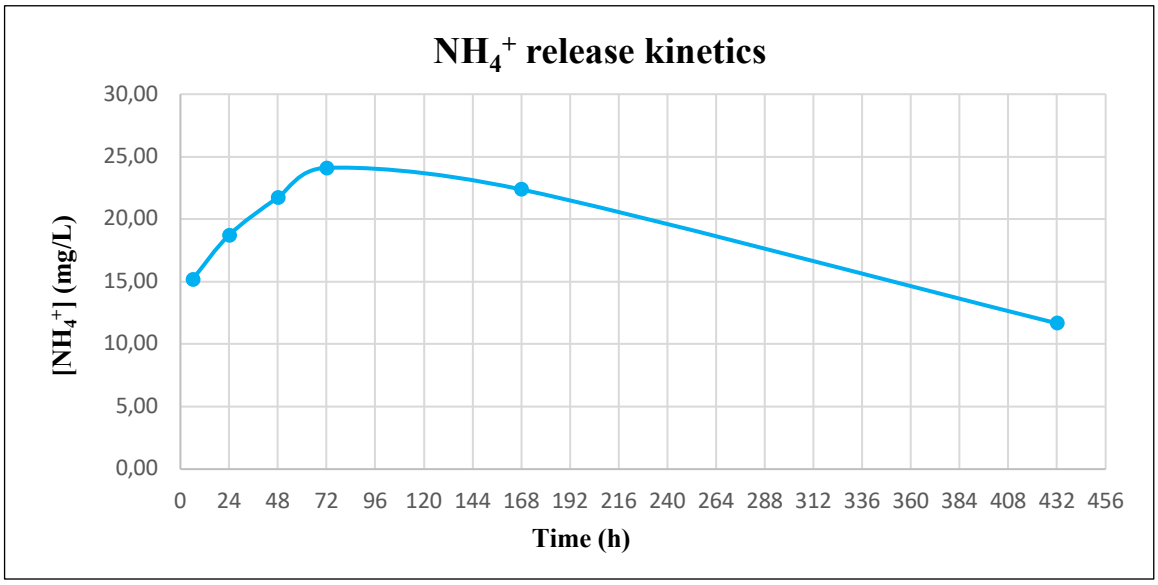

Figure 59: Ammonium release kinetics in water.

The graph displays the trend of NH_4^+release in water and it can be seen the achievement of a maximum at 72 h. Next, the amount of cation released into water also decreases due to oxidation phenomena that lead to the formation of the NO_3-ion. The trend observed on the chart suggests that zeolite releases slowly and in small doses the substances contained in it, corresponding to the description of slow-release fertilizer. The NH_4^+ ion release tests were performed for zeolites loaded with different K^+/ NH_4^+ ratios and for some zeolites loaded with digestate samples. The times and quantities issued for each sample are presented in Table 47 and the amount of zeolite treated is shown in brackets. Release kinetics can be viewed in Figure 60.

Table 47: NH_4^+ release over time for zeolite samples.

Time	**DIGESTATE 1.0 (10 g)**	**DIGESTATE 2.1 (15 g)**	**DIGESTATE 2.1 (20 g)**	**K/NH_4 1:9 (5 g)**	**K/NH_4 1:5 (5 g)**
h	mg/L NH_4^+	mg/L NH_4^+	mg/L NH_4^+	mg/L NH_4^+	mg/L NH_4^+
6	0,85	13,46	14,26	67,98	63,96
24	7,39	22,12	22,36	81,64	75,41
48	7,08	23,95	20,84	82,29	76,43
144	5,06	24,91	23,79	113,93	91,43
408	5,85	26,84	19,40	87,30	60,10

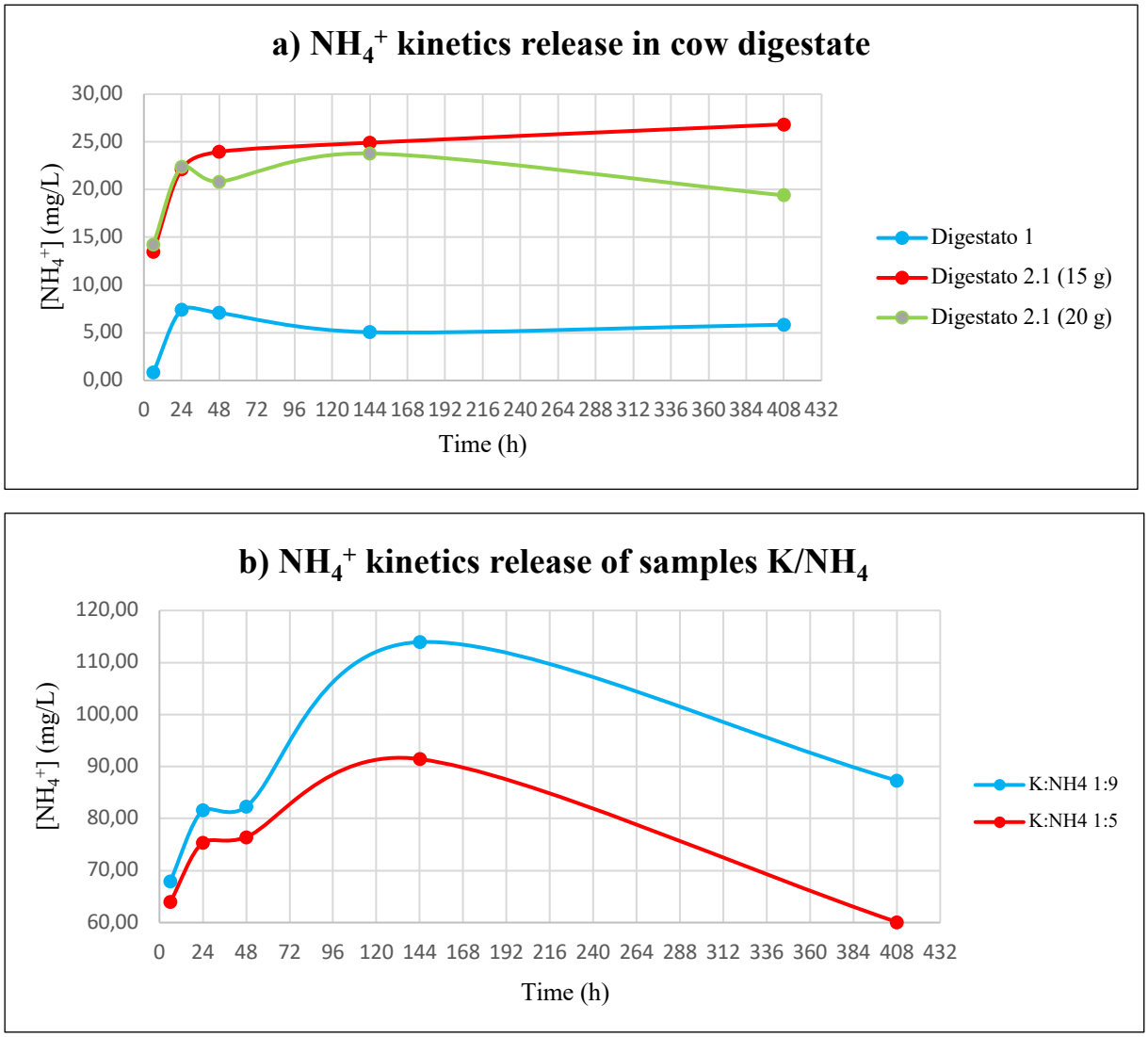

Figure 60: a) NH4+ release kinetics in water of zeolites loaded with digestate samples. b) NH4+ ion release kinetics in water of zeolites loaded with K:NH_4 samples.

As in the case described above, a larger initial release of the NH_4^+ ion (in this case in the first 24 h) is observed also for zeolites loaded with digestates followed by an approximately constant or slightly decreasing release of ammoniacal ion during time. The reason for the decrease in ammonium release can be traced back to the simultaneous oxidation of this ion in NO_3^- which is visible from the inversion in the slope of the curve in "Digestate 2.1" with 20 g of zeolite. In zeolite samples ammonium-rich with "Digestate 1" and "Digestate 2.1" with 15 g zeolite the curve reaches a maximum and keeps it almost unchanged over time. The difference in concentrations reflects the different concentrations of ammoniacal nitrogen present in zeolites. For zeolite samples enriched with standard solutions at different K^+/ NH_4^+ ratios, there is an equal trend in the two curves, with a sudden increase in NH_4^+ release in the first hours of contact with water. The trend reflects the previously shown trend of the standard solution of only NH_4^+.

At the same time, analyses were performed at the ICP-OES to verify the release of the K^+ ion from samples with different K:NH_4 ratios. The values are shown in Table 48 and Figure 61.

Table 48: Potassium release by zeolite.

Time	K^+ (K:NH_4 1:9)	K^+ (K:NH_4 1:5)
h	µg/L	µg/L
6	10345	13050
24	11750	16310
48	12420	16925
144	12320	17305
408	7950	9680

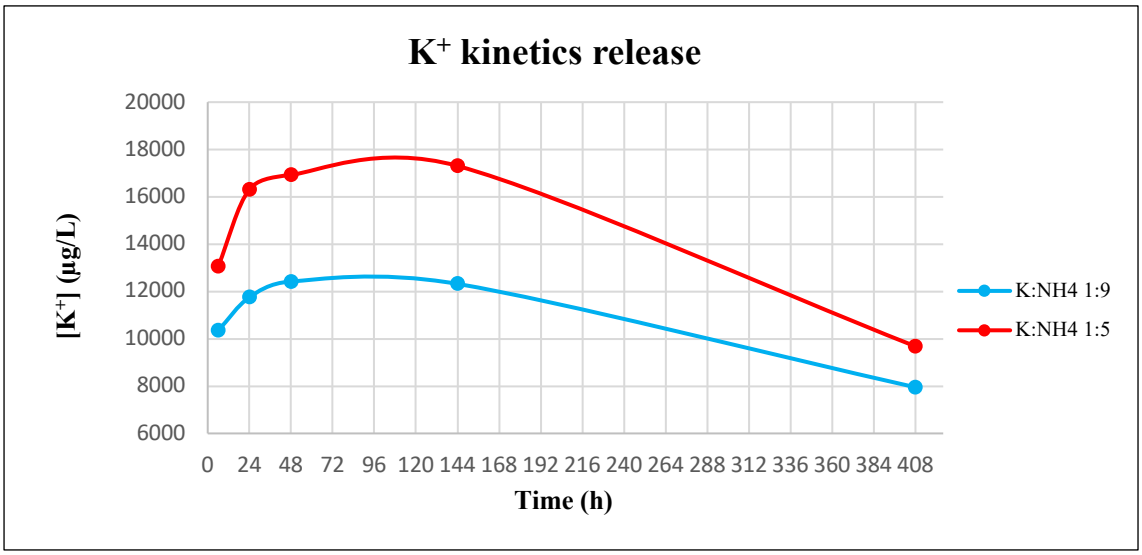

Figure 61: Potassium release by zeolite (graph).

The release kinetics of the K+ ion by zeolite is very similar to those observed for the NH_4^+ ion in the standard solution. Initially there is a very high release of this cation and then the amount of K^+ released decreases. The result shows, once again, that zeolite behaves like a slow-release fertilizer. After several months from the sampling of digesters 1.0 and 2.1, Kjeldahl distillations were again carried out to determine the residual content of NH_4^+ and total N. The results of these analyses can be seen in Table 49.

Table 49: Ammonium concentration in digestate samples.

SAMPLE	[NH_4^+] starting	[NH_4^+] final	[N] total
/	mg/L	mg/L	mg/L
Digestate 1.0	1726	226	334
Digestate 2.1	1990	956	1209

The tabulated values indicate that the sample "Digestate 1.0" has lost over time a high amount of NH_4^+ while the "Digestate 2.1" slightly less. The values for the total ammoniacal nitrogen content show that the second sample has a higher concentration of this compound. Following

the determination of the pH value, "Digestate 1.0" shows a pH =7 while "Digestate 2.1" a pH=8. In the first sample the pH value has changed over time, and this can be caused by the oxidation of ammoniacal nitrogen to nitric nitrogen which tends to acidify the environment. In the second digestate, however, the pH did not change significantly. To verify the presence and the content of NO_3^- released by the zeolites previously loaded, as well as the hypothesis of the transformation of NH_4^+ to NO_3^-, the content of this anion has been determined. The achieved results are shown in Table 50.

Table 50: Nitrates release by zeolite.

Time	DIGESTATE 1.0 (10 g)	DIGESTATE 2.1 (15 g)	DIGESTATE 2.1 (20 g)
h	mg/L NH_4^+	mg/L NH_4^+	mg/L NH_4^+
6	12,74	12,43	14,76
24	12,82	13,86	13,76
48	12,89	14,54	14,26
144	29,82	43,72	57,30
408	15,17	11,67	293,95

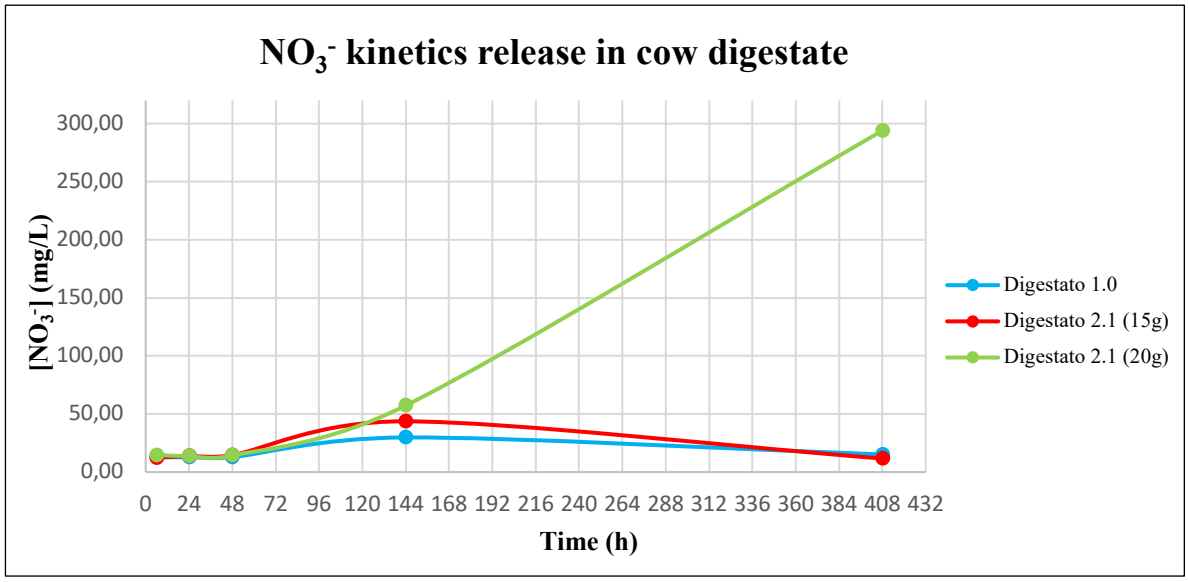

Figure 62: Nitrates kinetics release by zeolite.

The release kinetics of the NO_3^- ion in digestate samples shows the behavior of the curves is opposite to the curves regarding the release kinetics of NH_4^+. At the beginning the NO_3^- content is very low in solution but as time passes, the amount of this anion grows over time. The behavior is the same for digestate samples in contact with limited amounts of oxygen, while for sample "Digestate 2.1" with 20 g zeolite, in which the amount of oxygen in contact with the solution was much higher, there is an important transformation of NH_4^+ into NO_3^-.

10.1.14 Chemical Analyses of Zeolite: Strawberries cultivation

After the study of zeolite and its ammonium absorption characteristics, zeolite was tested as a slow-release fertilizer. Prior to the beginning and after the end of plant growth, the substrates from the various treatments were analyzed. The different amounts of nitrogen supplied to the different theses are shown in Table 51. The measurements were taken in triplicate. As Table shows, the NH_4-N and NO-N contents in the substrate were quite low. At the beginning of the growing cycle, N contribution to the plant was almost entirely dependent upon enriched zeolites. As indicated by the N % absorbed by the plant, the adsorption of nitrogen increased linearly with increased enriched zeolite intake [222].

Table 51: Nitrogen in its various forms measured at the start and at the beginning end of the strawberries growing cycle end absorbed by the plant (± SD).

Treatment	**NH_4^+ as N in soil (g)**	**NO_3^- as N in the soil (g)**	**NH_4^+ as N (g) intake zeolites**	**N tot at start (g)**	**NH_4^+ as N at end (g)**	**NO_3^- as N at end (g)**	**N tot at end (g)**	**Plant absorbed N (%)**
Control	0.189 ± 0.05 0.455 ± 0.03		-	0.64 ± 0.06 d	0.15 ± 0.02 c	0.24 ± 0.01 c	0.39 ± 0.02 c	40.22 ± 0.1 b
Zeolite - 30%			6.22 ± 0.11	6.87 ± 0,08 c	1.69 ± 0.06 b	0.59 ± 0.05 a	2.28 ± 0.07 b	66.76 ± 0.2 a
Zeolite			8.71 ± 0.13	9.36 ± 0.10 b	2.08 ± 0.07 b	0.48 ± 0.04 b	2.56 ± 0.07 ab	72.69± 0.3 a
Zeolite + 30%			11.2 ± 0.09	11.84 ± 0.15 a	2.46 ± 0.05 a	0.31 ± 0.02 c	2.77 ± 0.03 a	76.60 ± 0.3 a

Mean values followed by the same letter (a,b,c) are not significantly different at a $p \leq 0.05$ level.

10.1.15 Plant Growth and Flowering

Three weeks after the plants were transplanted to the treatment pots, the flower counts for each treatment (higher to lower) were as follows: zeolite > zeolite + 30% and zeolite − 30% > control, but only Zeolite and Control showed statistical difference (Table 52). The same result was observed for the total count of flowers per plant. These results confirm that, in general, N fertilization effectively promotes strawberry flower production, which was also observed by Durner [223].

Table 52: Effect of zeolite application on vegetative growth: flower count per plant.

	Days after transplant			
Treatment	**7**	**14**	**21**	**Total**
Control	0.1 ^{a}	1.6 ^{a}	0.6 ^{b}	2.3 ^{b}
Zeolite - 30%	0.2 ^{a}	2.1 ^{a}	1.5 ^{ab}	3.8 ^{ab}
Zeolite	0.3 ^{a}	1.8 ^{a}	2.5 ^{a}	4.6 ^{a}
Zeolite + 30%	0.3 ^{a}	2.1 ^{a}	1.5 ^{ab}	3.9 ^{ab}

Mean values followed by the same letter (a,b,c) are not significantly different at a $p \leq 0.05$ level.

Fertilizer treatments with N released by zeolite also improved strawberry plant growth. In fact, the treated plants showed a statistically higher leaf length, as summarized in Table 53.

Table 53: Effect of zeolite application on vegetative growth: average leaf length (cm).

	days after transplant		
Treatment	**7**	**14**	**21**
Control	3.13 [c]	3.31[c]	3.75 [c]
Zeolite - 30%	4.06 [a]	4.38 [a]	4.75 [a]
Zeolite	3.43 [b,c]	3.79 [b]	4.36 [b]
Zeolite + 30%	3.69 [a,b]	4.13 [a,b]	4.63 [a,b]

Mean values followed by the same letter (a,b,c) are not significantly different at a $p \leq 0.05$ level.

Different levels of zeolite added to strawberry plants resulted in increased leaf length during the growing season (Table 54). The treatment also significantly increased the number of leaves per plant compared to the control, particularly by the end of the trial. The plants treated with the highest amount of ammonium-enriched zeolite (zeolite + 30%) had the highest number of leaves per plant (15.1), while the control had the fewest (11.6). These results were consistent according to data literature [224], [225] .

Table 54: Effect of zeolite application on vegetative growth: number of leaves per plant.

	Days after transplant			
Treatment	**7**	**14**	**21**	**60**
Control	11.2 [a]	11.9 [a]	12.9 [a]	11.6 [b]
Zeolite - 30%	8.7 [a]	10.0 [a]	11.4 [a]	13.0 [a,b]
Zeolite	8.3 [a]	9.9 [a]	10.6 [a]	12.6 [a,b]
Zeolite + 30%	9.9 [a]	11.1 [a]	12.5 [a]	15.1 [a]

Mean values followed by the same letter (a,b) are not significantly different at a $p \leq 0.05$ level.

The data summarized in Table 54 exhibit a linear increase in the number of leaves per plant throughout the season for all zeolite treatments compared to the control. The control plants increased in the number of leaves per plant by only a small amount (3.6%), as opposed to the increases observed for zeolite − 30% (49.4%), zeolite (51.8%) and zeolite + 30% (52.5%). These results are evidence that the number of leaves per plant increased as the ammonium-enriched zeolite content in the substrate increased. By the end of the growing cycle, significant differences among the treatments and the control were revealed.

10.1.16 Plant Weights

The ammonium-charged zeolite treatment significantly affected the accumulation of water and nutrients, as demonstrated by the changes in plant weight measured in the experiment. At the end of the trial, the weight of the control plants was unchanged from their beginning weights. In contrast, the zeolite-treated plants weighed significantly more (Table 55). Prasad et al.[226]

also reported that a higher proportion of zeolite in a fertilizer substrate improved the vegetative growth (as evidenced by plant weight) of strawberry plants. In addition, in this case, the different amounts of zeolite added to cultural substrate correspond to different amounts of N.

Table 55: Effect of zeolite application on vegetative growth: plant fresh weight (g).

Treatment	day 0	day 60
Control	24.0 ^{a,A}	24.0 ^{c,A}
Zeolite - 30%	21.7 ^{a,B}	40.9 ^{a,A}
Zeolite	19.4 ^{a,B}	35.7 ^{b,A}
Zeolite + 30%	29.6 ^{a,B}	41.4 ^{a,A}

Mean values followed by the same letter (a,b,c,A,B,C) are not significantly different at a $p \leq 0.05$ level. Lowercase letters in the same column are used to compare treatments. Uppercase letters in the same row are used to compare storage times

10.1.17 Leaf Color and Chlorophyll Content

The mean values of the L* color parameter are displayed in Table 56. The upper side leaf L* parameter measures differed significantly among the treatments at the 14-, 21-, and 60-day intervals of the production cycle. Briefly, the L* values measured on the leaves decreased during the vegetative period and increased on the last day of the trial period. After 14 and 60 days, the treatments Zeolite − 30% and Control showed the highest values of L*, yielding a more brilliant color. This was probably related to the N content of the leaves; a high N content generally causes a darker color.

Table 56: Effect of zeolite application on leaves color: lightness parameter (L).*

	days after transplant			
L*	7	14	21	60
Control	42.37 ^{a,B}	41.81 ^{b,C}	40.80 ^{a,C}	44.99 ^{a,A}
Zeolite - 30%	42.37 ^{a,B}	41.35 ^{a,B}	37.51 ^{b,C}	47.91 ^{a,A}
Zeolite	42.37 ^{a,B}	38.16 ^{b,C}	34.79 ^{c,D}	44.19 ^{b,A}
Zeolite + 30%	42.37 ^{a,A}	39.44 ^{b,B}	36.92 ^{b,C}	43.52 ^{b,A}

Mean values followed by the same letter (a,b,A,B,C,D) are not significantly different at a $p \leq 0.05$ level. Lowercase letters in the same column are used to compare treatments. Uppercase letters in the same row are used to compare storage times.

The opposite trend was observed in leaf color (C) values (Table 57). During vegetative growth, the C values increased in all treatments, with higher values being recorded in the control treatment leaves which then decreased on the last day of analyses. This finding suggests that plants treated with high quantities of ammonium-enriched zeolite had less-brilliant (duller), lower saturated and darker green leaves compared to the control plant leaves. Changes in chlorophyll content determine changes in leaf color. The chlorophyll content was significantly affected by the amount of N released by enriched zeolite at all times of analysis (Table 57). The chlorophyll content was negatively affected in the control treatment and in the zeolite −

30%, i.e., the samples lost 20.3% and 11.3% of chlorophyll content, respectively. The zeolite and zeolite + 30% treatment leaves were significantly higher in chlorophyll content throughout vegetative growth, with no significant losses during the evaluated periods. More intense green leaf color resulting from higher chlorophyll contents was observed in treatments with higher ammonium-enriched zeolite concentrations.

Table 57: Effect of zeolite application on leaf color: Chroma parameter (C).*

	days after transplant			
C*	**7**	**14**	**21**	**60**
Control	15.92 ^{a,B}	24.14 ^{a,A}	24.90 ^{a,B}	9.76 ^{b,C}
Zeolite - 30%	15.92 ^{a,B}	18.70 ^{a,A}	17.57 ^{a,A,B}	16.8 ^{a,A,B}
Zeolite	15.92 ^{a,C}	19.21 ^{a,B}	23.87 ^{a,A}	9.29 ^{b,D}
Zeolite + 30%	15.92 ^{a,B}	21.12 ^{a,A}	17.37 ^{b,A}	8.83 ^{b,C}

Mean values followed by the same letter (a,b,A,B,C,D) are not significantly different at a $p \leq 0.05$ level. Lowercase letters in the same column are used to compare treatments. Uppercase letters in the same row are used to compare storage times.

Table 58: Effect of zeolite application on chlorophyll content: SPAD index.

	days after transplant			
SPAD	**7**	**14**	**21**	**60**
Control	45.60 ^{a,A}	37.25 ^{b,B}	35.33 ^{b,B}	36.33 ^{b,B}
Zeolite - 30%	45.60 ^{a,A}	41.50 $^{a,b,\ A,B}$	41.20 $^{a,b,\ A,B}$	40.46 ^{a,B}
Zeolite	45.60 ^{a,A}	45.43 ^{a,A}	43.74 ^{a,A}	41.92 ^{a,A}
Zeolite + 30%	45.60 ^{a,A}	42.60 ^{a,b,}	44.10 ^{a,A}	41.52 ^{a,A}

Mean values followed by the same letter(s) (a,b,A,B) are not significantly different at a $p \leq 0.05$ level. Lowercase letters in the same column are used to compare treatments. Uppercase letters in the same row are used to compare storage times.

10.1.18 Production

The addition of ammonium carried by zeolite resulted in a significant increase in the count of harvested fruits per plant, although the count increase was not proportional to the quantity of ammonium-enriched zeolite in the substrate (Table 59).

Table 59: Effect of zeolite application on vegetative growth: harvested fruits/plant, total fruit weight, count of stolons/plant.

Treatment	Harvested fruit per plant	Avg fruit weight (g)	Number of stolons/plants*
Control	4.2 ^{b}	6.1^{a}	0
Zeolite - 30%	6.7 ^{ab}	5.6^{a}	7
Zeolite	4.6 ^{b}	5.3^{a}	8
Zeolite + 30%	8.0 ^{a}	5.3^{a}	10

[1] Means values followed by the same letter a, b, ab are not significantly different at a $p \leq 0.05$ level. *Raw data

Generally, fruit size is inversely related to the number of fruits, but in this case, no significant differences were found in average fruit weight among the different treatments, even if the harvested fruits per plant were statistically different. The treatment with N released by zeolite

also increased the count of stolons/plant. Stolon is the vegetative propagation organ naturally produced by strawberries, and it is produced by the plant when nutrient availability is adequate [227]. No stolons were produced in the control treatment, which, according to Durner [219], is an indication that the plant is receiving a low amount of N.

10.1.19 Fruits

High sugar and relatively high acid contents are required for good flavor in strawberry fruit [228]. As shown in Table 60, the values for TSS and TA indicate significant differences among the treatments. The highest TSS (7.90 ◦Brix) and TA (134.04 m_{eq}/L) values were found in zeolite-treated samples, while the lowest were recorded in the control strawberries (6.87 ◦Brix and 103.7 m_{eq}/L), respectively. Ali et al.[229] similarly observed that different rates of N fertilizer significantly changed acidity in blackberry and reported that the use of N released by zeolites produced the highest acidity in strawberry. The observed data suggest that zeolites are efficient carriers of N to plants.

Table 60: Titratable Acidity (TA) (m_{eq}/l), Total Soluble Solid (TSS) (°Brix) and Total Phenolic Content (TPC) (mg Gallic Acid/100g FW).

	TA (meq/l)	TSS (°Brix)	TPC (mg Gallic Acid/100g FW)
Control	103.70 [c]	6.87 [c]	73.04 [b]
Zeolite - 30%	121.42 [b]	7.25 [b]	69.54 [c]
Zeolite	134.04 [a]	7.90 [a]	73.30 [b]
Zeolite + 30%	121.83 [b]	7.37 [b]	78.41 [a]

Mean values followed by the same letter(s) a,b,c) are not significantly different at a $p \leq 0.05$ level.

With respect to phenolic content, significant differences were found among treatments, with the highest phenolic contents having been observed in zeolite + 30%. Previous work on tomato [226] was also found that increased N fertilization positively affected the total phenolic content. The data obtained here suggest that adding ammonium-enriched zeolite to the cultural substrate is useful to raise the nutritional value of a product due to the known role of phenols as powerful antioxidants.

10.1.20 Microbial Abundances

The total bacteria, archaea, ammonia-oxidizing bacteria (AOB) and ammonia-oxidizing Archaea (AOA) in the substrates were all measured at the end of the period of plant growth (Table 61). The measurements were taken in triplicate and mean values and standard errors were calculated. Total bacteria and total archaea (data not shown) did not differ significantly in the presence of zeolite compared to the control. Overall, AOB were more abundant in zeolite-treated samples, in which AOA were less abundant than AOB, but not significantly

different from zeolite-treated samples, relative to the control. This might arise from the fact that AOB and AOA normally prefer to grow in different soil N conditions; specifically, AOB prefers high ammonia substrates while AOA prefers low ammonia substrates [230]. Data literature have showed that AOB are functionally more important than AOA in NH_3 oxidation in some agricultural soils. The increased abundance of AOB in the presence of ammonium-enriched zeolite suggests that it may favor a stable and active presence of AOB [231] that can release nitrate to the plant. On the other hand, and at the same time, the fact that AOB did not differ in the presence of different zeolite concentrations seems to confirm its slow-release capacity, as microbial communities are affected by nutrients in the substrate solution. However, in this experiment, it was impossible to clearly determine the extent of the effect of zeolite on AOB and other microbial communities with respect to the effect on N. This aspect needs to be evaluated in dedicated experiments in the future.

Table 61: Abundance of microbial markers in the growth substrate at the end of the experiment (± SD).

Treatment	Bacteria (Log copies g^{-1} dry soil)	AOB (Log copies g^{-1} dry soil)	AOA (Log copies g^{-1} dry soil)
Control	9.11 ± 0.30^{a}	4.49 ± 0.47^{b}	4.55 ± 0.39^{a}
Zeolite - 30%	9.33 ± 0.38^{a}	6.46 ± 0.37^{a}	4.57 ± 0.60^{a}
Zeolite	9.49 ± 0.15^{a}	6.73 ± 0.18^{a}	5.14 ± 0.46^{a}
Zeolite + 30%	9.42 ± 0.24^{a}	7.60 ± 0.31^{a}	4.74 ± 0.04^{a}

Means values followed by the same letter(s) (a,b) are not significantly different at a $p \leq 0.05$ level

10.2 Anionic nanosponges: synthesis characterization

10.2.1 Hypothesis of reaction mechanism

The synthesis mechanism can be described by two distinct phases, assumed to be responsible for the generation of the polymer network. For synthesis a basic environment (NaOH 0,2 M) has been chosen to catalyze the opening reaction of the epoxide ring present in the structure of the BDE/TTE or NGDE crosslinking agent (as described in Figure 64). This interaction would generate reactive species with negative charge (alcoxides), supposed to be the initial products of the reaction (first phase). Alcoxides, formed in this way, should not only interact with maltodextrin (GLU2) later, but should also be responsible for opening the ring of the reticulating agent (Figure 65), thus allowing the start of the polymerization step and therefore the growth of polymeric chains (second phase) [142]. In addition, the main strategy to introduce negative charges in the maltodextrin structure was to functionalize the polysaccharide skeleton by DABCO (initially used as catalyst of the reaction) and choline chloride. For characterization

of anionic nanosponges, it can be assumed a mechanism of reaction through which nanosponges can cross-link. Choline is introduced as a pendant group thanks to a reaction between the hydroxyl group of the choline and the electron-acceptor group of the cross-linker. As an example, the supposed mechanism is shown in figure for TTE crosslinker, in the absence or in presence of choline.

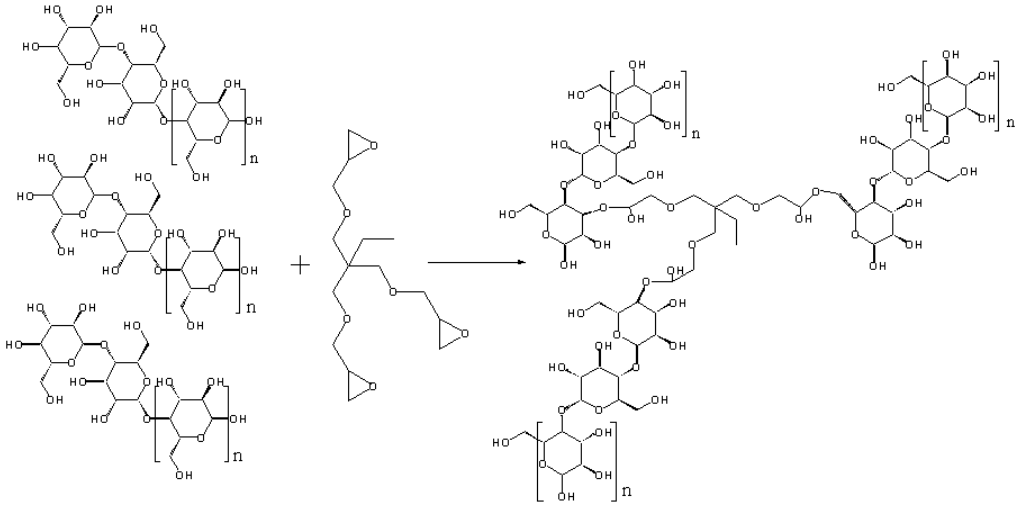

Figure 63: Cross-linking with TTE and maltodextrin in absence of choline.

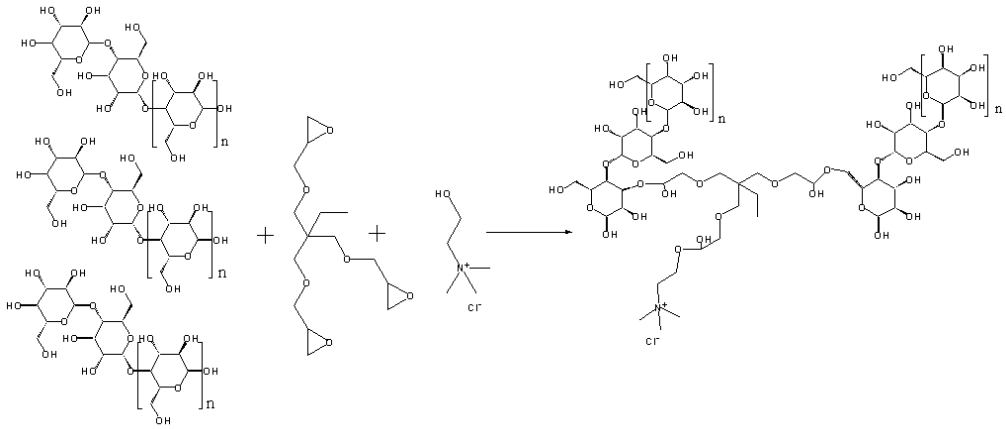

Figure 64: Cross-linking with TTE and maltodextrin with choline.

In addition to the cross-linking of polysaccharide chains, there is the formation of positively charged pendants (choline) in correspondence to the quaternary nitrogen.

10.2.2 Mass balance

The mass balances of water-synthesized nanosponges (BDE, TTE, NGDE) are reported below (Table 62):

Table 62: Massa balance anionic nanosponges.

NS	Mass Balance %	NS	Mass Balance %
GLUBDE	85,8	**GLUCHOBDE**	69,7
GLUTTE	88,1	**GLUCHOTTE**	81,0
GLUNGDE	86,3	**GLUCHONGDE**	78,0

Choline leads to a decrease in the mass balance of about 10%. This evidence may be attributed to choline's ability to bind the hydroxyl group nucleophilic addition reticule to the epoxy system. This results in a decrease of functional groups available for cross-linking and therefore the presence of free maltodextrins, which are subsequently removed during purification cycles.

10.2.3 TGA

Thermogravimetric analyses were conducted in a nitrogen atmosphere, with a temperature ramp of 10°C/min, up to a maximum temperature of 700 °C. The objective of this characterization is to evaluate the thermal stability of each product obtained. To compare the different samples, the onset temperature was used as the reference value, extrapolated from the intersection of the tangents of the degradation curve, before and after the degradative step, as shown in Figure 66:

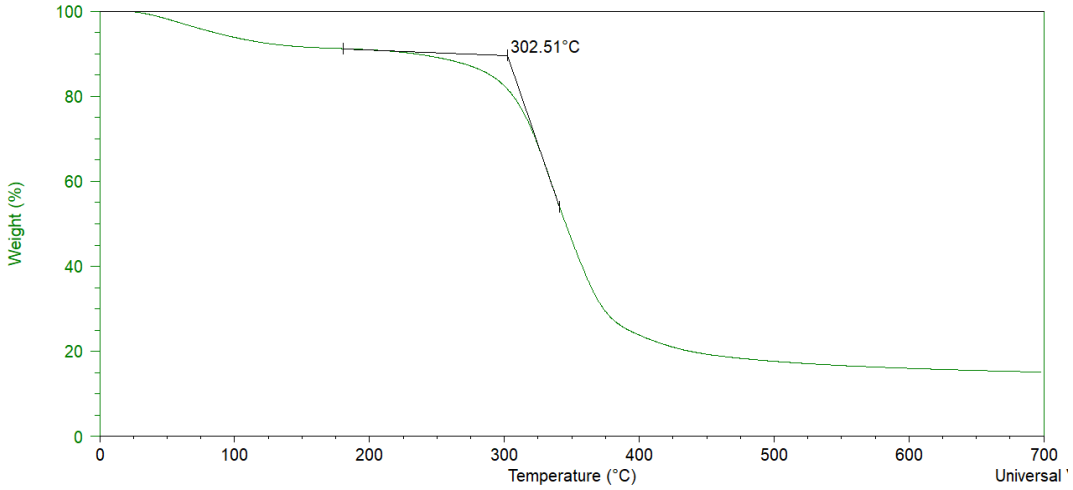

Figure 65: Thermogram of GLUBDE

The first weight loss, which occurs from room temperature up to 120 °C and equal to about 10% of the weight of the sample, is due to the desorption of the physiosorbed water on the material. The latter is hygroscopic because of the numerous hydroxyl groups that characterize the structure. The second weight loss, between 250 and 450 µc, concerns the degradation of the nanosponge in the absence of oxygen. This degradation represents the most important weight loss (about 70%). It was possible to observe the formation of a non-degradable residue (about 15% of the sample weight) under these conditions corresponding to the formation of

carbon structures. Below are reported the temperatures at which degradation occurs (T_{onset}) for nanosponges.

Table 63: Onset temperatures (°C) determined by the tangent method for anionic nanosponges.

NS	T_{onset}(°C)	NS	T_{onset}(°C)
GLUBDE	302,5	**GLUCHOBDE**	302,3
GLUTTE	282,2	**GLUCHOTTE**	270.9
GLUNGDE	288.6	**GLUCHONGDE**	281.2

These values, which vary between 270 and 320°C correspond to those of a typical thermal degradation profile of polysaccharides such as maltodextrins, whose depolymerize chains form multiple volatile fragmentation products which are removed from the nitrogen stream[232]. Lower thermal stability was observed in products containing choline chloride (on average 5 %). This evidence has been attributed to the ability of choline to react with a fraction of the epoxy groups of reticulation, thus subtracting these to the cross-linking reactions with the Glucidex 2 chains. A lower degree of cross-linking of the final product has been assumed, resulting in a decrease in thermal stability.

10.2.4 FTIR-ATR

The FTIR-ATR technique was used to characterize the polymers based on the type of functional groups present. The spectrum of each sample was compared with that of GLU2, to detect the characteristic bands of each synthesized nanosponge. The following figures show the recorded spectra.

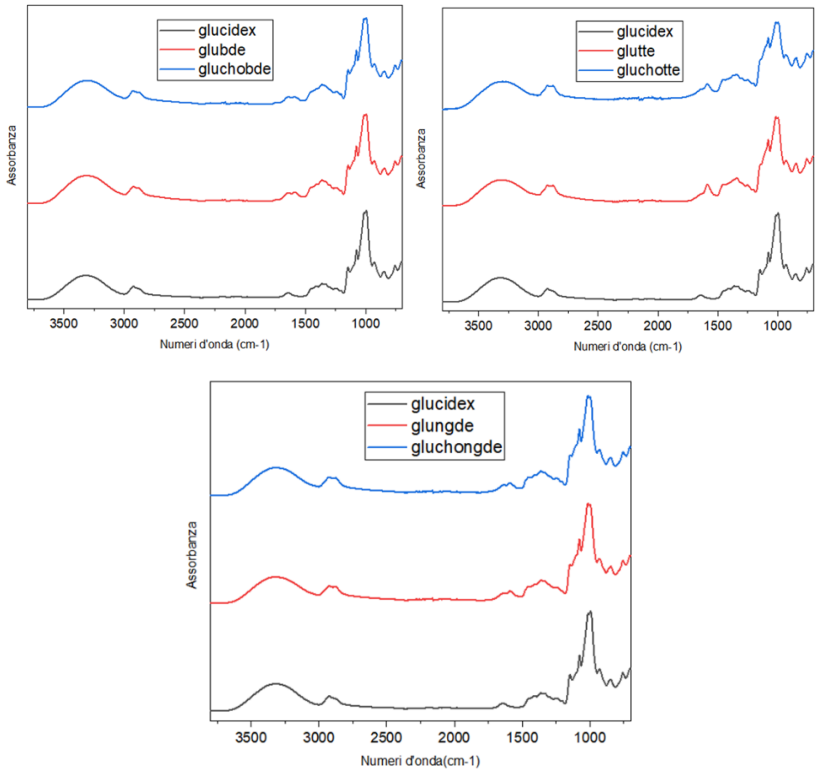

Figure 66: ATR spectra of anionic nanosponges.

The presence of carbonate bridges has been identified thanks to the characteristic bands of the carbonyl groups between 1700 and 1750 cm^{-1} in Figures 66. As regards the ether bridges responsible for cross-linking with epoxides, the overlapping of the signals due to the glycosidic bonds of maltodextrin did not allow detection. The presence of quaternary ammonium (responsible for functionalization with positive charge) was observed through contributions to about 1590 cm^{-1}. Unexpectedly, these signals were also observed in nanosponges synthesized in the absence of choline.

10.2.5 Elemental analysis

To understand the reasons for ATR evidence, an elementary analysis was carried out to study the composition of each product. Three replicates were carried out for each sample. The mean and the standard deviation for each determination are reported.

Table 64: Elemental analysis results of anionic nanosponges.

NS	% N	% C	% H
GLUBDE	**0,82**±1,5E-05	**43,61**±7,5E-02	**6,90**±6,0E-03
GLUCHOBDE	**0,84**±4,4E-05	**43,55**±1,1E-02	**6,77**±2,4E-03
GLUTTE	**1,05**±4,1E-03	**43,60**±3,0E-02	**6,59**±1,5E-04
GLUCHOTTE	**1,17**±2,8E-05	**43,13**±1,2E-01	**6,64**±3,0E-03
GLUNGDE	**0,65**±1,2E-04	**45,24**±7,3E-03	**7,19**±2,1E-02
GLUCHONGDE	**0,86**±3,0E-03	**45,28**±8,4E-01	**7,10**±3,0E-02

The amount of nitrogen is highlighted in cross-linked nanosponges choline-free (GLUBDE, GLUTTE, GLUNGDE). The only nitrogen-containing substance used in the synthesis is DABCO. Therefore, it was gathered that this amine does not act as reaction catalyst but is bound to the maltodextrin structure following the formation of a C-N bond with the cross-linker. Probably, this reaction involved the addition of the amine to the epoxy ring with its consequent opening and the formation of a quaternary ammonium salt. The following figure illustrates the just hypothesized reaction:

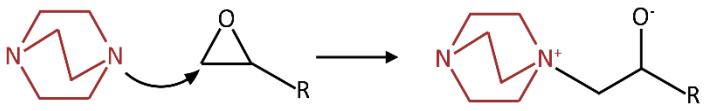

Figure 67: Nucleophilic addition reaction of DABCO on an epoxy system.

Furthermore, the nitrogen amount added by choline seems to play a marginal role compared to total nitrogen amount. With choline supplement, an increase of 0.21% nitrogen more a is observed (GLUCHONGDE), while DABCO represents 75-98% of the total nitrogen. These data have been attributed to a higher nitrogen nucleophilicity of DABCO, compared to the hydroxyl group of choline. The following table summarizes these findings:

Table 65: % N of DABCO and Choline contrinute to anionic nanospnges.

NS	%N DABCO	%N Choline
GLUBDE	100	0
GLUCHOBDE	98,35	1,65
GLUTTE	100	0
GLUCHOTTE	89,56	10,44
GLUNGDE	100	0
GLUCHONGDE	75,17	24,83

10.2.6 Potential-ζ

The results of potential-ζ measurements are given in the following tables. Below, data on epoxy-crosslinked nanosponges:

Table 66: Potential-ζ results of anionic nanosponges.

NS	Potential-ζ (mV)
GLUBDE	20,4
GLUCHOBDE	41,5
GLUTTE	41,4
GLUCHOTTE	36,9
GLUNGDE	44,2
GLUCHONGDE	44,5

Nanosponges not functionalized with choline but cross-linked with DABCO provided Potential-ζ values extremely like those related to choline functionalized nanosponges. This evidence indicates that the former is functionalized by positive charges thanks to the nucleophilic attack of DABCO on the epoxy system. This result is in line with what has been discussed in elementary analysis.

10.2.7 SEM Analysis

Anionic nanosponge samples (GLUBDE, GLUTTE, GLUNGDE) were morphologically characterized; the presence of trans-parent dimensionally polydisperse polymer granules could be observed (Fig. 68), whose size was roughly between a few tens to one hundred microns. The presence of amine-mediated reactions led to polymers characterized by increasing yellowing, proportional to the increasing amount of amine, when compared to the results observed from sample N. The SEM characterization revealed smooth external surfaces and the absence of macro-porosity. The porosity was further studied by gas-

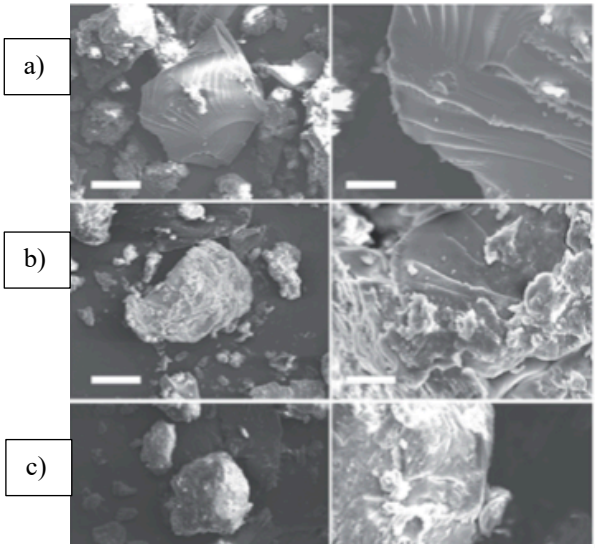

Figure 68: SEM analysis of a) GLUBDE, b) GLUTTE, c) GLUNGDE.

volumetric analysis, which concerned the bulky features of the resulting polymer granules. The specific surface areas were comprised roughly between 1 and 2 mg, while the absence of any meso- and micro-porosity was also observed.

10.3 Anionic nanosponges: abatement tests

Anionic nanosponges have been tested on nitrates, phosphates, glyphosate, Cr(VI), As(V) and As(III) at different concentrations. Nanosponges have been tested to assess the possibility that ion exchange is the predominant removal mechanism. In fact, other mechanisms of capture of the polluting anion by the nanosponge could act, such as an entrapment of the anionic species in the reticulated structure or phenomena of superficial adsorption. It is important to note, for future large-volume applications, that each synthesized nanosponge, when put in contact with the test solution, bulges. The absorption of large quantities of water by the materials obtained results in a considerable increase in volume, which may exceed 800% of the dry product volume. Three replicates were carried out for each measurement; the calculated average value and its standard deviation are reported. The percentage abatement was calculated by making the ratio between the final concentration of the filtered solution and the initial concentration put into contact with the nanosponge; the whole multiplied by 100.

10.3.1 Nitrates abatement tests

Table 67: % nitrates abatement of anionic nanosponges

Nitrate Concentration (mg/L)	**100**	**200**	**300**	**400**	**500**	**1000**
Nanosponge	% Abatement					
GLUBDE	62,9±3,4	34,73±3,7	30,15±2,9	29,0±2,6	21,38±2,8	18,0±2,9
GLUCHOBDE	55,6±3,7	45,10±3,3	38,86±2,8	30,0±2,9	25,77±3,8	20,0±3,1
GLUTTE	79,7±3,8	65,92±3,1	57,42±3,6	48,6±3,3	43,23±1,5	38,0±2,4
GLUCHOTTE	80,1±4,1	59,48±4,2	51,57±3,9	49,0±2,9	46,59±2,4	39,0±2,6
GLUNGDE	59,4±2,5	42,29±2,6	36,45±3,2	31,0±3,4	22,78±3,3	15,0±2,7
GLUCHONGDE	51,7±2,7	36,88±2,5	30,51±2,7	29,0±2,9	23,90±2,9	12,0±3,0

Table 68: nitrates mg/g abatement of anionic nanosponges.

Nitrate Concentration (mg/L)	**100**	**200**	**300**	**400**	**500**	**1000**
Nanosponge	mg/g abatement					
GLUBDE	6,29	10,95	12,34	11,6	10,69	18,0
GLUCHOBDE	5,56	9,02	11,66	12,00	12,89	20,0
GLUTTE	7,97	13,18	17,23	19,44	21,62	38,0
GLUCHOTTE	8,01	11,90	15,47	19,60	23,30	39,0
GLUNGDE	5,94	9,06	10,93	12,40	11,39	15,0
GLUCHONGDE	5,17	9,38	10,65	11,60	11,95	12,0

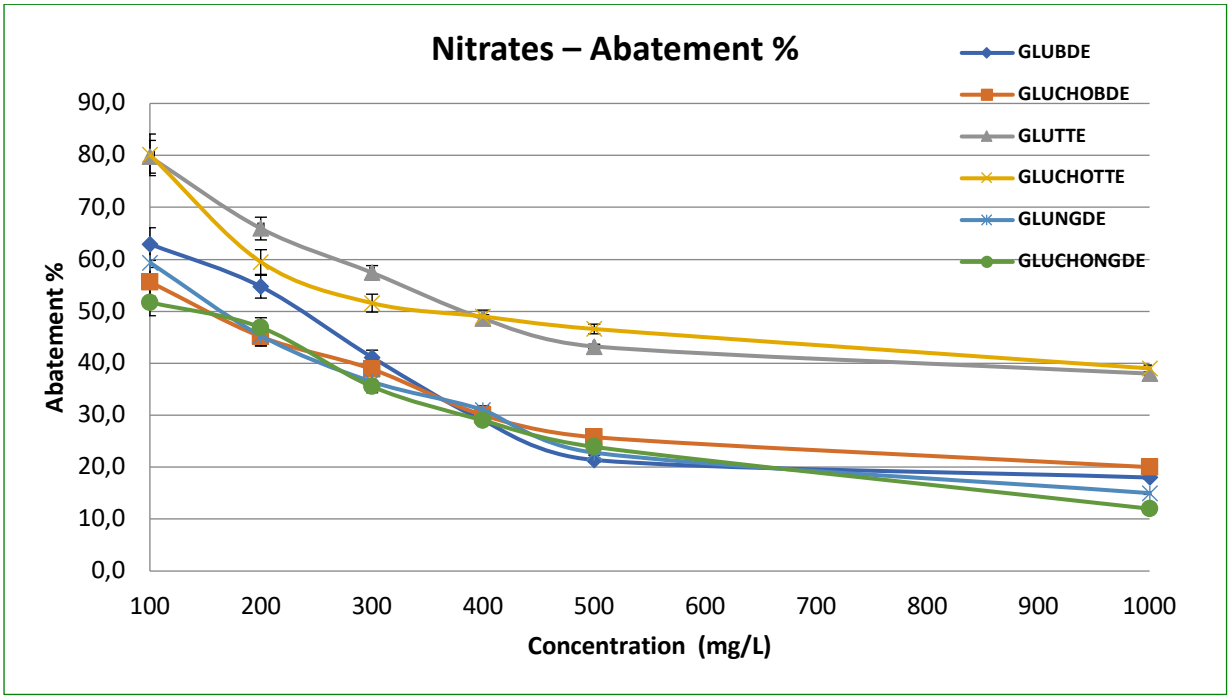

Figure 69: Removal efficiency % vs initial nitrate concentration for anionic nanosponges.

For each nanosponge, it is possible to observe how the removal efficiency percentage changes with the variation of the initial concentration of nitrate. Looking at the graph it could be seen an overall decrease in the percentage of removal efficiency as the nitrate concentration increases. This behavior can be explained by considering ion exchange phenomenon that occurs balancing adsorbed ions and ions in solution. As the concentration increases, the balance is shifted towards the ion exchange of the anions. For this reason, the milligrams of nitrate retained per gram of nanosponge increase. High concentrations were tested to assess the saturation of the nanosponge.

10.3.2 Phosphate abatement tests: removal efficiency and pH influence

The epoxy cross-linked nanosponges tested on nitrates and sulphates were also tested on four phosphate solutions with different pH values. These solutions were prepared starting from sodium orthophosphate, sodium mono-hydrogen phosphate and sodium dihydrogen phosphate dissolved in 1 L of ultrapure water in such quantities as to have the following pH values: 11.88; 8.49; 7.04; 5.25. Each solution was prepared at a different pH to test the abatement of nanosponges in different environmental background. Making a comparison among % removal efficiency of epoxy cross-linked nanosponges at different pH values, with the same initial phosphorus concentration, it is possible to note the presence of a maximum at 8,491 pH level.

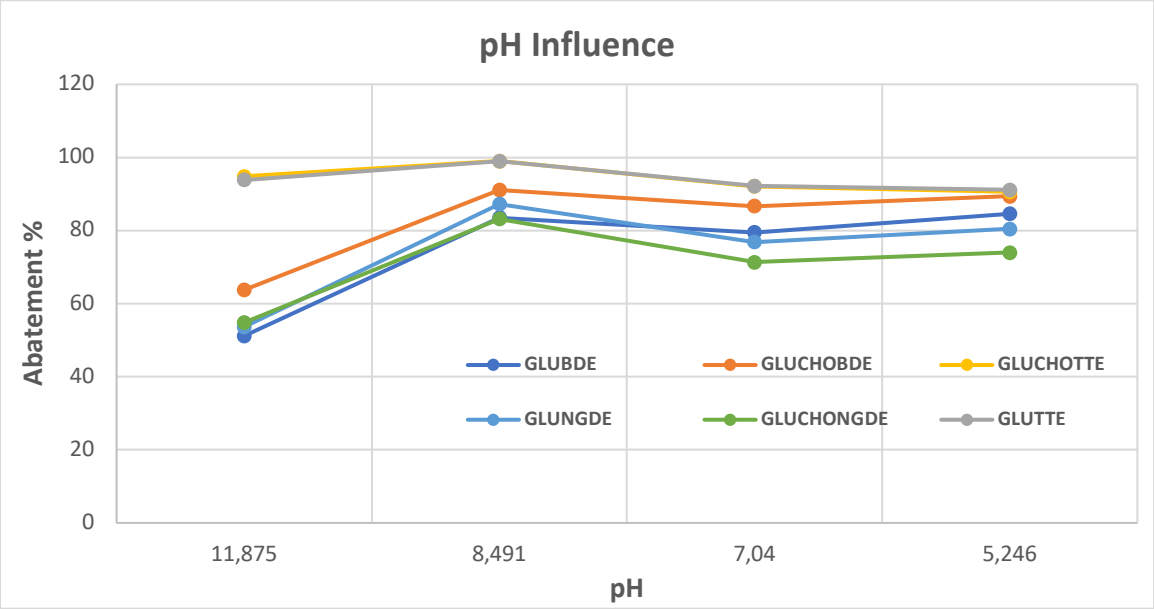

Figure 70: pH influence on abatement % of different nanosponges.

This trend can be explained by considering several aspects simultaneously. First of all, the ion exchange of the protonated forms of orthophosphate is in competition with the hydroxyl anion, which can be adsorbed by the positive charged group in nanosponge structure. At high pH values, it is possible to notice a drastic reduction in % abatement for all nanosponges except for those cross-linked with TTE, which always show very high abatement, maintaining the same trend. On the other hand, the low percentage of abatement at lower pH does not seem to undergo significant decreases and stays up to pH 5.25. In this pH range, the increase in the concentration of hydrogen ions is not in fact a contributing factor to hinder the abatement of anions. Indeed, the progressive decrease of hydroxyl ions promotes abatements less characterized by such competition. However, what is observed after the pH value of 8.49 is a decrease. To explain this decrease, it is necessary to consider the amphoteric character of the protonated forms of orthophosphate. Depending on the pH, phosphates come in three different forms: between pH 4 and 6, the most present form is dihydrogen phosphate; between pH 8 and 11, the predominant form is mono-hydrogen phosphate; at above pH 12.5 the orthophosphate anion becomes the most concentrated form. This situation is well illustrated in the speciation diagram shown in the following figure, where the distribution of orthophosphate species is expressed as α (ratio between the concentrations of the individual species and the total concentration) at different pH values:

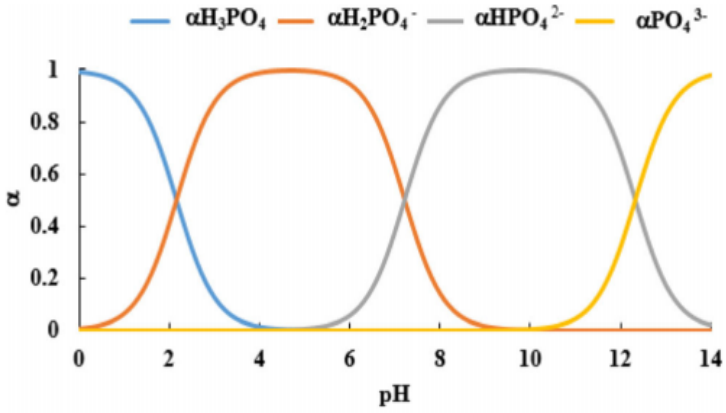

Figure 71: Phosphoric acid Bjerrum diagram.

Maximum abatement level at pH 8.49 represents the optimal tradeoff between a concentration of hydroxyl ions that do not predominate in the competition with the adsorption of phosphates and the concentration of these species in the less protonated forms. As more charged, these forms are adsorbed in larger quantities. Observing the speciation diagram just described (Figure 71), a high concentration of HPO_4^{2-}, a low concentration of $H_2PO_4^-$ and almost zero concentrations of PO_4^{3-} can be seen at pH 8.49.

10.3.3 Glyphosate abatement test

Several trials were performed to explore the possibility of glyphosate removal by nanosponges. A preliminary test was performed with a 100 mg/L solution of glyphosate on all nanosponges. The positive result gave rise to subsequent tests with lower concentrations (10 mg/L and 1 mg/L of glyphosate). As future perspective one of the main goals is to investigate nanosponges efficiency in glyphosate removal at lower concentrations, up to the legal limits imposed by European standards (0.1 µg/L). At this stage of the research, it was possible to identify the lowest quantifiable concentration with non-traditional and quickly technique (ICP-OES). For this reason, the instrument's limit of quantification (LOQ) was determined for glyphosate: 50 µg/L for the analytical line of phosphorus at 213.617 nm; 100 µg/L for the analytical line of phosphorus at 214.914 nm, while as regards the detection limits, an LOD of 25 µg/L was established for the line at 213.617 nm and 50 µg/L for that at 214.914 nm.

Table 69: Removal efficiency % of glyphosate for different nanosponges.

NS	Abatement % 100 mg/L GLY	Abatement % 10 mg/L GLY	Abatement % 1 mg/L GLY
GLUBDE	98,75±0,9	99,35±0,2	>98
GLUCHOBDE	97,71±1,2	99,31±0,3	>98
GLUTTE	98,28±0,7	98,10±0,5	89,70±2,1
GLUCHOTTE	97,77±0,6	99,08±0,7	93,33±1,7
GLUNGDE	96,48±1,4	99,44±0,4	>98
GLUCHONGDE	88,50±2,2	94,80±0,8	91,19±1,9

Glyphosate abatement tests provided high abatement values for all nanosponges. This evidence can be justified by the acid-base behavior of glyphosate in water. Glyphosate is a weak acid with four acid dissociation constants: two for the phosphonic group (pK_{a1} and pK_{a3}), one for the carboxyl group (pK_{a2}) and one for the amino group (pK_{a4}). The protonation equilibria of glyphosate are illustrated below:

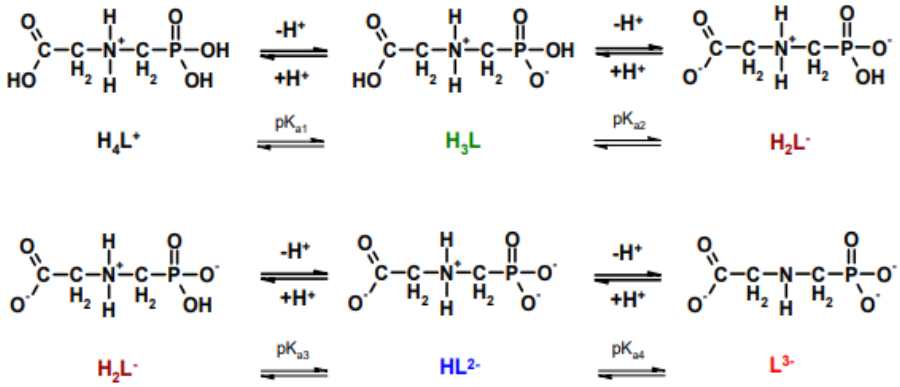

Figure 72: Deprotonation equilibria of glyphosate in water.

pKa values of glyphosate are shown in the following table:

Table 70: pKa values of glyphosate.

pK_{a1}	pK_{a2}	pK_{a3}	pK_{a4}
2,0	2,6	5,6	10,6

As a function of pH glyphosate forms in solution are distributed according to the following speciation diagram:

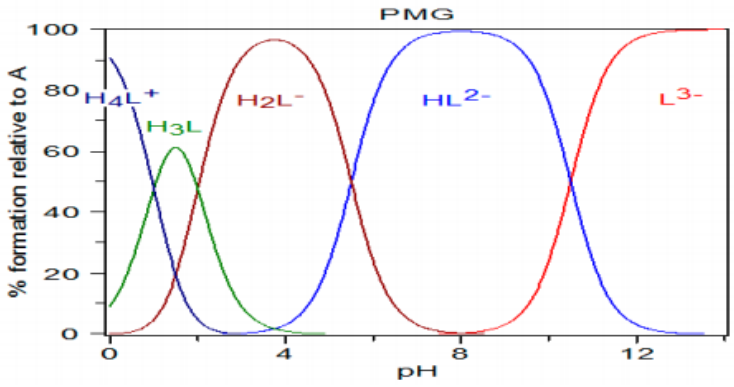

Figure 73: Bjerrum diagram of glyphosate in water.

Since tests were performed at neutral pH, it is assumed that the predominant form at the time of abatement is HL_2^-. The high number of negative charges in solution thus justifies the abatements. The data collected on the tests carried out did not allow to correlate an effect of the concentration on the percentage of abatement. As in the case of nitrates and sulphates, a further increase in the concentration of glyphosate is likely to result in a decrease in the percentage of killing. However, the study was directed towards lower concentrations.

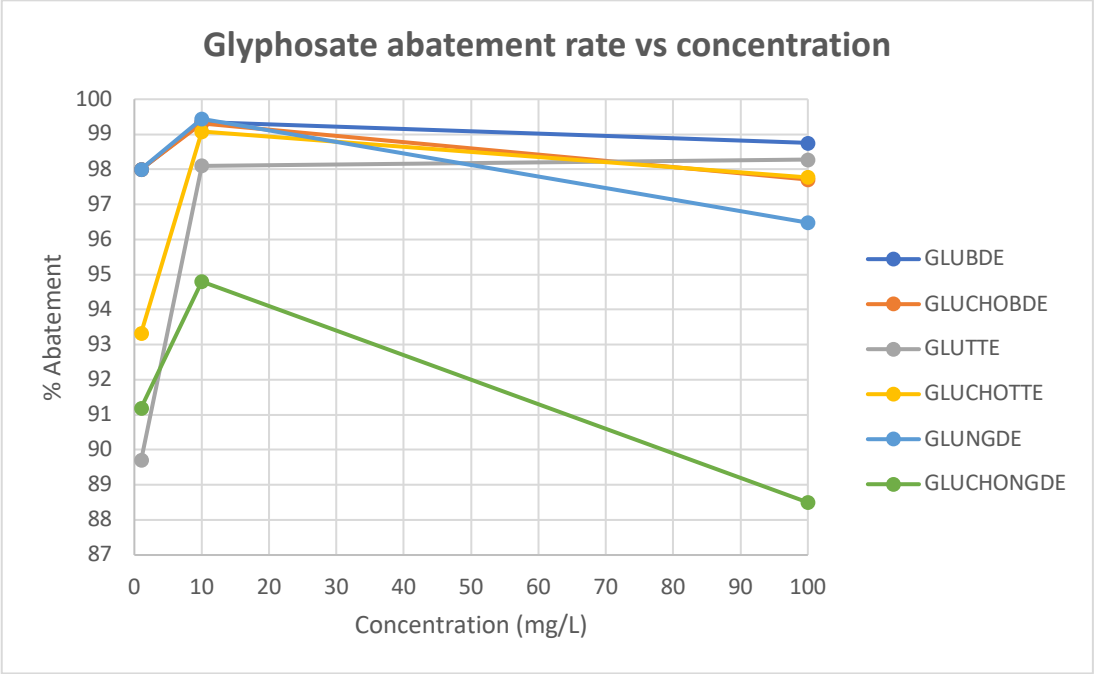

Figure 74: Dependence of the percentage of reduction of glyphosate in relation to the initial concentration for the different nanosponges tested. Variations in abatement rates are attributable to instrumental noise, as the concentration is close to the LOQ.

8.22.4 Comparison between glyphosate and sulphates

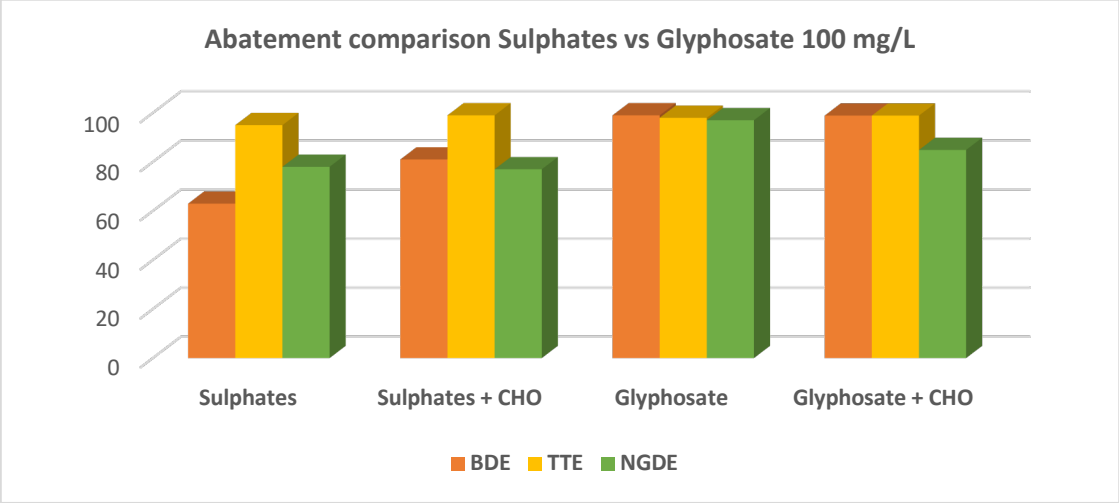

Figure 75: Comparison between glyphosate and sulphates by cationic nanosponges at 100 mg/l.

As additional evidence, a comparison was made between the removal of glyphosate and the removal of sulphates by cationic nanosponges at 100 mg/L. As a bicaric form, the predominant acid-base form in solution (HL^{2-}) is expected to yield reductions comparable to those of sulphates. Figure 75 show the comparison.

10.3.4 Chromium abatement tests

Table 71: Cr(VI) % abatement and mg/g abatement of anionic nanosponges.

Cr(VI) Concentration (mg/L)	**1**	**2**	**10**	**25**	**50**	**100**
Nanosponge	% Abatement					
GLUBDE	>99.7	99,8 ±	98,6 ±	92,0 ± 2,23	77,6 ±	66,7 ± 4,67
GLUCHOBDE	>99.7	99,7 ±	98,4 ±	93,7 ± 1,89	82,9 ±	75,2 ± 3,92
GLUTTE	>99.7	99,5 ±	98,8 ±	90,8 ± 2,78	87,9 ±	82,9 ± 2,56
GLUCHOTTE	>99.7	99,5 ±	99,3 ±	94,7 ± 3,29	89,5 ±	84,2 ± 3,77
GLUNGDE	>99.7	99,6 ±	98,7 ±	88,6 ± 1,23	78,1 ±	65,9 ± 2,45
GLUCHONGDE	99,6 ±	98,3 ±	95,6 ±	85,3 ± 1,69	76,3 ±	64,4 ± 1,29
Cr(VI) Concentration (mg/L)	**1**	**2**	**10**	**25**	**50**	**100**
Nanosponge	mg/g abatement					
GLUBDE	0.0997	0,1993	0,9870	2,0958	3,8554	6,6647
GLUCHOBDE	0.0984	0,1994	0,9828	2,1354	4,1385	7,5020
GLUTTE	0.0989	0,1909	0,9815	2,0642	4,3740	8,2574
GLUCHOTTE	0.0995	0,1986	0,9909	2,1509	4,4656	8,4111
GLUNGDE	0.0993	0,1991	0,9821	2,0224	3,8756	6,5521
GLUCHONGDE	0.0979	0,1918	0,9554	1,9562	3,9405	6,4151

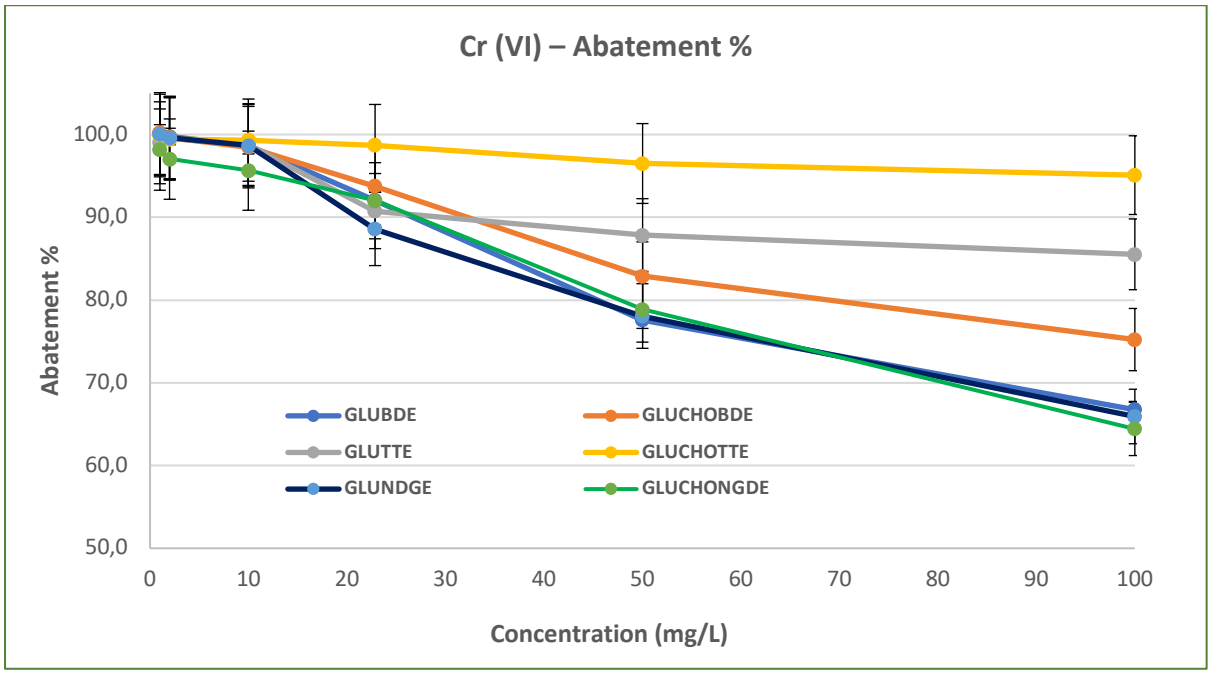

Figure 76: Removal efficiency vs contration of Cr(VI) for different nanosponges.

The graph shows the % reduction of Cr (VI) as a function of concentration, the tested range of which is from 0,1 ppm to 100 ppm. It is remarkable to see the high abatements performed by all nanosponges, (between 90-100%). Best performances despite concentration increasing are given by GLUCHOTTE. It should be noted that the detection limit of the instrument is 10 pbb, so some nanosponges are able to break down Cr (VI) below the legal limits for drinking water (10 ppb).

10.3.5 Arsenic abatement tests

Table 72: As(III) % abatement of anionic nanosponges.

NS	Abatement % 0,1 mg/L As(III)	Abatement % 1 mg/L As(III)	Abatement % 10 mg/L As(III)
GLUBDE	>95	>99,5	42,3 ± 2,56
GLUCHOBDE	>95	>99,5	45,6 ± 1,37
GLUTTE	85,9 ± 1,13	80,4 ± 1,17	23,8 ± 1,96
GLUCHOTTE	90,1 ± 1,28	82,9 ± 1,95	23,0 ± 1,66
GLUNGDE	88,6 ± 1,44	70,1 ± 1,45	20,7 ± 1,32
GLUCHONGDE	90 ± 1,73	75,7 ± 2,23	19,6 ± 1,67

Table 73: As(III) mg/g abatement of anionic nanosponges.

NS	mg As/g NS 0,1 mg/L As(III)	mg As/g NS 1 mg/L As(III)	mg As/g NS 10 mg/L As(III)
GLUBDE	0,0099	0,100	0,4175
GLUCHOBDE	0,0099	0,0991	0,3874
GLUTTE	0,0086	0,0801	0,2314
GLUCHOTTE	0,0089	0,0824	0,2244
GLUNGDE	0,0088	0,0696	0,1892
GLUCHONGDE	0,0090	0,0754	0,1889

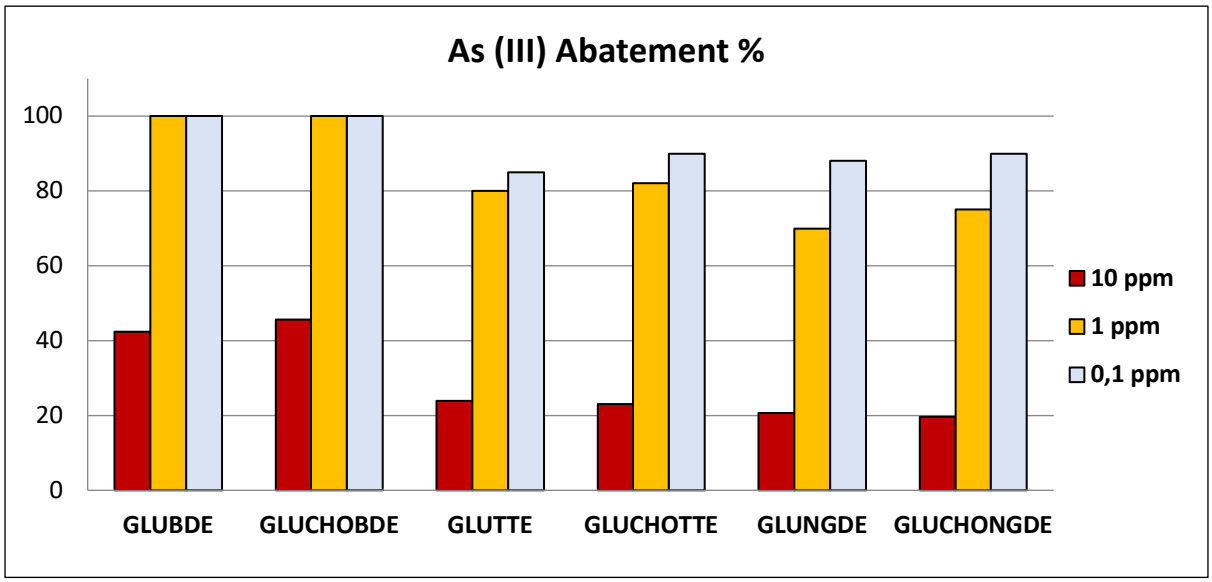

Figure 77: Removal efficiency of As(III) by anionic nanosponges.

Table 74: As(V) % abatement of anionic nanosponges.

NS	Abatement % 0,1 mg/L As(V)	Abatement % 1 mg/L As(V)	Abatement % 10 mg/L As(V)
GLUBDE	>95	>99,5	95,9 ± 2,45
GLUCHOBDE	>95	>99,5	95,1 ± 2,34
GLUTTE	>95	>99,5	95,9 ± 1,78
GLUCHOTTE	>95	>99,5	96,2 ± 1,37
GLUNGDE	>95	>99,5	90,7 ± 2,56
GLUCHONGDE	>95	>99,5	77,5 ± 2,33

Table 75: As(V) mg/g abatement of anionic nanosponges.

NS	mg As/g NS 0,1 mg/L As(V)	mg As/g NS 1 mg/L As(V)	mg As/g NS 10 mg/L As(V)
GLUBDE	0,0099	0,0995	0,9555
GLUCHOBDE	0,010	0,1002	0,9424
GLUTTE	0,0099	0,0993	0,9515
GLUCHOTTE	0,0099	0,0994	0,9567
GLUNGDE	0,010	0,1002	0,9029
GLUCHONGDE	0,010	0,0994	0,7721

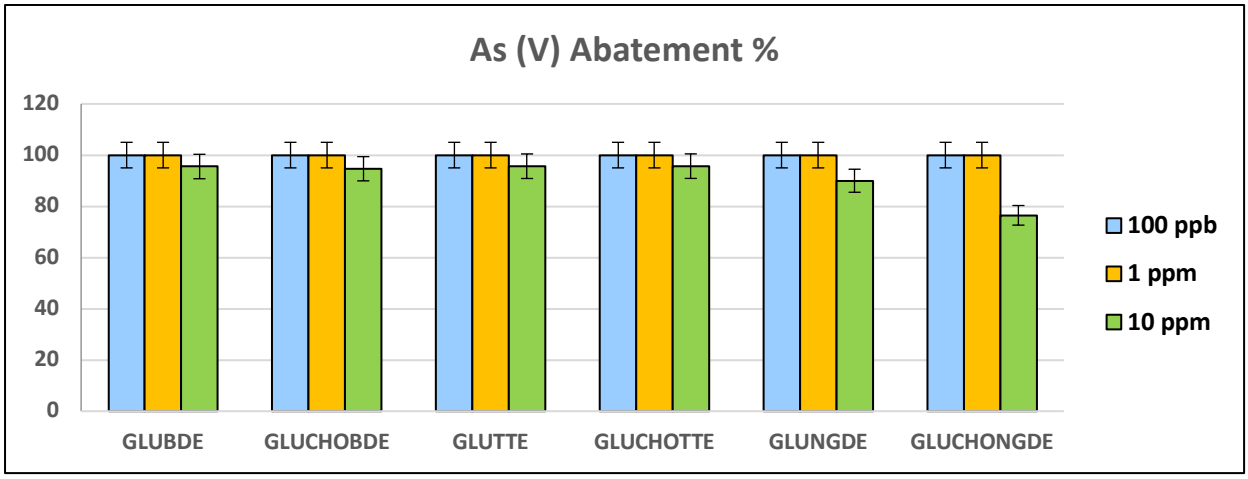

Figure 78: Removal efficiency of As(V) by anionic nanosponges.

Speaking of Arsenic, removal efficiency of As (V) and As (III) were both tested. High removal efficiency (90-100%) at different 3 concentrations tested for As (V) are noticeable, while As (III) did not give the same results, with lower abatement values. Also in this case, it should be noted that the detection limit of the instrument is 10 ppb, so some nanosponges are able to break down As below the legal limits for drinking water (10 ppb).

10.3.6 Release test

Release tests were carried out for all nanosponges tested for nitrates and Cr(VI) at 100 mg/L. The results obtained from the ICP-OES analysis are shown in Table 77.

Table 76: Water release tests for anionic nanosponges: nitrates and Cr(VI).

Nanosponge	Nitrates water release %	Cr(VI) Water release %
GLUBDE	4,34	3,56
GLUCHOBDE	4,56	3,68
GLUTTE	3,87	3,22
GLUCHOTTE	3,95	3,35
GLUNGDE	5,29	4,76
GLUCHONGDE	4,34	4,82

From the values observed it is clear that the release of nitrates and Cr(VI) ions into water is very low, a sign that the interaction between the functional groups present on the surface of the nanosponge and the ion is rather strong.

10.3.7 Rigeneration test: preliminary results

On the same nitrate and Cr(VI) nanosponges used for abatement tests were tested to see if regeneration was possible. A concentrated solution of NaCl at 10% was prepared and all the nanosponges were put in contact with the batch solution. For both nitrates and chromates, the release of the ion in water after 24h was > 80%. This preliminary test indicates that these anion nanosponges can be regenerated. However, further column tests should be carried out to verify a better regeneration. The difficulty in carrying out the column tests is focused on the considerable bulging of the nanosponges that would make it difficult to perform the test. Finally, an economic assessment should be carried out on the actual feasibility and convenience.

10.4 Cationic nanosponge synthesis

10.4.1 GLU2_BDE Mechanism cross-link reaction

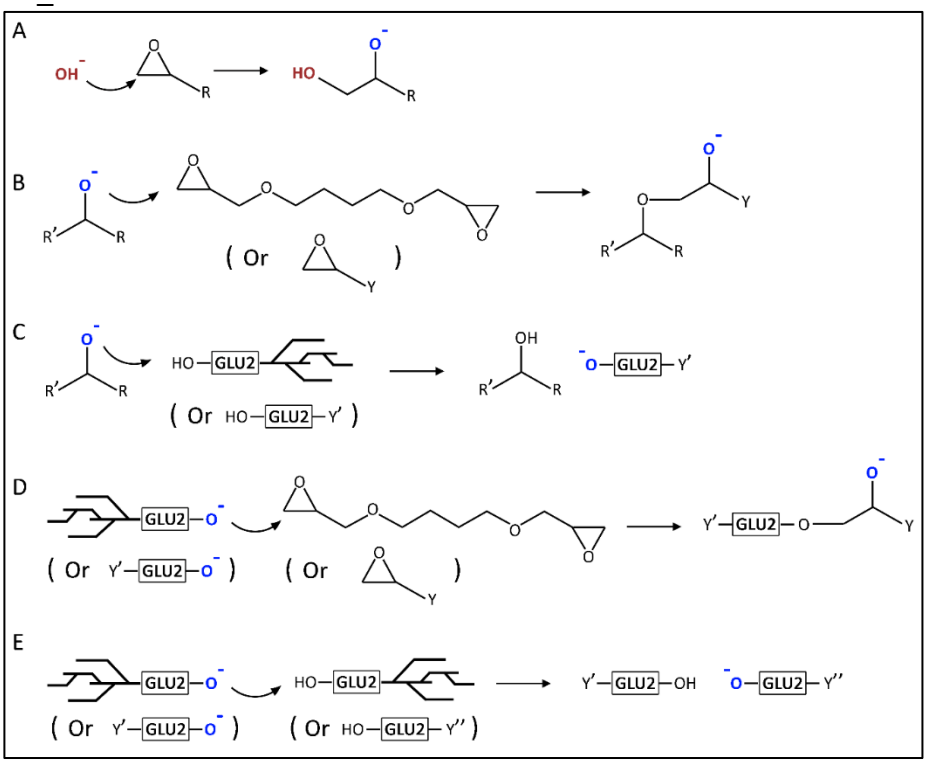

Figure 79: Mechanism of cross-linking reaction of GLU2_BDE based nanosponge in basic environment.

As the anionic nanosponges, synthesis mechanism can be described by two distinct phases, assumed to be responsible for the generation of the polymer network (Figure 79) [142].

For synthesis a basic environment (NaOH 0,2 M) has been chosen to catalyze the opening reaction of the epoxide ring present in the structure of the BDE crosslinking agent (as described in Figure 78 A). This interaction would generate reactive species with negative charge (alcoxides), supposed to be the initial products of the reaction (first phase). Alcoxides, formed in this way, should not only interact with maltodextrin (GLU2) later on, but should also be responsible for opening the ring of the reticulating agent (Figure 32 D), thus allowing the start of the polymerization step and therefore the growth of polymeric chains (second phase).[142] In addition, the main strategy for introducing negative charges in the maltodextrin structure was to functionalize the polysaccharide skeleton by species with carboxyl, sulphate or sulphonic groups. The introduction of these functional groups would allow better interaction between the adsorbent polymer and metal cations.

10.4.2 Mass Balance

Because of purification and drying in the oven, the amount of product has been expressed as a percentage mass balance, which is the ratio of the weight of the final product to the theoretical weight, which consists of the sum of the weight of the GLU2, BDE and functionalizing agent. For sulphonic nanosponges functionalized with 1,3-propylsulton and 1,4-butylsulton, the weight of the GLU2_BDE-based nanosponge was considered for the calculation of the theoretical weight and not that of maltodextrin. Percentages are given in Table 78.

Table 77: Mass balance % of cationic nanosponges.

Sulphonic Nanosponge	BM %
GLU2_BDE_CARK10%_NAOH	73
GLU2_BDE_CARK10%_H_2O	40
GLU2_BDE_CARK15%_H_2O	18
CARK15%_H_2Ob	28
PROPS10%_POSTSYNTH	78
PROPS20%_ POSTSYNTH	70
PROP30%_ POSTSYNTH	68
GLU2_BDE_1,4BUTS10%	41
BUTS20%_ POSTSYNTH	74
BUTS30%_ POSTSYNTH	69

Mass budgets range from 18% to 78%. The lowest values obtained are those for carrageenan-K-based and 1,4-butylsulton-based nanosponges, obtained by one-step synthesis. The main reason is ascribed to problems encountered during the synthesis and purification process.

10.4.3 Synthesis issues

As stated above, the lowest mass balance values are found for synthesis with 10% carrageenan-K and 15% w/w in aqueous medium and 1.4-butylsultone at 10% mol/mol obtained by one-step synthesis in a basic environment. This trend could be explained not only by problems of

recovery of the product following purification, but also by complications during synthesis. In fact, about the carrageenan-K nanosponges, the main difficulties were encountered in the formation of the gel (cross-linking reaction), which took more than an hour of time, at significantly higher temperatures and with a higher amount of reticulating agent, compared to the normal synthesis procedure (basic synthesis: GLU2_BDE). This is also since the reaction environment was not basic. In addition, the product achieved did not appear as a solid and friable gel block but was softer and more difficult to reduce to smaller pieces. These poor characteristics of final product affected the purification process because the polymer in contact with water, in addition to swelling, had the same consistency as a liquid gel, so the filter was easily clogged. In addition, the final product after drying in the oven was difficult to recover. After these issues, synthesis with carrageenan-K was re-done at 15% w/w (GLU2_BDE_CARK15%_H_2Ob) after 90 minutes a sticky gel and not a solid compact block were gotten. It was decided to leave it for a longer period of about 180 minutes. The final product has the same characteristics as the previous one and manifested the same problems both in the purification and in its recovery after drying in the stove. The same behavior was found for the one functionalized with the 1,4-butylsultone at 10% in moles, especially for final product characteristics of the, which always presented as a sticky gel. On the other hand, to make the reticulation reaction happen, temperature has been changed by raising it from 75°C to 85°C. The gel formation took place after 15 minutes, following the rise in temperature. The reticulation reaction was always allowed to take place for 90 minutes. In addition, with the same identical synthesis procedure with 10 % in moles of 1,3-propylsulton, the cross-linking reaction did not occur, even if the conditions varied. Therefore, because of these difficulties, sulton synthesis was performed by directly functionalizing the synthesized GLU2_BDE based nanosponge.

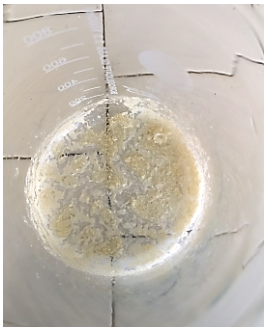

Figure 80: Nanosponge Glu2_bde_cark15b after drying in the stove at 70°C.

10.4.4 Nanosponge functionalize with carrageenin-K characterization: FTIR-ATR

To introduce sulfate groups was to use carrageenan-K, as a natural green biopolymer. The use of carrageenan-K is not only used to introduce negative charges on the surface of cross-linked polymers, but also to improve the swelling properties and mechanical properties of hydrogels. In a recent study, Tavakoli et al. [233] used carrageenan-K to modify the surface of a cross-linked hydrogel based on starch and cellulose, used in the biomedical field, to improve biocompatibility and mechanical resistance with a controlled degradation rate. The spectra of

carrageenan-K-based nanosponges (10% and 15% w/w) synthesized in both aqueous and basic environment are shown in Figure 81.

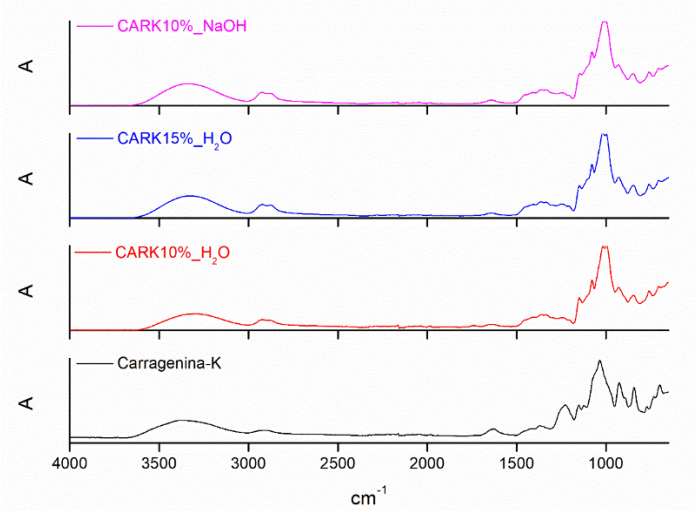

Figure 81: Spectra IR nanosponge based on carrageenan-K at 10 and 15% w/w in aqueous and 10% in basic environment.

Again, the interaction between maltodextrin and carrageenan-K should be confirmed by the presence of the sulphate group signal. However, by enlarging in the area from 1900 to 1100 cm^{-1} there are no differences with the spectrum related to the nanosponge GLU2_BDE. In fact, comparing the spectra of the three nanosponges based on carrageenan-K with that of the carrageenan-K as it is, in the first cited it is not found the presence of the signal of the sulphate group to approximately 1200 cm^{-1}, as it would have been expected.

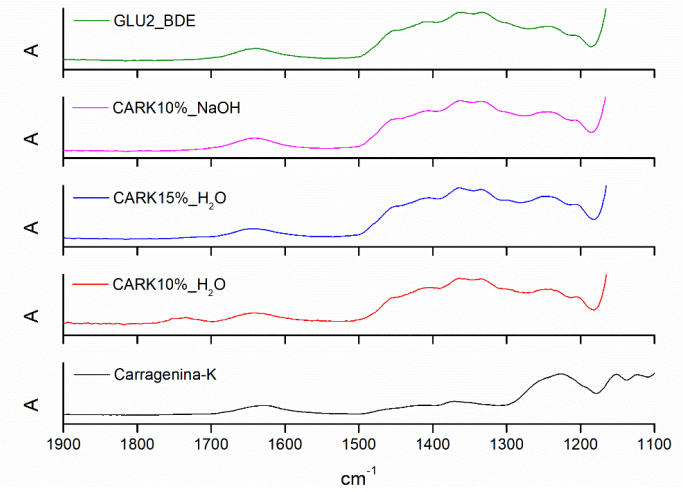

Figure 82: Magnification between 1900 and 1100 cm^{-1} to compare the spectra of carrageenan-K-based nanosponges with that of carrageenan-K and the GLU2_BDE-based nanosponge.

10.4.5 Nanosponge functionalize with carrageenin-K characterization: Elemental analyses

The following analysis was carried out to assess the presence of sulphur in the carrageenan-K-based nanosponge, at different percentages by weight. The values are given in Table 79.

Table 78: % S elemental analysis of cationic nanosponges.

Nanosponge	% S
GLU2_BDE_CARK10%_NaOH	0
GLU2_BDE_CARK10%_H_20	0,08
GLU2_BDE_CARK15%_H_2O_b	0,11
GLU2_BDE_CARK15%_H_2O	0,27

The percentages of sulfur detected are correlated with the amount of sulphate agent added. In fact, as the sulfate agent increases, there is an increase in the percentage of sulfur. However, the measured value for the 15% carrageenan-K nanosponge deviates from the previous synthesis. The cause could be ascribed to few sulphate groups due to a low interaction between maltodextrin and carrageenan-K during synthesis.

10.4.6 Nanosponge functionalize with carrageenin-K characterization: abatement tests

Table 80 and 81 show the abatement rates and mg/g of copper ions retained by carrageenan-K nanosponges at 10 and 15% w/w, synthesized in an aqueous medium. The nanosponge synthesized in the basic environment was not considered for abatement tests as the amount of sulfur was not detected. Initially, it was started with a standard copper solution of 25 mg/L.

Table 79: Copper abatement rates at 25 mg/L using 10 and 15% w/w carrageenan-K based nanosponges.

Cu solution 25 mg/L	% w/w car-K	% Abatement	mg/g
GLU2_BDE_CARK10%_H_2O	10	99,41	2,72
GLU2_BDE_CARK15%_H_2O	15	94,97	2,79
GLU2_BDE_CARK15%_H_2Ob	15	70,08	2,03

As can be observed from Table 80, this nanosponge has shown excellent abatement capacities, especially with 10% w/w of carrageenan-K. A decrease of the abatement percentages, increasing the amount of sulphate agent, can be attributed to synthesis issues encountered, because the two final products did not have the same characteristics as the 10% one. As a result, it was tried to increase the concentration of the copper solution to 50 mg/L, getting a decent percentage of abatement.

Table 80: Copper abatement rates at 50 mg/L using 10 and 15% w/w carrageenan-K based nanosponges.

Cu solution 50 mg/L	% w/w car-K	% Abatement	mg/g
GLU2_BDE_CARK10%_H_2O	10	47,13	2,74
GLU2_BDE_CARK15%_H_2O	15	66,84	4,15

For this second test was not tested the nanosponge GLU2_BDE_CARK15%_H2Ob, because already at low concentrations of the copper solution, the percentage of abatement was lower than the previous one. One of the reasons could be attributed to synthesis issues also due to a less likely linkage interaction between carrageenan-K and maltodextrin and consequently fewer active sites on the nanosponge, as can also be seen from the results of the CHNS analysis. In Figure 83 the comparison between nanosponges tested on copper solutions at different concentrations is shown in graph.

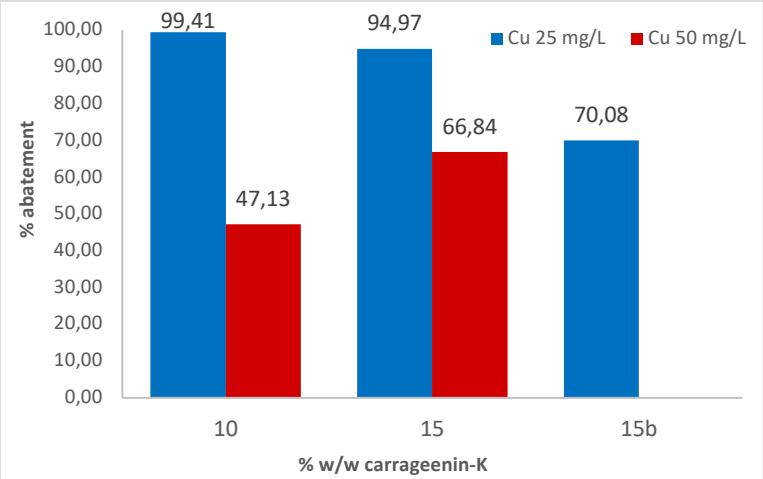

Figure 83: Comparison between % abatement of copper solutions 25 and 50 mg/L using the nanosponge based on carrageenan-K 10 and 15% w/w.

10.4.7 Nanosponge functionalize with sultons characterization: FTIR-ATR

The third strategy to achieve functionalized nanosponges with sulfonic groups was to introduce two types of sultons, (cyclic sulfonic esters), 1,3-proprilsultone and 1,4-butylsulton. Unlike the other two functionalizing agents this alternative turns out to be less "green". In fact, these two substances have limits in their use, as they are categorized as toxic. In any case, it has been hypothesized that during the synthesis, following the opening of the ring and the interaction with the nanosponge, the product should not cause environmental and human health problems. In literature there are research papers in which these two compounds are used to functionalize β-cyclodextrins, leading to sulfoalchileters-βCD, called SPE-βCD (with propylsulton) and SBE-βCD (with butylsulton), used in drug delivery (transport of medicines).[234] In Figure 84 and 85 the spectra of the basic nanosponge GLU2_BDE functionalized post-synthesis with 1,3-propylsulton or 1,4-butylsulton between 10 and 30% w/w. The spectra of the basic nanosponge GLU2_BDE functionalized post-synthesis with 1,3-propylsulton or 1,4-butylsulton between 10 and 30% w/w. Analysis was carried out to assess the presence of sulphonic groups following the interaction between the nanosponge and sulton. As can be seen from Figures 86 and 87, enlarging in the area between 1800 cm^{-1} and 1100 cm^{-1}, there is an evident increase of the peak

to about 1200 cm^{-1}, passing from 10% to 30% w/w of added sulton, confirming the presence of the sulfonic group in the nanosponge and sulton. As can be seen from Figures 86 and 87, enlarging in the area between 1800 cm^{-1} and 1100 cm^{-1}, there is an evident increase of the peak to about 1200 cm^{-1}, passing from 10% to 30% w/w of added sulton, confirming the sulfonic group in the nanosponge.

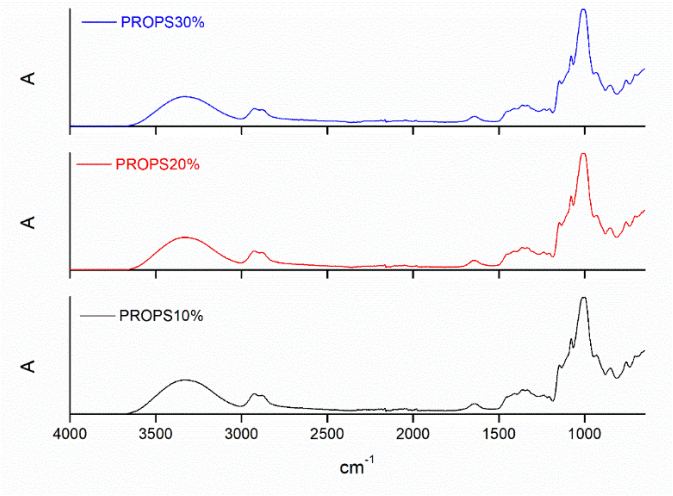

Figure 84: Nanosponge IR spectra based on 1,3-proprilsultone at 10, 20 and 30% w/w (post synthesis).

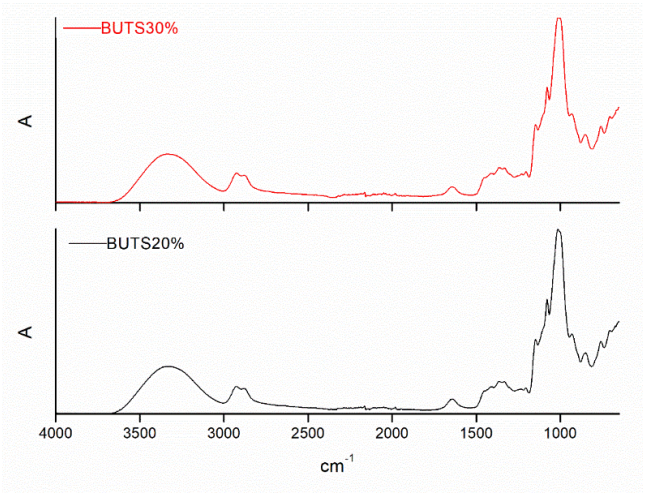

Figure 85: Nanosponge IR spectra based on 1,4-butylsultone at 20 and 30% w/w (post synthesis).

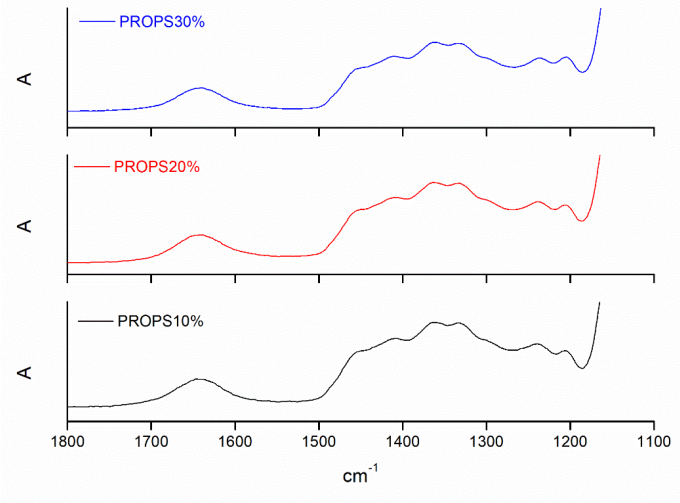

Figure 86: Magnification in the area between 1800 and 1100 cm-1 of the nanosponge spectra based on 1,3-proprilsultone at 10, 20 and 30% w/w (post synthesis).

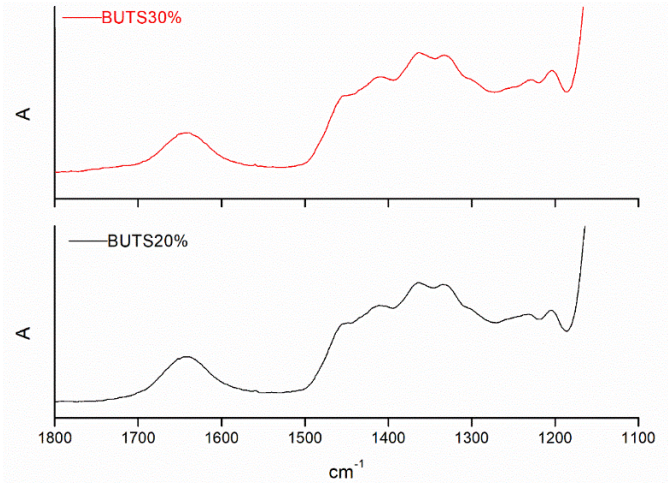

Figure 87: Magnification in the area between 1800 and 1100 cm-1 of the nanosponge spectra based on 1,4-butylsulton at 10, 20 and 30% w/w (post synthesis).

10.4.8 Nanosponge functionalize with sultons characterization: Elemental analyses

The following analysis was carried out to evaluate the amount of sulfur in nanosponges following the functionalization with sultons. The values are given in Table 82.

Table 81: %S of sultons in cationic nanosponges.

Nanosponge	%S
PROPS10% POSTSYNTH	0,25
PROPS20% POSTSYNTH	0,45
PROPILS30% POSTSYNTH	0,66
GLU2_BDE_1,4BUTS10%	0,41
BUTS20%_ POSTSYNTH	0,58
BUTILS30%_ POSTSYNTH	0,79

The trend sulfur found is correlated with the amount of sulton added. In fact, by increasing the percentage in weight there is an increase in the amount of sulfur present, corresponding to a likely increase in the sulfonic groups bound with the nanosponge, compared to other types of sulfonic nanosponges.

10.4.9 Nanosponge functionalize with sultons characterization: abatement tests

Table 22 shows the percentages of abatement and mg/g of copper ions retained by 1,3-propylsulton-based nanosponges from 10 to 30% w/w and from those based on 1,4-butylsultone at 20 and 30% w/w. It was started with a copper solution of 25 mg/L. The tests were carried out in bulk, using 100 mg of nanosponge in 10 ml of the copper solution at different concentrations.

Table 82: Copper abatement rates at 25 mg/L using 1,3-butylsultone-based nanosponges at 10, 20 and 30% w/w and based on 1,4-butylsultone at 20 and 30% w/w.

Cu solution 25 mg/L	**% w/w sulton**	**% Abatement**	**mg/g**
PROPS10%_POSTSYNTH	10	97,86	2,68
PROPS20%_ POSTSYNTH	20	99,38	2,72
PROPS30%_ POSTSYNTH	30	98,55	2,85
BUTS20%_ POSTSYNTH	20	100,00	3,06
BUTS30%_ POSTSYNTH	30	99,25	2,87
Cu solution 25 mg/L	**% mol/mol sulton**	**% Abatement**	**mg/g**
GLU2_BDE_1,4BUTS10%	10	88,19	2,43

The nanosponges tested have been shown to have a high efficiency in retaining Cu^{2+} ions, especially those with 20% sulton. For this reason, to evaluate a further abatement by increasing the concentration of copper to 50 mg/L, the percentages and mg/g of which are shown in Table 84.

Table 83: Copper abatement rates at 50 mg/L using 10, 20 and 30% w/w 1,3-propylsulton based nanosponges and at 20 and 30% w/w.

Cu solution 50 mg/L	**% w/w sulton**	**% Abatement**	**mg/g**
PROPS10%_ POSTSYNTH	10	77,50	4,51
PROPS20%_ POSTSYNTH	20	98,18	5,71
PROPS30%_ POSTSYNTH	30	98,94	6,25
BUTS20%_ POSTSYNTH	20	100,00	6,57
BUTS30%_POSTSYNTH	30	99,41	6,28
Cu solution 50 mg/L	**% mol/mol sulton**	**% Abatement**	**mg/g**
GLU2_BDE_1,4BUTS10%	10	63,11	3,85

Nanosponges with 20 and 30% sulton still maintain a high abatement efficiency, while for what concerns only that with 10% of 1,3-propylsulton, a clear decrease is observed due to a beginning of saturation of the sulfonic sites present in the nanosponge. This behavior can be compared with the elemental analysis at CHNS, which shows an increasing trend in the percentage of sulfur present in nanosponges, as sulton concentration increases, also indicating

a likely increase in sulphonic sites amount responsible for interaction with copper cations. Consequently, tests could also be performed at higher copper concentrations. In addition, both Table 22 and Table 23 also reported the values of the percentages of reduction of the nanosponge GLU2_BDE_1,4BUTS10%, synthesized with the one-step method described previously. It has been tested with both the 25 mg/L and 50 mg/L solution. The values are lower than the other nanosponges synthesized with the bi-step method. This behavior can be explained by the synthesis issues previous described. Figures 88 and 89 compare reductions of nanosponges functionalized with sulton, tested on copper solutions at two different concentrations.

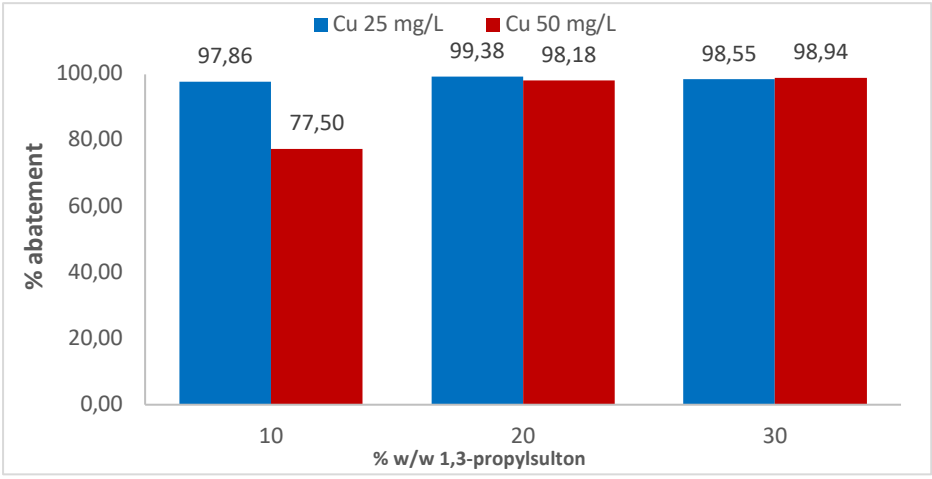

Figure 88: Comparison of the abatement percentages of the copper solution at 25 and 50 mg/L using the 1,3 propylsulton based nanosponge at 10, 20 and 30% w/w.

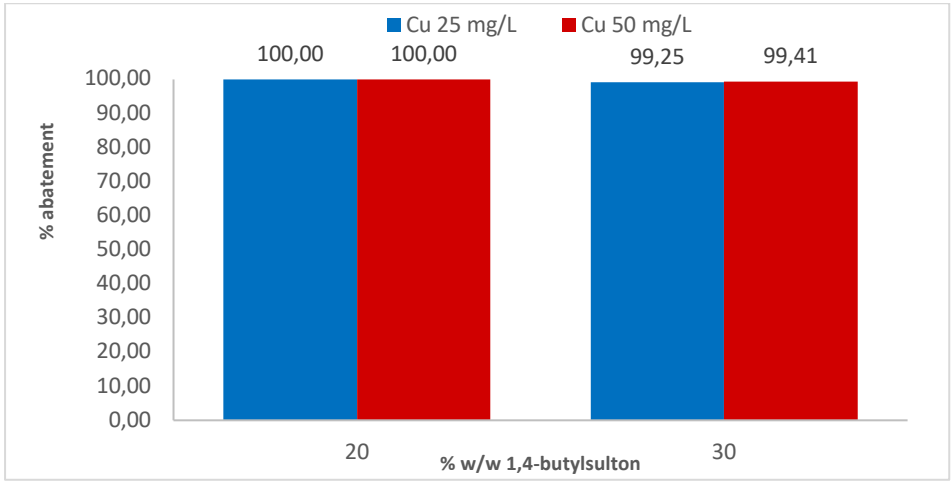

Figure 89: Comparison of abatement percentages of copper solution at 25 and 50 mg/L using 1,4-butylsultone based nanosponge at 20 and 30% w/w.

10.4.10 Nanosponge functionalize with sulphonic groups: a comparison

Figure 89 shows a comparison of the IR spectra of the sulphonic nanosponges, to evaluate how signals of the sulphate and sulfonic groups vary. By enlarging the area between 1900 and 1100

cm^{-1} the group stretching signal ($-SO^{3-}$) is much more evident for nanosponges functionalized with sultons.

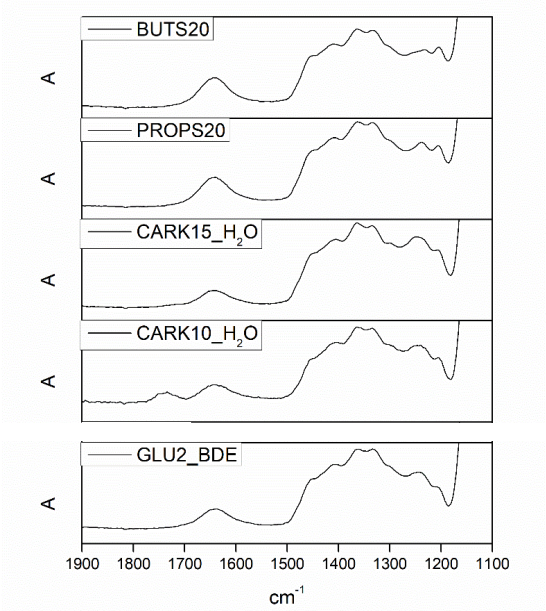

Figure 90: Comparison of the signals of the sulphonic groups of the nanosponge based on carrageenan-K at 10 and 15% w/w in water, of the 1,3-propylsulton and 1,4-butylsultone at 20% w/w (post synthesis) with GLU2BDE.

In Table 85, instead, the percentages of sulfur in the sulfonic nanosponges are summarized, measured by CHNS analysis.

Table 84: %S elemental analysis of cationic nanosponges.

Nanosponge	% S
GLU2_BDE_CARK10%_H_20	0,08
GLU2_BDE_CARK15%_H_2O_b	0,11
GLU2_BDE_CARK15%_H_2O	0,27
PROPS10%_POSTSINTH	0,25
PROPS20%_ POSTSINTH	0,45
PROPILS30%_ POSTSINTH	0,66
GLU2_BDE_1,4BUTS10%	0,41
BUTS20%_ POSTSINTH	0,58
BUTILS30%_ POSTSINTH	0,79

Increasing the amount of functionalizing agent also increases the percentage of sulfur (Figure 90). In addition, the higher values are observed for the functionalized base nanosponge, post synthesis with the 1,4-butylsulton, result that could be ascribed to a better interaction between the polymer and this type of sulton. In fact, the percentages are also higher than those functionalized with 1,3-propylsulton. No sulfur content values were reported for carrageenan-K-based nanosponges, synthesized in the basic environment, as the instrument did not detect the presence of sulfur. This behavior could be attributed to two phenomena:

1. the hydrolysis in the basic environment of the sulphate group, which could be removed as a result of the purification process of the nanosponge;
2. the instrument could not detect too low sulfur values, due to the presence of a few sulphate groups that bind to maltodextrin. Which would explain the fact that the polymer still retains a significant percentage of copper ions, compared to the GLU2_BDE-based nanosponge.

On the other hand, it is interesting to note that GLU2_BDE_1,4BUTS10% nanosponge, have a significant percentage of sulfur.

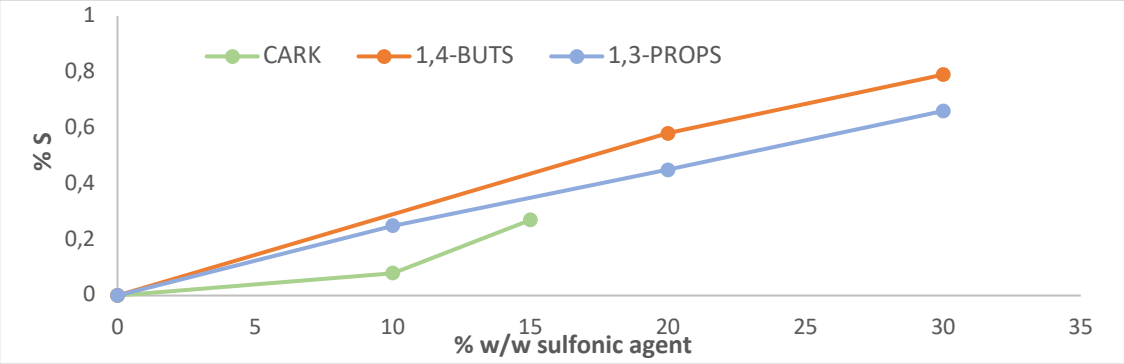

Figure 91: Trend of the percentage of sulfur present in nanosponges in relation to the percentage by weight of added sulphonic agent.

10.5 Synthesis optimization

Nanosponges functionalized with 10% sodium alginate, 10% carrageenan-K and 20 % 1,4-butylsulton (one-step synthesis) have been shown to have excellent adsorption features with Cu^{2+} ions. Therefore, it was decided to synthesize in greater amount to be able to carry out more tests and optimizing the synthesis.

10.5.1 Nanosponge synthesis with carrageenin-K al 10% w/w

The synthesis procedure is the same as described above. The reagents amount is listed in Table 86.

Table 85: Reagents and the respective amounts used for large synthesis.

NaOH 0,2 M	**28 ml**
GLU2	7 g
CARRAGEENIN-K	700 mg
BDE	5 ml

The temperature chosen for the entire synthesis procedure is 100 °C. In addition, due to the previous synthesis, it was decided to leave it for an intermediate time of 150 minutes. The final product was named as follows: GLU2_BDE_CARK10_BIS (Figure 92).

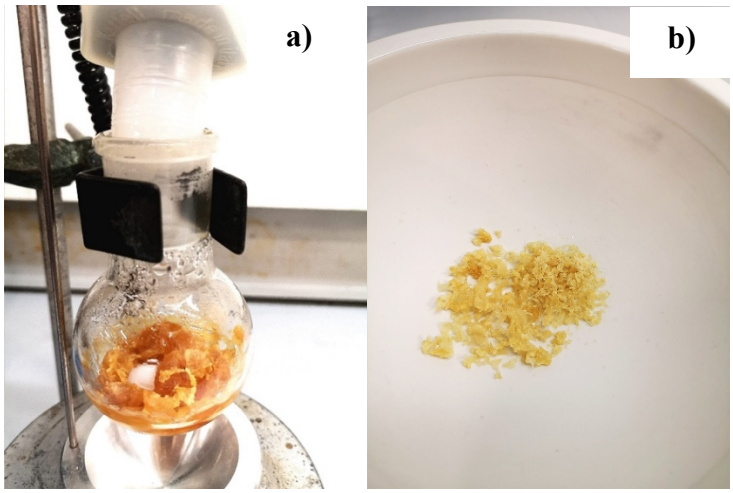

Figure 92: a) Nanosponge GLU2_BDE with 10% carrageenan-K before purification; b) after purification and drying in an oven at 70°C.

10.5.2 Bi-step Nanosponge synthesis with 1,4-butilsulton 20% w/w

The synthesis procedure is the same as described above. The reagents amount is listed in Table 87.

Table 86: Reagents and the respective amounts used for large synthesis.

NaOH 0,2 M	**50 ml**
GLU2_BDE	6 g
1,4-butilsulton	0,902 ml

The final product was named as follows: 1,4-BUTS20_POSTSINTH_BIS. Following the milling with mortar and pestle the three nanosponges are shown in Figure 93.

Figure 93: a) Sodium alginate based nanosponge; b) carrageenan-K and c) 1,4-butylsulton based nanosponge (post synthesis).

Mass balances are shown in Table 88.

Table 87: Mass balance of cationic nanosponges.

Nanosponge	**MB %**
GLU2_BDE	73
GLU2_BDE_CARK10	49
BUTS20_POSTSINTH	81

Mass balances values are congruent with previous synthesis. For the synthesis mechanism, as an example, Figure 94 shows a schematic representation of the functionalization of maltodextrin by the addition of 1,4-butylsulton. The same behavior can also be found for sodium alginate and carrageenan-K, added instead of sulton.

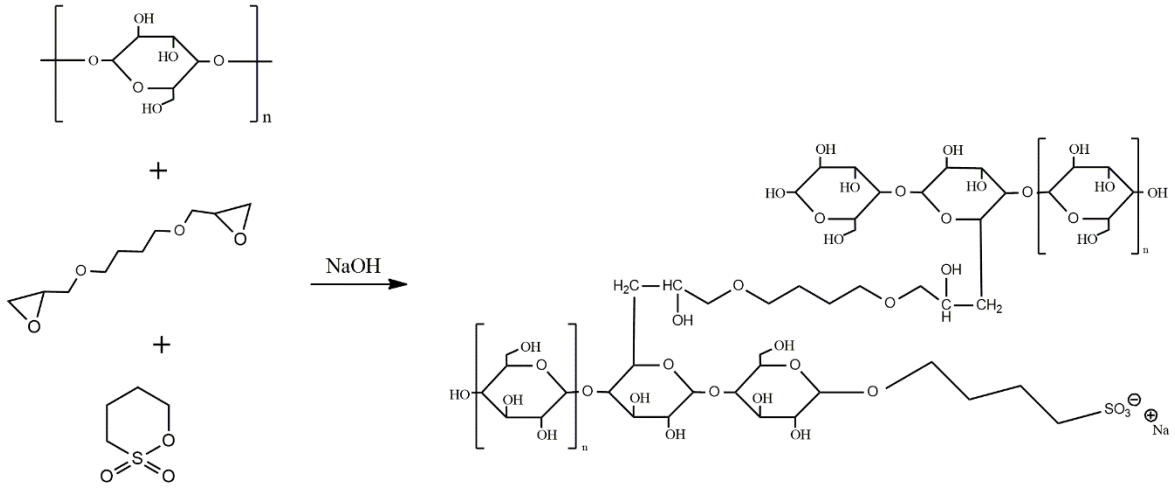

Figure 94:Schematic representation of the functionalization of maltodextrin by 1,4-butylsulton.

10.6 Cationic nanosponge final characterization

10.6.1 FTIR-ATR, TGA and Elemental analyses analyses

The following analyses have been carried out as in the previous cases to assess the presence of sulphonic agents and to confirm the interaction between maltodextrin or already synthesized nanosponge (case sultons) and functionalizing agents. The results were positive and fully comparable with the FTIR-ATR and TGA analyses already recorded for the first summaries. The results are given in Appendix I.

10.6.2 Potential-ζ

The potential-ζ measurement was also performed for each sample to assess the surface charge of the nanoparticles. The instrument performs three measurements for each sample and in addition the measurements have been performed in duplicate to have a replicability of the results. The averages of the calculated potential-ζ values for each sample and their standard deviation are given in Table 89.

Table 88: Potential-ζ final results.

Nanosponge	Potential-ζ (average)	St. Dev.
GLU2_BDE	-2,3	0,51
GLU2_BDE_CARK10%_H_2O_BIS	-6,6	0,93
BUTS20%_POSTISINTESI_BIS	-19,5	0,93

Due to sulfonic groups on the surface of the nanosponge, potential-ζ value is much more negative than GLU2_BDE. However, values are not as high as expected: the reason could be attributed to a lower stability of the polymer particles, which could easily aggregate.

10.6.3 Swelling test

One of the main characteristics of cross-linked polymers is that in water or other solvents they tend to swell.[235] For the three nanosponges examined, swelling tests were carried out

according to the method described in paragraph 6.5.5. The tests were performed in triplicate to obtain a replicability of the results, using distilled water at room temperature. The percentage swelling value has been calculated using the following formula:

$$\%\ swelling = \left(\frac{g_{(\ swelled\ polymer)} - g_{(dry\ polymer)}}{g_{(dry\ polymer)}}\right) \times 100,$$

In Table 90 the average of the values of swelling percentages and standard deviation are reported.

Table 89: Average values of swelling percentages.

Nanosponge	% (average)	St. Dev
BUTS20%_POSTSINTH_BIS	687,80	23,4
GLU2_BDE_CARK10%_BIS	436,44	5,3

Carrageenan-K nanosponges tend to swell less than the nanosponge functionalized with sulton. Swelling % is lower when compared with literature values in which the same nanosponge based GLU2_BDE, functionalized with amino groups, has been shown to have swelling properties far exceeding between 600% and 1400%. Generally, polymers with a high degree of cross-linking tend to swell little and there are suitable for environmental applications, especially for water treatment, as they can be packed into filtering devices and reused for multiple cycles. In a recent study, analogous polymers based on β-cyclodextrin and maltodextrin, crosslinked with citric acid or PMDA, were considered suitable for this type of application, as their swelling rates were below 400%.[141]

10.6.4 SEM analysis

Scanning electron microscope (SEM) analysis was instrumental in assessing the morphology of the following three maltodextrin nanosponges:

- BUTS20%-POSTSINTH_BIS, functionalized with 20% w/w of 1,4-butylsulton (Figure 95);
- GLU2_BDE_CARK10%_H2O _BIS, functionalized with 10% w/w carrageenan K in aqueous environment (Figure 96).

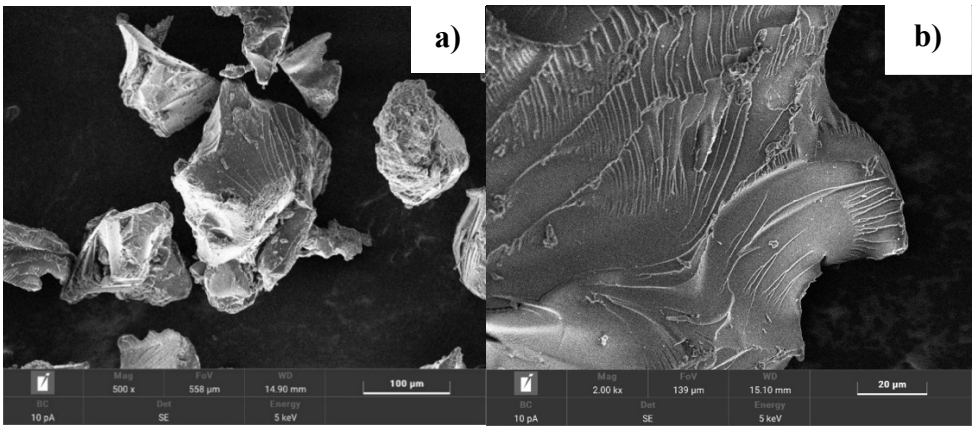

Figure 95: SEM images of polymer product granules 1.4BUTS20%-POSTSINTH_BIS. Magnification of 500x a) and 2kx b).

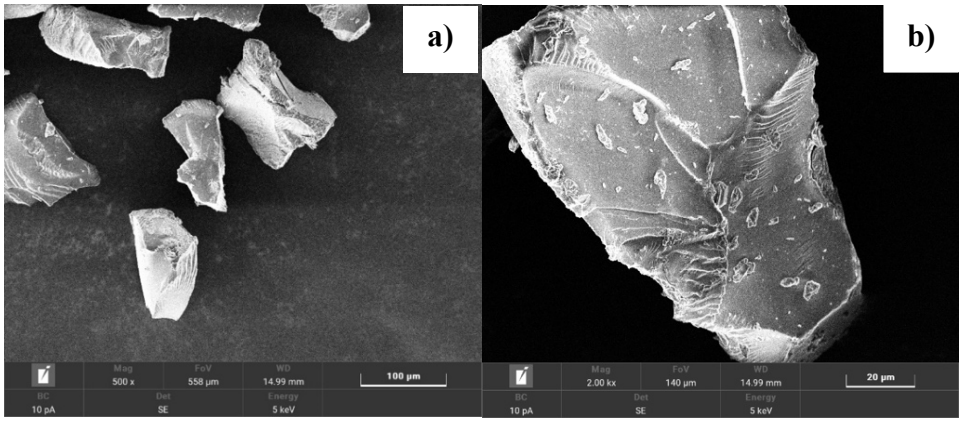

Figure 96: SEM images of polymer product GLU2_BDE_CAR10%_H2O_ BIS. Magnification of 500x a) and 2kx b).

The SEM characterization revealed that all nanosponges show an irregular morphology and a rather smooth outer surface. The presence of faults may have been caused by the grinding process of the final product.

10.7 Abatement test

The following nanosponges GLU2_BDE_CARK10%_BIS and BUTS20%_POSTSINTH_BIS have been tested by performing several abatement tests on different heavy metals at different concentrations. Copper (Cu^{2+}), chromium (Cr^{3+}), aluminum (Al^{3+}), nickel (Ni^{2+}), manganese (Mn^{2+}), lead (Pb^{2+}), cadmium (Cd^{2+}) and zinc (Zn^{2+}) were selected as heavy metals. It was used 250 mg of nanosponge in 25 ml of selected heavy metal stock solution. Initially, each o nanosponges was tested on a single metal solution with a concentration of 25 mg/L. After filtering the samples, they were analyzed at the ICP-OES. Table 91 shows the concentrations and pH values of the stock solutions used.

Table 90: Concentration mg/L and pH of standard solutions.

Heavy metal	Stock solution mg/L	pH
Cu	29,63	5
Cr (III)	31,59	5
Al	30,89	4
NI	19,97	5
Mn	10,71	4,5
Pb	28,51	5
Cd	21,84	5
Zn	36,70	4,5

The abatement rates and the mg/g of heavy metal retained by each of the three nanosponges tested are summarized in Table 92, while Figure 97 shows their comparison.

Table 91: Abatement rates and mg/g of heavy metals retained.

Nanosponge	Cu (%)	Cr^{3+} (%)	Al (%)	Ni (%)	Mn (%)	Pb (%)	Cd (%)	Zn (%)
GLU2_BDE_CARK10%	86,85	71,01	38,50	82,08	57,21	99,53	95,45	65,17
BUTS20_POSTSINTH	99,60	99,64	100,0	98,83	99,34	99,96	99,28	98,97
Nanosponge	**mg/g**	**mg/g**	**mg/g**	**mg/g**	**mg/g**	**mg/g**	**mg/g**	**mg/g**
GLU2_BDE_CARK10%	2,57	2,24	1,19	1,64	0,61	2,84	2,08	2,39
BUTS20%_POSTSINTH	2,95	3,15	3,09	1,97	1,06	2,85	2,17	3,63

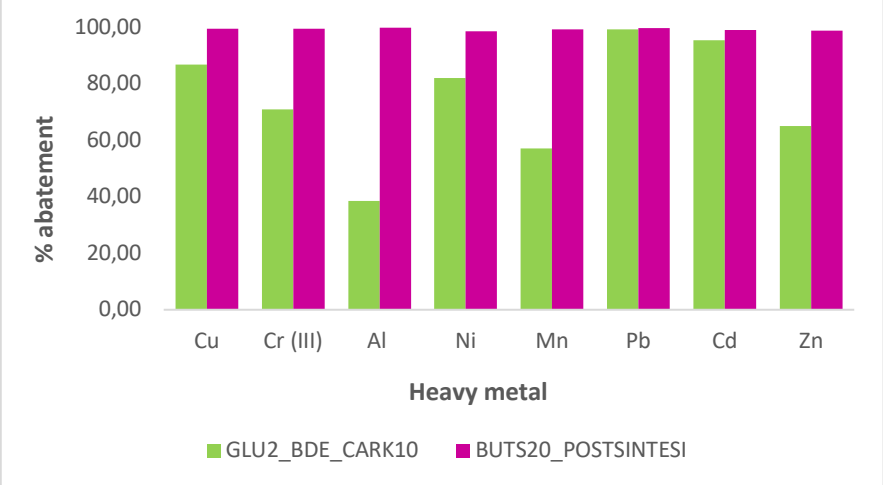

Figure 97: Comparison of the eight heavy metals abatement at 25 mg/L concertation.

All nanosponges have excellent adsorption capacities. By functionalizing maltodextrin with 20% w/w of 1,4-butylsulton, the adsorbent material showed excellent performance on all metals tested and especially on aluminum (as a tricaric ion), the abatement achieved was total. Even when the polysaccharide skeleton was functionalized with 10% w/w of sodium alginate, good abatement rates were found, comparable to the previous one, especially for copper, chromium, nickel, lead and cadmium. Carrageenan-K nanosponge has lower abatement values than the others: it is very efficient against lead and cadmium which demonstrate a likely affinity

for sulfur (>95%). Due to the excellent adsorbent capacity BUTS20%_POSTSINTH_BIS, these were tested on a metal mix with a total concentration of 50 mg/L. Samples were prepared using 250 mg of nanosponge in 25 ml of the metal mixture solution. The percentages of abatement and the mg/g of retained metal are shown in Table 93.

Table 92: Percentages of felling and mg/g from the 50 mg/L mix solution.

Nanosponge	**Cu (%)**	**Cr^{3+} (%)**	**Al (%)**	**Ni (%)**	**Mn (%)**	**Pb (%)**	**Cd (%)**	**Zn (%)**
BUTS20%_POSTSINTH	16,8	33,9	36,1	22,0	16,1	7,8	15,3	16,1
Nanosponge	**mg/g**	**mg/g**	**mg/g**	**mg/g**	**mg/g**	**mg/g**	**mg/g**	**mg/g**
BUTS20%_POSTSINTH	0,097	0,22	0,22	0,11	0,08	0,032	0,078	0,14

The resulting abatements are quite low both because the concentration of the solution of the metal mixture was quite high, and because metals enter competition: for some of them access to the active sites on the polymer is inhibited. This test allowed to estimate the probable mechanism of interaction between nanosponge and the eight heavy metal.

Considering the sample based on sodium alginate, the best abatement is found for the tricaric ion Cr (III) and for the bicaric ones such as Pb, Al and Ni. Alginate could impart mainly complexing properties, especially for lead, and in a small part of ion exchange features, as very similar to the tricaric ion Cr (III). 1,4-butylsultone-based nanosponge works very well with chromium (Cr^{3+}) and aluminum (Al^{3+}) as tricaric ions, and on average with bicaric ions such as copper, nickel, manganese, zinc and cadmium, has a lower percentage of lead. From these observations it can be assumed that is predominant both the effect of the charge and the size of the ion. Aluminum ion has a higher charge density and is retained slightly more than the Cr (III), which is larger. For bi-charged ion the results are quite similar, only nickel has a slightly higher value, as it is probably more like sulfur. From these considerations, it can be deduced that the 1,4-butylsulton could impart similar properties to those of an ion exchange resin, as the charge of the ion and consequently the pH of the solution plays a predominant role. In fact, commercial cationic resins generally interact better with high-charged ions, with small volume of hydration and that are very similar to the sulfonic group.[236] It was tried a test lowering the total concentration of the solution of the eight metals mixture to 10 mg/L. The concentrations of the stock solutions obtained from the ICP-OES are shown in Table 94. The results obtained, following analysis at ICP-OES, are summarized in Table 95, which shows the percentages of abatement and mg/g of the retained metal.

Table 93:Metal concentrations in the solution mix at 10 mg/L.

Heavy metal	Metal mix solution 10 mg/L
Cu	12,43
Cr (III)	13,37
Al	12,62
Ni	8,71
Mn	9,90
Pb	15,83
Cd	10,38
Zn	17,26

Table 94: Percentages of felling and i mg/g from the solution mix to 10 mg/L.

Nanosponge	Cu	Cr(III)	Al	Ni	Mn	Pb	Cd	Zn
BUTS20%_POSTSINTH	96,30	98,58	99,91	91,96	91,82	99,31	93,26	92,47
Nanosponge	**mg/g**	**mg/g**	**mg/g**	**mg/g**	**mg/g**	**mg/g**	**mg/g**	**mg/g**
BUTS20%_POSTSINTH	1,20	1,32	1,26	0,80	0,91	1,57	0,97	1,60

The percentages of abatement following these tests appear to be much higher. This nanosponge has values higher than 90%, comparable with those obtained from common commercial cationic resins [237][236][238], with the difference that this type of adsorbent material is mostly made up of cheap, sustainable, and easy-to-use raw materials such as maltodextrin. In Table 96 the comparison between the abatement with nanosponge based on 1,4-butylsultone to 20% (current study) and a cationic resin commercial [238] based on styrene-divinylbenzene, found in literature are shown. Compared to the commercial one, the nanosponge functionalized with butyl-sulton has however demonstrated comparable adsorption capacities, although it should be noted that these studies from the literature were carried out in the field and not under standard conditions as in this work.

Table 95: Comparison of abatement rates between the nanosponge 1.4BUTS20%_POSTSINTH and a commercial ion exchange resin.

Heavy metal	% Abatement 1,4BUTS20%_POSTSINTH (each metal 10 mg/L)	%Abatement commercial resin DOWEX50WX8[238] (real situation)
Ni	91,96	57,8
Cd	93,26	96,1
Pb	99,31	94,8
Zn	92,47	82,6
Cu	96,30	50

This test confirms the role of the two functionalizing agents in the nanosponge. As we can see from Table 96, sample also appears to be very similar to chromium, as a small part of the nanosponge could give ionic exchange. As regards butylsulton functionalized ion, the best abatement is again found for the aluminium tricaric ion, demonstrating that the following nanosponge has similar behavior of an ion exchange resin.

10.8 Adsorption kinetics

The following study was carried out on 1,4-BUTS20_POSTSINTH_BIS, using as metal the copper test, to evaluate their abatement efficiency at different times: after 15, 30 and 60 minutes.

Table 96: % abatement after 15, 30 and 60 minutes.

BUTS20%_POSTSINTH	t (min)	% Cu abatement	mg/g
	60 min	98,3	2,85
	30 min	98,1	2,85
	15 min	97,9	2,84

The results show that after 15 minutes the copper ions are almost completely abated. In fact, the values that are observed, leaving the nanosponge at greater times, are almost equal and the trend is almost linear.

10.9 Saturation test

The test was carried out on copper heavy metal alone for BUTS20%_POSTSINTESI_BIS nanosponges. The samples for the abatement tests used copper ion solution at increasing concentrations: 100, 400 and 1000 mg/L.

Table 97: Abatement percentages and mg/copper ions retained by loading the nanosponge with increasing concentrations of the copper solution.

Nanosponge	Concentration Cu mg/L	% Cu abatement	mg/g
BUTYLSULTON 20%	25	99,60	2,95
BUTYLSULTON 20%	100	91,84	1,02
BUTYLSULTON 20%	400	13,96	0,16
BUTYLSULTON 20%	1000	5,18	0,06

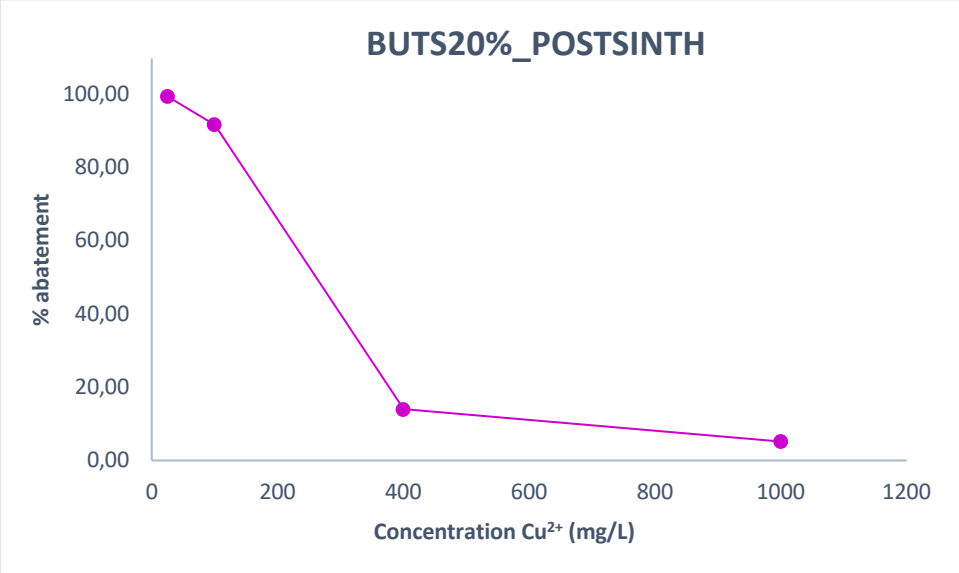

Figure 98: Abatement trend by loading the nanosponge with increasing concentrations of the copper solution.

Comparing the abatement rates with those with a stock solution of 25 mg/L of copper, a decrease is observed, as the active sites of the adsorbent system are becoming saturated. However, at 1000 mg/L, nanosponges retain a minimum percentage of copper cations.

10.10 Release test

Release tests were carried out for BUTS20_POSTSINTH_BIS nanosponges saturated with 100 mg/L copper solution.

Table 98: % release in water.

Nanosponge	Water release %
BUTS20%_POSTSINTH_BIS	0

Copper ions release into water is non-existent, a sign that the interaction between the functional groups present on the surface of the nanosponge and the copper cation is rather strong.

10.11 Nanosponge-metal interaction mechanism

For further confirmation as to whether the interaction mechanism between BUTS20_POSTSINTH_BIS and the metal cations is complexation or ion exchange, copper ion release tests were carried out one in 0 solution 0,01 M EDTA and the other in 0,01 M $CaCl_2$ solution. If the adsorption mechanism is an ion exchange, the active sites of adsorbent polymer release copper ions and bind to calcium, while if it is a complexion mechanism the metal will bind to EDTA, as the strongest complexing agent of the sulphonic groups. Nanosponges used are those previously charged with 1000 mg/L of copper solution.

Table 99: EDTA and CaCl2 % release.

BUTS20%_POSTSINTH_BIS	**Cu^{2+} total = 51,8 mg/L**	
	Release mg/L	**Release %**
In EDTA	56,2	100
In $CaCl_2$	43,93	84,81

The results confirmed the assumptions as previously theorize. Both nanosponges have a dual mechanism. By functionalizing the nanosponge with butylsultone, the release into $CaCl_2$ tends to increase significantly, as it acts as an ion exchange resin. However, all copper ions are also released in EDTA.

10.12 Biochar: Biomass characterization

10.12.1 Moisture content

The determination of the moisture content of each wood was measured by weighing about 1-2 g of sawdust, placed on aluminum paper, on an analytical balance. The samples were dried in oven at 120 ºC for 24 hours, after which they were weighed again to determine the dry weight (g) and consequently the moisture content (g).

Table 100: Determination of moisture content % (m/m) of woody biomass.

Biomasses	Wet weight (g)	Dry weight (g)	Moisture content (g)	Moisture (%)
Spruce	1,7524	1,624	0,1284	7,3
Corn cob	1,7348	1,5548	0,1800	10,4
Sawdust	1,4704	1,4439	0,0265	1,8
Hazelnut shells	2,0176	1,8738	0,1438	7,1
Cherry	1,7206	1,5585	0,1621	9,4
Gaggia	1,5341	1,3506	0,1835	12,0
Elder	1,7556	1,5537	0,2019	11,5
Walnut	1,8364	1,6930	0,1434	7,8
Jube	1,5526	1,4595	0,0931	6,0
Plum	1,6897	1,5896	0,1001	5,9
Fig	1,5255	1,3462	0,1793	11,8
Hazelnut tree	1,7093	1,6490	0,0603	3,5

The following formulae were used to determine the moisture content (grams and %):

$$Moisture\ content\ (g) = wet\ weight\ (g) - dry\ weight\ (g)$$

$$Moisture\ \% = \frac{Moisture\ content\ (g)}{wet\ weight\ \ (g)} * 100$$

It is possible to notice how the less aged woods such as fig, acacia and elderberry are those containing a higher percentage of water inside them, vice versa the spruce, jube and prune have a lower moisture content.

10.12.2 Ashes content

Woody biomass consists essentially of carbon, oxygen, and hydrogen. The nitrogen content is less than 0.1%, while the ash content does not exceed 0.2-0.3%. The determination of the ash was carried out by incineration at 550 ºC in porcelain crucibles previously brought to constant weight, placed for 15 min in oven at 120 ºC and afterwards in the desiccator, so that environmental humidity does not affect the measurement. Weigh about 1-2 g of the sample are inserted in crucibles inside the tubular furnace where the samples will be heated at 550 °C for 12 h and will turn into ash. The weight of the ashes + crucible is measured by carrying the

samples to constant weight in the same way as before. It is then possible to determine the weight of the ash (g) and subsequently its percentage weight, using the following formulae:

$$Ashes\ (g) = g\ (crucible + ash) - g\ crucible$$

$$\%\ m/m\ ashes/\ dry\ biomasses = \frac{ashes\ (g)}{dry\ biomass\ weight\ (g)} * 100$$

Table 101: Ashes content % determination.

.

Biomasses	Sawdust weight (g)	Ashes weight (g)	% m/m ashes
Spruce	1,6472	0,0110	0,67
Corn cob	1,5708	0,0344	2,19
Sawdust	1,3962	0,0169	1,21
Hazelnut shells	1,8796	0,0216	1,15
Cherry	1,5704	0,0143	0,91
Acacia	1,3667	0,0143	1,05
Elder	1,5755	0,0308	1,95
Core	1,7174	0,0366	2,13
Jube	1,4779	0,0299	2,02
Plum	1,5946	0,0227	1,42
Fig	1,3652	0,0513	3,76
Walnut	1,6310	0,0792	4,86

10.12.3 Biochar yields

Biochar corresponds to the solid carbon residue of the wood that has been heated in an oxygen-free environment (pyrolysis). This treatment removes moisture and volatile substances from the wood. The tables show the grams of each wood inserted in the furnace and the respective grams of biochar achieved for each temperature and the values in terms of yield % in biochar for all samples, at three temperatures.

Table 102: Comparison of yield % (w/w) in biochar at 550°C, 800°C, 1100°C.

Biomasses	Yield % 550 °C	Yield % 800 °C	Yield % 1100 °C
Spruce	27,80	24,02	23,11
Corn cob	25,03	24,50	24,07
Sawdust	27,11	26,62	25,16
Hazelnut shells	32,38	31,44	27,92
Cherry	26,46	25,23	23,37
Acacia	26,51	23,75	21,67
Elder	29,43	24,88	23,65
Walnut	28,85	25,14	23,58
Jube	30,73	26,92	24,57
Plum	28,62	24,31	23,65
Fig	29,24	28,85	26,71
Hazelnut tree	32,34	23,34	21,62

The biochar yield (%) was calculated with the following formula:

$$Biochar\ yield\ \% = \frac{biochar\ weight\ (g) * 100}{biomass\ weight\ (g)}$$

It is possible to see that the biochar yield is higher for samples that have been heated and have been produced at lower temperatures, which leads to the affirmation that biochar yield gradually decreases with the increase of the pyrolysis temperature.

10.12.4 pH determination

The effect of the biochar on the pH of the solution in which is placed in contact was evaluated. 0,5 g of each sample was inserted in 25 ml of water, placed inside Falcon-type tubes. The pH was measured after 72 hours of contact. The results show how the pH of the solution becomes alkaline because of contact with biochar. This phenomenon is caused by carbonates and oxides of alkali and alkaline earth metals in biochar. The samples that give the most alkalinization phenomena are those produced at 1100 °C: the increase in pH increases as the pyrolysis temperature with which the biochar was produced increases. This phenomenon also depends on the essence.

Table 103: pH measured on aqueous solutions after 72 hours of contact with different biochar samples.

Sample	pH (average)
Spruce 550 °C	8,705
Spruce 800 °C	10,136
Spruce 1100 °C	10,423
Cherry tree 550 °C	8,974
Cherry tree 800 °C	10,472
Cherry tree 1100 °C	11,013
Fig 550 °C	8,620
Fig 800 °C	10,131
Fig 1100 °C	10,489
Acacia 550 °C	8,581
Acacia 800 °C	10,007
Acacia 1100 °C	10,331
Jube 550° C	8,691
Jube 800 °C	10,52
Jube 1100 °C	10,974
Hazelnut shells 550 °C	9,082
Hazelnut shells 800 °C	11,932
Hazelnut shells 1100 °C	12,206
Walnut 550 °C	9,632
Walnut 800 °C	10,783
Walnut 1100 °C	11,113

Walnut 550 °C	9,561
Walnut 800 °C	10,13
Walnut 1100 °C	10,573
Plum 550 °C	9,036
Plum 800 °C	10,426
Plum 1100 °C	10,975
Elderberry 550 °C	10,10
Elder 800 °C	10,485
Elder 1100 °C	10,621
Poplar Sawdust 550 °C	9,03
Poplar Sawdust 800 °C	11,808
Poplar Sawdust 1100 °C	11,696
Corn cob 550 °C	9,537
Corn cob 800 °C	11,76
Corn cob 1100 °C	11,003
Commercial biochar	9,794
Commercial activated carbon	8,723

10.12.5 FTIR analysis

FTIR-IR analysis was performed to verify the presence and disappearance of functional groups on biochar at different temperatures. To achieve this, comparisons were made mainly by overlapping different spectra. It also occurred whether the acid treatment affected the spectrum bands, which did not happen.

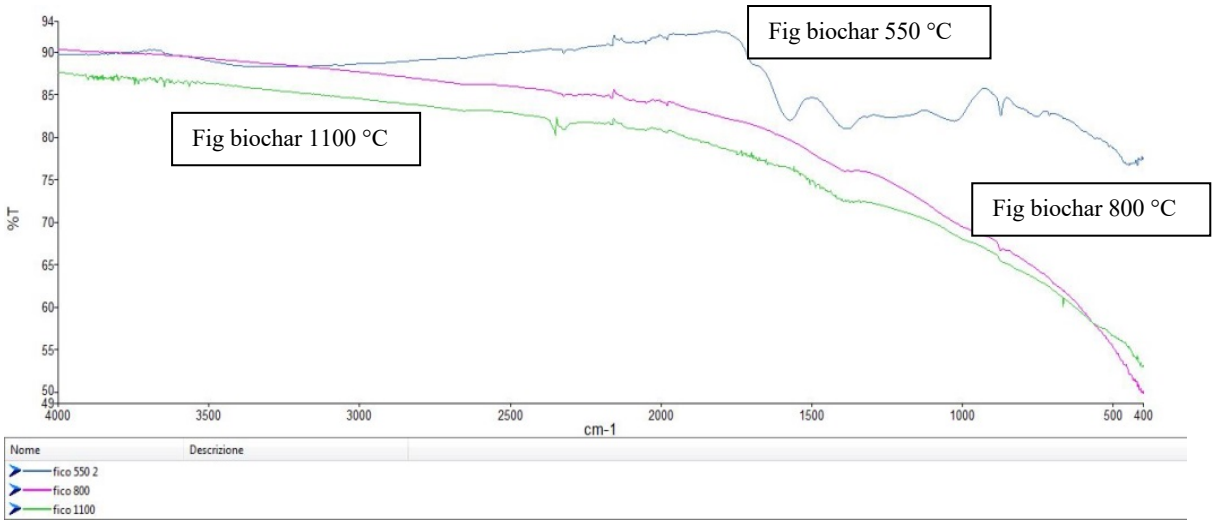

Figure 99: IR spectra of fig biochar.

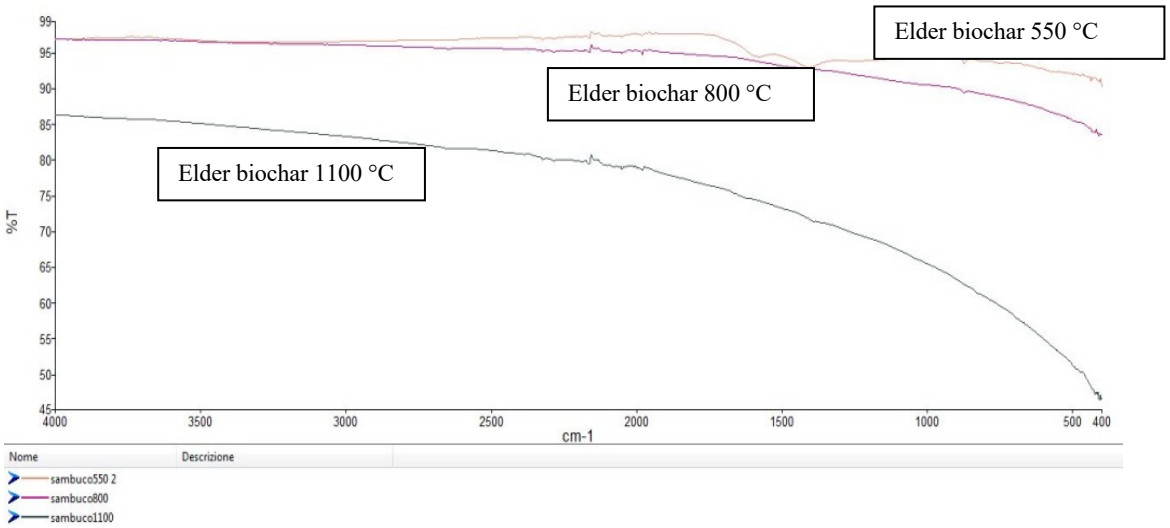

Figure 100: IR spectra of elder biochar.

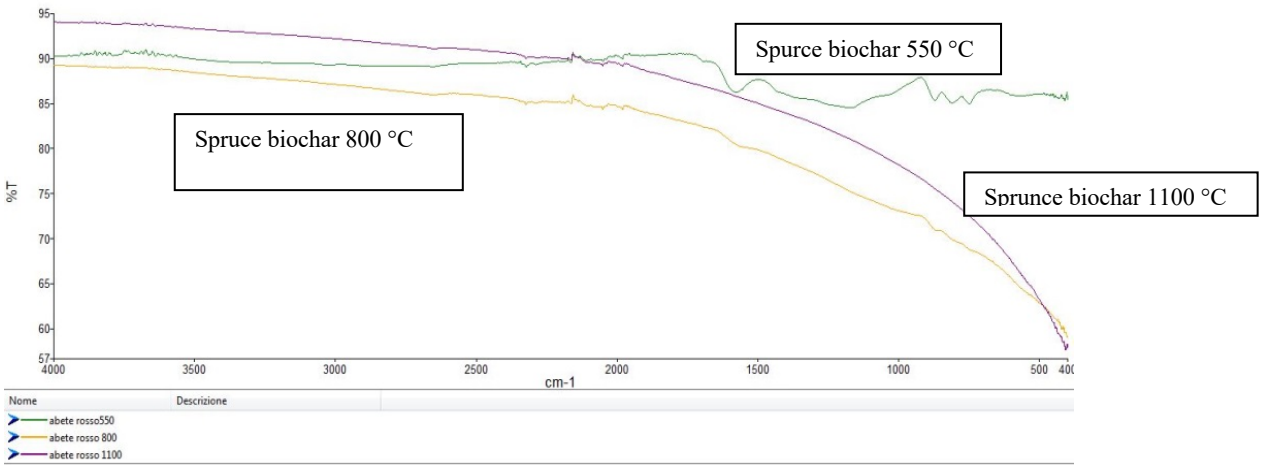

Figure 101: IR spectra of spruce biochar.

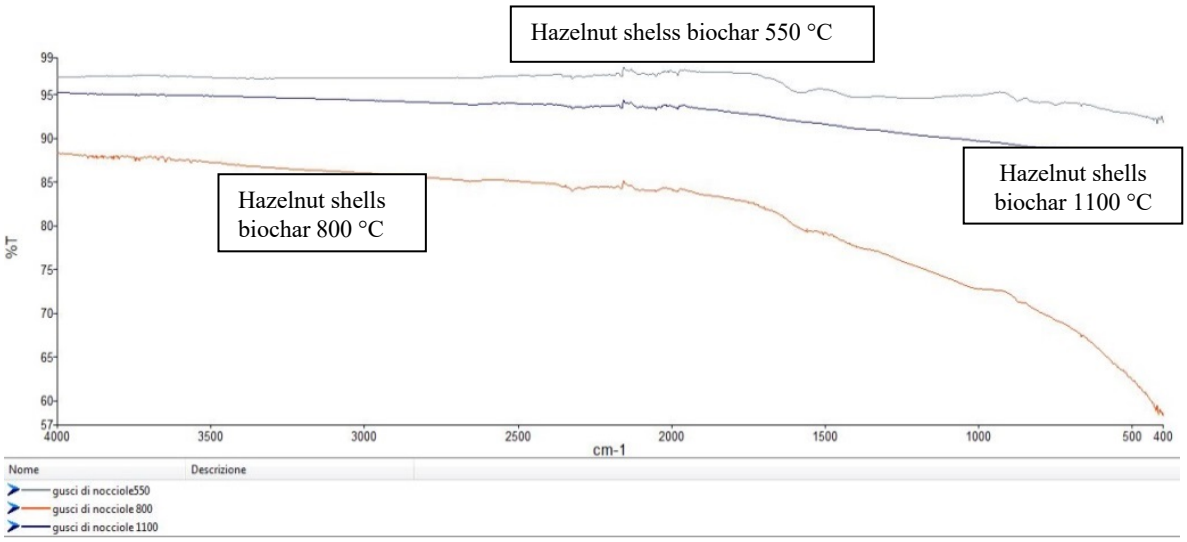

Figure 102: IR spectra of hazelnuts shells biochar.

As the pyrolysis temperature increases, biochar spectrum flattens, especially at 1100 °C, the spectrum usually corresponds to that of a totally amorphous material. Starting from the spectra of the biochar at 550 °C, it is possible to notice the presence of lignin through the peaks of the bonds C-O at 1200-1300 cm^{-1} and the peaks of the aromatic bonds C-H at 900-700 cm^{-1}. It is also found the presence of cellulose, from the slight bands related to groups O-H at 3600-3200 cm^{-1}, and those at 2950-2850 cm^{-1} of groups C-H aliphatic. It is also noted graphite bands present at 1600-1400 cm^{-1} relative C=C aromatic. As the pyrolysis temperature increases, first component that disappears is cellulose: the bands related to the stretching of the O-H bonds (3600-3200 cm^{-1}) and of the C-H bonds of the aliphatic groups (2950-2850 cm^{-1}) lose intensity. At the same time, there is an increase in the intensity of the C=C and C-H aromatic bands at 1600-1400 cm^{-1}, implying a high dehydration phenomenon and an increase in the aromaticity of the structure. These bands are attributable to the graphite structure. At 1100 °C, for almost all woods, graphite bands (1600-1400 cm^{-1}) disappear and the structure is amorphous. An interesting aspect is that the structures degradation of different biochar is slightly different some wood carbonizes differently, and this can be observed by spectra related to samples pyrolyzed at 800 °C and 1100 °C.

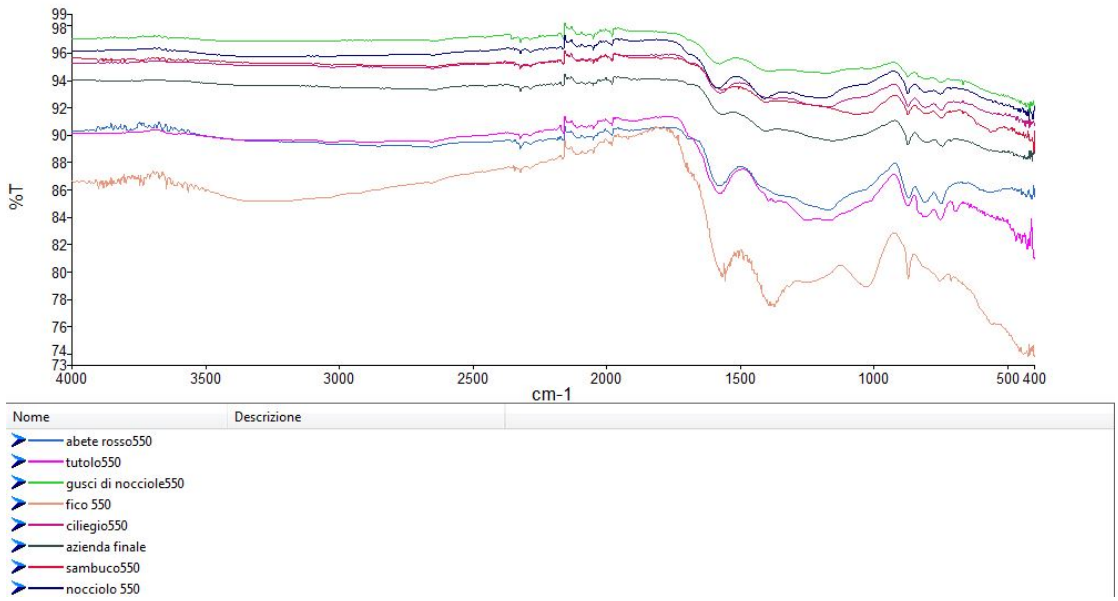

Figure 103: IR spectra comparison of all biochar at 550 °C.

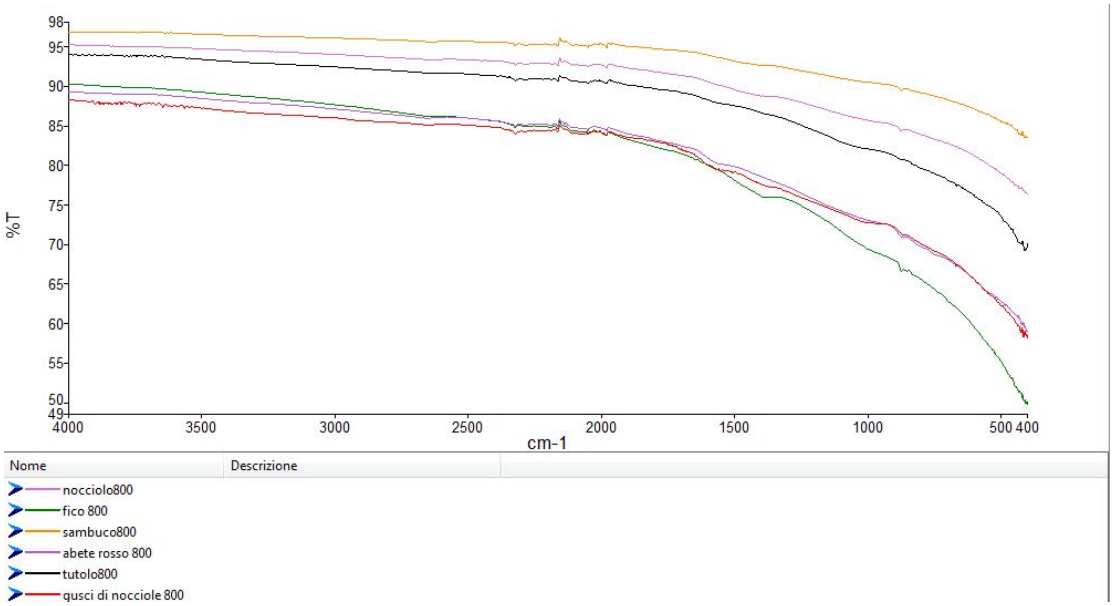

Figure 104: IR spectra comparison of all biochar at 800 °C.

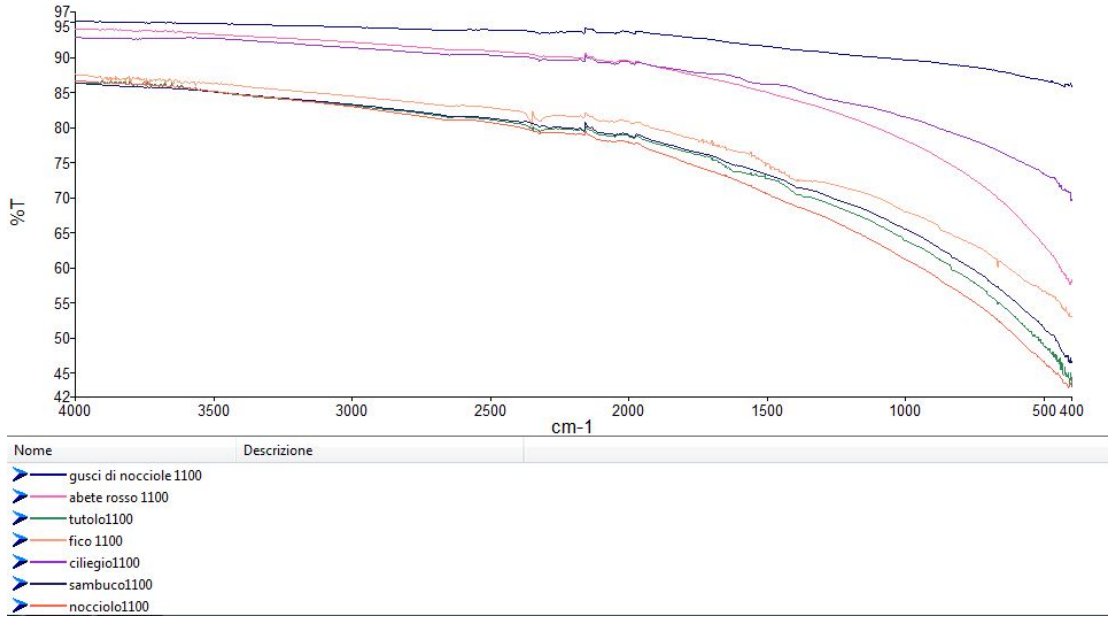

Figure 105: IR spectra comparison of all biochar at 1100 °C.

Cherry tree, corn cob, elder and fig biochar at 1100 °C, conserve their structure and a minimum of crystallinity, given by the presence of graphite, represented by bands at 1600-1400 cm^{-1}. In the case of cherry tree sample this may be due to the presence of resin. Other woods such as spruce and walnut biochar do not have this characteristic band.

10.12.6 Elemental analyses

Elemental analysis was carried out on some biochar samples. The analysis was carried out on samples with a mass of 2,5 mg to lower the error and standard deviation.

Table 104: Elemental analysis biochar results.

Sample	Nitrogen	Carbon	Hydrogen	Sulfur
	%	%	%	%
Commercial Biochar	0,73	74,62	1,97	0,00
Fig 550 °C	1,02	68,76	2,47	0,00
Fig 800 °C	0,99	73,00	0,89	0,00
Fig 1100 °C	0,85	75,69	0,52	0,00
Elder 550 °C	1,15	72,06	2,95	0,00
Elder 800 °C	1,00	79,55	0,99	0,00
Elder 1100 °C	0,96	80,91	0,58	0,00
Walnut wood 550 °C	0,57	69,12	2,57	0,00
Walnut wood 800 °C	0,60	68,32	0,88	0,00
Walnut wood °C	0,67	79,33	0,29	0,00
Spruce 550°C	0,28	80,19	2,54	0,00
Spruce 800°C	0,30	82,38	0,16	0,00
Spruce 1100°C	0,54	85,57	0,31	0,00

Best biochar samples (fig and elder biochar) have a nitrogen content of 0,9-0,15 that decreases slightly as pyrolysis temperature increases. On the other hand, spruce and walnut wood biochar sample, have a maximum nitrogen content of 0,67, which increases with the pyrolysis temperature but keeping values between 0,3 and 0,67. This would involve the presence of amino groups, which improve metal removal. The hydrogen content is also higher in elder and fig biochar but to a lesser extent. Carbon content is higher in spruce and walnut biochar and increases as the pyrolysis temperature increases. No biochar detected sulfur.

10.12.7 Porosity and surface area: BET isotherm analyses

To determine whether the biochar's abatement performance was due to the porosity of the material and the abatement was carried out on surface adsorption mechanism, gas volumetric measurements were carried out (isotherm BET) on the most promising samples (Fig 1100 °C, Elder 1100 °C and commercial biochar). The BET isotherm allows me to measure the total volume of gas (N_2) that the material can adsorb, expressed through the volume change of the substrate.

$$V = Vm\frac{Cp}{(po-p)[1+(C-1)*\frac{p}{po}]}$$

Where Vm corresponds to the volume of gas adsorbed by the first monolayer (thus corresponds to the capacity of the monolayer) and allows to calculate the specific surface of the substrate (m^2/g); C is the BET constant and represents the energy difference between the first monolayer (due to the substrate-adsorbed interaction) and the interaction energy between adsorbed

particles. This allows to calculate the net adsorption heat and the higher the interaction energy between substrate and adsorbed will be its value also influences the shape of the BET isotherm. Through these measurements, the values of the surface areas (m^2/g) and the volume of pores (cm^3/g) were determined, then their type. The results are as follows:

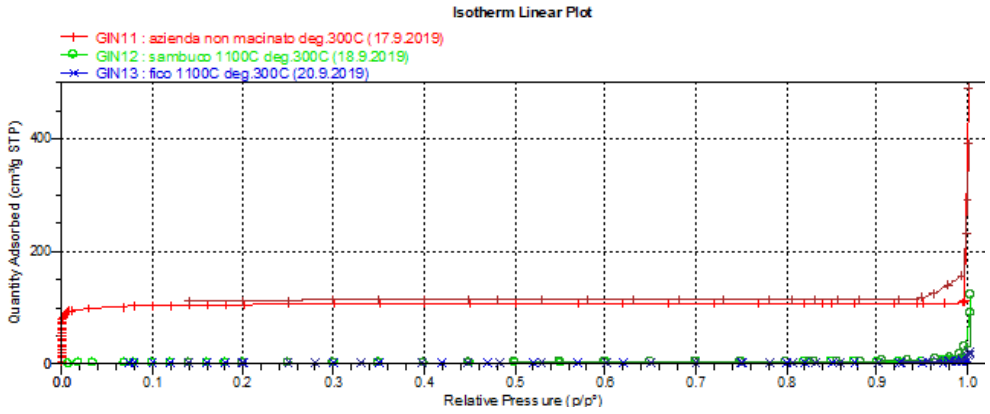

Figure 106: Commercial biochar and biochar BET Isotherm of Fig and Elder 1100 °C.

Commercial biochar is the only sample interesting from surface area e point of view. It gives an isotherm of type I, typical of microporous materials, has an area of 474 m^2/g from Langmuir model (more suitable than BET with microporous samples) and a volume of micropores of 0.13 cm^3/g (as evaluated by cumulative DFT graph):

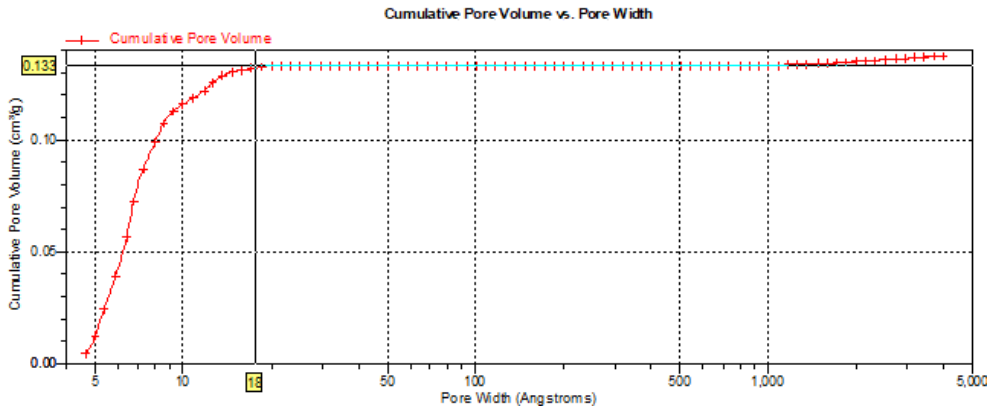

Figure 107: Cumulative graph DFT of commercial biochar and biochar of fig and elderberry 1100 °C.

In this second graph you can see how the pores are distributed:

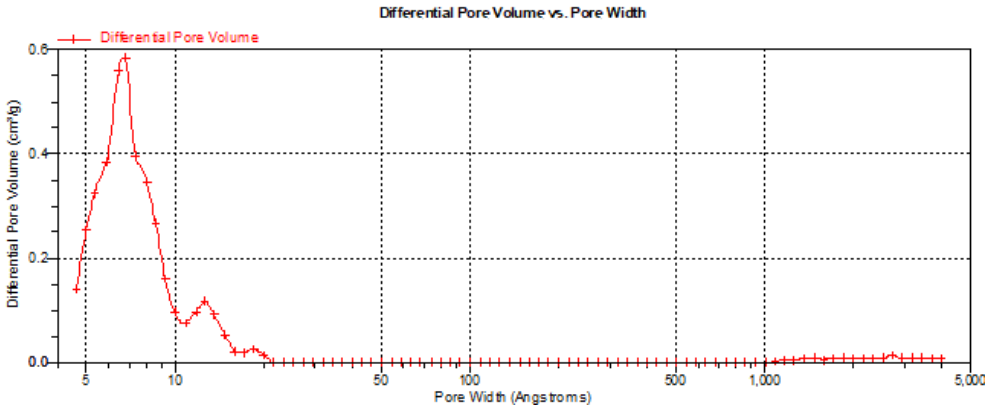

Figure 108: Pore distribution in commercial biochar.

Elderberry biochar 1100 °C and fig 1100 °C, have an area of 12 and 8 m^2/g, respectively, and an almost non-existent porosity. The observed change in area between the two is not significantly different. The table below shows the results obtained.

Table 105: Surface area and volume of micropores determined by BET isotherm.

Sample	Area (m^2/g)	Volume micropore (cm^3/g)
Commercial biochar	474	0,13
Elder 1100 °C	~12	N.D.
Fig 1100 °C	~8	N.D

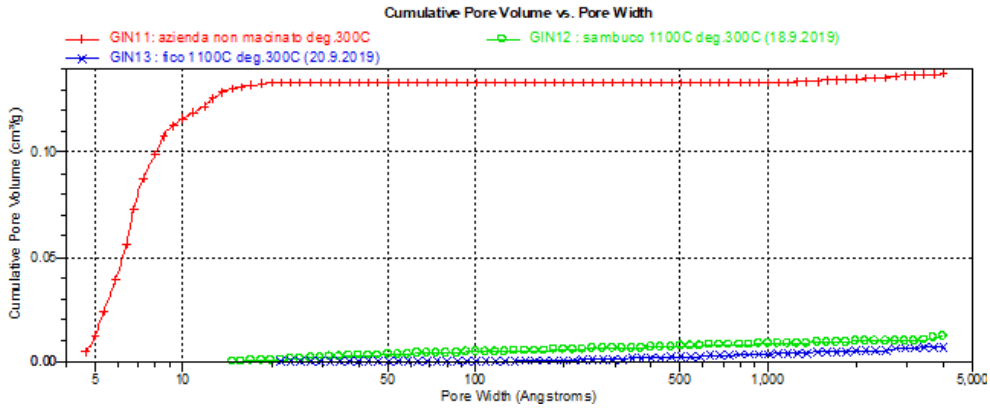

Figure 109: Micropore volume as function of diameter.

In conclusion, fig and elderberry samples at 1100 °C have low area and negligible porosity, which means that the micropores are not responsible for adsorption. It could be assumed that the abatement of the metals is due to the presence of ultra-micropores (under the 5 A of amplitude, not evaluable with N_2) that do not involve the superficial adsorption but rather the diffusion in the bulk. For some samples only area values were determined and not the whole isotherm, the results of which are as follows:

Table 106: Surface areas of some samples, determined without the use of the BET isotherm. It allows to observe how the surface area varies with the pyrolysis temperature.

Sample	Area (m^2/g)
Spruce 550 °C	82
Spruce 800 °C	322
Spruce 1100 °C	~ 9
Corn cob 550 °C	~ 1
Corn cob 800 °C	~ 1
Corn cob 1100 °C	~3
Hazelnut shells 800 °C	~ 8
Hazelnut shells 1100 °C	~ 8

Low values of areas lead to the exclusion metal abatement mechanism through surface adsorption. It can be said that biochar from different plant biomass is characterized by different values of areas and that such values typically become negligible when the material is produced at very high temperatures (1100 °C).

10.12.8 Morphology e surface features: SEM analysis

Through the SEM analysis it is possible to notice the changes that take place on the structure of the samples as the pyrolysis temperature increases. The analyses were performed on finely ground samples and using secondary electrons, working at increasing magnifications. The power set was 20.00 kV. Secondary electrons (SE) are electrons of low energy, coming from the surface of the sample, which define the surface morphology, highlighting the three-dimensional aspect.

1. *Spruce*

SEM images on spruce biochar show that its particles have dimensions of the order of 1 mm, an ordered lamellar structure but an irregular surface. Comparing the images from the samples at 800 °C and 1100 °C seems that the second is characterized by greater structural and superficial order.

a) 800 °C **b) 1100 °C**

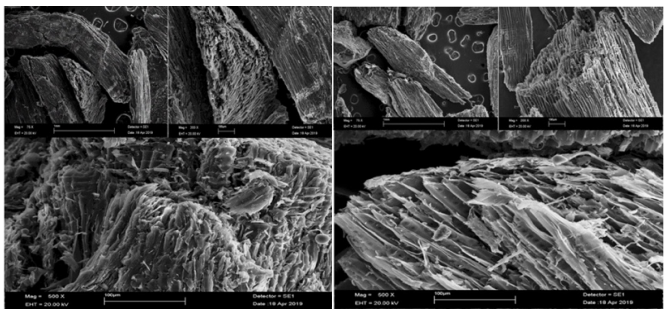

Figure 110: SEM images of spruce biochar a) 800 °C, b) 1100 °C.

2. *Corn cob*

The images show that corn cob particles have different dimensions and on average equal to 1 mm; in the images of the corn cob pyrolyzed at 800°C the structure appears spongy, while if you look at the images of 1100 °C it can be noticed the appearance of areas with structure like slats arranged evenly between them.

a) 800 °C. **b) 1100 °C**

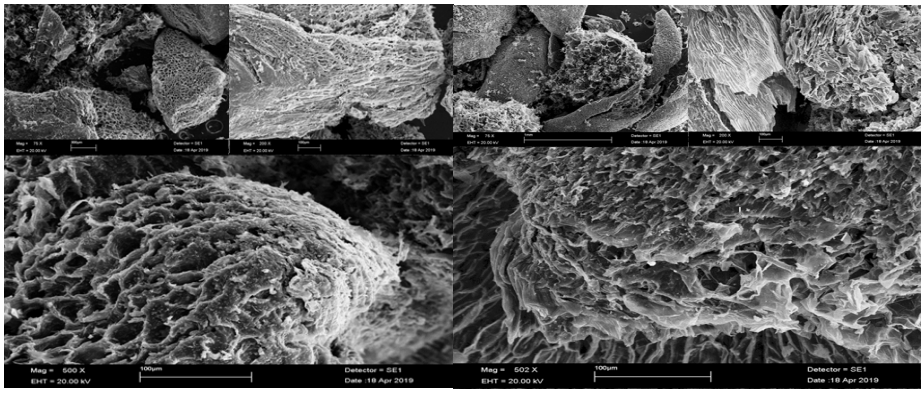

Figure 111: SEM images of corn cob biochar a) 800 °C, b) 1100 °C.

3. *Hazelnut shells*

Hazelnut shells biochar at 550 °C consists of particles of non-homogeneous size and an average of 1 mm; their structure is porous, and their surface is rough but smooth. The pyrolyzed sample at 1100 °C would appear to have a more lamellar structure and a less rough and more homogeneous surface.

a) 550 °C **b) 1100 °C**

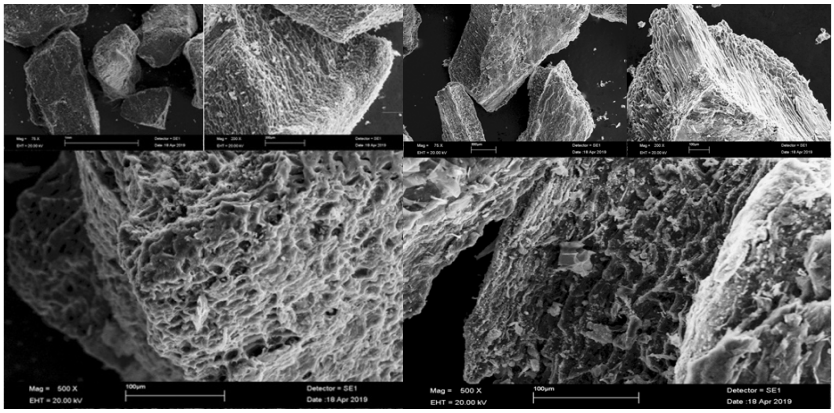

Figure 112: SEM images of hazelnut shells biochar a) 550 °C, b) 1100 °C

4. *Poplar sawdust*

The images of poplar sawdust biochar at 1100 °C are like spruce: particles of size greater than or equal to 1 mm and elongated shape, lamellar structure where in some points there are pores formed by the union between two adjacent lamellae held together by others perpendicular to them. This connection is highlighted by the circle on the image.

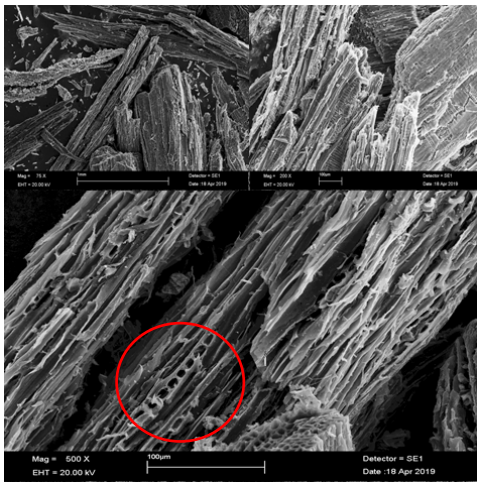

Figure 113: SEM image of poplar sawdust.

10.12.9 Metal release tests on non-treated biochar

1. *Neutral pH release:*

The untreated biochar has been extracted with water: in terms of metals concentration in mg/L has been assessed as a function of the pyrolysis temperature of the wood sample. The trends of each metal are different, the concentration of some metals increases as the pyrolysis temperature increases while for others it decreases or stays constant. It is possible to perform groupings biochar in which different wood essences show a similar behavior. As far as pH is concerned, no control was carried out by buffering solution, so it is possible to estimate the amount of calcination that causes an increase in pH for each type of wood and temperature. The final pH of all samples was about 10 and the analysis was performed in triple after 72 hours.

Table 107: Release macro-elements from the biochar in aqueous solution.

Metal release in water	Ca avg.	Mg avg.	Na avg.	K avg.	Ca Std. Dev	Mg Std. Dev	Na Std. Dev	K Std. Dev
	mg/l	mg/l	mg/l	mg/l	%	%	%	%
Spruce 550 °C	3,45	1,77	2,25	15,1	15,41	17,05	14,49	7,37
Spruce 800 °C	3,76	1,76	2,23	25,2	6,94	5,72	8,70	2,09
Spruce 1100 °C	7,98	3,67	2,57	41,5	6,34	7,12	32,25	22,34
Fig 550 °C	19,23	7,30	4,20	183,	7,37	4,06	27,80	3,23
Fig 800 °C	15,12	8,35	3,91	226,	6,22	6,44	2,61	2,46
Fig1100 °C	14,35	20,5	4,16	225,	5,80	3,04	15,82	1,65
Walnut 550 °C	15,72	7,76	3,81	47,5	11,13	4,07	7,13	11,48
Walnut 800 °C	17,52	7,45	3,10	40,2	5,60	3,76	31,11	3,21
Walnut 1100 °C	10,10	11,1	2,88	27,0	11,66	5,87	9,84	10,64
Elder 550 °C	9,67	6,99	2,84	55,9	9,33	3,19	12,25	5,70
Elder 800 °C	7,44	5,12	2,77	77,1	2,02	3,01	4,81	5,72
Elder 1100 °C	14,65	29,2	2,92	101,	11,58	5,91	3,34	7,19
Commercial Biochar	8,08	2,65	3,68	25,7	21,54	24,73	41,98	9,95
Active carbon	5,29	2,19	3,99	2,24	13,17	9,57	3,72	0,85

In all samples metal that is released in higher amounts is potassium and increases as the pyrolysis temperature increases, especially in spruce and elder biochar. Fig biochar shows clearly higher values compared to the other samples: the concentrations of sodium and potassium stays constant at varying temperatures, magnesium increases, and calcium decreases slightly. Spruce and elderberry biochar behave in a similar way: concentration of calcium, magnesium and potassium increases with the temperature while sodium stays stable. The elder biochar, however, releases double amounts metals, compared to samples of spruce with sodium exception.

Table 108: Release microelements from the biochar in aqueous solution.

Metal release in water	Al	Cd	Cr	Cu	Mn	Ni	Pb	Zn
	µg/l	µg/l	µg/l	µg/l	µg/l	µg/l	µg/l	µg/l
Spruce 550 °C	<20	<5	<20	<20	<20	<20	<20	<20
Spruce 800 °C	<20	<5	<20	<20	<20	<20	<20	<20
Spruce 1100 °C	<20	<5	<20	<20	<20	<20	<20	<20
Fig 550 °C	<20	<5	<20	<20	<20	<20	<20	<20
Fig 800 °C	<20	<5	<20	<20	<20	<20	<20	<20
Fig1100 °C	<20	<5	<20	<20	<20	<20	<20	<20
Walnut 550 °C	<20	<5	<20	<20	<20	<20	<20	<20
Walnut 800 °C	<20	<5	<20	<20	<20	<20	<20	<20
Walnut 1100 °C	<20	<5	<20	<20	<20	<20	<20	<20
Elder 550 °C	<20	<5	<20	<20	<20	<20	<20	<20
Elder 800 °C	<20	<5	<20	<20	<20	<20	<20	<20
Elder 1100 °C	<20	<5	<20	<20	<20	<20	<20	<20
Commercial	<20	<5	<20	<20	<20	<20	<20	<20
Active carbon	<20	<5	<20	<20	<20	<20	<20	<20

2. *Metal release at pH 4*

Release tests at pH 4 were performed in a buffer solution with acetic acid 0,01 M and under pH control, acidifying the samples after 24 hours of mixing with concentrated acetic acid to restore the pH to the desired value. Filtration and analysis were conducted after 72 hours. These tests showed that, working at pH below neutrality, most metals are released at higher concentrations.

Table 109: Release macro-elements from the biochar in solution at pH 4.

Metal release at pH =4	Ca avg	Mg avg	Na avg	K avg	Ca Std. Dev	Mg Std. Dev	Na Std. Dev	K Std. Dev
	mg/l	mg/l	mg/l	mg/l	%	%	%	%
Spruce 550 °C	18,60	5,98	3,65	54,12	9,30	3,18	24,81	1,81
Spruce 800 °C	20,83	5,64	3,60	52,35	8,81	4,63	10,09	2,80
Spruce 1100 °C	21,95	5,79	4,10	53,33	1,74	20,69	19,05	4,12
Fig 550 °C	210,24	40,01	7,23	311,00	5,93	0,60	20,51	3,99
Fig 800 °C	259,29	41,72	6,00	305,47	1,34	0,60	30,95	2,40
Fig1100 °C	239,65	47,44	6,08	251,95	0,41	2,22	8,64	1,95
Walnut 550 °C	463,33	30,56	6,84	130,56	9,90	1,72	26,88	3,11
Walnut 800 °C	469,69	28,50	6,36	134,25	7,69	3,59	11,06	2,73
Walnut 1100 °C	475,93	31,00	6,08	134,83	3,78	10,61	19,72	6,79
Elder 550 °C	74,92	29,22	5,01	144,51	1,32	3,91	5,81	8,66
Elder 800 °C	102,00	28,56	5,38	139,07	18,93	3,15	32,44	3,32
Elder 1100 °C	72,63	42,03	5,07	132,34	9,51	1,96	20,96	9,95
Commercial	185,17	8,89	5,72	48,68	4,86	14,26	16,11	3,73
Active carbon	79,54	13,79	1,70	4,80	11,83	4,53	11,23	5,83

Metals released are much higher than the neutral pH test and potassium and calcium are higher amounts in all samples. The sodium concentrations are similar for the different essences and have a constant trend for the three temperatures. Calcium has low value in spruce biochar but very high in the other samples, especially walnut, and its concentration does not vary with the temperature. The concentration of magnesium released stays constant in spruce and walnut biochar while slightly increasing with the temperature in elderberry and fig biochar. Potassium released decrease slightly as the pyrolysis temperature increases, Higher amount of calcium released in the samples produced at 550 °C occurs in all sample's exception for walnut biochar.

Table 110: Release microelements from the biochar in solution at pH 4.

Metal release at pH =4	Cd average	Cr average	Cu average	Pb average	Al average	Ni average	Mn average	Zn average	Al Std. Dev.	Ni Std. Dev.	Mn Std. Dev.	Zn Std. Dev
	µg/l	µg/l	µg/l	µg/l	µg/l	µg/l	µg/l	µg/l	%	%	%	%
Spruce 550 °C	<5	< 20	< 20	< 20	< 20	< 20	930,1	398,9			1,49	8,78
Spruce 800 °C	<5	< 20	< 20	< 20	< 20	< 20	921,7	299,9			2,15	18,05
Spruce 1100 °C	<5	< 20	< 20	< 20	< 20	< 20	934,1	252,1			5,01	14,88
Fig 550 °C	<5	< 20	< 20	< 20	< 20	< 20	68,5	234,6			3,68	1,41
Fig 800 °C	<5	< 20	< 20	< 20	< 20	< 20	66,8	298,0			1,79	3,19
Fig1100 °C	<5	< 20	< 20	< 20	68,8	< 20	132,2	123,3	39,9		4,94	0,55
Walnut 550 °C	<5	< 20	< 20	< 20	< 20	< 20	3615.0	342,5			9,79	7,16
Walnut 800 °C	<5	< 20	< 20	< 20	< 20	< 20	3755,3	302,1			3,95	2,12
Walnut 1100 °C	<5	< 20	< 20	< 20	< 20	< 20	3302,9	138,2			5,65	24,0
Elder 550 °C	<5	< 20	< 20	< 20	< 20	< 20	332,2	230,2			8,57	33,9
Elder 800 °C	<5	< 20	< 20	< 20	< 20	< 20	217,2	296,9			12,67	14,1
Elder 1100 °C	<5	< 20	< 20	< 20	78,23	< 20	193,4	155,6	38,0		3,78	13,4
Commercial Biochar	<5	< 20	< 20	< 20	< 20	< 20	1500,1	531,5			6,34	14,3
Active carbon	<5	< 20	< 20	< 20	14465	34,72	234,2	212,7	7,21	5,89	1,77	7,24

Working at acidic pH, manganese and zinc release occur in all samples and in the biochar. Fig and elderberry biochar at the highest temperature show traces of aluminum, which is in large amount in the activated carbon, together with nickel. This is probably due to the source material with which it was produced. The Walnut biochar has higher amounts of manganese than all other samples, excluding the commercial biochar. Zinc released decreases with the pyrolysis temperature, because during pyrolysis the environment is reducing and low melting elements, such as zinc, cadmium, and lead, evaporate.

3. Metal release at pH=1

Release tests at pH=1 was performed only on activated carbon and commercial biochar sample, in triplicate, by inserting 0,5 g of biochar into 25 ml of 0,1 M hydrochloric acid solution within Falcon-type tubes. The ICP-OES analysis was carried out after 72 hours, after pH check and filtration. The pH stays constant. The pH=1 release test allows metals to be fully extracted from biochar and the total content was determined. As noted, the commercial biochar contains mainly calcium and potassium while the activated carbon is mainly rich in calcium and magnesium.

Table 111: Release of macro-elements in solution at pH 1.

Metal release at pH =1	Ca average	Mg average	Na average	K average	Ca Std. Dev	Mg Std. Dev	Na Std. Dev	K Std. Dev
	mg/l	mg/l	mg/l	mg/l	%	%	%	%
Commercial biochar	228,1	8,80	3,09	57,2	13,2	17,2	10,1	28,4
Active carbon	147,6	30,6	4,77	8,86	9,12	8,98	4,56	12,2

Table 112: Release of microelements in solution at pH 1.

Metal release pH =1	Al avg	Cd avg	Cr avg	Cu avg	Ni avg	Pb avg	Mn avg	Zn avg	Al Std Dev	Cr Std Dev	Cu Std Dev	Ni Std Dev	Pb Std Dev	Mn Std Dev	Zn Std Dev
	µg/L	µg/L	µg/L	µg/L	µg/L	µg/L	µg/L	µg/L	%	%	%	%	%	%	%
Commercial biochar	1020,7	<5	37,0	147,7	13,4	11,2	2996,8	733,4	16,5	27,4	4,9	46,7	20,8	10,1	2,1
Active carbon	123542,8	<5	43,8	139,2	56,8	<20	783,8	232,8	7,5	89,5	27	17,4	17,2	1,0	5,4

The above results show high content of aluminum in activated carbon while the presence of manganese and traces of lead in the commercial biochar was found.

10.13 Abatement tests

The data and information collected during the various abatement tests are reported in following paragraphs. The results are expressed as percentage of metal retained; this value was obtained by analysis of the solution before and after contact with the biochar. At this point the following formula is used to convert the µg/L in %:

$$metal\ retained\ (\%) = \frac{Metal\ concentration\ retained\left(\frac{\mu g}{L}\right)}{Metal\ concentration\ in\ stock\ solution\ \left(\frac{\mu g}{L}\right)} * 100$$

10.13.1 Abatement tests: 2 mg/l at pH 1

The first abatement test was carried out with a 2 mg/l solution prepared at pH=1 with nitric acid. 1 gram of biochar was weighed into 12 Falcon-type test tubes to which 50 ml of solution was added, placed under orbital shaker for 72 hours and finally filtered and analyzed. The absorption is very poor because there is too much competition between the metal cations and the ion H_3O^+.

Abatement 2 mg/L pH 1:	Al	Cd	Cr	Cu	Mn	Ni	Pb	Zn
	%	%	%	%	%	%	%	%
Spruce 550 °C	28,9	10,4	30,1	12,4	0,0	9,8	52,8	5,1
Spruce 800 °C	27,8	10,7	30,3	23,2	0,0	13,3	60,4	8,4
Spruce 1100 °C	35,2	12,8	35,2	23,9	0,0	13,9	60,7	12,9
Walnut shells 550 °C	0,0	12,9	33,6	17,2	28,3	12,5	56,8	10,9
Walnut shells 800 °C	10,3	12,1	28,3	25,2	27,8	17,8	60,3	15,8
Walnut shells 1100 °C	9,9	16,4	35,7	29,5	29,0	17,4	62,6	17,3
Poplar sawdust 550 °C	10,0	11,1	22,1	16,4	22,4	10,5	58,0	10,7
Poplar sawdust 800 °C	10,2	16,3	28,2	21,9	19,2	17,0	60,0	12,4
Poplar sawdust 1100 °C	11,0	18,4	32,7	42,4	26,0	19,2	74,5	19,5
Corn cob 550 °C	25,0	13,1	30,6	23,4	27,8	12,7	53,6	0,0
Corn cob 800 °C	26,8	12,1	30,4	30,7	29,4	14,8	60,7	0,0
Corn cob 1100 °C	31,5	16,2	36,8	32,4	30,5	14,7	65,4	0,0

Table 113: Abatement % of different biochar samples in solution at pH 1.

By observing the results, it is possible to notice how the percentages of metal abatement slightly increase with the pyrolysis temperature. The results are however low, on average 20-30% abatement except lead with a good result that almost 75%.

10.13.2 Abatement tests: 2 mg/l at pH 6

The choice to work at pH=6 is dictated by the fact that this pH is the most common for natural waters, so this test is the most representative. To work as much as possible at these pH conditions, it was necessary to use biochar samples which had undergone acid treatment and to correct the pH with dilute acetic acid or 0,1 M sodium acetate before carrying out the analyses. All the analyses were conducted after 24, 48 and 72 hours of biochar-solution contact, to observe the process progress over time. Only the analysis performed after 72 hours was done in triple to determine the percentage standard deviation.

- *Aluminum*

Table 114: Abatement % of aluminum in solution (2 mg/l pH 6.)

Sample	**Al**		**Al average**	**Std. Dev**
Metal amount retained	***%***	***%***	***%***	***%***
Time	***24 h***	***48 h***	***72 h***	***72 h***
Spruce 550 °C	40,11	54,12	98,50	1,19
Spruce 800 °C	23,77	29,19	99,51	0,34
Spruce 1100 °C	67,48	99,76	99,97	0,06
Cherry tree 550 °C	82,21	92,15	99,70	0,25
Cherry tree 800 °C	64,88	70,87	99,82	0,15
Cherry tree 1100 °C	96,70	99,00	99,77	0,31
Fig 550 °C	93,54	100,0	99,20	0,66
Fig 800 °C	93,54	100,0	100,0	0,00
Fig 1100 °C	88,57	95,00	99,16	1,47
Acacia 550 °C	71,15	84,41	92,04	7,00
Acacia 800 °C	39,28	43,99	76,55	2,46
Acacia 1100 °C	76,17	88,96	94,04	2,80
Jube 550 °C	75,26	99,33	100,0	1,60
Jube 800 °C	49,35	61,03	81,64	2,09
Jube 1100 °C	93,54	99,76	100,0	0,00
Walnuts shells 550 °C	29,15	40,40	97,15	3,38
Walnuts shells 800 °C	13,03	90,88	97,66	2,66
Walnuts shells 1100 °C	56,77	67,02	99,72	0,49
Stone wood 550 °C	65,09	69,00	82,97	2,66
Stone wood 800 °C	58,04	63,33	64,00	2,01
Stone wood 1100 °C	94,53	96,00	99,63	0,64
Walnut 550 °C	46,07	61,91	94,40	1,47
Walnut 800 °C	90,74	99,00	99,89	0,19
Walnut 1100 °C	72,63	94,55	99,04	0,85
Plum 550 °C	59,07	87,87	93,21	0,49
Plum 800 °C	34,75	47,42	87,55	4,24
Plum 1100 °C	92,63	100,0	100,0	0,00
Elder 550 °C	79,00	80,00	88,90	2,65
Elder 800 °C	90,00	90,00	94,64	2,26
Elder 1100 °C	99,00	99,00	100,0	0,00
Poplar sawdust 550 °C	36,76	44,29	99,53	0,23
Poplar sawdust 800 °C	37,08	46,34	99,13	0,76
Poplar sawdust 1100 °C	92,47	97,20	99,54	0,80
Corn cob 550 °C	49,96	66,57	99,60	0,40
Corn cob 800 °C	83,33	97,73	100,0	0,00
Corn cob 1100 °C	79,37	70,60	99,68	0,55
Commercial biochar	82,06	94,08	100,0	0,00
Active carbon	-	-	100,0	0,00

Looking at the data, it is possible to say that aluminum is retained between 80 and 100% from all biochar for all three temperatures and this result is reached after 72 hours. Some sample such as fig, cherry, and elderberry biochar after only 24 hours achieve excellent results. Other features that improve abatement efficiency is the pyrolysis temperature: most of the best results have been found on biochar produced at 1100 °C. Aluminum abatement increase a lot with time (the best results are after 72 hours) and to a lesser extent with the pyrolysis temperature. Many biochar at 800°C is less efficient than those produced at 550 °C and 1100 °C, probably because they lack the functional groups in biochar produced at 550 °C and lack the a peculiar graphitic structure resulting at 1100 °C. Spruce biochar behaves in a similar way to plum biochar, as the pyrolysis temperature and the time increase the abatement efficiency. On the other hand, fig and elderberry biochar show high abatement % right no matter pyrolysis temperature.

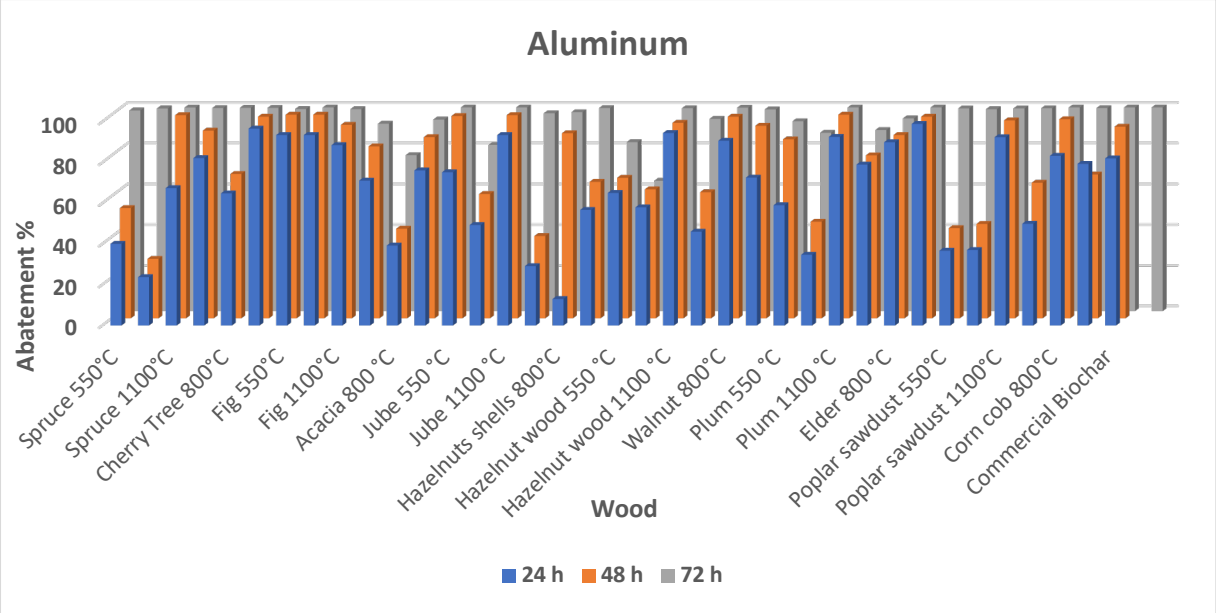

Figure 114: Abatement % of aluminum according to essence, time and temperature.

- *Chromium*

Table 115: % abatement of chromium in solution (2 mg/l at pH 6).

Sample	**Cr**		**Cr average**	**Std. Dev.**
Metal amount retained	***%***	***%***	***%***	***%***
Time	***24 h***	***48 h***	***72 h***	***72 h***
Spruce 550 °C	30,62	33,50	33,18	4,61
Spruce 800 °C	25,20	34,02	38,90	2,10
Spruce 1100 °C	51,39	71,75	76,86	5,28
Cherry tree 550 °C	20,59	23,04	23,49	1,69
Cherry tree 800 °C	28,69	30,04	30,05	3,00
Cherry tree 1100 °C	58,29	60,57	65,09	6,45
Fig 550 °C	55,65	60,80	60,31	2,97
Fig 800 °C	73,23	80,12	81,64	2,13
Fig 1100 °C	99,66	99,00	99,48	0,37
Acacia 550 °C	54,32	54,76	53,23	1,50
Acacia 800 °C	39,84	40,95	37,88	9,16
Acacia 1100 °C	70,76	69,13	69,77	2,90
Jube 550 °C	62,21	63,14	63,67	2,62
Jube 800 °C	37,10	37,34	42,34	3,42
Jube 1100 °C	84,45	80,58	80,42	0,87
Walnuts shells 550 °C	33,24	41,24	48,40	11,31
Walnuts shells 800 °C	36,84	48,72	48,01	3,25
Walnuts shells 1100 °C	75,08	90,61	97,58	1,94
Stone wood 550 °C	56,56	58,01	75,22	2,51
Stone wood 800 °C	54,27	59,83	57,24	1,25
Stone wood 1100 °C	86,77	85,93	89,20	3,52
Walnut 550 °C	45,32	52,79	55,79	1,02
Walnut 800 °C	61,07	64,79	66,72	1,24
Walnut 1100 °C	61,54	62,64	69,83	0,10
Plum 550 °C	44,58	45,96	42,86	4,12
Plum 800 °C	40,39	41,11	42,55	4,60
Plum 1100 °C	75,05	79,05	75,70	4,91
Elder 550 °C	65,31	68,79	63,32	3,18
Elder 800 °C	66,81	69,59	69,42	4,37
Elder 1100 °C	99,12	99,50	99,87	0,09
Poplar sawdust 550 °C	27,22	30,09	30,23	9,08
Poplar sawdust 800 °C	29,01	37,24	39,40	4,09
Poplar sawdust 1100 °C	71,10	80,04	85,39	0,86
Corn cob 550 °C	41,19	47,64	47,44	3,45
Corn cob 800 °C	55,62	60,99	60,55	1,03
Corn cob 1100 °C	79,74	80,57	86,88	2,98
Commercial biochar	93,51	95,37	99,56	0,09
Active carbon	-	-	99,96	0,08

The results show high chromium abatement already after 24 hours and stays constant during time. The best results are achieved in biochar produced at 1100 °C: abatement percentages are all between 70 and 100%. Chrome abatement increases much with the pyrolysis temperature, the process depends closely on it. Fig and elderberry biochar 1100 °C had the most abatement efficiency.

Figure 115: Reduction % of chromium as a function of essence, time and temperature.

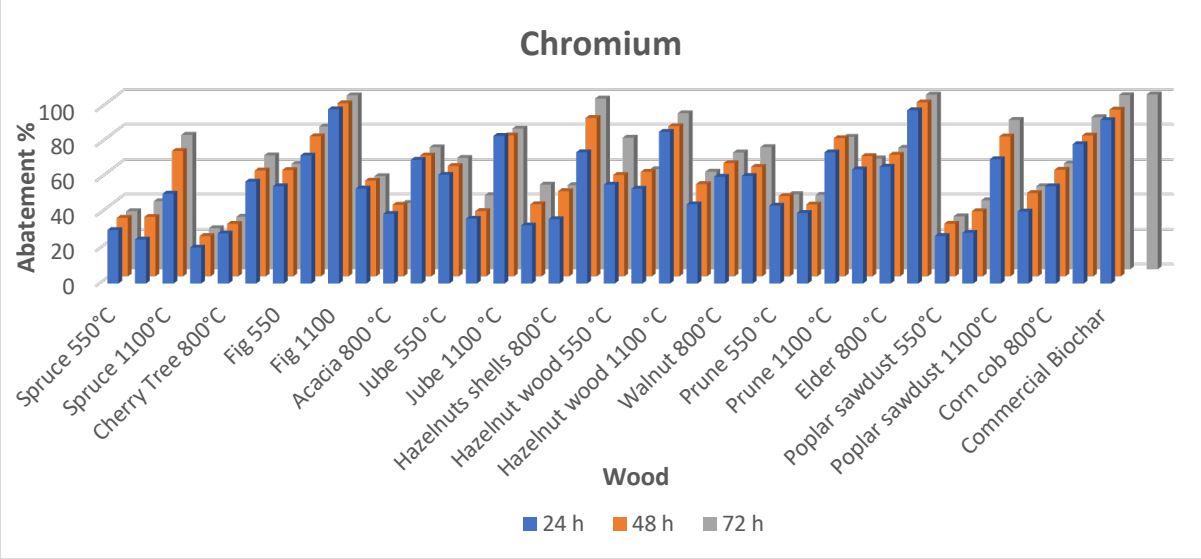

- *Copper*

Table 116: Abatement of copper in solution (2 mg/l at pH 6).

Sample	Cu		Cu average	Std. Dev.
Metal amount retained	***%***	***%***	***%***	***%***
Time	***24 h***	***48 h***	***72 h***	***72 h***
Spruce 550° C	21,17	27,39	43,35	4,15
Spruce 800 °C	20,83	30,41	47,57	2,19
Spruce 1100 °C	25,70	40,89	88,10	1,93
Cherry tree 550 °C	57,38	63,54	68,36	0,87
Cherry tree 800 °C	73,94	77,09	79,78	2,21
Cherry tree 1100 °C	91,73	93,19	93,45	1,97
Fig 550 °C	57,76	65,11	79,47	1,51
Fig 800 °C	90,90	94,26	94,96	0,95
Fig 1100 °C	97,46	98,26	98,80	0,11
Acacia 550 °C	47,00	58,45	67,81	0,92
Acacia 800 °C	38,54	38,96	63,31	0,62
Acacia 1100 °C	78,97	79,77	87,16	1,96
Jube 550 °C	56,75	77,21	80,14	1,49
Jube 800 °C	46,45	60,34	62,77	1,70
Jube 1100 °C	90,14	91,99	91,63	1,53
Walnuts shells 550 °C	7,34	10,69	54,72	1,80
Walnuts shells 800 °C	5,55	28,27	39,16	3,17
Walnuts shells 1100 °C	53,04	64,02	95,15	1,76
Stone wood 550 °C	56,35	56,64	58,18	1,15
Stone wood 800 °C	85,65	85,27	85,76	1,36
Stone wood 1100 °C	92,10	94,78	97,30	1,73
Walnut 550 °C	17,25	26,46	47,04	6,40
Walnut 800 °C	65,16	78,34	80,89	1,04
Walnut 1100 °C	84,01	91,19	93,29	3,72
Plum 550 °C	31,48	46,20	71,29	1,59
Plum 800 °C	64,82	77,17	77,03	1,08
Plum 1100 °C	84,68	90,24	91,16	3,23
Elder 550 °C	58,10	56,44	77,11	4,64
Elder 800 °C	95,63	97,26	99,69	3,66
Elder 1100 °C	98,86	99,11	98,88	0,27
Poplar sawdust 550 °C	13,47	15,83	32,69	2,61
Poplar sawdust 800 °C	32,21	38,69	53,47	1,52
Poplar sawdust 1100 °C	57,89	59,78	91,26	1,55
Corn cob 550 °C	26,65	37,48	51,90	4,56
Corn cob 800 °C	48,50	51,29	56,44	2,87
Corn cob 1100 °C	62,91	64,86	66,16	2,48
Commercial biochar	93,01	95,96	98,80	0,32
Active carbon	-	-	99,27	0,21

Best results are found on biochar 1100 °C after 72 hours. Copper abatement % increase with pyrolysis temperature and with time of contact between biochar and the solution. If it is considered only samples produced at 1100 °C, abatement percentage varies between 80% and 99% depending on the wood essence. Fig and elder biochar continue to be the most performing samples.

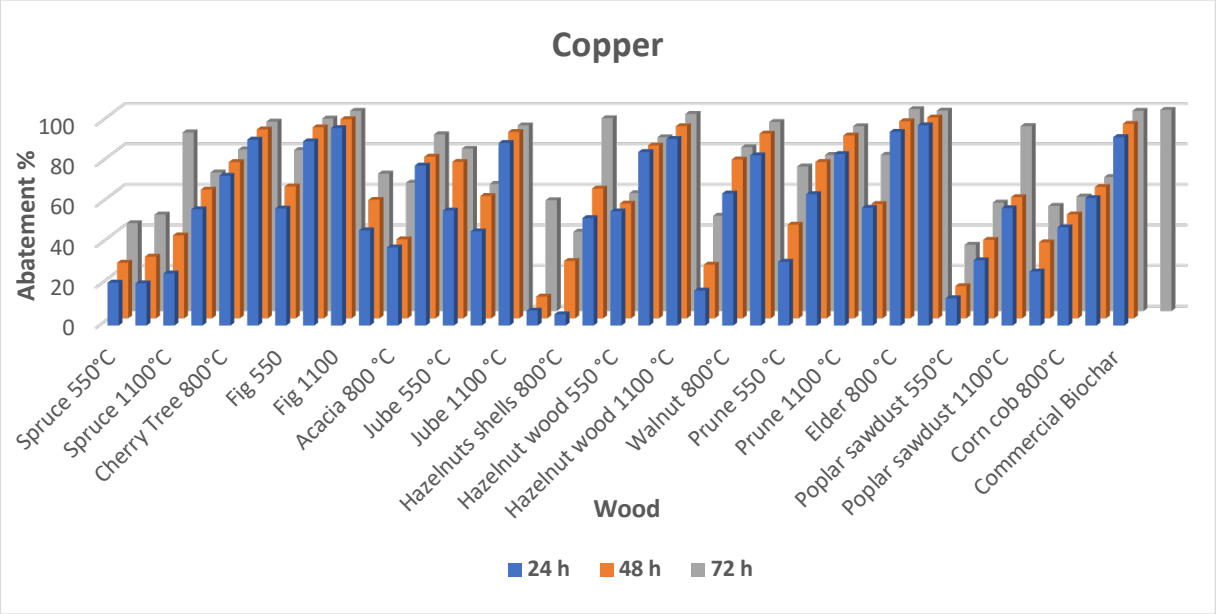

Figure 116: Abatement % of copper as a function of essence, time and temperature.

- *Lead*

Table 117: Abatement of lead in solution (2 mg/l pH 6).

Sample	**Pb**		**Pb agerage**	**Std. Dev.**
Metal amount retained	%	%	%	%
Time	24 h	48 h	72 h	72 h
Spruce 550° C	35,49	40,69	69,82	3,89
Spruce 800 °C	27,82	30,76	68,96	2,62
Spruce 1100 °C	20,68	38,15	85,84	2,46
Cherry tree 550 °C	40,05	59,46	69,04	1,95
Cherry tree 800 °C	43,61	64,14	75,34	0,86
Cherry tree 1100 °C	70,79	85,17	95,54	2,93
Fig 550 °C	90,45	97,00	97,70	1,27
Fig 800 °C	94,02	96,00	96,16	3,23
Fig 1100 °C	99,09	99,30	99,82	0,72
Acacia 550 °C	33,17	54,65	85,21	5,20
Acacia 800 °C	29,26	50,29	84,97	4,40
Acacia 1100 °C	49,49	67,75	93,90	3,10
Jube 550 °C	76,51	83,64	95,46	0,82
Jube 800 °C	50,92	54,75	85,16	1,87
Jube 1100 °C	99,01	99,10	99,47	0,30
Walnuts shells 550 °C	27,26	70,97	88,57	1,34
Walnuts shells 800 °C	23,67	77,25	94,36	3,79
Walnuts shells 1100 °C	58,10	68,59	98,10	1,00
Stone wood 550 °C	65,16	84,33	93,19	1,08
Stone wood 800 °C	44,64	60,76	88,12	3,11
Stone wood 1100 °C	72,58	87,80	99,05	0,41
Walnut 550 °C	73,83	75,51	87,78	0,95
Walnut 800 °C	88,86	89,00	95,73	1,02
Walnut 1100 °C	88,82	90,33	96,74	0,13
Plum 550 °C	49,62	54,35	82,36	0,78
Plum 800 °C	43,84	45,30	76,65	6,41
Plum 1100 °C	91,18	92,21	94,33	1,45
Elder 550 °C	48,17	75,47	94,07	1,33
Elder 800 °C	71,63	90,09	96,47	2,21
Elder 1100 °C	82,95	95,09	99,75	0,14
Poplar sawdust 550 °C	30,81	32,59	83,27	3,44
Poplar sawdust 800 °C	36,78	41,61	86,15	0,50
Poplar sawdust 1100 °C	54,67	54,80	96,15	2,03
Corn cob 550 °C	37,26	45,05	95,30	1,56
Corn cob 800 °C	65,70	78,99	96,99	0,55
Corn cob 1100 °C	65,16	68,70	97,55	0,49
Commercial biochar	98,59	99,00	99,73	0,43
Active carbon	-	-	99,97	0,06

Lead is retained in high percentages, very close to 100%, by all the samples pyrolyzed both at low and high temperatures and after 72 hours of contact. The phenomenon depends mainly on the time and to a lesser extent on the temperature.

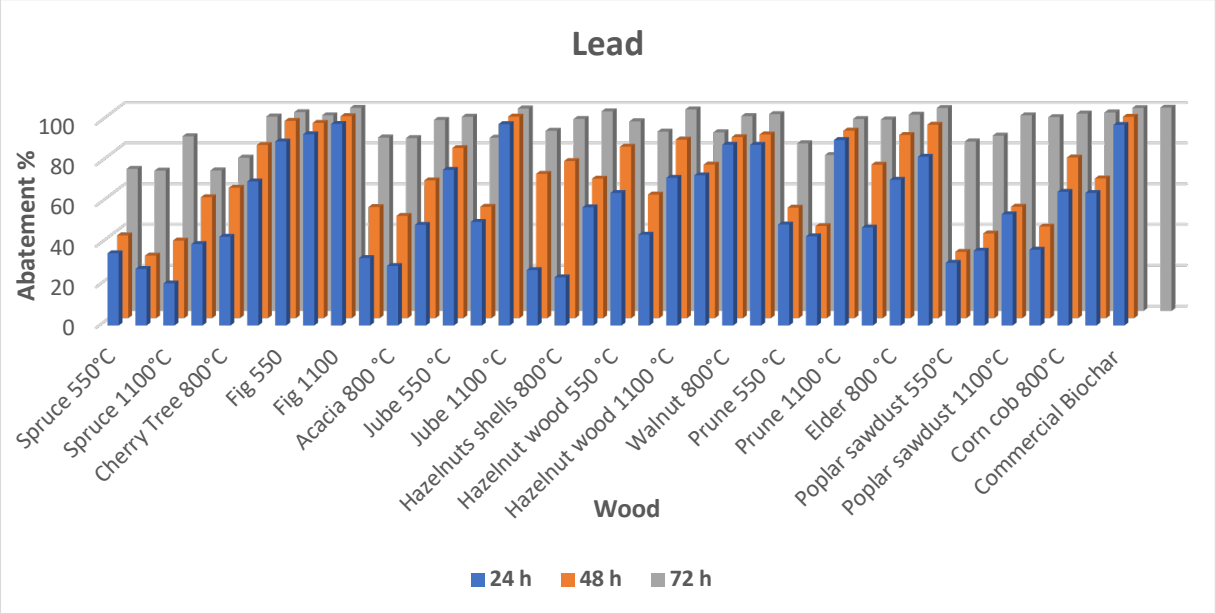

Figure 117: Abatement % of lead as a function of essence, time and temperature

- *Zinc*

Table 118: Reduction of zinc in solution (2 mg/l pH 6).

Sample	**Zn**		**Zn average**	**Std. Dev.**
Metal amount retained	***%***	***%***	***%***	***%***
Time	***24 h***	***48 h***	***72 h***	***72 h***
Spruce 550° C	10,85	40,98	48,22	8,31
Spruce 800 °C	11,96	41,72	45,29	11,04
Spruce 1100 °C	17,48	53,04	59,71	1,28
Cherry tree 550 °C	19,66	26,85	76,22	9,76
Cherry tree 800 °C	20,13	23,78	76,55	11,08
Cherry tree 1100 °C	22,89	33,19	94,99	2,64
Fig 550 °C	22,69	28,89	91,19	0,94
Fig 800 °C	25,68	32,62	95,78	0,11
Fig 1100 °C	79,84	86,84	96,50	0,58
Acacia 550 °C	27,88	28,40	50,61	3,12
Acacia 800 °C	21,94	27,73	49,22	2,19
Acacia 1100 °C	23,55	29,37	51,64	2,65
Jube 550 °C	19,46	26,36	46,76	9,43
Jube 800 °C	18,83	28,64	47,13	5,16
Jube 1100 °C	20,98	28,98	51,93	5,40
Walnuts shells 550 °C	28,04	37,10	70,26	1,80
Walnuts shells 800 °C	26,64	45,23	68,45	3,17
Walnuts shells 1100 °C	34,09	49,04	68,56	1,76
Stone wood 550 °C	29,48	35,45	66,10	0,39
Stone wood 800 °C	21,96	30,74	65,49	5,13
Stone wood 1100 °C	29,26	35,43	68,87	1,39
Walnut 550 °C	22,96	48,97	75,36	1,64
Walnut 800 °C	25,02	46,80	75,25	1,10
Walnut 1100 °C	27,29	45,28	76,77	1,40
Plum 550 °C	11,42	15,44	52,11	2,26
Plum 800 °C	9,64	14,47	52,85	5,18
Plum 1100 °C	10,89	17,69	53,76	7,33
Elder 550 °C	18,50	21,72	61,44	4,07
Elder 800 °C	31,54	32,39	76,02	5,66
Elder 1100 °C	72,75	80,69	93,45	4,38
Poplar sawdust 550 °C	9,74	11,82	64,67	2,10
Poplar sawdust 800 °C	9,60	45,07	64,83	2,43
Poplar sawdust 1100 °C	10,91	12,84	66,68	1,72
Corn cob 550 °C	10,50	34,29	68,02	1,07
Corn cob 800 °C	12,13	51,13	67,00	3,37
Corn cob 1100 °C	15,27	71,57	66,26	0,71
Commercial biochar	84,95	92,34	93,85	1,79
Active carbon	-	-	93,28	2,28

Zinc abatement increases considerably with time and to a lesser extent with the pyrolysis temperature at which the sample was produced. Looking at the results, except for elder and fig sample, biochar abatement % are similar, whether produced at high temperatures or low. Zinc abatement % are on average lower than those of previous metals and vary between 50 and 90%.

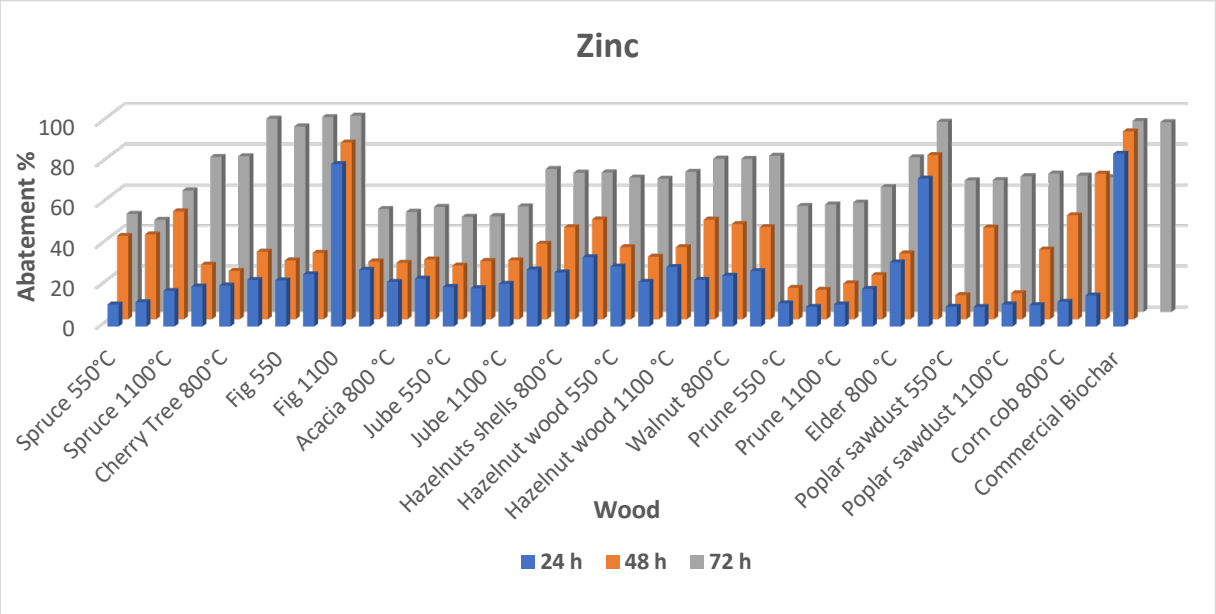

Figure 118: Abatement % of zinc as a function of essence, time and temperature.

- *Cadmium*

Table 119: Reduction of cadmium in solution (2 mg/l pH 6).

Sample	Cd		Cd average	Std. Dev.
Metal amount retained	***%***	***%***	***%***	***%***
Time	***24 h***	***48 h***	***72 h***	***72 h***
Spruce 550° C	5,13	6,56	46,65	9,55
Spruce 800 °C	5,64	6,88	45,98	3,71
Spruce 1100 °C	1,06	1,64	50,38	13,27
Cherry tree 550 °C	28,12	39,95	37,34	17,96
Cherry tree 800 °C	26,72	38,57	44,74	12,94
Cherry tree 1100 °C	28,00	35,29	63,84	1,29
Fig 550 °C	25,78	34,39	56,56	13,66
Fig 800 °C	20,18	24,95	63,52	2,84
Fig 1100 °C	61,68	76,66	77,21	6,58
Acacia 550 °C	27,93	37,60	51,32	1,04
Acacia 800 °C	25,43	30,32	45,32	5,29
Acacia 1100 °C	26,80	42,67	61,60	4,16
Jube 550 °C	19,91	26,65	60,01	4,72
Jube 800 °C	8,87	13,61	46,13	7,07
Jube 1100 °C	19,88	25,20	71,10	3,13
Walnuts shells 550 °C	4,28	6,58	40,97	1,34
Walnuts shells 800 °C	3,94	7,07	38,21	2,80
Walnuts shells 1100 °C	6,18	8,69	49,51	10,02
Stone wood 550 °C	32,35	14,76	56,98	4,60
Stone wood 800 °C	25,60	36,37	54,80	7,46
Stone wood 1100 °C	37,16	45,01	73,56	0,27
Walnut 550 °C	12,95	18,81	36,44	5,58
Walnut 800 °C	20,61	30,18	32,89	5,79
Walnut 1100 °C	9,73	15,40	37,70	6,85
Plum 550 °C	8,84	13,88	49,60	2,14
Plum 800 °C	7,79	10,99	49,25	1,89
Plum 1100 °C	9,95	14,17	57,25	8,19
Elder 550 °C	28,53	39,46	69,61	3,69
Elder 800 °C	27,79	42,86	62,49	2,68
Elder 1100 °C	47,62	53,82	89,34	0,26
Poplar sawdust 550 °C	5,73	35,25	39,80	10,58
Poplar sawdust 800 °C	5,60	36,79	36,70	10,69
Poplar sawdust 1100 °C	4,58	37,33	41,52	11,47
Corn cob 550 °C	3,95	6,18	47,37	16,34
Corn cob 800 °C	5,59	8,33	45,21	6,95
Corn cob 1100 °C	3,02	25,02	56,45	7,05
Commercial biochar	56,84	65,63	97,85	0,36
Active carbon	-	-	95,64	1,60

As regards cadmium, retain percentages is lower than other metals and vary, on average, between 30 and 70% after 72 hours of contact. The abatement increases and depends mainly on time and to a lesser extent on the pyrolysis temperature, even if the greatest abatement occurs in the samples produced at 1100 °C. Elder biochar 1100 °C is the most performing among the samples.

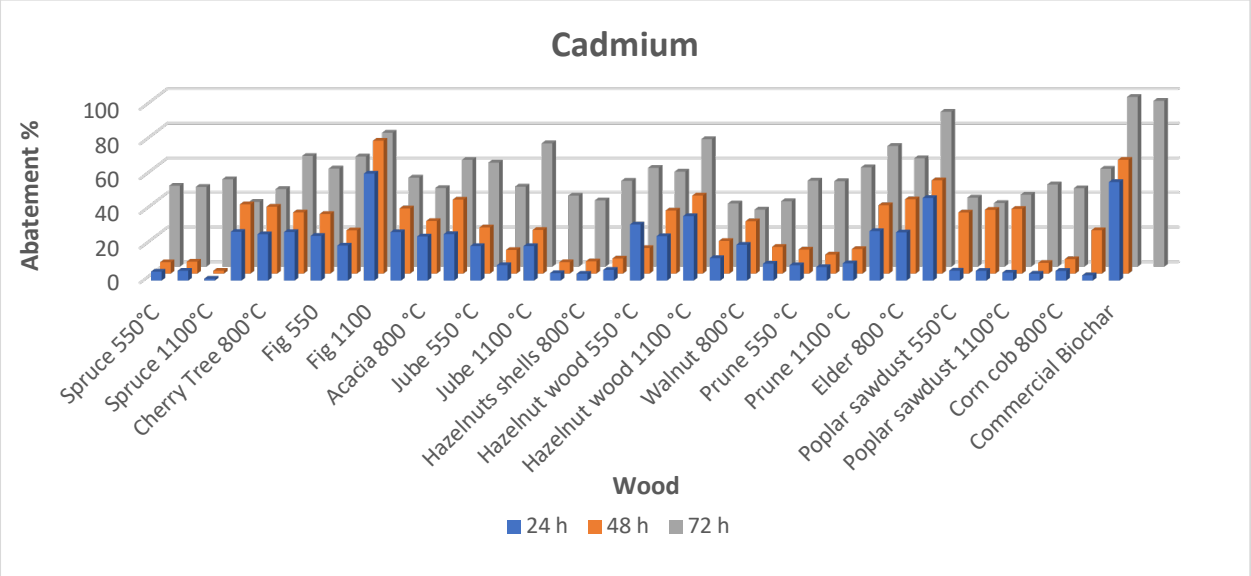

Figure 119: Abatement % of cadmium as a function of essence, time and temperature.

- *Manganese*

Table 120: Abatement % of manganese in solution (2 mg/l pH 6).

Sample	Mn		Mn Average	Std. Dev
Metal amount retained	***%***	***%***	***%***	***%***
Time	***24 h***	***48 h***	***72 h***	***72 h***
Spruce 550° C	6,61	6,93	32,91	14,37
Spruce 800 °C	7,36	8,06	36,17	5,00
Spruce 1100 °C	2,79	4,20	45,87	23,68
Cherry tree 550 °C	7,51	10,63	32,44	1,27
Cherry tree 800 °C	8,14	17,61	36,39	4,98
Cherry tree 1100 °C	9,35	20,24	45,66	8,00
Fig 550 °C	13,92	17,85	53,23	3,75
Fig 800 °C	12,23	15,40	52,96	3,46
Fig 1100 °C	33,92	36,09	73,30	6,31
Acacia 550 °C	26,43	29,40	35,25	11,68
Acacia 800 °C	24,77	31,22	38,51	5,89
Acacia 1100 °C	25,20	29,89	47,31	5,92
Jube 550 °C	12,14	14,66	30,80	1,84
Jube 800 °C	11,42	15,16	33,71	6,71
Jube 1100 °C	13,00	17,66	52,23	2,55
Walnuts shells 550 °C	8,17	9,89	32,04	3,07
Walnuts shells 800 °C	7,41	8,84	34,08	11,07
Walnuts shells 1100 °C	9,15	9,81	42,76	1,59
Stone wood 550 °C	19,07	21,24	38,84	5,65
Stone wood 800 °C	24,00	25,93	41,07	7,58
Stone wood 1100 °C	31,72	41,71	55,72	9,65
Walnut 550 °C	8,91	14,17	31,62	20,10
Walnut 800 °C	6,16	11,16	31,45	24,19
Walnut 1100 °C	8,52	12,32	35,24	5,85
Plum 550 °C	10,95	15,09	36,79	1,50
Plum 800 °C	10,78	12,51	35,76	5,09
Plum 1100 °C	10,48	14,19	44,94	5,86
Elder 550 °C	26,18	27,79	55,68	3,25
Elder 800 °C	24,20	28,04	47,38	4,38
Elder 1100 °C	28,89	43,96	72,74	1,52
Poplar sawdust 550 °C	6,93	6,98	27,82	19,10
Poplar sawdust 800 °C	6,96	8,36	25,54	13,38
Poplar sawdust 1100 °C	6,60	8,41	31,96	7,48
Corn cob 550 °C	5,61	7,73	28,90	5,87
Corn cob 800 °C	7,26	9,32	32,39	5,70
Corn cob 1100 °C	5,81	5,79	35,12	1,87
Commercial biochar	56,53	69,98	86,15	1,48
Active carbon	-	-	81,49	5,06

Manganese is cut down by 70% from all samples and after 72 hours of biochar-solution contact, typically around 30-40%. Acceptable results are achieved only after 72 h. Pyrolysis temperature is not particularly relevant for abatement tests, even if the samples at 1100°C are generally more performing. Fig and elder biochar continue to be the most effective sample and reaching greater than 70% abatement.

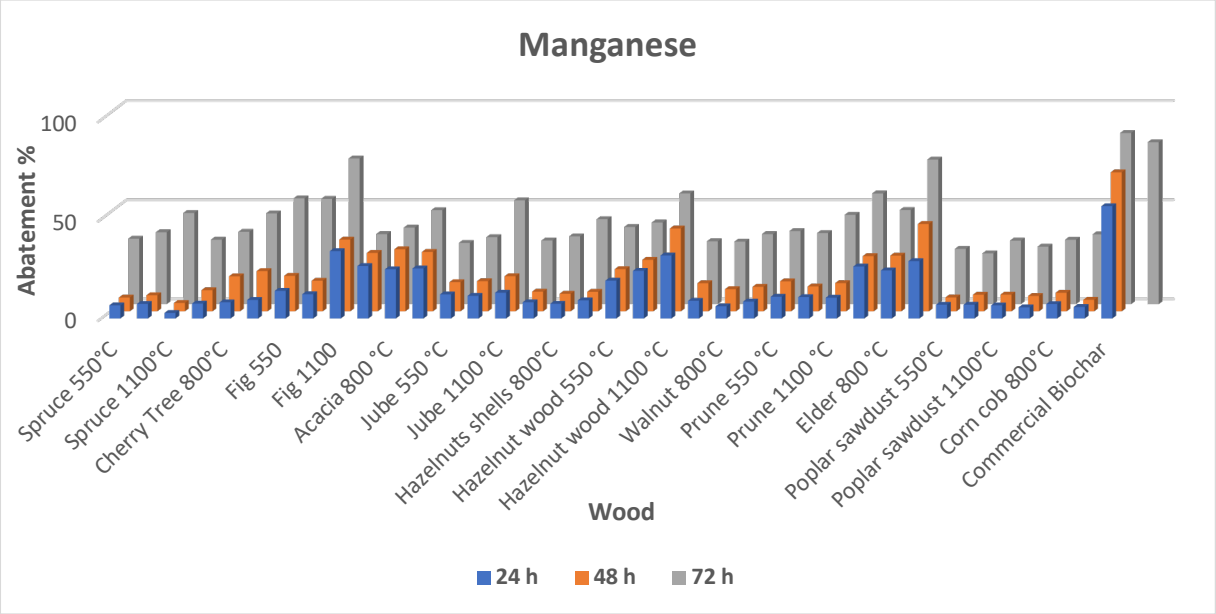

Figure 120: Abatement % of manganese as a function of essence, time and temperature.

- *Nickel*

Table 121: Reduction of nickel in solution (2 mg/l pH 6).

Sample	Ni		Ni average	Std. Dev.
Metal amount retained	%	%	%	%
Time	24 h	48 h	72 h	72 h
Spruce 550° C	4,02	6,00	39,25	14,66
Spruce 800 °C	5,40	5,41	42,21	7,73
Spruce 1100 °C	8,66	10,28	46,65	8,61
Cherry tree 550 °C	26,82	27,46	41,60	1,42
Cherry tree 800 °C	25,04	26,49	44,84	4,78
Cherry tree 1100 °C	26,80	27,46	54,48	9,96
Fig 550 °C	13,08	18,07	43,65	14,03
Fig 800 °C	21,70	27,03	56,99	7,56
Fig 1100 °C	51,83	58,59	73,66	1,71
Acacia 550 °C	26,43	36,33	43,48	8,10
Acacia 800 °C	24,54	26,06	45,31	9,03
Acacia 1100 °C	24,43	29,37	56,12	5,14
Jube 550 °C	11,28	13,97	48,16	4,63
Jube 800 °C	7,97	12,34	43,74	9,77
Jube 1100 °C	14,33	19,75	60,65	2,48
Walnuts shells 550 °C	5,69	7,19	35,60	2,73
Walnuts shells 800 °C	2,43	6,03	37,01	2,58
Walnuts shells 1100 °C	5,54	7,64	51,33	2,19
Stone wood 550 °C	31,42	36,55	46,73	0,75
Stone wood 800 °C	25,50	36,12	51,15	5,34
Stone wood 1100 °C	34,39	40,92	63,66	4,98
Walnut 550 °C	7,59	11,64	33,13	4,51
Walnut 800 °C	20,58	30,57	38,65	6,72
Walnut 1100 °C	7,31	13,83	42,25	2,76
Plum 550 °C	7,32	12,22	45,41	3,15
Plum 800 °C	7,48	10,98	45,06	3,50
Plum 1100 °C	9,04	13,34	48,66	9,27
Elder 550 °C	27,44	32,31	62,28	2,12
Elder 800 °C	25,82	39,71	68,81	11,77
Elder 1100 °C	47,66	60,33	89,06	5,44
Poplar sawdust 550 °C	5,65	5,80	36,45	14,02
Poplar sawdust 800 °C	5,36	7,47	33,92	14,15
Poplar sawdust 1100 °C	2,84	6,25	39,44	9,77
Corn cob 550 °C	3,83	5,41	42,16	3,06
Corn cob 800 °C	5,31	8,87	44,38	5,51
Corn cob 1100 °C	1,51	3,01	43,40	7,25
Commercial biochar	24,36	52,57	96,40	1,66
Active carbon	-	-	95,97	1,41

Nickel behaves in a similar way to manganese and cadmium: the percentages of abatement are, generally, medium low (they vary between 30 and 60%) and increase with time, while pyrolysis temperature is not particularly relevant on the process. Samples at 1100 ºC are usually more performing, especially fig and elder samples.

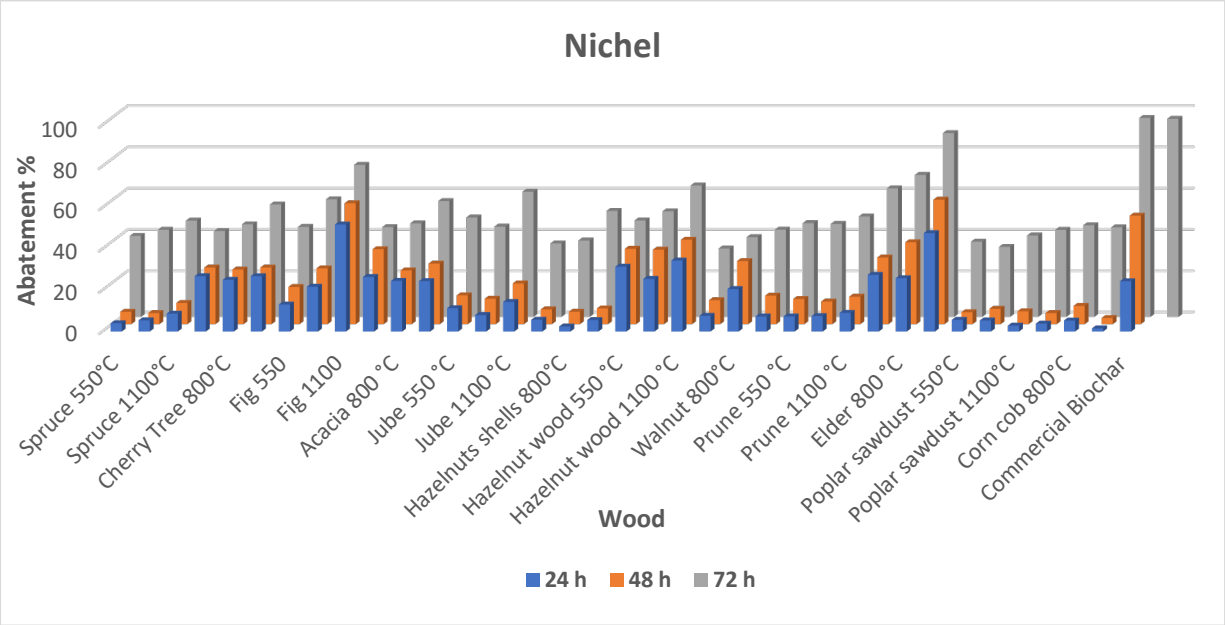

Figure 121: Nickel abatement as a function of essence, time and temperature.

10.13.3 Abatement tests

From the data collected and considering only the samples produced at 1100 °C after 72 hours, it is possible to split metals into two categories, each characterized by similar trends, in terms of abatement percentages and behavior (dependence on time and temperature). Metals such as aluminum, copper and lead appear to be almost totally retained by all samples while zinc and chromium are shot down in lower percentages but still greater than 50% by all woods. It has also been found that this phenomenon depends mainly on the pyrolysis temperature, and it is for this reason that biochar 1100 °C turn out to be more performing than those produced at lower temperatures.

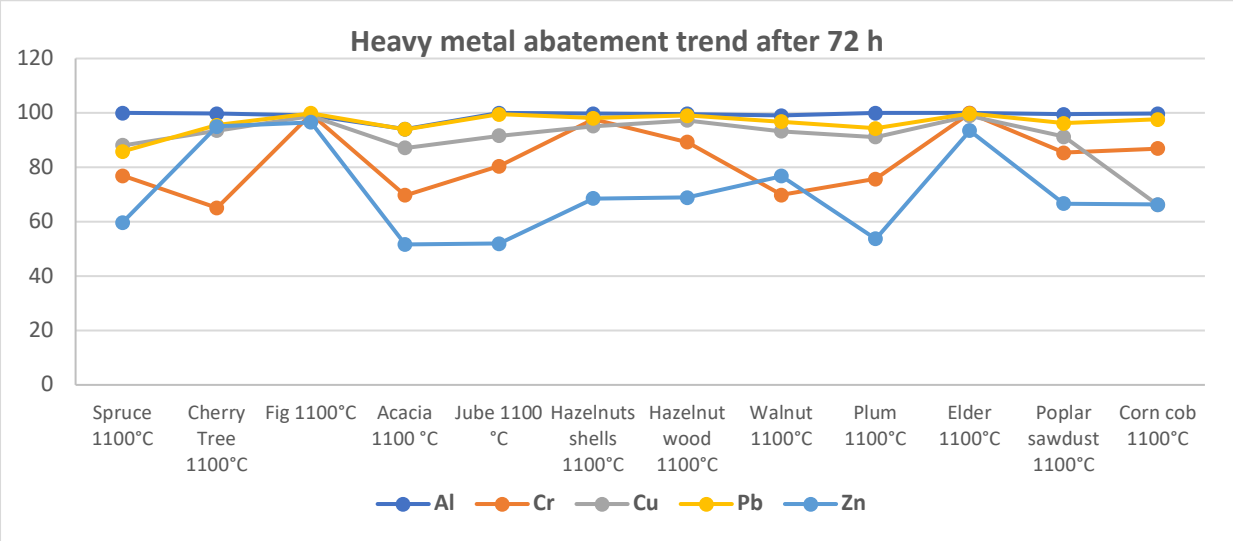

Figure 122: Reduction of the percentage of aluminum, chromium, copper, lead and zinc according to the essence.

Cadmium, manganese, and nickel show a different pattern: they are cut down in lower percentages, on average between 30 and 80%, and the abatement increases mainly with time and to a lesser extent with the pyrolysis temperature, although biochar 1100 °C are the most performing.

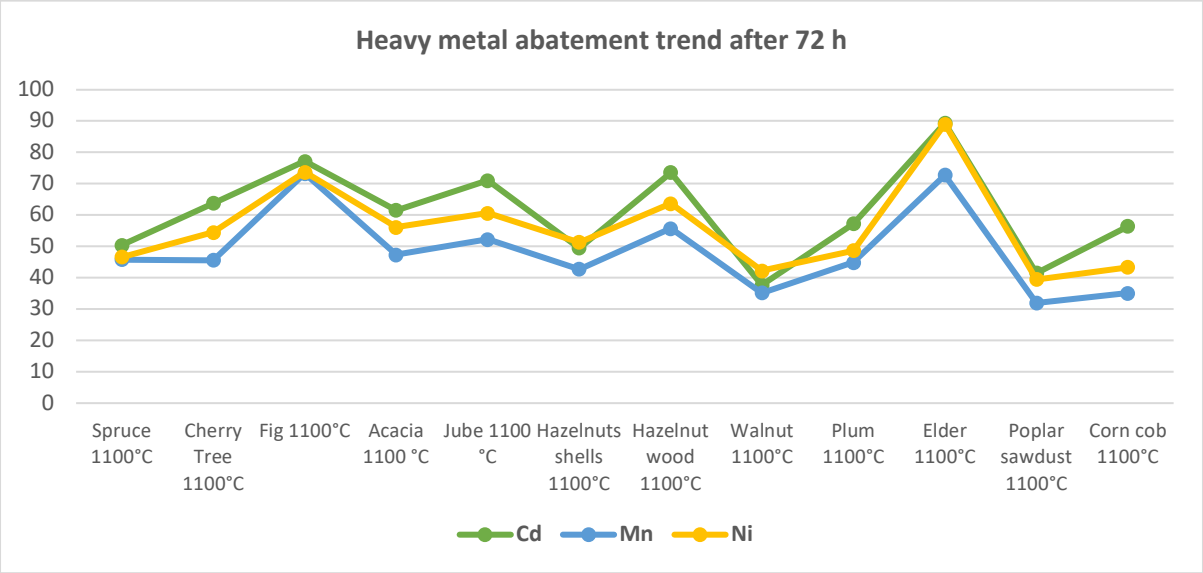

Figure 123: Percentage reduction of cadmium, manganese and nickel as a function of the essence.

10.13.4 Woody biochar vs active carbon: a comparison

Unlike most samples, the commercial biochar and activated carbon were not produced in the laboratory but were supplied by the company NeraBiochar srl. These samples can reduce percentages equal to 99% of all metals tested (except for manganese which is cut down around 80%,). A comparison on best performing samples is shown in the following graph.

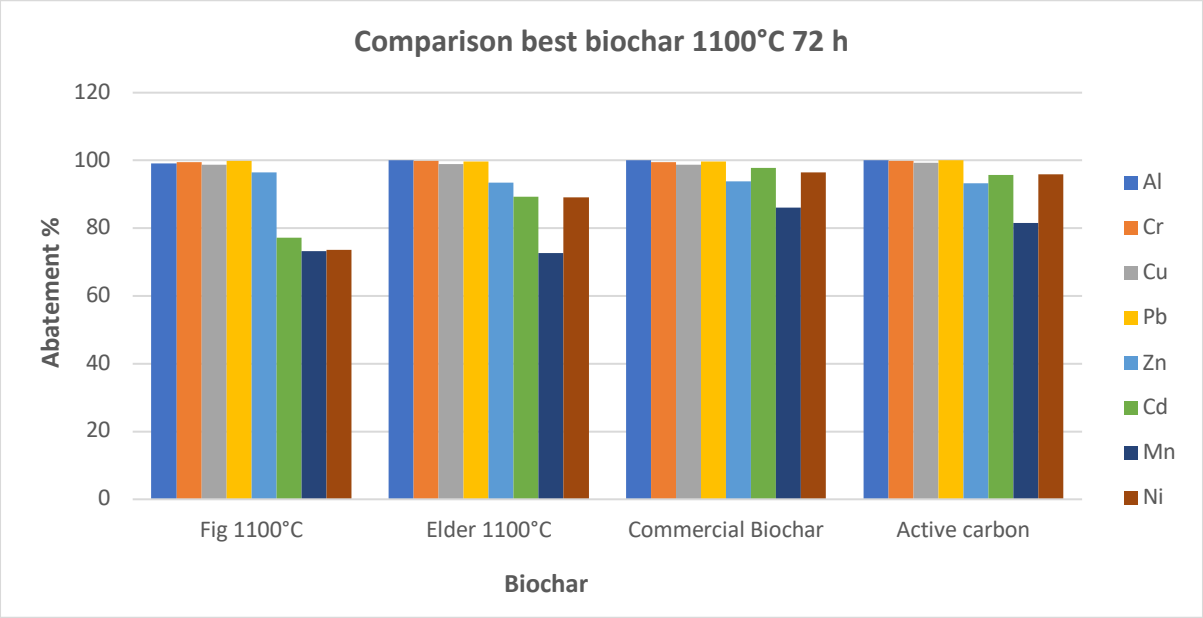

Figure 124: Comparison of commercial biochar and activated carbon abatement capabilities with the most performing samples produced in the laboratory.

If we compare commercial samples with best performing woods produced by in the lab (fig and elderberry biochar 1100 °C), it can be said that activated carbon and commercial biochar yield slightly higher abatement percentages than elderberry biochar for cadmium, manganese, and nickel. This difference is probably due to the starting material and industrial processes to produce activated carbon and commercial biochar. It should be considered also the samples produced in lab have not undergone any treatment with the aim of improving their detention.

10.13.5 Abatement tests: 2 mg/l at pH 4 on performing samples

This test was carried out on best samples using 0,5 g biochar and 25 ml of a solution metal mix solution 2 mg/l buffered with acetic acid. Analysis was performed in duplicate, after 72 hours the solution taken filtered and acidified.

Table 122: pH influence on % abatement.

% metal retained in 72h	Al average	Cd average	Cr average	Cu average	Mn average	Ni average	Pb average	Zn average
pH=4	%	%	%	%	%	%	%	%
Commercial biochar	77,44	15,41	61,43	87,22	0	19,96	84,73	0
Cherry tree 1100 °C	60,65	30,52	23,18	53,24	22,63	26,22	75,65	20
Fig 1100 °C	79,19	27,76	28,89	71,31	20,87	25,93	78,35	22
Walnut 1100 °C	82,11	41,17	35,63	67,83	33,64	43,11	84,83	0
Elder 1100 °C	80,74	37,53	31,19	63,46	34,21	39,87	80,31	0

	Al Std. Dev.	Cd Std. Dev.	Cr Std. Dev.	Cu Std. Dev.	Mn Std. Dev.	Ni Std. Dev.	Pb Std. Dev.	Zn Std. Dev.
	%	%	%	%	%	%	%	%
Commercial biochar	1,36	14,18	6,97	0,43	0	4,16	4,83	
Cherry tree 1100 °C	4,15	4,69	1,54	4,36	20,42	19,85	2,7	0
Fig 1100 °C	3,83	4,98	5,77	1,69	13,22	10,59	1,87	6,43
Walnut 1100 °C	0,78	12,87	3,18	2,97	13,66	4,22	2,2	
Elder 1100 °C	6,01	6,04	4,31	2,94	9,25	10,53	0,89	

When the pH of the aqueous matrix is less than 5, biochar's abatement efficiency is worse than when the pH >6. Under such conditions, Al, Cu and Pb are always retained in higher percentages than other metals. The graph below allows to compare the efficiency of the abatement as a function of pH and shows that working at pH=6, abatement percentage is higher.

10.13.6 Abatement tests: 1 mg/l at pH 6 on best performing samples

This abatement test was carried out only on the best samples inserting 0,5 g biochar with 50 ml of 1 mg/l solution of metals into Falcon type specimens. By decreasing the concentration but doubling the volume, the absolute metal amount stays constant. Analysis at the ICP-OES was performed on the solution taken after 72 hours of contact with biochar. The purpose of this test is to assess how the abatement varies as the concentration of the solution varies: it was decided to lower metal concentration in solution. Looking at the results it can be said that the abatement rates are very high for all metals, even for those that were absorbed less (Cd, Mn, Ni) during the tests on 2 mg/l.

Table 123: Results: reduction of % 1 mg/l and pH 6 on best performing samples.

Abatement % 1 mg/l	Al average	Cd average	Cr average	Cu average	Mn average	Ni average	Pb average	Zn average
72 h, pH= 6	%	%	%	%	%	%	%	**%**
Commercial biochar	99,5	93,3	99,9	98,9	53,1	94,9	95,3	73,7
Cherry tree 1100 °C	100	76,7	86,2	93,6	65,7	70,1	96,1	37,9
Fig 1100 °C	97,5	88,8	99,9	99	78,8	93,6	95,5	89,6
Walnut 1100 °C	99,5	73,2	99,3	91,9	67,1	72,8	97,1	39,2
Elder 1100 °C	99,9	79,5	99	94,7	61,2	66,5	97,2	40
	Al Std. Dev.	**Cd Std. Dev.**	**Cr Std. Dev.**	**Cu Std. Dev.**	**Mn Std. Dev.**	**Ni Std. Dev.**	**Pb Std. Dev.**	**Zn Std. Dev.d**
	%	%	%	%	%	%	%	%
Commercial biochar	0,7	2,4	0,2	0,3	0,6	0,1	5,1	3,4
Cherry tree 1100 °C	0	1	19,5	3,1	3,7	3,3	2,1	0,4
Fig 1100 °C	3,6	2,8	0,2	0,2	2	4,9	6,1	0,9
Walnut 1100 °C	0,8	14,5	0,7	8,5	2,4	4,4	2,3	7,1
Elder 1100 °C	0,2	2,4	1,2	1,6	1	2,5	2,7	3,3

10.13.7 Abatement tests: 0,1 mg/l at pH 6 on best performing samples

The abatement test on 0,1 mg/l of metals was carried out on best performing biochar by inserting 1 g of each in 1L of solution. The analysis was performed after 72 hours. The purpose of this test was to assess the trend of biochar abatement as concentration and dilution in the aqueous environment varied.

Table 124: Results: reduction of 0.1 mg/l and pH 6 on best performing samples.

Abatement % 0,1 mg/l	Al	Cd	Cr	Cu	Mn	Ni	Pb	Zn
72 h, pH= 6	%	%	%	%	%	%	%	%
Commercial biochar	44,2	40,8	56,6	74,5	0,0	45,8	67,2	0,0
Cherry tree 1100 °C	100,0	7,6	80,6	69,0	5,4	7,1	68,0	2,8
Fig 1100 °C	86,9	21,3	91,7	87,1	11,0	21,5	83,5	3,2
Walnut 1100 °C	56,9	51,1	96,3	89,8	17,0	17,1	0,0	0,0
Elder 1100 °C	100,0	8,4	93,7	72,0	6,8	8,8	69,1	1,4

These results are generally much lower than lower volumes of solution, which leads to the conclusion that when biochar is too dispersed, its abatement efficiency are lowered.

10.13.8 Abatement tests at pH=6: a comparison

The following graphs show how abatement percentages vary with the varying concentration in solution. The comparison concerns three tests carried out at pH=6, those carried out on solutions at concentrations of 0,1 mg/l, 1 mg/l and 2 mg/l for samples showing best performance.

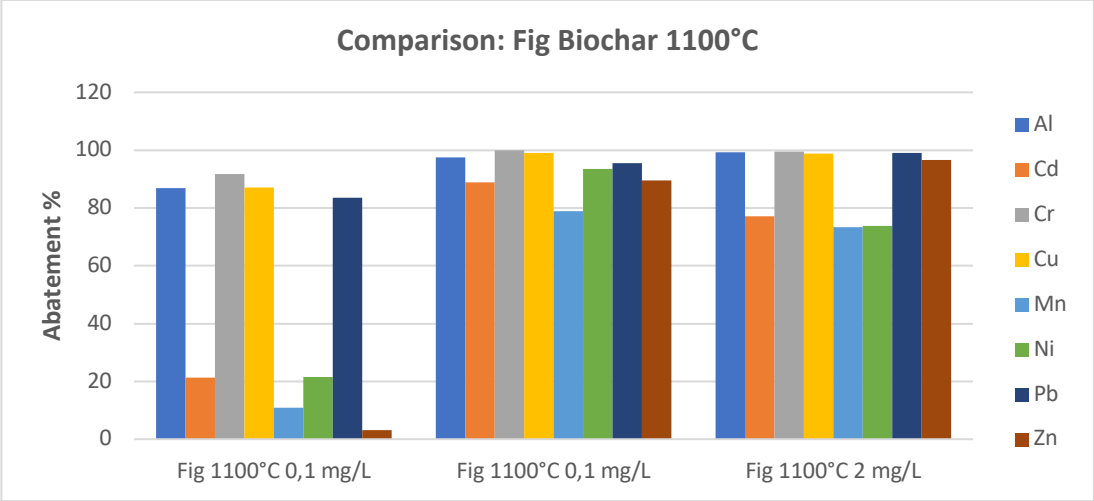

Figure 125: Concentration effect on biochar's abatement capacities of Fig 1100°C.

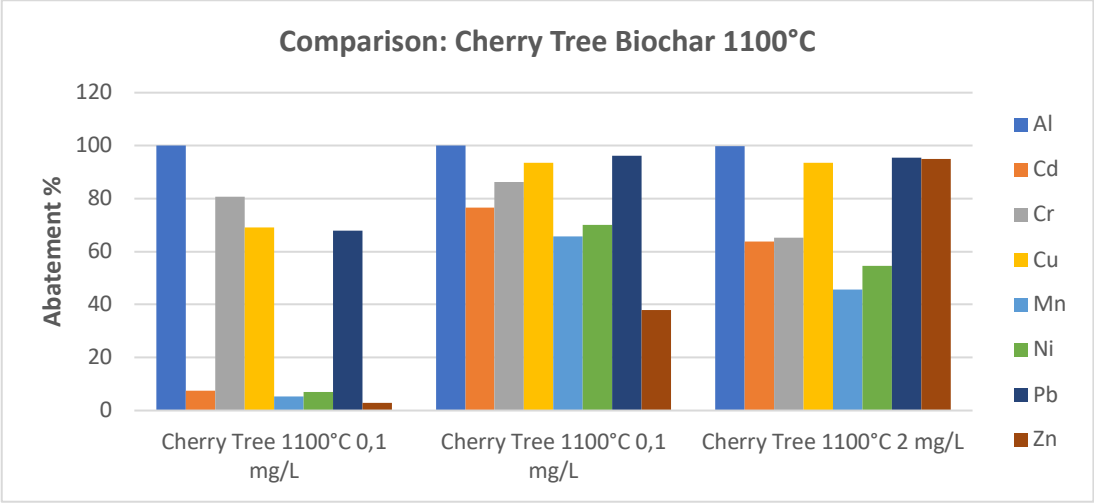

Figure 126: Concentration effect on biochar's abatement capacities of Cherry Tree 1100°C.

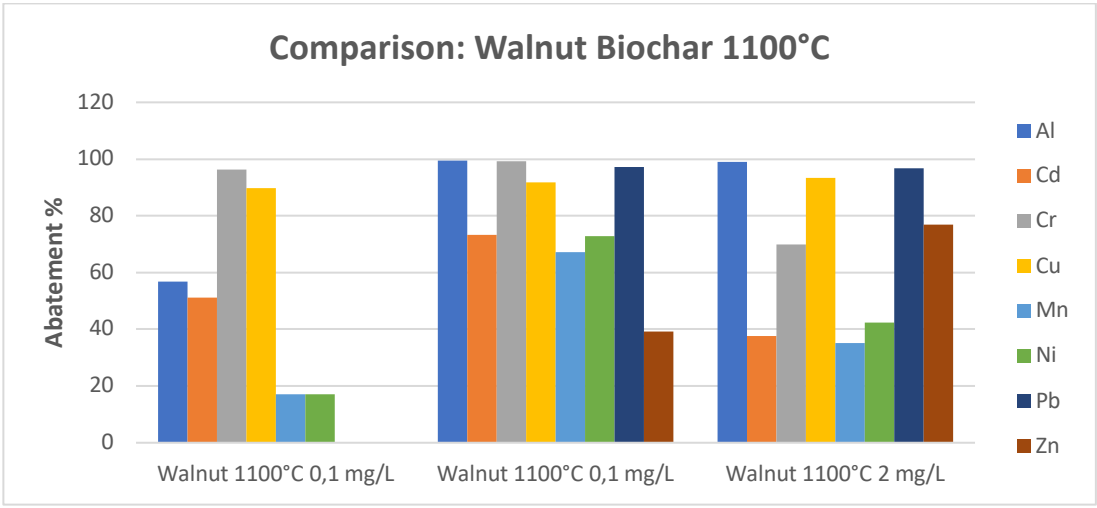

Figure 127: Concentration effect on biochar's abatement capacities of Walnut 1100°C.

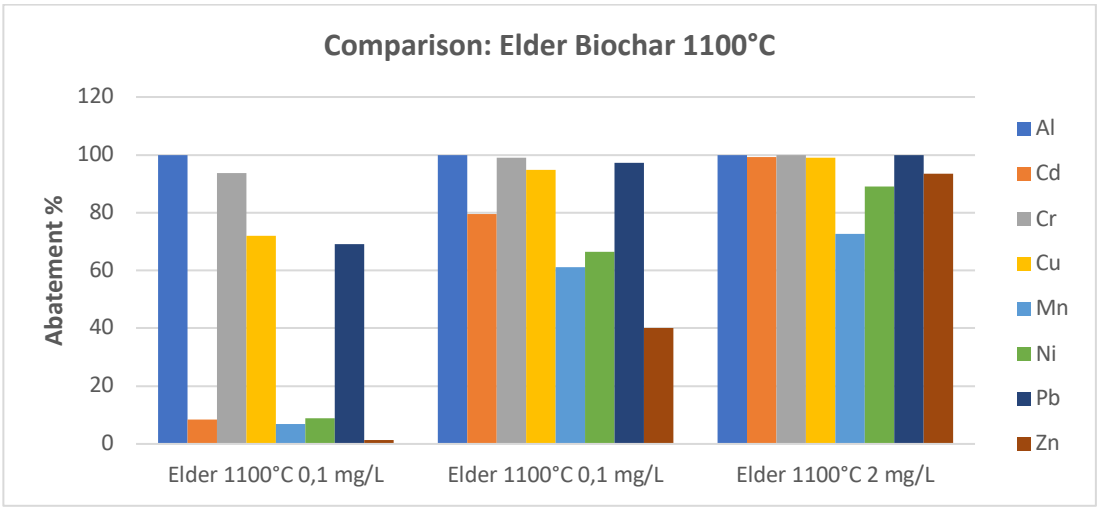

Figure 128: Concentration effect on biochar's abatement capacities of Elder 1100°C.

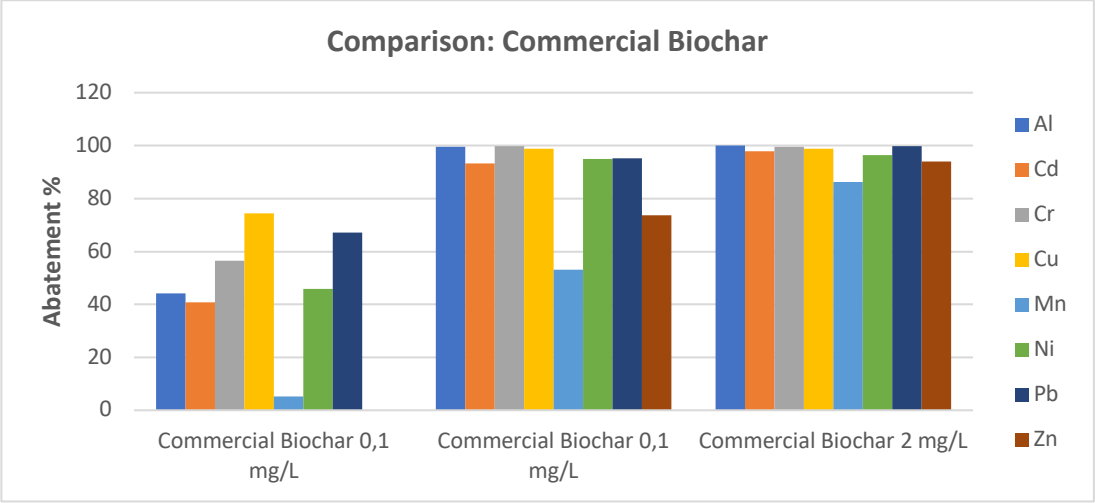

Figure 129: Concentration effect on biochar's abatement capacities of Commercial biochar 1100°C.

Lowest abatement percentages of are found in all the samples during the test at 0,1 mg/l in 1L. The commercial biochar and elder biochar 1100 °C are more performing during the test conducted on 2 mg/l, vice versa, the other samples show on average higher abatement during the test carried out at 1 mg/l. Aluminum, chromium, copper and lead are felled in high percentages at all three concentration conditions and by all woods, excluding walnut and commercial biochar which show low values. Zinc is retained in higher percentages, by all samples, during the 2 mg/l test, and cadmium, manganese and nickel are retained better during the 1 mg/l test, but this does not occur in commercial biochar and elder biochar samples.

10.13.9 Release tests

The release tests were carried out after the abatement test at pH=6 to 2 mg/l. To better understand the mechanisms involved in retention process and release of retained metals. It was also intended to check whether any pH changes in aqueous matrix may cause metals to return to solution. These measurements were performed on the samples which showed the best abatement feature. Biochar containing the adsorbed metals were placed in contact with 50 ml of ultrapure water buffered with acetate buffer to reach the desired pH. After 30 minutes the first withdrawal was made. If the release of metals was found at this stage, the abatement mechanism could be traced back to ionic exchange phenomena. Subsequently the pH was lowered from 6 to 4 and after 5 days the analysis was carried out again. The results obtained are shown in the tables and are expressed as a withheld percentage. Only on tests performed after five days the standard deviation has been calculated.

Table 125: % of metal retained after 30 minutes of the biochar's stay in water.

% Retained after dopo 30 min in water (pH 6)	Al	Cd	Cr	Cu	Mn	Ni	Pb	Zn
	% metal retained							
Commercial biochar	99,9	98,5	100,0	100,0	90,4	97,6	100,0	97,6
Fig 1100 °C	100,0	77,9	100,0	99,8	79,5	91,8	100,0	89,8
Elder 1100 °C	100,0	65,7	99,9	99,3	79,4	82,4	99,2	81,9
Cherry tree 1100 °C	99,9	68,5	99,3	94,3	87,4	81,4	89,2	75,4
Walnut 1100 °C	100,0	70,8	99,8	94,5	87,6	89,0	84,1	71,1

Observing the results, it emerges that the commercial biochar can retain almost all the metals, excluding manganese which is retained at 90%. The other biochar samples retain aluminum and chromium very well, while copper, manganese, nickel and lead are retained in percentages between 80-100%. Cadmium and zinc are metals released in higher amount, but the retained percentages remain significant (65-90%). These results make it possible to affirm that the ionic exchange phenomena influence only a small part of the abatement process. Finally, the retained percentages are shown, measured after 5 days of permanence of the biochar with a buffer solution of pH 4.

Table 126: % metal retained after 5 days of permanence of the biochar in a buffer solution having pH 4.

% Retained after 5 days in solution at pH= 4	Al	Cd	Cr	Cu	Mn	Ni	Pb	Zn
	% Abatement							
Commercial biochar	99	95	100	100	74	95	100	97
Fig 1100 °C	100	52	100	99	71	73	98	68
Elder 1100 °C	92	58	91	96	79	61	63	55
Cherry tree 1100 °C	84	66	87	87	85	81	72	75
Walnut 1100 °C	74	65	73	55	84	77	39	71
	Al Std. Dev.	**Cd Std. Dev.**	**Cr Std. Dev.**	**Cu Std. Dev.**	**Mn Std. Dev.**	**Ni Std. Dev.**	**Pb Std. Dev.**	**Zn Std. Dev.**
	%	%	%	%	%	%	%	%
Commercial biochar	0,4	0,8	0	0,2	1,8	1,1	0,7	2,2
Fig 1100 °C	0,3	23,7	0	0	3,9	13,4	0,6	30,5
Elder 1100 °C	12,2	6,5	12,8	14,6	0,8	16,3	55,2	55,4
Cherry tree 1100 °C	15,3	7,3	7,9	6,3	2,3	10,5	22	5,8
Walnut 1100 °C	7	0,5	1,5	7,1	1,7	2,1	10,5	1,7

Looking at the results we can say that the commercial biochar continues to retain > 95% all metals previously retained. It is noted that aluminum and chromium stay the most retained metals, whereas cadmium is the least retained metal (65-50%); other metals are retained in high percentages, between 60 and 90%.

11 Conclusion and Future Perspective

1. ***ZEOLITE:*** The aim of first part of the study was too lower ammoniacal nitrogen content in cow and pig digestate to comply Nitrates Directive and allow its spreading in crops. To reach this purpose, zeolite has been used as natural retainer of NH_4^+ ion: after treating the digestate, it may subsequently be used as a slow-release fertilizer by the same farmer or sold. In this case, there would be a double advantage: the first one is to be within law parameters and the second one is to gain a profit that would amortize the costs of wastewater treatment plant. From the preliminary tests carried out to verify the competition between the ions NH_4^+ and K^+ for zeolite cavities, it was found an increase of K^+ and a decrease in the absorption of ammoniacal nitrogen has been reported. This was an important factor to consider knowing the composition of the digestate to be treated. The NH_4^+ content in samples does not differ much from one digestate to another, while other elements are more variable and is attributable to the anaerobic digester feeding. These digestors require, in addition to animal waste, some plant material to have a production of CH_4 sufficient to meet the costs associated with this technology. The results are different for the digestates examined and depend on their composition. Tests for the ammonium abatement in digesters with increasing amounts of zeolite and in the pilot plant have demonstrated, once again, that the difference in composition affects the ammonium holding capacity to reach the 60% retention target. The analyses carried out to determine the abatement and release kinetics of zeolite for NH_4^+ ion show that clinoptilolite is a mineral that gradually releases it over time. K^+ release tests also confirm this behavior, decreasing the released cation content over time. The use of natural zeolite as a retainer of NH_4^+ ion has an ecological, agricultural, and economic advantage. Ecological advantage is shown because of zeolite natural origin and is widely available since it is widespread globally. At agricultural level, zeolite is useful as its unique characteristics make it rather suitable as a slow-release fertilizer and as a water tract, as demonstrated by the promising results of the strawberry study using zeolite used to cull ammonium. Strawberry plants treated with ammonium-enriched zeolite showed positive effects in growth and photosynthetic activity measures; however, it wasn't possible to identify a unique trend with enriched zeolites added to the substrate. All the data point to

environmental benefits for more widespread use of zeolite in livestock waste treatment. Zeolite represents an economic advantage: it is available at a low price (100-300 euro/tons) and is less expensive than the current processes. Also, following its loading with the NH_4^+ ion, you can spread it directly in field as a fertilizer or regenerate and use it again as a retainer. The use of zeolites is a valuable contribution to this by pursuing of sustainable agriculture, which aims to an optimum use of nutrients in livestock waste and production waste. The future aims of this study could be focused on ammonium retention in different types of zeolites, in the ratio between the size and ion abatement capacity, in zootechnical effluents treatment of prior to their release into the digester. In addition, it would be appropriate to verify the real fertilizer capacity of the zeolites charged following digestate treatment, zeolites charged with different concentrations not only of NH_4^+ but also of K^+, and their impact on plant growth and fruit formation. In conclusion, the knowledge of the composition of the digestate and the treatment of the latter with zeolites favors a greater spreading in the field of the digester product avoiding problems of nitrogen release. Ammonium nitrogen could be released during field spreading while, during the time spent in the soil. Soil is potentially prone to nitrates leaching that inevitably end up in the nearby water sources. Since natural zeolites do not pollute the environment and make agronomic improvements.

2. ***NANOSPONGES:*** The second part of the research work focused on functionalized nanosponges (in granular form) based on cross-linked commercial maltodextrins, through green synthesis methods. The choice of maltodextrins as a raw material has been favored as they are low-cost, soluble in aqueous solvents and as a result, they are considered more sustainable alternatives than the raw materials used in common commercial ion exchange resins or other adsorbent materials. For the synthesis, a commercial maltodextrin derived from maize starch, called Glucidex2®, (with equivalent dextrose, DE=2), crosslinked by 1,4-diglycyledyether (BDE), in a basic environment (NaOH 0,2 M) or simply aqueous. The 1,4-diglycylidene ether has been shown to be an excellent alternative to conventional reticulating agents less 'green' (for example, epichlorohydrin or glutaraldehyde), thanks to its low toxicity, biocompatibility, and good solubility in water. In addition, it has proven very efficient in cross-linking maltodextrins. In addition to BDE, other cross-linkers such as TTE

have been tested, and the reagent is less green than NGDE. By varying the percentages in weight of functionalizing agents, we have obtained two types of nanosponges:

a) Anionic nanosponges, using the 3 cross-linkers, the DABCO (initially used as reaction catalyst) and choline chloride as a cationic functionalizing agent.
b) using reagents with sulphate or sulphonic groups such as carrageenan-K or sultons (1,3-propylsulton and 1,4-butylsulton).

Overall, it was possible to obtain insoluble cross-linked polymers, in granular form, with rather green synthesis methods, both for the reagents used and for the chosen reaction conditions.

For *anionic nanosponges* cross-linked with epoxide in aqueous solution, choline chloride was found to be insignificant for charge conferral. Data on elemental analysis potential-ζ and FTIR-ATR spectra analysis have shown that anionic nanosponges functionalization is associated with DABCO linked to the crosslinking agent. In fact, it is DABCO that creates a quaternary ammonium and gives predominantly positive charge to the polymer. The abatement of all the anions analyzed was high. Nitrates are cut down around 50 to 80% when the concentration is 100 mg/L. Given the limits of nitrates in different water compartments, efficiencies of this type, with such concentrations, the abatement percentage has been decreasing with the increase in concentration. This behavior has been associated with the nature of the ion exchange mechanism. The phosphates retainment showed a dependence on pH. The observed trend foresees an increase in the percentage of felling up to a maximum of pH 8,49. If this value is exceeded, the abatement decreases rapidly. This pH value has been identified as the optimal compromise between a high concentration of the most charged species and competition with hydroxyl. The increasing concentration of orthophosphate and mono-hydrogen phosphate as the pH increases, promotes the abatement. On the other hand, the competition with hydroxyl in the ionic exchange, is higher with the increase of the pH and disadvantages the abatement. Glyphosate showed very high retainment at all concentrations tested. Such efficiencies have been associated with the predominant presence of the species having two negative formal charges (HL^{2-}). The instrument used for the analysis of glyphosate (ICP-OES) showed a LOQ of 50 μg/L, it was not possible to perform abatement tests below this limit of quantification. Equally positive results were obtained for the killing of highly polluting species such as Cr(VI), As(V) and As(III). The major flaw of these materials is their tendency to swell a lot,

which could compromise their applicability in the industrial field. In the future, further improvements to all synthesis parameters can be optimized. For this reason, the focus will be more on NGDE and BDE, to the detriment of TTE, which has a certain toxicity. Always in this context, particular attention should be paid to the choice of the functionalizing amine. DABCO, in fact, is not free from toxicity on aquatic life. Finally, given the positive results of the glyphosate abatement, further abatement tests at lower and lower concentrations will have to be carried out to fall below the legal limit set by the European Union of 0,1 μg/L. This requires the use of more sensitive analytical techniques.

Carrageenan-K and sultons were used for *cationic nanosponges*. Carrageenan-K is natural biopolymers derived from brown algae and red algae. It is biocompatible and used for the formation of cross-linked hydrogels in the biomedical and environmental field. The less green alternative is represented by sultons, cyclic sulfonic esters, characterized by acute toxicity and relatively higher cost than the other reagents used. However, from various research papers in literature they have played an important role in the functionalization of β-cyclodextrin, for biomedical applications, such as in the controlled release of drugs. As for TTE and DABCO, the main cause of danger would be the handling of these reagents. Even the synthesis conditions adopted are quite mild with temperatures in the range of 75 °C-100 °C, reaction times not exceeding two hours and with the possibility of obtaining the final product in one step, without the use of organic solvents either as a reaction medium or for the purification process. These adsorbent materials have been used to abate various heavy metals from standard aqueous solutions at different concentrations. The 10% w/w carrageenan-K-based nanosponges with sulphate and sulfonic groups showed average adsorption capacity. However, even if greener, the synthesis involved more difficulties than the other types, which is why it is necessary to find solutions to improve the characteristics of the final product. The best performance was observed for post-synthesis functionalized nanosponges with 20% w/w of 1.4-butylsulton, despite the less green characteristics for the functionalizing agent used. The use of these adsorbent systems has allowed us to achieve the almost total removal of the metal cations tested, especially tri-charged ions, thus being able to compare them to ion exchange resins. Given the excellent results, the adsorption mechanism speed (after only 15 minutes), the synthesis methods simplicity and their attractive properties as biocompatibility, insolubleness in water and the lower

tendency to swell in aqueous solutions, these adsorbent materials could provide a green alternative for the removal of metallic cations in wastewater. In fact, given the tendency to swell less than anionic nanosponges, they could be exploited in column for their continuous use. Another promising possibility could be the synthesis of two-functional nanosponges by functionalizing maltodextrin with both sodium alginate and 1,4-butylsulton. Surely, another very important test to evaluate is the regeneration of the nanosponges synthesized for their possible recycling and reuse.

Despite the promising features of both types of nanosponges, the main limit for their future scale-up, could be attributed to a difficult recovery of microparticles, which often require further processes such as sedimentation and centrifugation, and therefore additional costs. Similar problems may occur during the synthesis process, due to the viscosity of the gel, which could lead to difficulties in the cleaning of the reactor and in the recovery of the product itself. In addition, from a synthetic point of view, it is necessary to find systems that guarantee a homogenous heating as well as an efficient agitation system.

3. ***BIOCHAR***: In the third part of the research work the aim was to test different biochar at different temperatures for heavy metals abatement. The type of biomass to produce biochar greatly influence its capabilities and the mechanisms of metal abatement. Varying the type of biomass, varies the structure, the mineral content, the surface porosity, the abundance of functional groups on the biochar. Excellent results have been obtained using biochar of light and porous woods, such as fig and elder. They correspond to some of the samples which, even if produced at 1100 °C, still have a minimum of crystallinity in the structure given by the presence of graphite (detected through FTIR measurements) and aromatic phenomena. The temperature at which biomass is pyrolyzed influences the abatement properties and mechanisms involved in the process. In general, biochar produced at 1100 °C were those that allowed to break down the highest percentages of metals, probably thanks to the electrostatic interactions that occur between the electrons π of the aromatic structures of the biochar and metal cations. Often better results were found on pyrolyzed samples at 550 °C than those produced at 800 °C, this may be since there were still active functional groups on the surface able to establish weak bonds with the metal ions in solution. Through the abatement tests of 1 mg/l and 0,1 mg/l, it was evaluated, respectively, how the biochar's abatement capacity varies as the concentration of metals in solution

decreases, increasing the volume, keeping the absolute metal amount constant. In general, as the concentration of metal ions decreases, the abatement capacities increase, from 2 to 1 mg/l, but if the concentration decreases by ten times, its abatement properties drastically decrease. If compare the best results obtained during all the abatement tests, with the limits defined by the Legislation on drinking water, it is possible to say that the biochar does not allow sufficient abatement to the potabilization of water, because only chromium, aluminum and copper are cut down to a percentage that is below the legal limits. If wastewater limits are taken into account, they can be respected after purification with the biochar with the exception of cadmium, since its legal limit is extremely low (5 μg/l) and the cation is poorly killed by the biochar. It should be noted that the results obtained in this study work came from batch abatement tests, so further testing should be carried out by working in columns as they could lead to more satisfactory results. Typically, the higher the pH of the solution in contact with the biochar, the lower the concentrations of metals in the water appear, because as the pH increases these metals precipitate. It was chosen to work at a pH of as much as possible equal to 6, that is like that of natural water. The results show the abatement efficiency is higher when the pH of the solution is 6 than when it is less than or equal to 4, better results could be obtained at even higher pH. High pH values may not be a problem for the purification of industrial wastewater. During the post-cull release tests, it was also shown that lowering the pH from 6 to 4 the metals did not return in solution but remained well retained by the biochar, excluding the fact that the retention mechanism was labile. In addition, the data show that, to break down most metals, it usually takes 72 hours of contact with the biochar. The process is therefore rather slow, it does not allow the removal of metals in a single and rapid passage, so, if the solution was represented by a continuous flow, it should recirculate several times on the biochar itself to be able to purify.

To date, it is considered very important to carry out, develop, enhance and promote research and experimentation related to the application of vegetable and residual raw materials in industrial production cycles, verifying their possible impact on the natural environment, nutrient cycles and waste recycling. Materials such as biochar are perfectly classifiable as new products of green chemistry, for many reasons, first, the biochar is obtained from agricultural or industrial waste, otherwise considered as waste then substances to be disposed of (often through combustion in the open air, or

alternatively become costs to the enterprise). Using such waste to produce a material that is marketable on the market means revaluing it, turning it into a resource, which automatically implies an increase in profit, if the process is carried out in an advantageous way. Turning a waste into a resource is one of the basic principles of the circular economy. Many recent studies show that the biochar can be used in different sectors, such as agriculture in which it finds applications as a soil improver, zootechnics where it can be used as a probiotic animal food. In the literature are known especially the ability of the biochar to remove inorganic pollutants such as heavy metals, pharmaceutical substances, and organic pollutants (VOCs) demonstrating that the adsorption of pollutants by biochar is an effective and cost-effective method, applicable in environmental treatment [60] and for water purification as an alternative to other adsorbent systems such as ion exchange resins. As far as the end-of-life problem of spent filters is concerned, it needs to be further studied and deepened. However, few studies have been carried out on the regeneration of the biochar used for the abatement of heavy metals, since if retained by the material they are difficult to desorb. Therefore, as a future perspective we should focus primarily on determining effective surface changes for the biochar (activation)to improve its felling capacity and the recyclability of the material when loaded with metal pollutants. Another future perspective is to focus on how to recycle the contaminated biochar in different technological applications, rather than how to regenerate it and reuse it as a filter. Biochar containing heavy metals may be used as an alternative to carbon-based synthetic nanomaterials (such as nano tubes) to produce supercapacitors, or, in the field of catalysis, as a catalyst or catalyst carrier. At the same time, it will be important to transform the technologies studied in the laboratory in actual industrial applications, considering the economic aspects and the end of life of the material, both to be deeply investigated.

12 APPENDIX I

12.1 Cationic Nanosponges: characterization of optimize synthesis

12.1.1 FTIR-ATR Analyses

In figures are shown the IR spectra of:

- GLU2_BDE_CARK10%_H_2O_BIS,
- BUTS20%_POSTSINTESI_BIS.

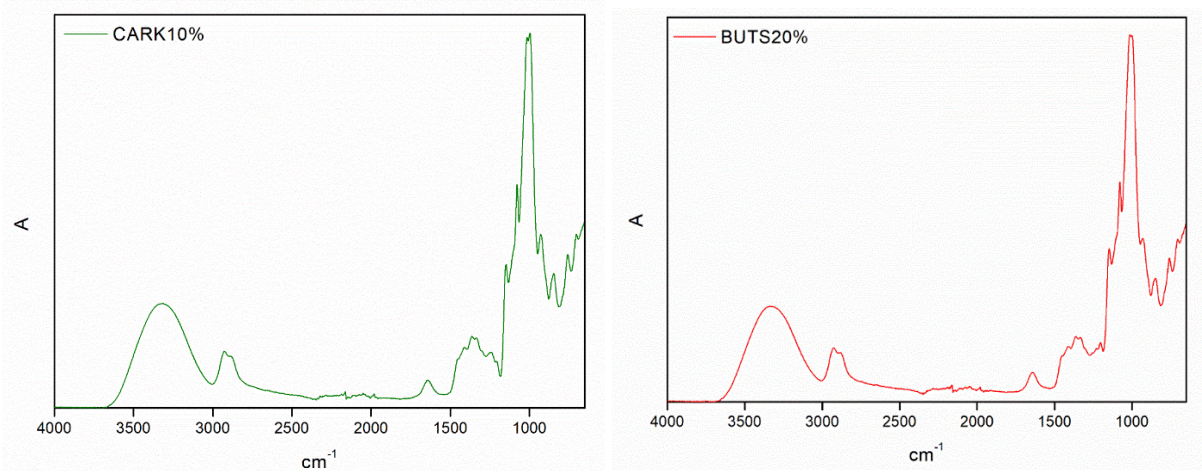

Figure 130: IR spectra GLU2_BDE_CARK10%_H2O_BIS

12.1.2 TGA analyses

Thermogravimetric analyses were carried out to assess the thermal stability of nanosponges. It is worked in an inert N_2 atmosphere, starting from a temperature of 50 °C to 700 °C. The thermograms of nanosponges are shown in figure 131:

• GLU2_BDE_CARK10%_H2O_BIS;

• BUTS20_POSTISINTH_BIS.

In all thermograms are identified two main phenomena of weight loss: the first, between 50 °C and 200°C, corresponding to the volatilization of the water adsorbed on the surface of the nanosponge, while the second, between 200 °C and 450 °C on the pyrolysis phenomenon of polymers, from which onset temperatures are derived, as shown in following table. In addition, because of the second step of weight loss, a stable carbon residue is obtained above 700 °C, corresponding to 18.1% for the nanosponge based on sodium alginate, 11.9% for that with carrageenan-K and 15% for that with 1,4-butylsulton, relative to the polymer's initial weight.

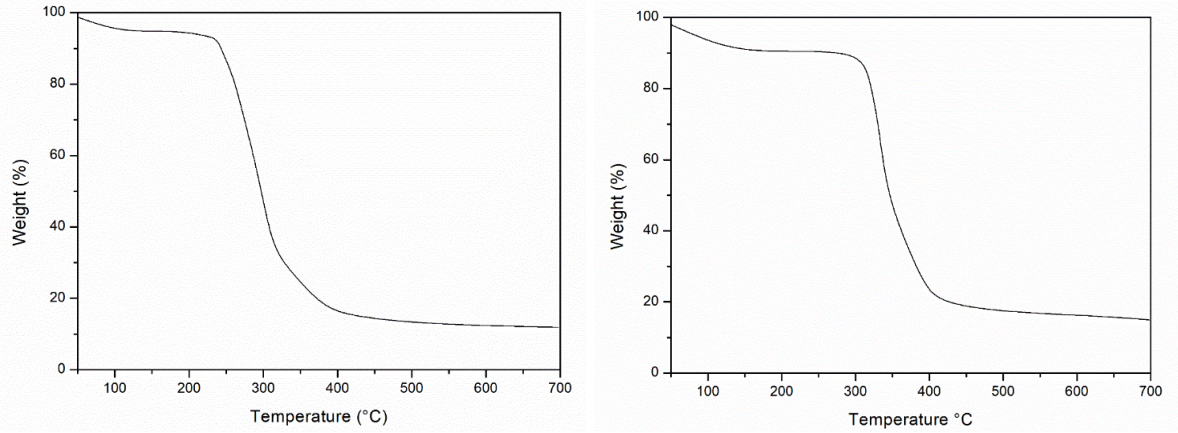

Figure 131: Thermograms of GLU2_BDE_CARK10%_H2O in N2 BUTS20_POSTISINTH in N_2.

T_{onset}, get by the curve were compared to GLU2_BDE.

Table 127: Onset temperatures of cationic nanosponges

Nanosponge	T_{onset} (°C)	Gas
GLU2_BDE	279	N_2
GLU2_BDE_CARK10%_H_2O_BIS	252	N_2
BUTS20%_POSTISINTESI_BIS	316	N_2

As for the carrageenan-K nanosponge, the presence of these two functionalizing agents tends to decrease the thermal stability of the polymer. In contrast, the presence of 1,4-butylsultone tends to increase the thermal stability of the nanosponge. In addition, for BUTS20%_POSTISINTH_BIS nanosponge, a thermogravimetric analysis in air was also performed to simulate its eventual disposal through the incineration process, since there are no certainties regarding its safety both for the environment and for man, due to 1,4-butylsulton.

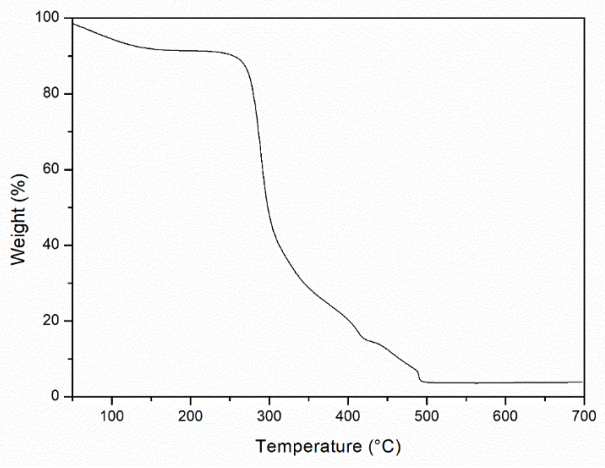

Figure 132: Thermogram of BUTS20_POSTISINTH in air.

The thermogram profile is similar when compared to nitrogen one (Figure 132). However, in the reactive atmosphere the pyrolysis phenomenon is anticipated, in fact there is a lower onset temperature (275 °C). It is interesting to note that the carbon residue, obtained because of the pyrolysis phenomenon of the polymer, is much smaller (3.8% compared to the initial weight), and is stable over 500 °C.

12.1.3 Elemental analysis

For sulphonic nanosponges, the elemental analysis was carried out to assess the percentage of Sulphur as shown in Table 129.

Table 128: Elemental analysis.

Nanosponge	% S
GLU2_BDE_CARK10%_H_20	0,1
BUTS20%_POSTSINTH	1,07

Obviously, by increasing the amount of sulfonic agent from 500 mg to 700 mg, there is an increase in the percentage of sulfur.

13 APPENDIX II

13.1 Calibration curve

13.1.1 Zeolite

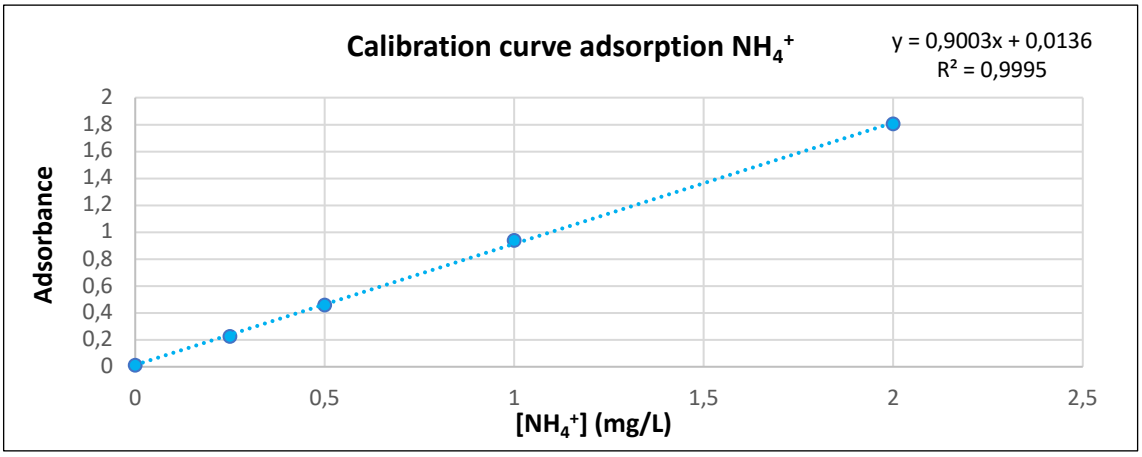

Figure 134: Calibration curve adsorption NH4+.

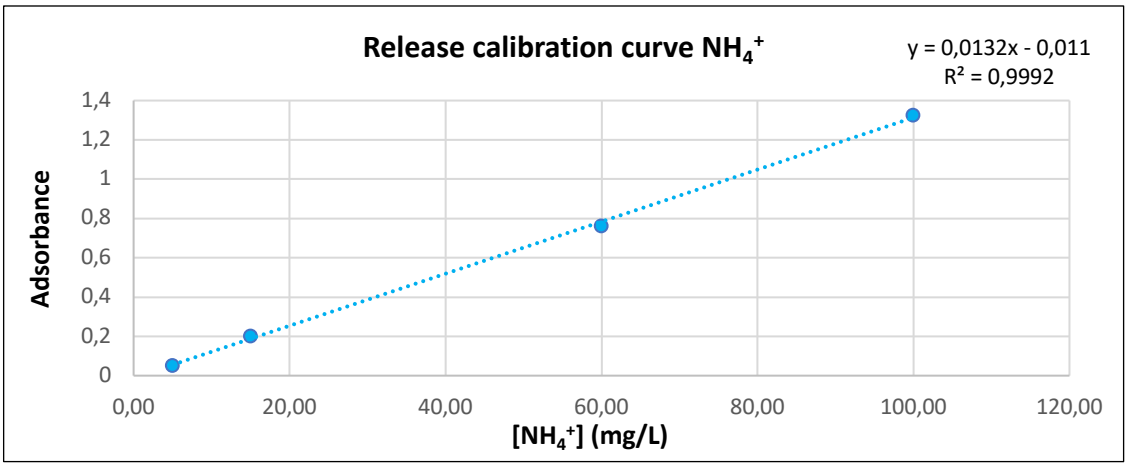

Figure 133: Release calibration curve NH4+

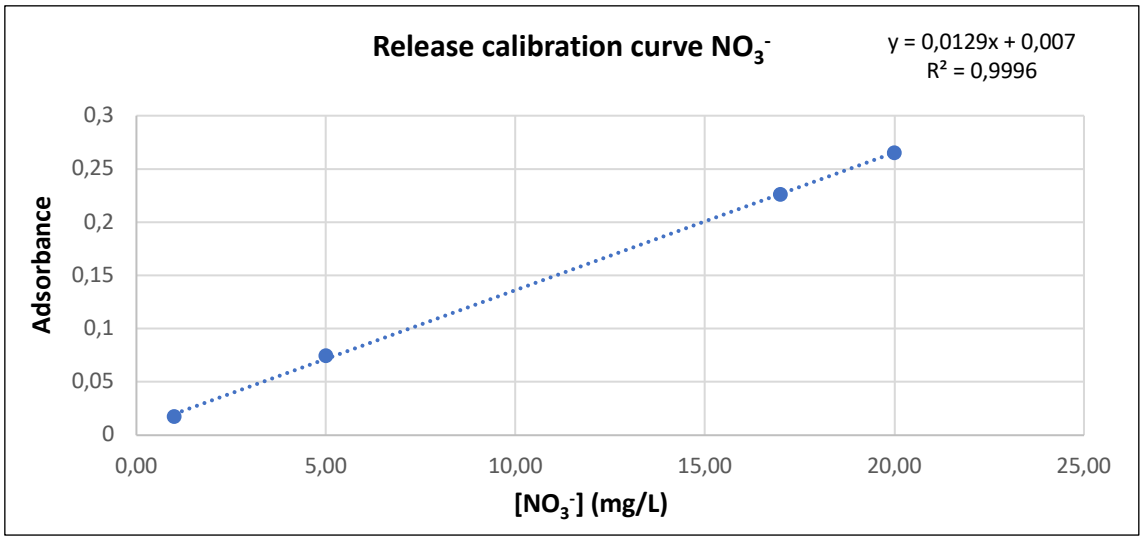

Figure 137: Release calibration curve NO3-

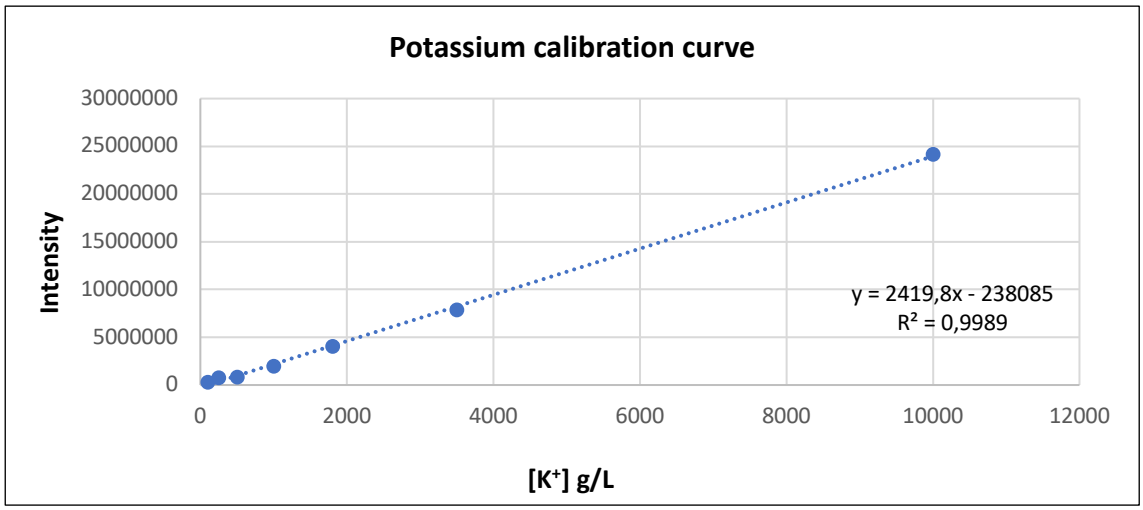

Figure 136: Potassium calibration curve

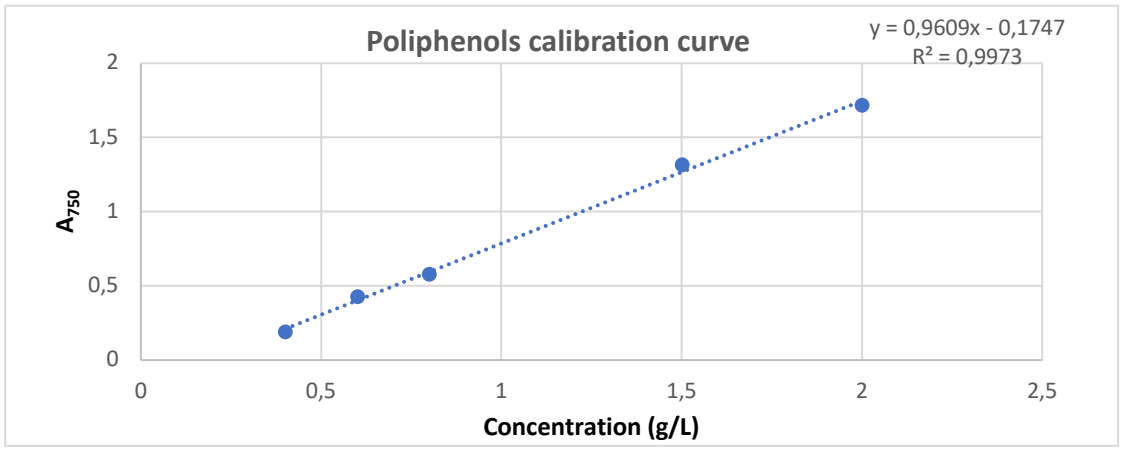

Figure 135: Polyphenols calibration curve

Concentration (g/L) gallic acid					
2	1,5	1	0,8	0,6	0,4

13.2 Nanosponges

- Nitrates

Table 129: Nitrates standard concentrations.

Standard	Concentration (mg/L)	Area
Nitrates	1	0,08
	2,5	0,244
	5	0,501
	7,5	0,769
	10	1,049
	25	2,796

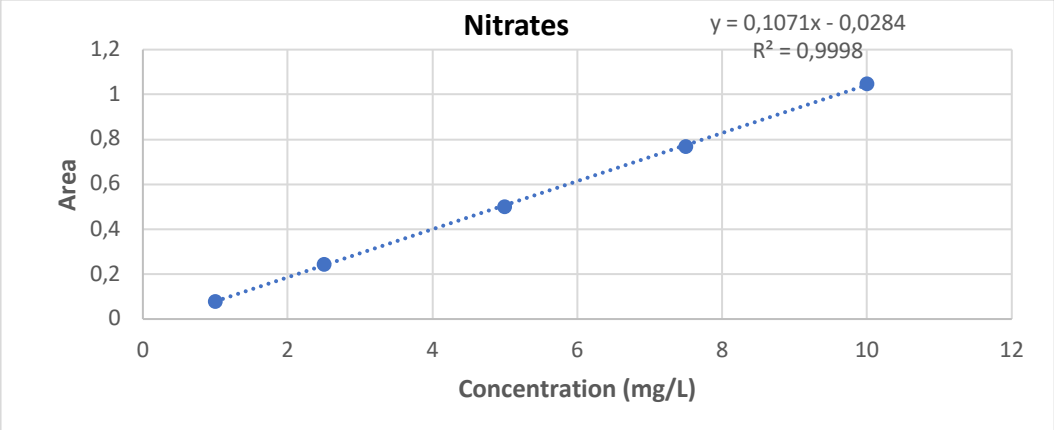

Figure 138: Nitrates calibration curve.

- Phosphates

The analysis of total phosphorus by ICP-OES was carried out by constructing the following calibration lines by selecting the analytical lines of phosphorus at 213,617 and 214,914 nm. The average of the results obtained with the two lines gave the figure reported in the discussion of the results. The following table shows the straight-line data for the analytical row of phosphorus at 213,617 nm:

Table 130: P 213,617 nm standard concentrations

Concentration P (mg/L)	Intensity
0,16	5,69E+03
0,33	1,15E+04
0,65	2,35E+04
1,63	5,92E+04
3,26	1,18E+05

8,15	3,00E+05
16,30	5,98E+05
32,61	1,18E+06
65,22	2,44E+06
130,44	4,89E+06

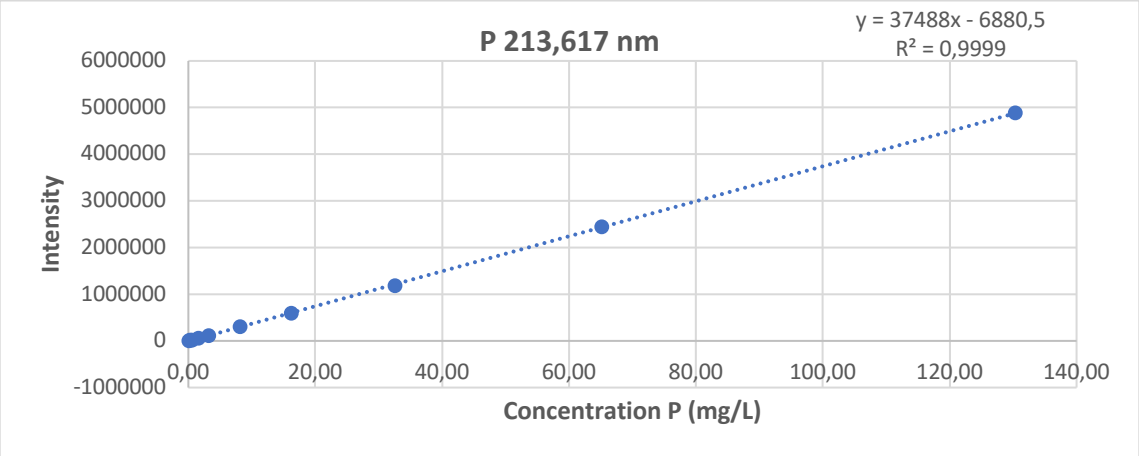

Figure 139: P 213,617 nm calibration curve.

P 214,914 nm:

Table 131: P 214,914 nm standard calibrations.

Concentration P (mg/L)	**Intensity**
0,16	1,63E+03
0,33	3,19E+03
0,65	6,36E+03
1,63	1,55E+04
3,26	3,09E+04
8,15	7,76E+04
16,30	1,56E+05
32,61	3,06E+05
65,22	6,36E+05
130,44	1,24E+06

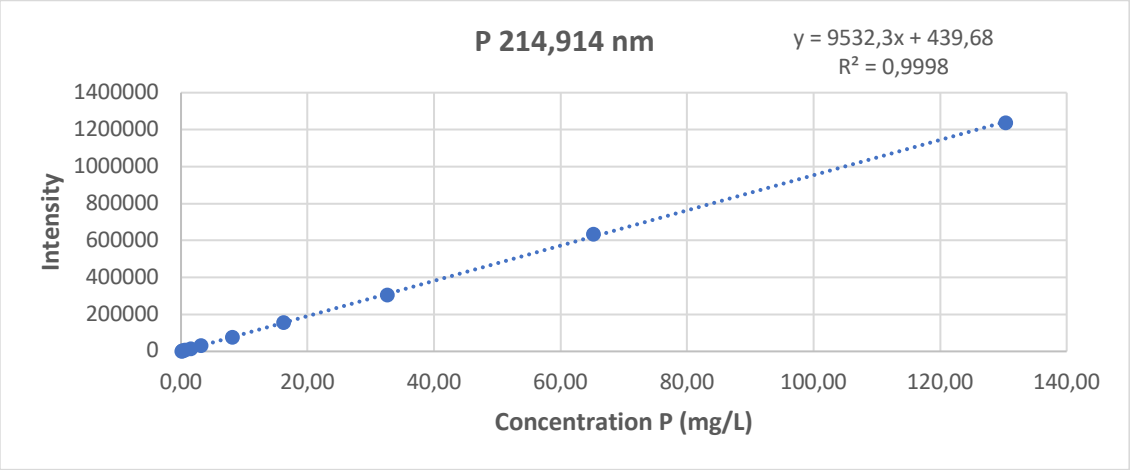

Figure 140: P 214,914 nm calibration curve.

- Glyphosate

P 213,617 nm:

Concentration GLY (mg/L)	**Intensity P 213,617 nm**	**Intensity 214,914 nm:**
0,1	4,89E+02	4,89E+02
0,25	1,11E+03	1,11E+03
0,5	2,30E+03	2,30E+03
1	4,70E+03	4,70E+03
2,5	1,19E+04	1,19E+04
5	2,46E+04	2,46E+04
10	5,25E+04	5,25E+04
25	1,30E+05	1,30E+05
50	2,64E+05	2,64E+05
100	5,42E+05	5,42E+05

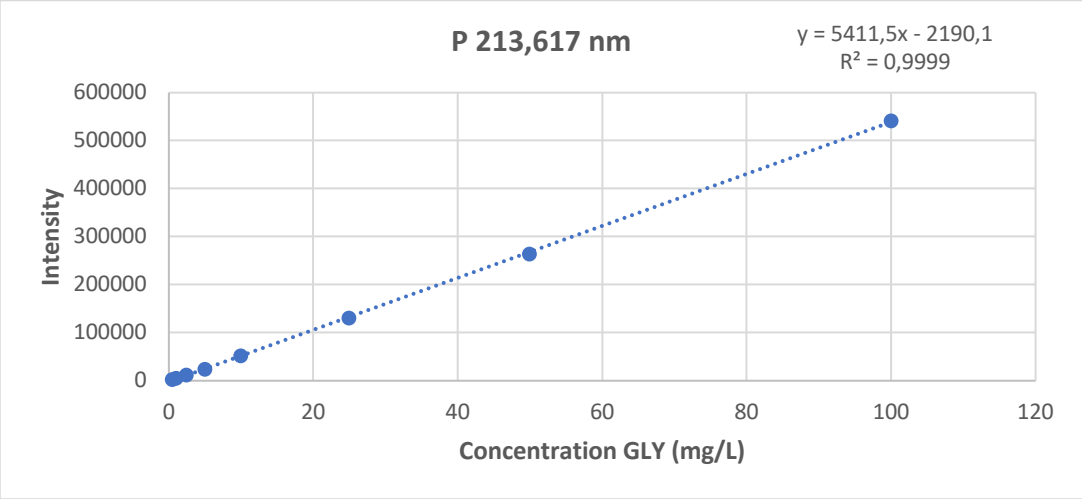

Figure 141: Glyphosate calibration curve P 213,617 nm.

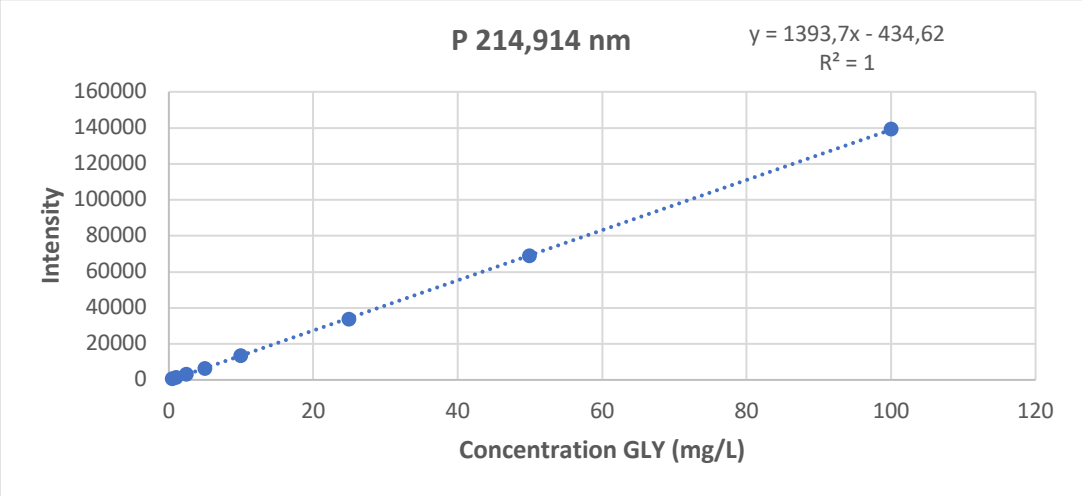

Figure 142: Glyphosate calibration curve P 214,914 nm.

For 10 and 1 mg/L tests, these standards were used:

Concentration	Intensity	Intensity
0,05	2,88E+02	6,22E+01
0,1	4,89E+02	5,72E+01
0,25	1,11E+03	2,61E+02
0,5	2,30E+03	6,17E+02
1	4,70E+03	1,21E+03
2,5	1,19E+04	3,10E+03
0,05	2,88E+02	6,22E+01
0,1	4,89E+02	5,72E+01
0,25	1,11E+03	2,61E+02
0,5	2,30E+03	6,17E+02

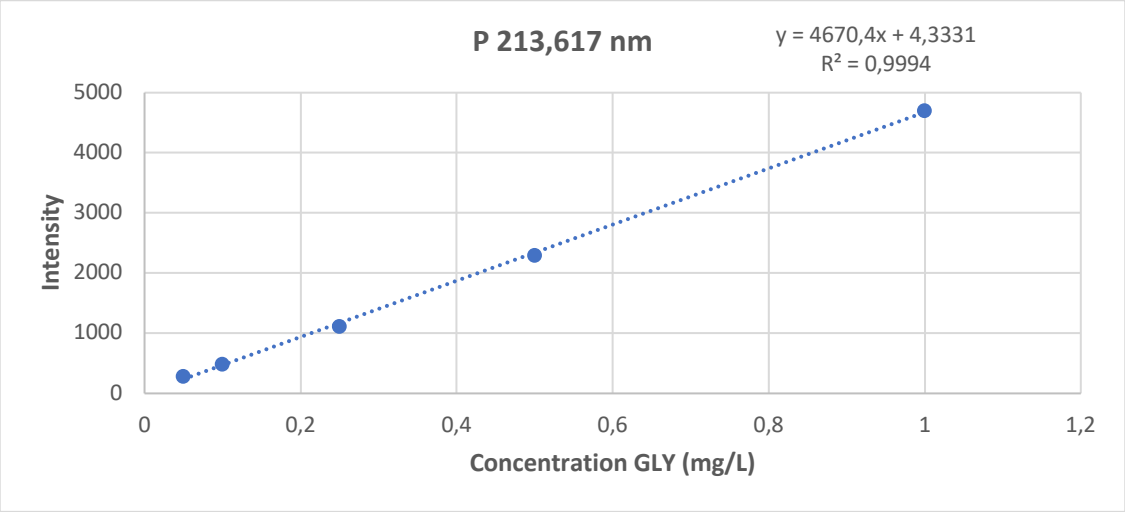

Figure 143: Second glyphosate calibration curve P 213,617 nm.

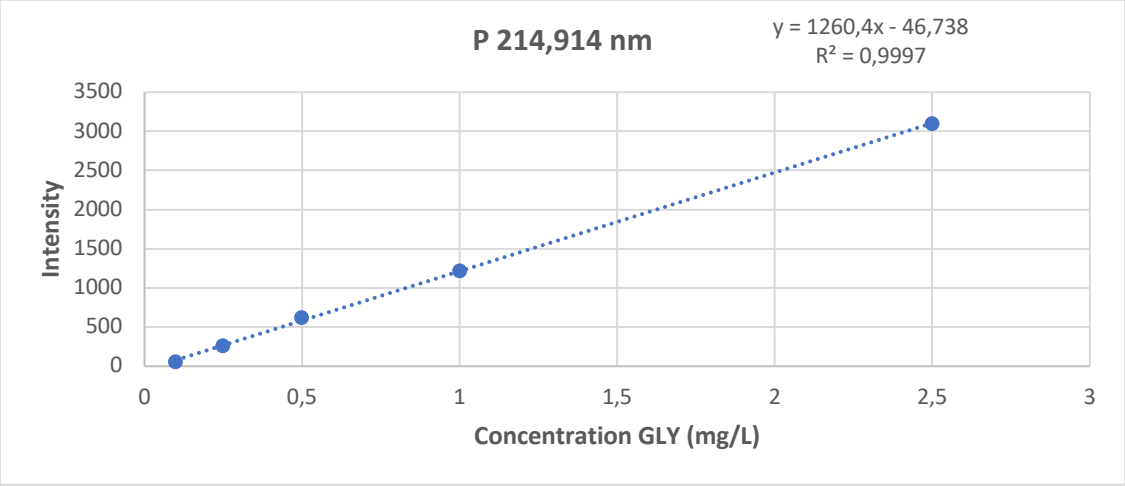

Figure 144: ond glyphosate calibration curve P 219,914 nm.

- Cr (VI)

Table 132: Cr(VI) standard concentrations.

Conc. (µg/L)	*Intensity*
2,5	1865,5
5	3731
10	7462
20	15126
50	37433
100	70486
250	178389
500	354184
1000	710468

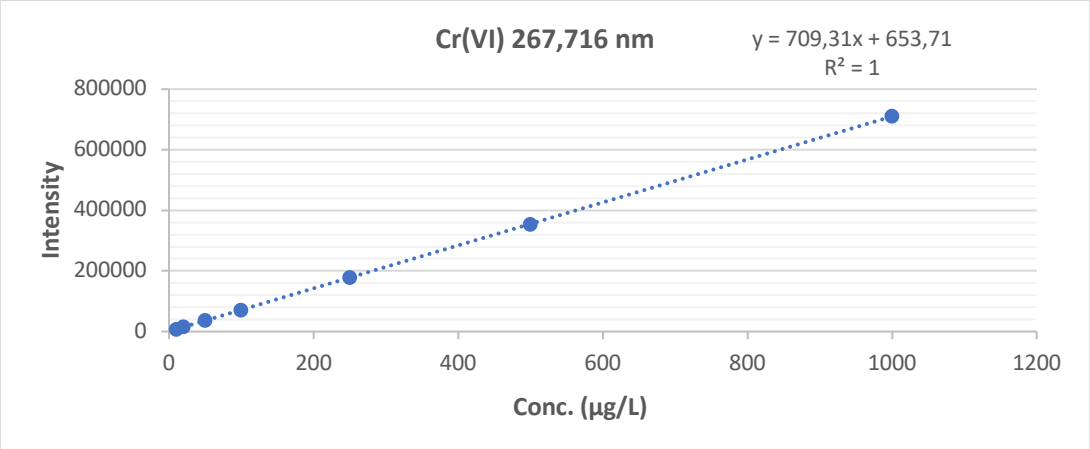

Figure 145: Cr(VI) calibration curve.

Arsenic: 193,393 nm

Table 133: Arsenic 193,696 nm standard concentrations.

Conc. (mg/L)	*Intensity*
10	*432916*
5	*211329*
2	*86040*
1	*45647*
0,5	*34805*
0,25	*28519*
0,1	*9298*
0,05	*4785*
0,025	*2304*

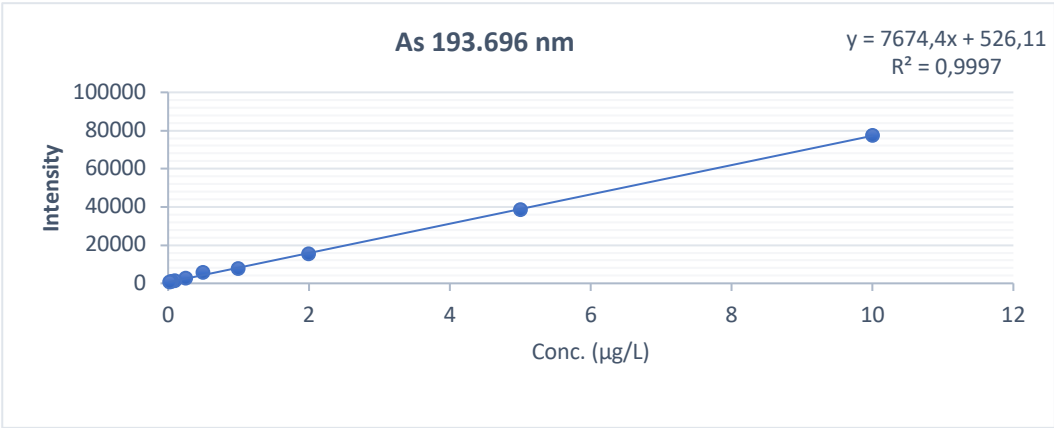

Figure 146: As 193.696 nm calibration curve.

Arsenic: 228,812 nm

Table 134: As 228,819 nm standard concentrations.

Conc. (mg/L)	*Intensity*
10	*432916*
5	*211329*
2	*86040*
1	*45647*
0,5	*34805*
0,25	*28519*
0,1	*9298*
0,05	*4785*
0,025	*2304*

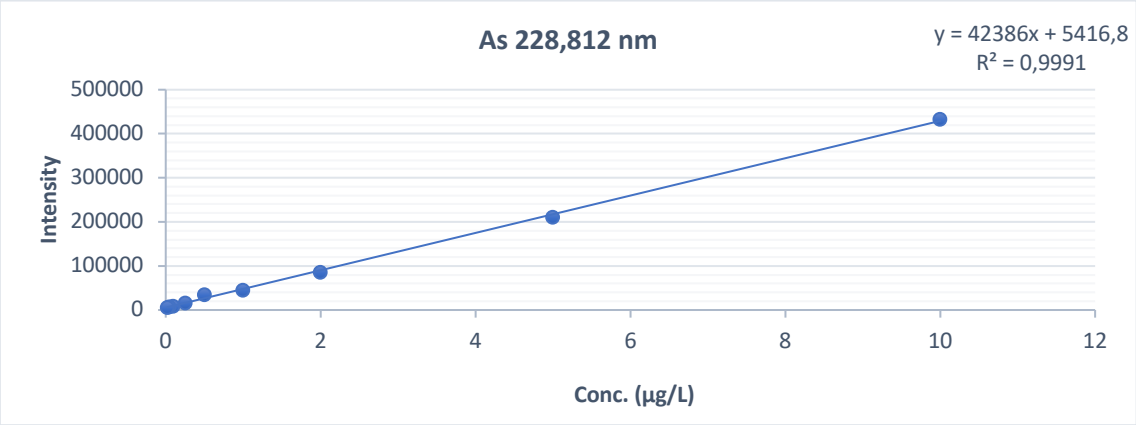

Figure 147: As 228,819 nm calibration curve.

Arsenic: 188,979 nm

Table 135: As 188,979 nm standard calibration.

Conc. (mg/L)	*Intensity*
10	*77462*
5	*38630*
2	*15504*
1	*7793*
0,5	*5547*
0,25	*2440*
0,1	*1159*
0,05	*866*
0,025	*534*

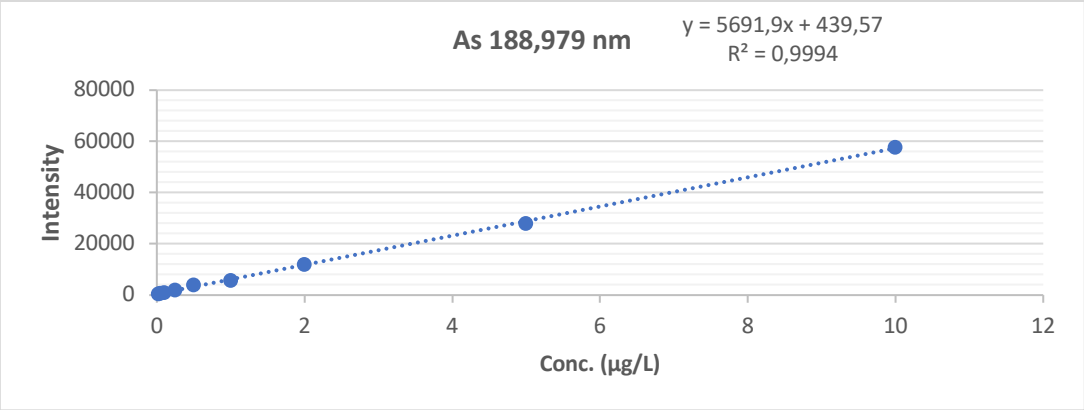

Figure 148: As 188,979 calibration curve.

Arsenic: 197,197 nm

Table 136: As 197,197 nm standard calibration.

Conc. (mg/L)	*Intensity*
10	*57791*
5	*27972*
2	*11942*
1	*5786*
0,5	*4098*
0,25	*1914*
0,1	*983*
0,05	*768*
0,025	*420*

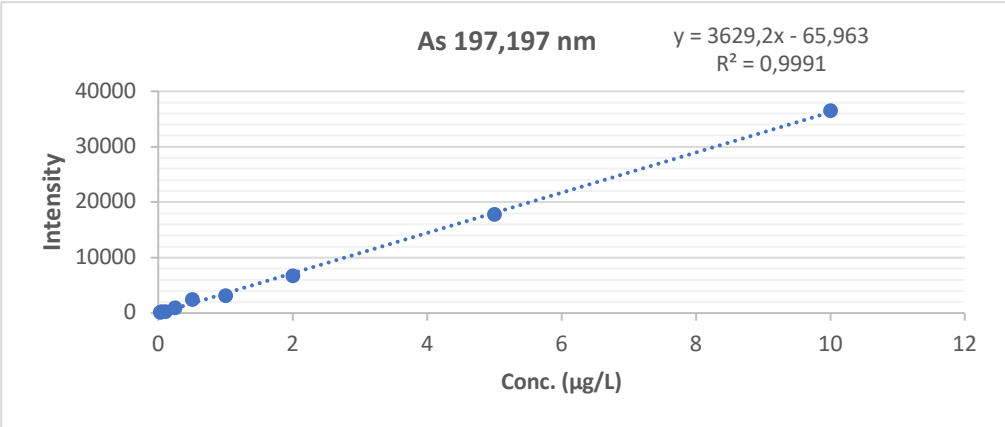

Figure 149: As 197,197 nm calibration curve.

14 BIBLIOGRAPHY

[1] S. R. Carpenter, N. F. Caraco, D. L. Correll, R. W. Howarth, A. N. Sharpley, and V. H. Smith, "Nonpoint pollution of surface waters with phosphorus and nitrogen," *Ecological Applications*, vol. 8, no. 3, pp. 559–568, 1998.

[2] I. P.U., C. C.C., I. F.C., F. I.F., and O. C.A., "A Review of Environmental Effects of Surface Water Pollution," *International Journal of Advanced Engineering Research and Science*, vol. 4, no. 12, pp. 128–137, 2017, doi: 10.22161/ijaers.4.12.21.

[3] Epa USA, "FEDERAL WATER POLLUTION CONTROL ACT," 1972.

[4] J. Manuel, "Nutrient pollution: A persistent threat to waterways," *Environmental Health Perspectives*, vol. 122, no. 11, pp. A305–A309, Nov. 2014, doi: 10.1289/ehp.122-A304.

[5] E. Páll, M. Niculae, T. Kiss, C. D. Şandru, and M. Spînu, "Human impact on the microbiological water quality of the rivers," *Journal of Medical Microbiology*, vol. 62, no. PART 11. pp. 1635–1640, Nov. 2013. doi: 10.1099/jmm.0.055749-0.

[6] S. C. Chapra, L. A. Camacho, and G. B. McBride, "Impact of global warming on dissolved oxygen and bod assimilative capacity of the world's rivers: Modeling analysis," *Water (Switzerland)*, vol. 13, no. 17, Sep. 2021, doi: 10.3390/w13172408.

[7] J. Vidmar, T. Zuliani, P. Novak, A. Drinčić, J. Ščančar, and R. Milačič, "Elements in water, suspended particulate matter and sediments of the Sava River," *Journal of Soils and Sediments*, vol. 17, no. 7, pp. 1917–1927, Jul. 2017, doi: 10.1007/s11368-016-1512-4.

[8] Y. Zhao, C. Feng, Q. Wang, Y. Yang, Z. Zhang, and N. Sugiura, "Nitrate removal from groundwater by cooperating heterotrophic with autotrophic denitrification in a biofilm-electrode reactor," *Journal of Hazardous Materials*, vol. 192, no. 3, pp. 1033–1039, 2011, doi: 10.1016/j.jhazmat.2011.06.008.

[9] P. Hammond, M. Suttie, V. T. Lewis, A. P. Smith, and A. C. Singer, "Detection of untreated sewage discharges to watercourses using machine learning," *npj Clean Water*, vol. 4, no. 1, Dec. 2021, doi: 10.1038/s41545-021-00108-3.

[10] J. E. Cloern, "Our evolving conceptual model of the coastal eutrophication problem," *Marine Ecology Progress Series*, vol. 210, pp. 223–253, 2001, doi: 10.3354/meps210223.

[11] D. L. Correll, "The role of phosphorus in the eutrophication of receiving waters: A review," *Journal of Environmental Quality*, vol. 27, no. 2, pp. 261–266, 1998, doi: 10.2134/jeq1998.00472425002700020004x.

[12] V. H. Smith, "Eutrophication of freshwater and coastal marine ecosystems: A global problem," *Environmental Science and Pollution Research*, vol. 10, no. 2, pp. 126–139, 2003, doi: 10.1065/espr2002.12.142.

[13] B. C. (Bryson C.) Bates, Z. Kundzewicz, S. Wu, J. Palutikof, and Intergovernmental Panel on Climate Change. Working Group II, *Climate change and water*.

[14] N. W. Arnell, S. J. Halliday, R. W. Battarbee, R. A. Skeffington, and A. J. Wade, "The implications of climate change for the water environment in England," *Progress in Physical Geography*, vol. 39, no. 1, pp. 93–120, Feb. 2015, doi: 10.1177/0309133314560369.

[15] J. A. Duran-Encalada, A. Paucar-Caceres, E. R. Bandala, and G. H. Wright, "The impact of global climate change on water quantity and quality: A system dynamics approach to the US–Mexican

transborder region," *European Journal of Operational Research*, vol. 256, no. 2, pp. 567–581, Jan. 2017, doi: 10.1016/j.ejor.2016.06.016.

[16] A. Schlutow, W. Schröder, and T. Scheuschner, "Assessing the relevance of atmospheric heavy metal deposition with regard to ecosystem integrity and human health in Germany," *Environmental Sciences Europe*, vol. 33, no. 1, Dec. 2021, doi: 10.1186/s12302-020-00391-w.

[17] J. Briffa, E. Sinagra, and R. Blundell, "Heavy metal pollution in the environment and their toxicological effects on humans," *Heliyon*, vol. 6, no. 9. Elsevier Ltd, Sep. 01, 2020. doi: 10.1016/j.heliyon.2020.e04691.

[18] T. M. Ansari, I. L. Marr, and N. Tariq, "Heavy Metals in Marine Pollution Perspective–A Mini Review," *Journal of Applied Sciences*, vol. 4, no. 1, pp. 1–20, 2003, doi: 10.3923/jas.2004.1.20.

[19] M. L. Sall, A. K. D. Diaw, D. Gningue-Sall, S. Efremova Aaron, and J. J. Aaron, "Toxic heavy metals: impact on the environment and human health, and treatment with conducting organic polymers, a review," *Environmental Science and Pollution Research*, vol. 27, no. 24, pp. 29927–29942, 2020, doi: 10.1007/s11356-020-09354-3.

[20] P. D. Millner, *Manure Management*, 1st ed. Elsevier Inc., 2009. doi: 10.1016/B978-0-12-374186-8.00004-5.

[21] A. Tallou, A. Haouas, M. Y. Jamali, K. Atif, S. Amir, and F. Aziz, *Review on Cow Manure as Renewable Energy*, vol. 17. Springer International Publishing, 2020. doi: 10.1007/978-3-030-37794-6_17.

[22] R. K. Hubbard and R. R. Lowrance, "Chapter 5 Management of Dairy Cattle Manure," in *US Department of Agriculture, Agricultural Research Service, US*, no. Coletti, 1998, pp. 91–102.

[23] E. Pattey, M. K. Trzcinski, and R. L. Desjardins, "Quantifying the reduction of greenhouse gas emissions as a result of composting dairy and beef cattle manure," *Nutrient Cycling in Agroecosystems*, vol. 72, no. 2, pp. 173–187, 2005, doi: 10.1007/s10705-005-1268-5.

[24] D. R. Külling *et al.*, "Emissions of ammonia, nitrous oxide and methane from different types of dairy manure during storage as affected by dietary protein content," *Journal of Agricultural Science*, vol. 137, no. 2, pp. 235–250, 2001, doi: 10.1017/s0021859601001186.

[25] D. Hill *et al.*, "Dairy manure as a potential source of crop nutrients and environmental contaminants," *Journal of Environmental Sciences (China)*, vol. 100, no. 3, pp. 117–130, 2021, doi: 10.1016/j.jes.2020.07.016.

[26] V. S. Varma *et al.*, "Dairy and swine manure management – Challenges and perspectives for sustainable treatment technology," *Science of the Total Environment*, vol. 778, p. 146319, 2021, doi: 10.1016/j.scitotenv.2021.146319.

[27] C. Font-palma, "Methods for the Treatment of Cattle Manure — A Review," 2019.

[28] O. Oenema, D. Oudendag, and G. L. Velthof, "Nutrient losses from manure management in the European Union," *Livestock Science*, vol. 112, no. 3, pp. 261–272, 2007, doi: 10.1016/j.livsci.2007.09.007.

[29] D. Ruiz, G. San Miguel, B. Corona, A. Gaitero, and A. Domínguez, "Environmental and economic analysis of power generation in a thermophilic biogas plant," *Science of the Total Environment*, vol. 633, pp. 1418–1428, 2018, doi: 10.1016/j.scitotenv.2018.03.169.

[30] O. A. Arikan, W. Mulbry, and S. Lansing, “Effect of temperature on methane production from field-scale anaerobic digesters treating dairy manure,” *Waste Management*, vol. 43, pp. 108–113, 2015, doi: 10.1016/j.wasman.2015.06.005.

[31] M. Abdallah, A. Shanableh, M. Adghim, C. Ghenai, and S. Saad, “Biogas production from different types of cow manure,” *2018 Advances in Science and Engineering Technology International Conferences, ASET 2018*, pp. 1–4, 2018, doi: 10.1109/ICASET.2018.8376791.

[32] S. Husted, L. S. Jensen, and S. S. Jlerrgensen, “Reducing Ammonia Loss from Cattle Slurry by the Use of Acidifying Additives : the Role of the Buffer System,” no. 1987, pp. 335–349, 1991.

[33] B. Van Der Stelt, P. C. J. Van Vliet, J. W. Reijs, E. J. M. Temminghoff, and W. H. Van Riemsdijk, “Effects of dietary protein and energy levels on cow manure excretion and ammonia volatilization,” *Journal of Dairy Science*, vol. 91, no. 12, pp. 4811–4821, 2008, doi: 10.3168/jds.2006-449.

[34] P. Sefeedpari, T. Vellinga, S. Ra, M. Shari, P. Shine, and S. H. Pishgar-komleh, “Technical , environmental and cost-bene fi t assessment of manure management chain : A case study of large scale dairy farming,” vol. 233, 2019, doi: 10.1016/j.jclepro.2019.06.146.

[35] F. Gioelli, M. P. Bernal, D. Fangueiro, H. Trindade, L. S. Jensen, and O. Oenema, “Stakeholder perceptions of manure treatment technologies in Denmark , Italy , the Netherlands and Spain,” *Journal of Cleaner Production*, vol. 172, pp. 1620–1630, 2018, doi: 10.1016/j.jclepro.2016.10.162.

[36] A. Masoni, L. Ercoli, U. Pisa, S. Superiore, and S. Anna, “Azoto nel terreno,” no. 3, pp. 211–241.

[37] A. N. Hristov *et al.*, “Review: Ammonia emissions from dairy farms and beef feedlots,” *Canadian Journal of Animal Science*, vol. 91, no. 1, pp. 1–35, 2011, doi: 10.4141/CJAS10034.

[38] O. Martins, “Loss of Nitrogenous Compounds during Composting of Animal Wastes,” vol. 42, pp. 103–111, 1992.

[39] N. Zhang *et al.*, “Reducing Ammonia Emissions from Dairy Cattle Production via Cost-E ff ective Manure Management Techniques in China,” 2019, doi: 10.1021/acs.est.9b04284.

[40] G. M. Shah, G. A. Shah, J. C. J. Groot, O. Oenema, and E. A. Lantinga, “Agriculture , Ecosystems and Environment Irrigation and lava meal use reduce ammonia emission and improve N utilization when solid cattle manure is applied to grassland,” *“Agriculture, Ecosystems and Environment,”* vol. 160, pp. 59–65, 2012, doi: 10.1016/j.agee.2011.07.017.

[41] B. Amon, V. Kryvoruchko, T. Amon, and S. Zechmeister-boltenstern, “Methane , nitrous oxide and ammonia emissions during storage and after application of dairy cattle slurry and influence of slurry treatment,” vol. 112, no. 2006, pp. 153–162, 2012, doi: 10.1016/j.agee.2005.08.030.

[42] Y. Hou *et al.*, “Agriculture , Ecosystems and Environment Feed use and nitrogen excretion of livestock in EU-27,” *“Agriculture, Ecosystems and Environment,”* vol. 218, pp. 232–244, 2016, doi: 10.1016/j.agee.2015.11.025.

[43] S. M. McGinn, T. Coates, T. K. Flesch, and B. Crenna, “Ammonia emission from dairy cow manure stored in a lagoon over summer,” *Canadian Journal of Soil Science*, vol. 88, no. 4, pp. 611–615, 2008, doi: 10.4141/CJSS08002.

[44] J. Webb *et al.*, *An Assessment of the Variation of Manure Nitrogen Efficiency throughout Europe and an Appraisal of Means to Increase Manure-N Efficiency*, vol. 119. Elsevier, 2013. doi: 10.1016/B978-0-12-407247-3.00007-X.

[45] F. Hassanat *et al.*, “Replacing alfalfa silage with corn silage in dairy cow diets: Effects on enteric methane production, ruminal fermentation, digestion, N balance, and milk production,” *Journal of Dairy Science*, vol. 96, no. 7, pp. 4553–4567, 2013, doi: 10.3168/jds.2012-6480.

[46] Y. Ye *et al.*, “A critical review on ammonium recovery from wastewater for sustainable wastewater management,” *Bioresource Technology*, vol. 268, no. June, pp. 749–758, 2018, doi: 10.1016/j.biortech.2018.07.111.

[47] A. Beckinghausen, M. Odlare, E. Thorin, and S. Schwede, “From removal to recovery: An evaluation of nitrogen recovery techniques from wastewater,” *Applied Energy*, vol. 263, no. February, p. 114616, 2020, doi: 10.1016/j.apenergy.2020.114616.

[48] J. P. van der Hoek, R. Duijff, and O. Reinstra, “Nitrogen recovery from wastewater: Possibilities, competition with other resources, and adaptation pathways,” *Sustainability (Switzerland)*, vol. 10, no. 12, 2018, doi: 10.3390/su10124605.

[49] A. Iddya *et al.*, “Efficient ammonia recovery from wastewater using electrically conducting gas stripping membranes,” *Environmental Science: Nano*, vol. 7, no. 6, pp. 1759–1771, 2020, doi: 10.1039/c9en01303b.

[50] C. Wu, H. Yan, Z. Li, and X. Lu, “Ammonia recovery from high concentration wastewater of soda ash industry with membrane distillation process,” *Desalination and Water Treatment*, vol. 57, no. 15, pp. 6792–6800, 2016, doi: 10.1080/19443994.2015.1010233.

[51] S. Xiang *et al.*, “New progress of ammonia recovery during ammonia nitrogen removal from various wastewaters,” *World Journal of Microbiology and Biotechnology*, vol. 36, no. 10, pp. 1–20, 2020, doi: 10.1007/s11274-020-02921-3.

[52] N. Nasir *et al.*, “Removal of ammonia nitrogen from rubber industry wastewater using zeolite as adsorbent,” *Malaysian Journal of Fundamental and Applied Sciences*, vol. 15, no. 6, pp. 862–866, 2019.

[53] W. Zhang, R. Fu, L. Wang, J. Zhu, J. Feng, and W. Yan, “Rapid removal of ammonia nitrogen in low-concentration from wastewater by amorphous sodium titanate nano-particles,” *Science of the Total Environment*, vol. 668, pp. 815–824, 2019, doi: 10.1016/j.scitotenv.2019.03.051.

[54] M. Altinbas, I. Ozturk, and A. F. Aydin, “Ammonia recovery from high strength agro industry effluents,” *Water Science and Technology*, vol. 45, no. 12, pp. 189–196, 2002, doi: 10.2166/wst.2002.0426.

[55] Y. Ahn, “Sustainable nitrogen elimination biotechnologies : A review,” vol. 41, pp. 1709–1721, 2006, doi: 10.1016/j.procbio.2006.03.033.

[56] Z. Hu, T. Lotti, M. van Loosdrecht, and B. Kartal, “Nitrogen removal with the anaerobic ammonium oxidation process,” *Biotechnology Letters*, vol. 35, no. 8, pp. 1145–1154, 2013, doi: 10.1007/s10529-013-1196-4.

[57] T. Lotti *et al.*, “RIMOZIONE COMPLETAMENTE AUTOTROFA DELL ’ AZOTO CON,” vol. 1, 2014.

[58] E. Marañón, A. M. Salter, L. Castrillón, S. Heaven, and Y. Fernández-nava, “Reducing the environmental impact of methane emissions from dairy farms by anaerobic digestion of cattle waste,” vol. 31, pp. 1745–1751, 2011, doi: 10.1016/j.wasman.2011.03.015.

[59] J. B. Holm-nielsen, T. Al Seadi, and P. Oleskowicz-popiel, “Bioresource Technology The future of anaerobic digestion and biogas utilization,” *Bioresource Technology*, vol. 100, no. 22, pp. 5478–5484, 2009, doi: 10.1016/j.biortech.2008.12.046.

[60] J. Bacenetti, M. Negri, M. Fiala, and S. González-garcía, “Science of the Total Environment Anaerobic digestion of different feedstocks : Impact on energetic and environmental balances of biogas process,” *Science of the Total Environment, The*, vol. 463–464, pp. 541–551, 2013, doi: 10.1016/j.scitotenv.2013.06.058.

[61] C. Rico, H. García, and J. L. Rico, “Physical-anaerobic-chemical process for treatment of dairy cattle manure,” *Bioresource Technology*, vol. 102, no. 3, pp. 2143–2150, 2011, doi: 10.1016/j.biortech.2010.10.068.

[62] Y. Li, J. Zhao, J. Krooneman, G. Jan, and W. Euverink, “Science of the Total Environment Strategies to boost anaerobic digestion performance of cow manure : Laboratory achievements and their full-scale application potential,” vol. 755, 2021, doi: 10.1016/j.scitotenv.2020.142940.

[63] B. Shehu, U. Ibn, and N. Ismail, “ANAEROBIC DIGESTION OF COW DUNG FOR,” vol. 7, no. 2, pp. 169–172, 2012.

[64] P. Taylor, A. Lehtomäki, and L. Björnsson, “Two-Stage Anaerobic Digestion of Energy Crops : Methane Production , Nitrogen Mineralisation and Heavy Metal Mobilisation CROPS : METHANE PRODUCTION , NITROGEN,” no. October 2014, pp. 37–41, 2010, doi: 10.1080/09593332708618635.

[65] F. Battini, A. Agostini, A. K. Boulamanti, J. Giuntoli, and S. Amaducci, “Science of the Total Environment Mitigating the environmental impacts of milk production via anaerobic digestion of manure : Case study of a dairy farm in the Po Valley,” *Science of the Total Environment, The*, vol. 481, pp. 196–208, 2014, doi: 10.1016/j.scitotenv.2014.02.038.

[66] A. Normak, J. Suurpere, K. Orupõld, E. Jõgi, and E. Kokin, “Simulation of anaerobic digestion of cattle manure,” no. 1, pp. 167–174, 2012.

[67] J. C. H. Shih, “Chapter 14 Development of Anaerobic Digestion of Animal Waste : From Laboratory , Research and Commercial Farms to a Value-Added New Product,” no. Tietjen, pp. 339–352, 1975.

[68] I. M. Nasir, T. I. Mohd. Ghazi, R. Omar, and A. Idris, “Bioreactor performance in the anaerobic digestion of cattle manure: A review,” *Energy Sources, Part A: Recovery, Utilization and Environmental Effects*, vol. 36, no. 13, pp. 1476–1483, 2014, doi: 10.1080/15567036.2010.542439.

[69] H. B. Nielsen, Z. Mladenovska, P. Westermann, and B. K. Ahring, “Comparison of Two-Stage Thermophilic (68 ° C / 55 ° C) Anaerobic Digestion With One-Stage Thermophilic (55 ° C) Digestion of Cattle Manure,” 2004, doi: 10.1002/bit.20037.

[70] I. M. Nasir, T. I. Mohd Ghazi, and R. Omar, “Anaerobic digestion technology in livestock manure treatment for biogas production: A review,” *Engineering in Life Sciences*, vol. 12, no. 3, pp. 258–269, 2012, doi: 10.1002/elsc.201100150.

[71] T. Abbasi, S. M. Tauseef, and S. A. Abbasi, “Anaerobic digestion for global warming control and energy generation — An overview,” *Renewable and Sustainable Energy Reviews*, vol. 16, no. 5, pp. 3228–3242, 2012, doi: 10.1016/j.rser.2012.02.046.

[72] Y. Li, L. Li, and J. Yu, “Applications of Zeolites in Sustainable Chemistry,” *Chem*, vol. 3, no. 6, pp. 928–949, 2017, doi: 10.1016/j.chempr.2017.10.009.

[73] K. Ramesh and D. D. Reddy, “Zeolites and Their Potential Uses in Agriculture,” *Advances in Agronomy*, vol. 113, pp. 219–241, 2011, doi: 10.1016/B978-0-12-386473-4.00004-X.

[74] A. Hedstrom, “ION EXCHANGE OF AMMONIUM IN ZEOLITES: A LITERATURE REVIEW,” *Project Management Journal*, vol. 2, no. 2, pp. 29–50, 2012.

[75] S. Wang and Y. Peng, “Natural zeolites as effective adsorbents in water and wastewater treatment,” *Chemical Engineering Journal*. 2010. doi: 10.1016/j.cej.2009.10.029.

[76] V. K. Jha and S. Hayashi, “Modification on natural clinoptilolite zeolite for its NH4+ retention capacity,” *Journal of Hazardous Materials*, vol. 169, no. 1–3, pp. 29–35, 2009, doi: 10.1016/j.jhazmat.2009.03.052.

[77] M. Kithome, J. W. Paul, L. M. Lavkulich, and A. A. Bomke, “Effect of pH on ammonium adsorption by natural zeolite clinoptilolite,” *Communications in Soil Science and Plant Analysis*, vol. 30, no. 9–10, pp. 1417–1430, 1999, doi: 10.1080/00103629909370296.

[78] S. Montalvo, C. Huiliñir, R. Borja, E. Sánchez, and C. Herrmann, “Application of zeolites for biological treatment processes of solid wastes and wastewaters – A review,” *Bioresource Technology*, vol. 301, no. January, p. 122808, 2020, doi: 10.1016/j.biortech.2020.122808.

[79] R. J. Mc Veigh and L. R. Weatherley, “Effect of other cations in wastewaters on the ion-exchange removal of ammonium ion,” *Developments in Chemical Engineering and Mineral Processing*, vol. 7, no. 1–2, pp. 69–84, 1999, doi: 10.1002/apj.5500070108.

[80] M. Pansini, “Natural zeolites as cation exchangers for environmental protection,” *Mineralium Deposita*, vol. 31, no. 6, pp. 563–575, 1996, doi: 10.1007/BF00196137.

[81] G. Costamagna *et al.*, “Characterization and use of absorbent materials as slow-release fertilizers for growing strawberry: Preliminary results,” *Sustainability (Switzerland)*, vol. 12, no. 17, 2020, doi: 10.3390/SU12176854.

[82] S. J. Leghari, G. M. Laghari, A. H. Laghari, and T. Ahmed, “Role of Nitrogen for Plant Growth and Development : A review ces inEnvironmental Biology Role of Nitrogen for Plant Growth rowth and Development : A Review,” no. November, 2016.

[83] E. Castro, P. Mañas, and J. de Las Heras, “Effects of Wastewater Irrigation in Soil Properties and Horticultural Crop (Lactuca Sativa L.),” *Journal of Plant Nutrition*, vol. 36, no. 11, pp. 1659–1677, 2013, doi: 10.1080/01904167.2013.805221.

[84] J. E. Cloern, “Our evolving conceptual model of the coastal eutrophication problem,” *Marine Ecology Progress Series*, vol. 210, pp. 223–253, 2001, doi: 10.3354/meps210223.

[85] N. A. Jaworski, R. W. Howarth, and L. J. Hetling, “Atmospheric deposition of nitrogen oxides onto the landscape contributes to coastal eutrophication in the Northeast United States,” *Environmental Science and Technology*, vol. 31, no. 7, pp. 1995–2004, 1997, doi: 10.1021/es960803f.

[86] D. J. Conley, “Biogeochemical nutrient cycles and nutrient management strategies,” *Hydrobiologia*, vol. 410, pp. 87–96, 1999, doi: 10.1023/A:1003784504005.

[87] S. R. Carpenter, N. F. Caraco, D. L. Correll, R. W. Howarth, A. N. Sharpley, and V. H. Smith, “Nonpoint pollution of surface waters with phosphorus and nitrogen,” *Ecological Applications*, vol. 8, no. 3, pp. 559–568, 1998.

[88] J. H. Gakstatter, A. F. Bartsch, and C. A. Callahan, “The impact of broadly applied effluent phosphorus standards on eutrophication control,” *Water Resources Research*, vol. 14, no. 6, pp. 1155–1158, 1978, doi: 10.1029/WR014i006p01155.

[89] A. Masoni and L. Ercoli, *Azoto nel terreno*, no. 3. 2010.

[90] H. H. Comly, “Cyanosis in Infants Caused by Nitrates in Well Water,” *JAMA: The Journal of the American Medical Association*, vol. 257, no. 20, pp. 2788–2792, 1987, doi: 10.1001/jama.1987.03390200128027.

[91] M. J. Hill, “Nitrate toxicity: Myth or reality?,” *British Journal of Nutrition*, vol. 81, no. 5, pp. 343–344, 1999.

[92] Repubblica Italiana, “Decreto Legislativo 2 febbraio 2001, n. 31: Attuazione della direttiva 98/83/CE relativa alla qualità delle acque destinate al consumo umano,” *Gazzetta Ufficiale*, no. 52, pp. 1–21, 2001.

[93] APAT (Italian Agency for Environmental Protection and Technical Services), *L ’ inquinamento da nitrati di origine agricola nelle acque interne in Italia*. 2005.

[94] Archna, S. K. Sharma, and R. C. Sobti, “Nitrate removal from ground water: A review,” *E-Journal of Chemistry*, vol. 9, no. 4, pp. 1667–1675, 2012, doi: 10.1155/2012/154616.

[95] Mohsenipour et al, “Removal Techniques of Nitrate from Water,” *Asian journal of chemistry*, vol. 30, no. 18, pp. 2424–2430, 2018.

[96] B. I. Dvorak and S. O. Skipton, “Drinking Water Treatment : Reverse Osmosis,” *University of Nebraska-Lincoln, Institute of Agriculture and Natural Resources*, no. Mcl, 2008.

[97] W. P. Michalski and D. J. D. Nicholas, “The adaptation of Rhodopseudomonas sphaeroides f. sp. denitrificans for growth under denitrifying conditions,” *Journal of General Microbiology*, vol. 130, no. 1, pp. 155–165, 1984.

[98] Y. Zhao, C. Feng, Q. Wang, Y. Yang, Z. Zhang, and N. Sugiura, “Nitrate removal from groundwater by cooperating heterotrophic with autotrophic denitrification in a biofilm-electrode reactor,” *Journal of Hazardous Materials*, vol. 192, no. 3, pp. 1033–1039, 2011, doi: 10.1016/j.jhazmat.2011.06.008.

[99] H. Gross and K. Truetler, “Biological denitrification process with hydrogen-oxidizing bacteria for drinking water treatment.,” *Aqua London*, no. 5, pp. 288–290, 1986.

[100] J. J. Schoeman, “Nitrate-nitrogen removal with small-scale reverse osmosis, electrodialysis and ion-exchange units in rural areas,” *Water SA*, vol. 35, no. 5, pp. 721–728, 2009, doi: 10.4314/wsa.v35i5.49198.

[101] C. Gorman, C. Seidel, V. Jensen, and J. Darby, “An assessment of the state of nitrate treatment alternatives,” in *American Water Works Association Annual Conference and Exposition 2011, ACE 2011*, 2011, pp. 5514–5528.

[102] Y.-H. Kim, E.-D. Hwang, W. S. Shin, J.-H. Choi, T. W. Ha, and S. J. Choi, “Treatments of stainless steel wastewater containing a high concentration of nitrate using reverse osmosis and nanomembranes,” *Desalination*, vol. 202, no. 1–3, pp. 286–292, 2007, doi: 10.1016/j.desal.2005.12.066.

[103] R. Rautenbach, W. Kopp, G. van Opbergen, and R. Hellekes, “Nitrate reduction of well water by reverse osmosis and electrodialysis - studies on plant performance and costs,” *Desalination*, vol. 65, no. C, pp. 241–258, 1987, doi: 10.1016/0011-9164(87)90137-8.

[104] H. M. Azam *et al.*, “Phosphorous in the environment: characteristics with distribution and effects, removal mechanisms, treatment technologies, and factors affecting recovery as minerals in natural and engineered systems,” *Environmental Science and Pollution Research*, vol. 26, no. 20, pp. 20183–20207, 2019, doi: 10.1007/s11356-019-04732-y.

[105] D. L. Correll, “The role of phosphorus in the eutrophication of receiving waters: A review,” *Journal of Environmental Quality*, vol. 27, no. 2, pp. 261–266, 1998, doi: 10.2134/jeq1998.00472425002700020004x.

[106] R. A. Corrales and J. L. Maclean, “Impacts of harmful algae on seafarming in the Asia-Pacific areas,” *Journal of Applied Phycology*, vol. 7, no. 2, pp. 151–162, 1995, doi: 10.1007/BF00693062.

[107] V. H. Smith, “Eutrophication of freshwater and coastal marine ecosystems: A global problem,” *Environmental Science and Pollution Research*, vol. 10, no. 2, pp. 126–139, 2003, doi: 10.1065/espr2002.12.142.

[108] European Comission, “2008/56/CE Del Parlamento Europeo E Del Consiglio,” *Gazzetta ufficiale dell’Unione europea*, vol. 164, pp. 19–40, 2008.

[109] European Comission, “2000/60/CE Del Parlamento Europeo E Del Consiglio,” vol. 37, pp. 1–282, 2014.

[110] “Decreto Legislativo 3 aprile 2006, n. 152 Norme in materia ambientale.,” 2013.

[111] D. Cordell, J.-O. Drangert, and S. White, “The story of phosphorus: Global food security and food for thought,” *Global Environmental Change*, vol. 19, no. 2, pp. 292–305, 2009, doi: 10.1016/j.gloenvcha.2008.10.009.

[112] *AEA, 2010. L’ambiente in Europa — Stato e prospettive nel 2010: Sintesi. Agenzia europea dell’ambiente, Copenaghen.* 2010.

[113] G. K. Morse, S. W. Brett, J. A. Guy, and J. N. Lester, “Review: Phosphorus removal and recovery technologies,” *Science of the Total Environment*, vol. 212, no. 1, pp. 69–81, 1998, doi: 10.1016/S0048-9697(97)00332-X.

[114] J. Y. Lee *et al.*, “Nutrient removal from hydroponic wastewater by a microbial consortium and a culture of Paracercomonas saepenatans,” *New Biotechnology*, vol. 41, pp. 15–24, 2018, doi: 10.1016/j.nbt.2017.11.003.

[115] E. Eggers, A. H. Dirkzwager, and H. Van der Honing, “Full-scale experiences with phosphate crystallisation in a crystalactor,” *Water Science and Technology*, vol. 24, no. 10, pp. 333–334, 1991.

[116] L. Peng, H. Dai, Y. Wu, Y. Peng, and X. Lu, “A comprehensive review of phosphorus recovery from wastewater by crystallization processes,” *Chemosphere*, vol. 197, pp. 768–781, 2018, doi: 10.1016/j.chemosphere.2018.01.098.

[117] Consiglio della comunità europea, “Direttiva 91/271/CEE del Consiglio, del 21 maggio 1991, concernente il trattamento delle acque reflue urbane.,” vol. 43, no. 10, pp. 8509–8515, 1991.

[118] “World Health Organization & International Programme on Chemical Safety. (1994). Glyphosate https://apps.who.int/iris/handle/10665/40044”.

[119] L. P. Agostini *et al.*, “Effects of glyphosate exposure on human health: Insights from epidemiological and in vitro studies,” *Science of the Total Environment*, vol. 705, 2020, doi: 10.1016/j.scitotenv.2019.135808.

[120] A. D. Baylis, “Why glyphosate is a global herbicide: Strengths, weaknesses and prospects,” *Pest Management Science*, vol. 56, no. 4, pp. 299–308, 2000, doi: 10.1002/(SICI)1526-4998(200004)56:4<299::AID-PS144>3.0.CO;2-K.

[121] P. J. Landrigan and F. Belpoggi, “The need for independent research on the health effects of glyphosate-based herbicides,” *Environmental Health: A Global Access Science Source*, vol. 17, no. 1, 2018, doi: 10.1186/s12940-018-0392-z.

[122] J. P. Myers *et al.*, “Concerns over use of glyphosate-based herbicides and risks associated with exposures: A consensus statement,” *Environmental Health: A Global Access Science Source*, vol. 15, no. 1, 2016, doi: 10.1186/s12940-016-0117-0.

[123] T. Bøhn, M. Cuhra, T. Traavik, M. Sanden, J. Fagan, and R. Primicerio, “Compositional differences in soybeans on the market: Glyphosate accumulates in Roundup Ready GM soybeans,” *Food Chemistry*, vol. 153, pp. 207–215, 2014, doi: 10.1016/j.foodchem.2013.12.054.

[124] IARC, *IARC Monographs on the evaluation of carcinogenic risks to humans - volume 112: Some organophosphate insecticides and herbicides - Glyphosate*, vol. 112. 2017.

[125] A. Paganelli, V. Gnazzo, H. Acosta, S. L. López, and A. E. Carrasco, “Glyphosate-based herbicides produce teratogenic effects on vertebrates by impairing retinoic acid signaling,” *Chemical Research in Toxicology*, vol. 23, no. 10, pp. 1586–1595, 2010, doi: 10.1021/tx1001749.

[126] A. Laborde *et al.*, “Children’s health in Latin America: The infuence of environmental exposures,” *Environmental Health Perspectives*, vol. 123, no. 3, pp. 201–209, 2015, doi: 10.1289/ehp.1408292.

[127] G. M. Williams *et al.*, “A review of the carcinogenic potential of glyphosate by four independent expert panels and comparison to the IARC assessment,” *Critical Reviews in Toxicology*, vol. 46, pp. 3–20, 2016, doi: 10.1080/10408444.2016.1214677.

[128] “Conclusion on the peer review of the pesticide risk assessment of the active substance glyphosate,” *EFSA Journal*, vol. 13, no. 11, 2016, doi: 10.2903/j.efsa.2015.4302.

[129] OMS, “Summary Report from the May 2016 Joint FAO/WHO Meeting on Pesticide Residues,” *Meeting on pesiticide residues. Summary Report*, no. May, pp. 9–13, 2016.

[130] E.U. Commission, “Regolamento di Esecuzione (UE) 2016/1313 della Commissione del 1 agosto 2016 che modifica il regolamento di esecuzione (UE) n. 540/2011 per quanto riguarda le condizioni di approvazione della sostanza attiva glifosato,” vol. 13, no. 11, pp. 1–3, 2016.

[131] Ministero della Salute, “Decreto: revoca di autorizzazioni all’immissione in commercio e modifica delle condizioni d’impiego di prodotti fitosanitari contenenti la sostanza attiva glifosate in attuazione del regolamento di esecuzione (UE) 2016/1313 della Commissione del 1°agosto,” 2016, doi: 10.1017/CBO9781107415324.004.

[132] Council of the European Union, “Council Directive 98/83/EC of 3 November 1998 on the quality of water intended for human consumption,” *Documents in European Community Environmental Law*, pp. 865–878, 2010, doi: 10.1017/cbo9780511610851.055.

[133] X. Ding and K. L. Yang, “Development of an oligopeptide functionalized surface plasmon resonance biosensor for online detection of glyphosate,” *Analytical Chemistry*, vol. 85, no. 12, pp. 5727–5733, 2013, doi: 10.1021/ac400273g.

[134] H. Lan *et al.*, “Removal of glyphosate from water by electrochemically assisted MnO 2 oxidation process,” *Separation and Purification Technology*, vol. 117, pp. 30–34, 2013, doi: 10.1016/j.seppur.2013.04.012.

[135] A. Grandcoin, S. Piel, and E. Baurès, “AminoMethylPhosphonic acid (AMPA) in natural waters: Its sources, behavior and environmental fate,” *Water Research*, vol. 117, no. January 2018, pp. 187–197, 2017, doi: 10.1016/j.watres.2017.03.055.

[136] G. M. Fu *et al.*, "Optimization of liquid-state fermentation conditions for the glyphosate degradation enzyme production of strain Aspergillus oryzae by ultraviolet mutagenesis," *Preparative Biochemistry and Biotechnology*, vol. 46, no. 8, pp. 780–787, 2016, doi: 10.1080/10826068.2015.1135462.

[137] J. Shen, J. Huang, H. Ruan, J. Wang, and B. Van der Bruggen, "Techno-economic analysis of resource recovery of glyphosate liquor by membrane technology," *Desalination*, vol. 342, pp. 118–125, 2014, doi: 10.1016/j.desal.2013.11.041.

[138] D. Guo, N. Muhammad, C. Lou, D. Shou, and Y. Zhu, "Synthesis of dendrimer functionalized adsorbents for rapid removal of glyphosate from aqueous solution," *New Journal of Chemistry*, vol. 43, no. 1, pp. 121–129, 2019, doi: 10.1039/c8nj04433c.

[139] R. B. Shrivastava, P. Singh, J. Bajpai, and A. K. Bajpai, "Polysaccharide-Based Nanosorbents in Water Remediation," *Application of Nanotechnology in Water Research*, vol. 9781118496, pp. 79–113, 2014, doi: 10.1002/9781118939314.ch5.

[140] R. B. Shrivastava, P. Singh, J. Bajpai, and A. K. Bajpai, "Polysaccharide-Based Nanosorbents in Water Remediation," *Application of Nanotechnology in Water Research*, vol. 9781118496, pp. 79–113, 2014, doi: 10.1002/9781118939314.ch5.

[141] I. Corsi *et al.*, "Environmentally sustainable and ecosafe polysaccharide-based materials for water nano-treatment: An eco-design study," *Materials*, vol. 11, no. 7, 2018, doi: 10.3390/ma11071228.

[142] I. Corsi *et al.*, "Environmentally sustainable and ecosafe polysaccharide-based materials for water nano-treatment: An eco-design study," *Materials*, vol. 11, no. 7, 2018, doi: 10.3390/ma11071228.

[143] E. da R. Zavareze, D. H. Kringel, and A. R. G. Dias, "Nano-scale polysaccharide materials in food and agricultural applications," *Advances in Food and Nutrition Research*, vol. 88, pp. 85–128, 2019, doi: 10.1016/bs.afnr.2019.02.013.

[144] G. Eggleston, J. W. Finley, and M. John, *Gillian Eggleston, John W. Finley, and John M. deMan 4*. 2018.

[145] E. da R. Zavareze, D. H. Kringel, and A. R. G. Dias, "Nano-scale polysaccharide materials in food and agricultural applications," *Advances in Food and Nutrition Research*, vol. 88, pp. 85–128, 2019, doi: 10.1016/bs.afnr.2019.02.013.

[146] G. Eggleston, J. W. Finley, and M. John, *Gillian Eggleston, John W. Finley, and John M. deMan 4*. 2018.

[147] M. Haroon *et al.*, *Chemical modification of starch and its application as an adsorbent material*, vol. 6, no. 82. 2016. doi: 10.1039/c6ra16795k.

[148] M. Haroon *et al.*, *Chemical modification of starch and its application as an adsorbent material*, vol. 6, no. 82. 2016. doi: 10.1039/c6ra16795k.

[149] A. R. Pedrazzo *et al.*, "for the Removal of Heavy Metals," pp. 1–14, 2019.

[150] B. Tian, S. Hua, Y. Tian, and J. Liu, "Cyclodextrin-based adsorbents for the removal of pollutants from wastewater: a review," *Environmental Science and Pollution Research*, vol. 28, no. 2, pp. 1317–1340, 2021, doi: 10.1007/s11356-020-11168-2.

[151] B. Tian, S. Hua, Y. Tian, and J. Liu, "Cyclodextrin-based adsorbents for the removal of pollutants from wastewater: a review," *Environmental Science and Pollution Research*, vol. 28, no. 2, pp. 1317–1340, 2021, doi: 10.1007/s11356-020-11168-2.

[152] G. Crini and M. Morcellet, “Synthesis and applications of adsorbents containing cyclodextrins,” *Journal of Separation Science*, vol. 25, no. 13, pp. 789–813, 2002, doi: 10.1002/1615-9314(20020901)25:13<789::AID-JSSC789>3.0.CO;2-J.

[153] G. Crini and M. Morcellet, “Synthesis and applications of adsorbents containing cyclodextrins,” *Journal of Separation Science*, vol. 25, no. 13, pp. 789–813, 2002, doi: 10.1002/1615-9314(20020901)25:13<789::AID-JSSC789>3.0.CO;2-J.

[154] I. Krabicová *et al.*, “History of cyclodextrin nanosponges,” *Polymers*, vol. 12, no. 5, pp. 1–23, 2020, doi: 10.3390/POLYM12051122.

[155] I. Krabicová *et al.*, “History of cyclodextrin nanosponges,” *Polymers*, vol. 12, no. 5, pp. 1–23, 2020, doi: 10.3390/POLYM12051122.

[156] A. P. Sherje, B. R. Dravyakar, D. Kadam, and M. Jadhav, “Cyclodextrin-based nanosponges: A critical review,” *Carbohydrate Polymers*. 2017. doi: 10.1016/j.carbpol.2017.05.086.

[157] C. Cecone, G. Costamagna, M. Ginepro, and F. Trotta, “One-step sustainable synthesis of cationic high-swelling polymers obtained from starch-derived maltodextrins,” *RSC Advances*, vol. 11, no. 13, pp. 7653–7662, 2021, doi: 10.1039/d0ra10715h.

[158] Q. Liu, Y. Zhou, J. Lu, and Y. Zhou, “Novel cyclodextrin-based adsorbents for removing pollutants from wastewater: A critical review,” *Chemosphere*, vol. 241, no. 130, p. 125043, 2020, doi: 10.1016/j.chemosphere.2019.125043.

[159] A. R. Pedrazzo *et al.*, “for the Removal of Heavy Metals,” pp. 1–14, 2019.

[160] C. Cecone, G. Costamagna, M. Ginepro, and F. Trotta, “One-step sustainable synthesis of cationic high-swelling polymers obtained from starch-derived maltodextrins,” *RSC Advances*, vol. 11, no. 13, pp. 7653–7662, 2021, doi: 10.1039/d0ra10715h.

[161] Q. Liu, Y. Zhou, J. Lu, and Y. Zhou, “Novel cyclodextrin-based adsorbents for removing pollutants from wastewater: A critical review,” *Chemosphere*, vol. 241, no. 130, p. 125043, 2020, doi: 10.1016/j.chemosphere.2019.125043.

[162] M. Zhang *et al.*, “Adsorption performance and mechanisms of Pb(II), Cd(II), and Mn(II) removal by a β-cyclodextrin derivative,” *Environmental Science and Pollution Research*, vol. 26, no. 5, pp. 5094–5110, 2019, doi: 10.1007/s11356-018-3989-4.

[163] N. Reddy, R. Reddy, and Q. Jiang, “Crosslinking biopolymers for biomedical applications,” *Trends in Biotechnology*, vol. 33, no. 6, pp. 362–369, 2015, doi: 10.1016/j.tibtech.2015.03.008.

[164] N. Reddy, R. Reddy, and Q. Jiang, “Crosslinking biopolymers for biomedical applications,” *Trends in Biotechnology*, vol. 33, no. 6, pp. 362–369, 2015, doi: 10.1016/j.tibtech.2015.03.008.

[165] Y. Zhou, Y. Hu, W. Huang, G. Cheng, C. Cui, and J. Lu, “A novel amphoteric B-cyclodextrin-based adsorbent for simultaneous removal of cationic/anionic dyes and bisphenol A,” *Chemical Engineering Journal*, vol. 341, no. 130, pp. 47–57, 2018, doi: 10.1016/j.cej.2018.01.155.

[166] M. Zhang *et al.*, “Adsorption performance and mechanisms of Pb(II), Cd(II), and Mn(II) removal by a β-cyclodextrin derivative,” *Environmental Science and Pollution Research*, vol. 26, no. 5, pp. 5094–5110, 2019, doi: 10.1007/s11356-018-3989-4.

[167] F. Zhao, E. Repo, D. Yin, Y. Meng, S. Jafari, and M. Sillanpää, “EDTA-Cross-Linked β-Cyclodextrin: An Environmentally Friendly Bifunctional Adsorbent for Simultaneous Adsorption of Metals and Cationic Dyes,” *Environmental Science and Technology*, vol. 49, no. 17, pp. 10570–10580, 2015, doi: 10.1021/acs.est.5b02227.

[168] C. Rodriguez-Tenreiro, C. Alvarez-Lorenzo, A. Rodriguez-Perez, A. Concheiro, and J. J. Torres-Labandeira, "New cyclodextrin hydrogels cross-linked with diglycidylethers with a high drug loading and controlled release ability," *Pharmaceutical Research*, vol. 23, no. 1, pp. 121–130, 2006, doi: 10.1007/s11095-005-8924-y.

[169] F. Zhao, E. Repo, D. Yin, Y. Meng, S. Jafari, and M. Sillanpää, "EDTA-Cross-Linked β-Cyclodextrin: An Environmentally Friendly Bifunctional Adsorbent for Simultaneous Adsorption of Metals and Cationic Dyes," *Environmental Science and Technology*, vol. 49, no. 17, pp. 10570–10580, 2015, doi: 10.1021/acs.est.5b02227.

[170] T. Yu, Z. Xue, X. Zhao, W. Chen, and T. Mu, "Green synthesis of porous β-cyclodextrin polymers for rapid and efficient removal of organic pollutants and heavy metal ions from water," *New Journal of Chemistry*, vol. 42, no. 19, pp. 16154–16161, 2018, doi: 10.1039/c8nj03438a.

[171] Y. Zhou, Y. Hu, W. Huang, G. Cheng, C. Cui, and J. Lu, "A novel amphoteric B-cyclodextrin-based adsorbent for simultaneous removal of cationic/anionic dyes and bisphenol A," *Chemical Engineering Journal*, vol. 341, no. 130, pp. 47–57, 2018, doi: 10.1016/j.cej.2018.01.155.

[172] T. Yu, Z. Xue, X. Zhao, W. Chen, and T. Mu, "Green synthesis of porous β-cyclodextrin polymers for rapid and efficient removal of organic pollutants and heavy metal ions from water," *New Journal of Chemistry*, vol. 42, no. 19, pp. 16154–16161, 2018, doi: 10.1039/c8nj03438a.

[173] D. Cai, T. Zhang, F. Zhang, and X. Luo, "Quaternary ammonium β-cyclodextrin-conjugated magnetic nanoparticles as nano-adsorbents for the treatment of dyeing wastewater: Synthesis and adsorption studies," *Journal of Environmental Chemical Engineering*, vol. 5, no. 3, pp. 2869–2878, 2017, doi: 10.1016/j.jece.2017.06.001.

[174] D. Cai, T. Zhang, F. Zhang, and X. Luo, "Quaternary ammonium β-cyclodextrin-conjugated magnetic nanoparticles as nano-adsorbents for the treatment of dyeing wastewater: Synthesis and adsorption studies," *Journal of Environmental Chemical Engineering*, vol. 5, no. 3, pp. 2869–2878, 2017, doi: 10.1016/j.jece.2017.06.001.

[175] C. F. Carolin, P. S. Kumar, A. Saravanan, G. J. Joshiba, and M. Naushad, "Efficient techniques for the removal of toxic heavy metals from aquatic environment: A review," *Journal of Environmental Chemical Engineering*, vol. 5, no. 3, pp. 2782–2799, 2017, doi: 10.1016/j.jece.2017.05.029.

[176] J. Briffa, E. Sinagra, and R. Blundell, "Heavy metal pollution in the environment and their toxicological effects on humans," *Heliyon*, vol. 6, no. 9, p. e04691, 2020, doi: 10.1016/j.heliyon.2020.e04691.

[177] J. Briffa, E. Sinagra, and R. Blundell, "Heavy metal pollution in the environment and their toxicological effects on humans," *Heliyon*, vol. 6, no. 9, p. e04691, 2020, doi: 10.1016/j.heliyon.2020.e04691.

[178] Canyon Hydro *et al.*, "We are IntechOpen , the world ' s leading publisher of Open Access books Built by scientists , for scientists TOP 1 %," *Intech*, vol. 32, no. July, pp. 137–144, 2013.

[179] K. H. Vardhan, P. S. Kumar, and R. C. Panda, "A review on heavy metal pollution, toxicity and remedial measures: Current trends and future perspectives," *Journal of Molecular Liquids*, vol. 290, p. 111197, 2019, doi: 10.1016/j.molliq.2019.111197.

[180] Canyon Hydro *et al.*, "We are IntechOpen , the world ' s leading publisher of Open Access books Built by scientists , for scientists TOP 1 %," *Intech*, vol. 32, no. July, pp. 137–144, 2013.

[181] T. M. Ansari, I. L. Marr, and N. Tariq, “Heavy Metals in Marine Pollution Perspective–A Mini Review,” *Journal of Applied Sciences*, vol. 4, no. 1, pp. 1–20, 2003, doi: 10.3923/jas.2004.1.20.

[182] P. B. Tchounwou, C. G. Yedjou, A. K. Patlolla, and D. J. Sutton, *Molecular, clinical and environmental toxicicology Volume 3: Environmental Toxicology*, vol. 101. 2012. doi: 10.1007/978-3-7643-8340-4.

[183] V. Masindi and K. L. Muedi, “Environmental Contamination by Heavy Metals,” *Heavy Metals*, 2018, doi: 10.5772/intechopen.76082.

[184] V. Masindi and K. L. Muedi, “Environmental Contamination by Heavy Metals,” *Heavy Metals*, 2018, doi: 10.5772/intechopen.76082.

[185] D. Ciszewski and T. M. Grygar, “A Review of Flood-Related Storage and Remobilization of Heavy Metal Pollutants in River Systems,” *Water, Air, and Soil Pollution*, vol. 227, no. 7, 2016, doi: 10.1007/s11270-016-2934-8.

[186] D. Ciszewski and T. M. Grygar, “A Review of Flood-Related Storage and Remobilization of Heavy Metal Pollutants in River Systems,” *Water, Air, and Soil Pollution*, vol. 227, no. 7, 2016, doi: 10.1007/s11270-016-2934-8.

[187] M. A. Barakat, “New trends in removing heavy metals from industrial wastewater,” *Arabian Journal of Chemistry*, vol. 4, no. 4, pp. 361–377, 2011, doi: 10.1016/j.arabjc.2010.07.019.

[188] P. K. Gautam, R. K. Gautam, S. Banerjee, M. C. Chattopadhyaya, and J. D. Pandey, “Heavy metals in the environment: Fate, transport, toxicity and remediation technologies,” *Heavy Metals: Sources, Toxicity and Remediation Techniques*, no. March 2017, pp. 101–130, 2016.

[189] R. Mingkhwan and S. Worakhunpiset, “Heavy metal contamination near industrial estate areas in Phra Nakhon Si Ayutthaya Province, Thailand and human health risk assessment,” *International Journal of Environmental Research and Public Health*, vol. 15, no. 9, 2018, doi: 10.3390/ijerph15091890.

[190] P. Saha and B. Paul, “Assessment of heavy metal toxicity related with human health risk in the surface water of an industrialized area by a novel technique,” *Human and Ecological Risk Assessment*, vol. 25, no. 4, pp. 966–987, 2019, doi: 10.1080/10807039.2018.1458595.

[191] S. I. Shupack, “The chemistry of chromium and some resulting analytical problems,” 1991. doi: 10.1289/ehp.91927.

[192] N. Greenwood and A. Earnshaw, “24 - Manganese, Technetium and Rhenium BT - Chemistry of the Elements (Second Edition),” in *Chemistry of the Elements*, 1997. doi: http://dx.doi.org/10.1016/B978-0-7506-3365-9.50030-4.

[193] J. Barnhart, “Occurrences, Uses, and Properties of Chromium,” *Regulatory Toxicology and Pharmacology*, 1997, doi: 10.1006/rtph.1997.1132.

[194] “Arsenic, Antimony and Bismuth,” in *Chemistry of the Elements*, 1997. doi: 10.1016/b978-0-7506-3365-9.50019-5.

[195] A. Mudhoo, S. K. Sharma, V. K. Garg, and C. H. Tseng, “Arsenic: An overview of applications, health, and environmental concerns and removal processes,” *Critical Reviews in Environmental Science and Technology*, 2011, doi: 10.1080/10643380902945771.

[196] F. T. Jones, “A broad view of arsenic,” *Poultry Science*. 2007. doi: 10.1093/ps/86.1.2.

[197] M. L. Sall, A. K. D. Diaw, D. Gningue-Sall, S. Efremova Aaron, and J. J. Aaron, “Toxic heavy metals: impact on the environment and human health, and treatment with conducting organic

polymers, a review," *Environmental Science and Pollution Research*, vol. 27, no. 24, pp. 29927–29942, 2020, doi: 10.1007/s11356-020-09354-3.

[198] A. Pilger and H. W. Rüdiger, "8-Hydroxy-2′-deoxyguanosine as a marker of oxidative DNA damage related to occupational and environmental exposures," *International Archives of Occupational and Environmental Health*. 2006. doi: 10.1007/s00420-006-0106-7.

[199] F. Henkler, J. Brinkmann, and A. Luch, "The role of oxidative stress in carcinogenesis induced by metals and xenobiotics," *Cancers*. 2010. doi: 10.3390/cancers2020376.

[200] P. K. Gautam, R. K. Gautam, S. Banerjee, M. C. Chattopadhyaya, and J. D. Pandey, "Heavy metals in the environment: Fate, transport, toxicity and remediation technologies," *Heavy Metals: Sources, Toxicity and Remediation Techniques*, no. March 2017, pp. 101–130, 2016.

[201] N. Muisa, Z. Hoko, and P. Chifamba, "Impacts of alum residues from Morton Jaffray Water Works on water quality and fish, Harare, Zimbabwe," *Physics and Chemistry of the Earth*, vol. 36, no. 14–15, pp. 853–864, 2011, doi: 10.1016/j.pce.2011.07.047.

[202] N. Muisa, Z. Hoko, and P. Chifamba, "Impacts of alum residues from Morton Jaffray Water Works on water quality and fish, Harare, Zimbabwe," *Physics and Chemistry of the Earth*, vol. 36, no. 14–15, pp. 853–864, 2011, doi: 10.1016/j.pce.2011.07.047.

[203] Md. A. Rahman, Md. A. Hashem, Md. S. Rana, and Md. R. Islam, "Manganese in potable water of nine districts, Bangladesh: human health risk," *Environmental Science and Pollution Research*, 2021, doi: 10.1007/s11356-021-14016-z.

[204] G. Ungureanu, S. Santos, R. Boaventura, and C. Botelho, "Arsenic and antimony in water and wastewater: Overview of removal techniques with special reference to latest advances in adsorption," *Journal of Environmental Management*. 2015. doi: 10.1016/j.jenvman.2014.12.051.

[205] P. F. Tee *et al.*, "Review on hybrid energy systems for wastewater treatment and bio-energy production," *Renewable and Sustainable Energy Reviews*, vol. 54, pp. 235–246, 2016, doi: 10.1016/j.rser.2015.10.011.

[206] A. Azimi, A. Azari, M. Rezakazemi, and M. Ansarpour, "Removal of Heavy Metals from Industrial Wastewaters: A Review," *ChemBioEng Reviews*, vol. 4, no. 1, pp. 37–59, 2017, doi: 10.1002/cben.201600010.

[207] F. Fu and Q. Wang, "Removal of heavy metal ions from wastewaters: A review," *Journal of Environmental Management*, vol. 92, no. 3, pp. 407–418, 2011, doi: 10.1016/j.jenvman.2010.11.011.

[208] F. Fu and Q. Wang, "Removal of heavy metal ions from wastewaters: A review," *Journal of Environmental Management*, vol. 92, no. 3, pp. 407–418, 2011, doi: 10.1016/j.jenvman.2010.11.011.

[209] A. Pohl, "Removal of Heavy Metal Ions from Water and Wastewaters by Sulfur-Containing Precipitation Agents," *Water, Air, and Soil Pollution*, vol. 231, no. 10, 2020, doi: 10.1007/s11270-020-04863-w.

[210] A. Pohl, "Removal of Heavy Metal Ions from Water and Wastewaters by Sulfur-Containing Precipitation Agents," *Water, Air, and Soil Pollution*, vol. 231, no. 10, 2020, doi: 10.1007/s11270-020-04863-w.

[211] M. A. Barakat, "New trends in removing heavy metals from industrial wastewater," *Arabian Journal of Chemistry*, vol. 4, no. 4, pp. 361–377, 2011, doi: 10.1016/j.arabjc.2010.07.019.

[212] M. C. Benalia, L. Youcef, M. G. Bouaziz, S. Achour, and H. Menasra, “Removal of Heavy Metals from Industrial Wastewater by Chemical Precipitation: Mechanisms and Sludge Characterization,” *Arabian Journal for Science and Engineering*, 2021, doi: 10.1007/s13369-021-05525-7.

[213] M. S. Oncel, A. Muhcu, E. Demirbas, and M. Kobya, “A comparative study of chemical precipitation and electrocoagulation for treatment of coal acid drainage wastewater,” *Journal of Environmental Chemical Engineering*, vol. 1, no. 4, pp. 989–995, 2013, doi: 10.1016/j.jece.2013.08.008.

[214] G. Crini and E. Lichtfouse, “Advantages and disadvantages of techniques used for wastewater treatment,” *Environmental Chemistry Letters*, vol. 17, no. 1, pp. 145–155, 2019, doi: 10.1007/s10311-018-0785-9.

[215] M. S. Oncel, A. Muhcu, E. Demirbas, and M. Kobya, “A comparative study of chemical precipitation and electrocoagulation for treatment of coal acid drainage wastewater,” *Journal of Environmental Chemical Engineering*, vol. 1, no. 4, pp. 989–995, 2013, doi: 10.1016/j.jece.2013.08.008.

[216] M. C. Benalia, L. Youcef, M. G. Bouaziz, S. Achour, and H. Menasra, “Removal of Heavy Metals from Industrial Wastewater by Chemical Precipitation: Mechanisms and Sludge Characterization,” *Arabian Journal for Science and Engineering*, 2021, doi: 10.1007/s13369-021-05525-7.

[217] S. T. Hussain and S. A. Khaleefa Ali, “Removal of Heavy Metal by Ion Exchange Using Bentonite Clay,” *Journal of Ecological Engineering*, vol. 22, no. 1, pp. 104–111, 2020, doi: 10.12911/22998993/128865.

[218] B. Alyüz and S. Veli, “Kinetics and equilibrium studies for the removal of nickel and zinc from aqueous solutions by ion exchange resins,” *Journal of Hazardous Materials*, vol. 167, no. 1–3, pp. 482–488, 2009, doi: 10.1016/j.jhazmat.2009.01.006.

[219] S. M. Moosavirad, R. Sarikhani, E. Shahsavani, and S. Z. Mohammadi, “Removal of some heavy metals from inorganic industrial wastewaters by ion exchange method,” *Journal of Water Chemistry and Technology*, vol. 37, no. 4, pp. 191–199, 2015, doi: 10.3103/S1063455X15040074.

[220] R. Shrestha *et al.*, “Technological trends in heavy metals removal from industrial wastewater: A review,” *Journal of Environmental Chemical Engineering*, vol. 9, no. 4, p. 105688, 2021, doi: 10.1016/j.jece.2021.105688.

[221] N. P. Raval, P. U. Shah, and N. K. Shah, “Adsorptive removal of nickel(II) ions from aqueous environment: A review,” *Journal of Environmental Management*, vol. 179, pp. 1–20, 2016, doi: 10.1016/j.jenvman.2016.04.045.

[222] M. Karnib, A. Kabbani, H. Holail, and Z. Olama, “Heavy metals removal using activated carbon, silica and silica activated carbon composite,” *Energy Procedia*, vol. 50, pp. 113–120, 2014, doi: 10.1016/j.egypro.2014.06.014.

[223] M. N. Rashed, M. A. Eltaher, and A. N. A. Abdou, “Adsorption and photocatalysis for methyl orange and Cd removal from wastewater using TiO2/sewage sludge-based activated carbon nanocomposites,” *Royal Society Open Science*, vol. 4, no. 12, 2017, doi: 10.1098/rsos.170834.

[224] N. P. Raval, P. U. Shah, and N. K. Shah, “Adsorptive removal of nickel(II) ions from aqueous environment: A review,” *Journal of Environmental Management*, vol. 179, pp. 1–20, 2016, doi: 10.1016/j.jenvman.2016.04.045.

[225] R. Shrestha *et al.*, “Technological trends in heavy metals removal from industrial wastewater: A review,” *Journal of Environmental Chemical Engineering*, vol. 9, no. 4, p. 105688, 2021, doi: 10.1016/j.jece.2021.105688.

[226] N. Morin-Crini, J. N. Staelens, S. Loiacono, B. Martel, G. Chanet, and G. Crini, “Simultaneous removal of Cd, Co, Cu, Mn, Ni, and Zn from synthetic solutions on a hemp-based felt. III. Real discharge waters,” *Journal of Applied Polymer Science*, vol. 137, no. 24, pp. 1–10, 2020, doi: 10.1002/app.48823.

[227] E. A. Abdelrahman, E. T. Abdel-Salam, S. M. El Rayes, and N. S. Mohamed, “Facile synthesis of graft copolymers of maltodextrin and chitosan with 2-acrylamido-2-methyl-1-propanesulfonic acid for efficient removal of Ni(II), Fe(III), and Cd(II) ions from aqueous media,” *Journal of Polymer Research*, vol. 26, no. 11, 2019, doi: 10.1007/s10965-019-1920-4.

[228] S. Wang, B. Gao, Y. Li, Y. S. Ok, C. Shen, and S. Xue, “Biochar provides a safe and value-added solution for hyperaccumulating plant disposal: A case study of Phytolacca acinosa Roxb. (Phytolaccaceae),” *Chemosphere*, vol. 178, pp. 59–64, 2017, doi: 10.1016/j.chemosphere.2017.02.121.

[229] A. Bagreev, T. J. Bandosz, and D. C. Locke, “Pore structure and surface chemistry of adsorbents obtained by pyrolysis of sewage sludge-derived fertilizer,” 2001.

[230] S. Sohi, E. Lopez-Capel, R. Bol, and F. Jülich, “Biochar, Climate Change and Soil: A Review to Guide Future Research Sustainable Subsoil Management View project Optimisation of value chains for biogas production in Denmark (Biochain) View project,” 2009. [Online]. Available: https://www.researchgate.net/publication/228656328

[231] M. I. Inyang *et al.*, “A review of biochar as a low-cost adsorbent for aqueous heavy metal removal,” *Critical Reviews in Environmental Science and Technology*, vol. 46, no. 4. Taylor and Francis Inc., pp. 406–433, Feb. 16, 2016. doi: 10.1080/10643389.2015.1096880.

[232] H. Li, X. Dong, E. B. da Silva, L. M. de Oliveira, Y. Chen, and L. Q. Ma, “Mechanisms of metal sorption by biochars: Biochar characteristics and modifications,” *Chemosphere*, vol. 178. Elsevier Ltd, pp. 466–478, 2017. doi: 10.1016/j.chemosphere.2017.03.072.

[233] M. Ahmedna, W. E. Marshall, A. A. Husseiny, R. M. Rao, and I. Goktepe, “The use of nutshell carbons in drinking water filters for removal of trace metals,” *Water Research*, vol. 38, no. 4, pp. 1062–1068, 2004, doi: 10.1016/j.watres.2003.10.047.

[234] T. Chen *et al.*, “Influence of pyrolysis temperature on characteristics and heavy metal adsorptive performance of biochar derived from municipal sewage sludge,” *Bioresource Technology*, vol. 164, pp. 47–54, 2014, doi: 10.1016/j.biortech.2014.04.048.

[235] W. Yang *et al.*, “Impact of biochar on greenhouse gas emissions and soil carbon sequestration in corn grown under drip irrigation with mulching,” *Science of the Total Environment*, vol. 729, Aug. 2020, doi: 10.1016/j.scitotenv.2020.138752.

[236] S. Yoo, S. S. Kelley, D. C. Tilotta, and S. Park, “Structural Characterization of Loblolly Pine Derived Biochar by X-ray Diffraction and Electron Energy Loss Spectroscopy,” *ACS Sustainable Chemistry and Engineering*, vol. 6, no. 2, pp. 2621–2629, Feb. 2018, doi: 10.1021/acssuschemeng.7b04119.

[237] M. Keiluweit, P. S. Nico, M. Johnson, and M. Kleber, “Dynamic molecular structure of plant biomass-derived black carbon (biochar),” *Environmental Science and Technology*, vol. 44, no. 4, pp. 1247–1253, 2010, doi: 10.1021/es9031419.

[238] K. H. Kim *et al.*, “Investigation of physicochemical properties of biooils produced from yellow poplar wood (Liriodendron tulipifera) at various temperatures and residence times,” *Journal of Analytical and Applied Pyrolysis*, vol. 92, no. 1, pp. 2–9, 2011, doi: 10.1016/j.jaap.2011.04.002.

[239] Z. L. Zhang *et al.*, “Investigating the structure of non-graphitising carbons using electron energy loss spectroscopy in the transmission electron microscope,” *Carbon*, vol. 49, no. 15, pp. 5049–5063, 2011, doi: 10.1016/j.carbon.2011.07.023.

[240] A. S. Marriott *et al.*, “Investigating the structure of biomass-derived non-graphitizing mesoporous carbons by electron energy loss spectroscopy in the transmission electron microscope and X-ray photoelectron spectroscopy,” *Carbon*, vol. 67, pp. 514–524, 2014, doi: 10.1016/j.carbon.2013.10.024.

[241] J. Park, I. Hung, Z. Gan, O. J. Rojas, K. H. Lim, and S. Park, “Activated carbon from biochar: Influence of its physicochemical properties on the sorption characteristics of phenanthrene,” *Bioresource Technology*, vol. 149, pp. 383–389, 2013, doi: 10.1016/j.biortech.2013.09.085.

[242] B. Singh, Y. Fang, B. C. C. Cowie, and L. Thomsen, “NEXAFS and XPS characterisation of carbon functional groups of fresh and aged biochars,” *Organic Geochemistry*, vol. 77, pp. 1–10, Dec. 2014, doi: 10.1016/j.orggeochem.2014.09.006.

[243] G. Abdul, X. Zhu, and B. Chen, “Structural characteristics of biochar-graphene nanosheet composites and their adsorption performance for phthalic acid esters,” *Chemical Engineering Journal*, vol. 319, pp. 9–20, 2017, doi: 10.1016/j.cej.2017.02.074.

[244] C. E. Brewer, K. Schmidt-Rohr, J. A. Satrio, and R. C. Brown, “Characterization of biochar from fast pyrolysis and gasification systems,” *Environmental Progress and Sustainable Energy*, vol. 28, no. 3, pp. 386–396, Oct. 2009, doi: 10.1002/ep.10378.

[245] J. Park, I. Hung, Z. Gan, O. J. Rojas, K. H. Lim, and S. Park, “Activated carbon from biochar: Influence of its physicochemical properties on the sorption characteristics of phenanthrene,” *Bioresource Technology*, vol. 149, pp. 383–389, 2013, doi: 10.1016/j.biortech.2013.09.085.

[246] J. H. Yuan, R. K. Xu, and H. Zhang, “The forms of alkalis in the biochar produced from crop residues at different temperatures,” *Bioresource Technology*, vol. 102, no. 3, pp. 3488–3497, Feb. 2011, doi: 10.1016/j.biortech.2010.11.018.

[247] A. R. A. Usman *et al.*, “Chemically Modified Biochar Produced from Conocarpus Wastes: An Efficient Sorbent for Fe(II) Removal from Acidic Aqueous Solutions.”

[248] M. Uchimiya, I. M. Lima, K. Thomas Klasson, S. Chang, L. H. Wartelle, and J. E. Rodgers, “Immobilization of heavy metal ions (CuII, CdII, NiII, and PbII) by broiler litter-derived biochars in water and soil,” *Journal of Agricultural and Food Chemistry*, vol. 58, no. 9, pp. 5538–5544, May 2010, doi: 10.1021/jf9044217.

[249] T. Chen *et al.*, “Influence of pyrolysis temperature on characteristics and heavy metal adsorptive performance of biochar derived from municipal sewage sludge,” *Bioresource Technology*, vol. 164, pp. 47–54, 2014, doi: 10.1016/j.biortech.2014.04.048.

[250] R. Subedi *et al.*, “Greenhouse gas emissions and soil properties following amendment with manure-derived biochars: Influence of pyrolysis temperature and feedstock type,” *Journal of Environmental Management*, vol. 166, pp. 73–83, Jan. 2016, doi: 10.1016/j.jenvman.2015.10.007.

[251] M. I. Al-Wabel, A. Al-Omran, A. H. El-Naggar, M. Nadeem, and A. R. A. Usman, “Pyrolysis temperature induced changes in characteristics and chemical composition of biochar produced

from conocarpus wastes," *Bioresource Technology*, vol. 131, pp. 374–379, 2013, doi: 10.1016/j.biortech.2012.12.165.

[252] H. Zhang, R. P. Voroney, and G. W. Price, "Effects of temperature and processing conditions on biochar chemical properties and their influence on soil C and N transformations," *Soil Biology and Biochemistry*, vol. 83, pp. 19–28, Apr. 2015, doi: 10.1016/j.soilbio.2015.01.006.

[253] O. R. Harvey, B. E. Herbert, R. D. Rhue, and L. J. Kuo, "Metal interactions at the biochar-water interface: Energetics and structure-sorption relationships elucidated by flow adsorption microcalorimetry," *Environmental Science and Technology*, vol. 45, no. 13, pp. 5550–5556, Jul. 2011, doi: 10.1021/es104401h.

[254] Y. Liang, X. Cao, L. Zhao, X. Xu, and W. Harris, "Phosphorus Release from Dairy Manure, the Manure-Derived Biochar, and Their Amended Soil: Effects of Phosphorus Nature and Soil Property," *Journal of Environmental Quality*, vol. 43, no. 4, pp. 1504–1509, Jul. 2014, doi: 10.2134/jeq2014.01.0021.

[255] M. Inyang, B. Gao, P. Pullammanappallil, W. Ding, and A. R. Zimmerman, "Biochar from anaerobically digested sugarcane bagasse," *Bioresource Technology*, vol. 101, no. 22, pp. 8868–8872, Nov. 2010, doi: 10.1016/j.biortech.2010.06.088.

[256] S. Koutcheiko, C. M. Monreal, H. Kodama, T. McCracken, and L. Kotlyar, "Preparation and characterization of activated carbon derived from the thermo-chemical conversion of chicken manure," *Bioresource Technology*, vol. 98, no. 13, pp. 2459–2464, Sep. 2007, doi: 10.1016/j.biortech.2006.09.038.

[257] B. Purevsuren *et al.*, "The characterisation of tar from the pyrolysis of animal bones," *Fuel*, vol. 83, no. 7–8, pp. 799–805, May 2004, doi: 10.1016/j.fuel.2003.10.011.

[258] R. Cárdenas-Navarro, L. López-Pérez, P. Lobit, O. Escalante-Linares, V. Castellanos-Morales, and R. Ruíz-Corro, "Diagnosis of N status in strawberry (Fragaria x ananassas Duch)," in *Acta Horticulturae*, Aug. 2004, vol. 654, pp. 257–262. doi: 10.17660/ActaHortic.2004.654.29.

[259] R. Malekian, J. Abedi-Koupai, and S. S. Eslamian, "Influences of clinoptilolite and surfactant-modified clinoptilolite zeolite on nitrate leaching and plant growth," *Journal of Hazardous Materials*, vol. 185, no. 2–3, pp. 970–976, Jan. 2011, doi: 10.1016/j.jhazmat.2010.09.114.

[260] R. G. Mcguire, "Reporting of Objective Color Measurements."

[261] J. P. Stanoeva, M. Stefova, K. B. Andonovska, A. Vankova, and T. Stafilov, "Phenolics and mineral content in bilberry and bog bilberry from Macedonia," *International Journal of Food Properties*, vol. 20, pp. S863–S883, Dec. 2017, doi: 10.1080/10942912.2017.1315592.

[262] O. I., A.-R. F., A. J., O. L., Q. M., and H. A., "Effect of Harvesting Date and Variety of Date Palm on Antioxidant Capacity, Phenolic and Flavonoid Content of Date Palm (Phoenix Dactylifera)," *Journal of Food and Nutrition Research*, vol. 2, no. 8, pp. 499–505, Aug. 2014, doi: 10.12691/jfnr-2-8-11.

[263] J. Donhauser and B. Frey, "Alpine soil microbial ecology in a changing world," *FEMS Microbiology Ecology*, vol. 94, no. 9. Oxford University Press, Sep. 01, 2018. doi: 10.1093/femsec/fiy099.

[264] E. F. Durner, "Plant architecture of 'Albion' strawberry (Fragaria × ananassa Duch.) is not influenced by light source during conditioning," *AIMS Agriculture and Food*, vol. 3, no. 3, pp. 246–265, 2018, doi: 10.3934/AGRFOOD.2018.3.246.

[265] A. Gül, D. Erŏul, and A. R. Ongun, “Comparison of the use of zeolite and perlite as substrate for crisp-head lettuce,” *Scientia Horticulturae*, vol. 106, no. 4, pp. 464–471, Nov. 2005, doi: 10.1016/j.scienta.2005.03.015.

[266] F. Aydın Temel and A. Kuleyin, “Ammonium removal from landfill leachate using natural zeolite: kinetic, equilibrium, and thermodynamic studies,” *Desalination and Water Treatment*, vol. 57, no. 50, pp. 23873–23892, 2016, doi: 10.1080/19443994.2015.1136964.

[267] E. Turhan and A. Eris, “Effects of sodium chloride applications and different growth media on ionic composition in strawberry plant,” *Journal of Plant Nutrition*, vol. 27, no. 9, pp. 1653–1665, 2004, doi: 10.1081/PLN-200026009.

[268] J. C. Caruana, J. W. Sittmann, W. Wang, and Z. Liu, “Suppressor of Runnerless Encodes a DELLA Protein that Controls Runner Formation for Asexual Reproduction in Strawberry,” *Molecular Plant*, vol. 11, no. 1. Cell Press, pp. 230–233, 2018. doi: 10.1016/j.molp.2017.11.001.

[269] B. Mitcham, “Quality Assurance for Strawberries: A Case Study,” 1996.

[270] L. Ali, B. W. Alsanius, A. K. Rosberg, B. Svensson, T. Nielsen, and M. E. Olsson, “Effects of nutrition strategy on the levels of nutrients and bioactive compounds in blackberries,” *European Food Research and Technology*, vol. 234, no. 1, pp. 33–44, Jan. 2012, doi: 10.1007/s00217-011-1604-8.

[271] F. M. Prasad *et al.*, “Effect of Different Levels of Bioneema and Nitrogenous Fertilizer on Bio Chemical Constituents in Tomato (Lycopersicon esculentum Mill.) C.V. Money Maker,” *World Journal of Chemistry*, vol. 1, no. 1, pp. 28–29, 2006.

[272] R. Delgado, R. González, and P. Martín, “INTERACTION EFFECTS OF NITROGEN AND POTASSIUM FERTILIZATION ON ANTHOCYANIN COMPOSITION AND CHROMATIC FEATURES OF TEMPRANILLO GRAPES EFFETS D’INTERACTION ENTRE FERTILISATION AZOTÉE ET FERTILISATION POTASSIQUE SUR LA COMPOSITION ANTHOCYANIQUE ET LES CARACTÉRISTIQUES CHROMATIQUES DU RAISIN CV. TEMPRANILLO,” 2006.

[273] H. J. Di *et al.*, “Ammonia-oxidizing bacteria and archaea grow under contrasting soil nitrogen conditions,” *FEMS Microbiology Ecology*, vol. 72, no. 3, pp. 386–394, Jun. 2010, doi: 10.1111/j.1574-6941.2010.00861.x.

[274] L. Ali, B. W. Alsanius, A. K. Rosberg, B. Svensson, T. Nielsen, and M. E. Olsson, “Effects of nutrition strategy on the levels of nutrients and bioactive compounds in blackberries,” *European Food Research and Technology*, vol. 234, no. 1, pp. 33–44, Jan. 2012, doi: 10.1007/s00217-011-1604-8.

[275] N. C. Banning, L. D. Maccarone, L. M. Fisk, and D. v. Murphy, “Ammonia-oxidising bacteria not archaea dominate nitrification activity in semi-arid agricultural soil,” *Scientific Reports*, vol. 5, Jun. 2015, doi: 10.1038/srep11146.

[276] R. Gorra, M. Coci, R. Ambrosoli, and H. J. Laanbroek, “Effects of substratum on the diversity and stability of ammonia-oxidizing communities in a constructed wetland used for wastewater treatment,” *Journal of Applied Microbiology*, vol. 103, no. 5, pp. 1442–1452, Nov. 2007, doi: 10.1111/j.1365-2672.2007.03357.x.

[277] M. Castro-Cabado, F. J. Parra-Ruiz, A. L. Casado, and J. San Román, “Thermal crosslinking of maltodextrin and citric acid. Methodology to control the polycondensation reaction under processing conditions,” *Polymers and Polymer Composites*, vol. 24, no. 8, pp. 643–654, 2016, doi: 10.1177/096739111602400803.

[278] S. Tavakoli, M. Kharaziha, S. Nemati, and A. Kalateh, “Nanocomposite hydrogel based on carrageenan-coated starch/cellulose nanofibers as a hemorrhage control material,” *Carbohydrate Polymers*, vol. 251, no. August 2020, p. 117013, 2021, doi: 10.1016/j.carbpol.2020.117013.

[279] R. Challa, A. Ahuja, J. Ali, and R. K. Khar, “Cyclodextrins in drug delivery: An updated review,” *AAPS PharmSciTech*, vol. 6, no. 2, pp. 329–357, 2005, doi: 10.1208/pt060243.

[280] J. Y. C. Lim, S. S. Goh, S. S. Liow, K. Xue, and X. J. Loh, “Molecular gel sorbent materials for environmental remediation and wastewater treatment,” *Journal of Materials Chemistry A*, vol. 7, no. 32, pp. 18759–18791, 2019, doi: 10.1039/c9ta05782j.

[281] B. Alyüz and S. Veli, “Kinetics and equilibrium studies for the removal of nickel and zinc from aqueous solutions by ion exchange resins,” *Journal of Hazardous Materials*, vol. 167, no. 1–3, pp. 482–488, 2009, doi: 10.1016/j.jhazmat.2009.01.006.

[282] S. T. Hussain and S. A. Khaleefa Ali, “Removal of Heavy Metal by Ion Exchange Using Bentonite Clay,” *Journal of Ecological Engineering*, vol. 22, no. 1, pp. 104–111, 2020, doi: 10.12911/22998993/128865.

[283] S. M. Moosavirad, R. Sarikhani, E. Shahsavani, and S. Z. Mohammadi, “Removal of some heavy metals from inorganic industrial wastewaters by ion exchange method,” *Journal of Water Chemistry and Technology*, vol. 37, no. 4, pp. 191–199, 2015, doi: 10.3103/S1063455X15040074.

15 Final report of academic activities - PhD Programme in Chemical and Material Sciences

1st year:

Presentations

Oral presentation:

1. *"Use of nano-structural materials for abatement of nitrates in natural and wastewater", G. Costamagna, S. Mariotti, and M. Ginepro, XXVII Congresso Divisione Chimica Analitica (Società Chimica Italiana), Bologna, Italy, September 2018*
2. *"By-products analysis of a pyrolysis plant powered by plastic waste materials for energy's production", Merck & Elsevier Young Chemists Symposium (MEYCS 2018)", S. Mariotti, G. Costamagna, and M. Ginepro, Merck & Elsevier Young Chemists Symposium (MEYCS 2018), Rimini, Italy, 19-21 November 2018*

Poster presentation:

1. *"Use of nano-structural materials for abatement of nitrates in natural and waste water", , G. Costamagna, S. Mariotti, and M. Ginepro, XXVII Congresso Divisione Chimica Analitica (Società Chimica Italiana), Bologna, Italy, September 2018*
2. *"By-products analysis of a pyrolysis plant powered by plastic waste materials for energy's production", Merck & Elsevier Young Chemists Symposium (MEYCS 2018)", G. Costamagna, S. Mariotti and M. Ginepro, Merck & Elsevier Young Chemists Symposium (MEYCS 2018), Rimini, Italy, 19-21 November 2018*

PhD Courses Attended

Course title	Instructor	University / Department	Hours	CFU
An insight into epistemological and didactic issues related with science teaching	Prof. E. Ghibaudi, Prof. G. Cerrato	Department of Chemistry, University of Turin	8	2
Interactive laboratory to stimulate an attitude to outreach activities on basic physico-chemical phenomena	Prof. G. Magnacca, Prof. G. Berlier	Department of Chemistry, University of Turin	12	3
English for Scientific Academic Purposes for Phd Students	Prof. J. Robinson, Prof. P. Gambino	Department of Chemistry, Dottorati in Scienza della Natura in collaborazione con L'Istituto Universitario di Studi Europei	30	7.5
Corso di formazione	Online	Scuole di dottorato	4	1

generale per lavoratori in materia di igiene e sicurezza				

PhD Schools Attended

- We Food Academy – Alla scoperta delle fabbriche del gusto, Vicenza, 2-4 November 2018
- Emergence and Organization of Life, Bardonecchia – Villaggio Olimpico, Italy, 20-21 June 2019.

Seminars, Conferences Attended

- Merck & Elsevier Young Chemists Symposium 2018, Società Chimica Italiana, Rimini, Italy, 19-21 November 2018.
- Sviluppi nella Tecnologia e nelle Applicazioni SFE, Incontro di aggiornamento sulla tecnica di Estrazione con Fluidi Supercritici – Settore didattico Università di Milano, Milan, Italy, 22th November 2018.
- Looking for Mobility? Funding Schemes, Recognition of Academic Titles, pan-European defined, contribution pension solution for research organizations and researchers, APAC Project etc. – Department of Chemistry, Aula Cannizzaro, Torino, Italy, 9th May 2019.
- Patenting and Knowledge Transfer - Aquality and Paracat H2020 MSCA ITNs Projects – Torino, Italy, 15th May 2019.
- Lean Thinking – Aquality and Paracat H2020 MSCA ITNs Projects – Department of Chemistry, Torino, Italy, 16th May 2019.
- NIS Colloquium – AQUAlity & Project O Dissemination – Department of Chemistry, Torino, Italy, 16-17 May 2019

2nd year

Papers

- *Characterization and Use of Absorbent Materials as Slow-Release Fertilizers for Growing Strawberry: Preliminary Results.*

Giulia Costamagna, Valentina Chiabrando, Enrica Fassone, Ilaria Mania, Roberta Gorra, Marco Ginepro and Giovanna Giacalone, **Sustainability (MDPI), 2020, 12, 6854; doi: 10.3390/su12176854.**

Presentations

Oral presentation:

1. *"Use of nano-structural materials for pollutant removal in water treatment", G. Costamagna, S. Mariotti, and M. Ginepro, XXVIII Congresso Divisione Chimica*

Analitica (Società Chimica Italiana), Bari, Italy, September 2019, ISBN: 978-88-94952-10-0.

2. *"Innovative materials for As(III) and As(V) removal in water treatment", Merck & Elsevier Young Chemists Symposium (MYCS 2019)", G. Costamagna, L. Defereria, S. Caro and M. Ginepro, Merck & Elsevier Young Chemists Symposium (MYCS 2019), Rimini, Italy, 25-27th November 2019, ISBN: 978-88-94952-15-5*

Poster presentation:

1. *"Use of biochar as water purification system in waters contaminated by heavy metals", G. Costamagna, S. Mariotti, C. Bezzi and M. Ginepro, XXVIII Congresso Divisione Chimica Analitica (Società Chimica Italiana), Bari, Italy, September 2019, ISBN: 978-88-94952-10-0*
2. *"Innovative materials for As(III) and As(V) removal in water treatment", Merck & Elsevier Young Chemists Symposium (MYCS 2019)", G. Costamagna, L. Defereira, S. Caro and M. Ginepro, Merck & Elsevier Young Chemists Symposium (MYCS 2019), Rimini, Italy, 25-27th November 2019, ISBN: 978-88-94952-15-5*
3. "*Preservation of fresh-cut fruit with polyphenols and essential oils extracted with Microwave Assisted Extraction technique",* Giulia COSTAMAGNA*, Lisa GHIDETTI, Valentina CHIABRANDO, Giovanna GIACALONE, Marco GINEPRO, *Green Chemistry Online Postgraduate Summer School, 6-10th, University Ca' Foscari, Venice, Book of Abstract, page 62.*

PhD Courses Attended

Course title	Instructor	University / Department	Hours	CFU
Raman Day 2020	Alessandro Damin – Eliano Diana – Sergio Favero-Longo – Simona Ferrando – Daniele Giordano – Paolo Olivero – Jasmine Petriglieri – Federico Picollo – Francesco Turci	Department of Chemistry, University of Turin	8	2
Electrochemical Energy Storage and Conversion Systems	Mauro Sgori	Department of Chemistry, University of Turin	10	2,5

IDROGEOLOGIA AMBIENTALE: LA CONTAMINAZIONE DELLE ACQUE SOTTERRANEE	Prof. Domenico de Luca and Prof. Manuela Lasagna	Deparment of Earth Sciences	8	2

PhD Schools Attended

- Green Chemistry Online Postgraduate Summer School, University of Ca' Foscari, Venice, 6- 10 July 2020.

Seminars, Conferences Attended

- XXVIII Congresso della Divisione di Chimica Analitica – Società Chimica Italiana, Bari, 22-26 September 2019.
- Merck & Elsevier Young Chemists Symposium 2019, Società Chimica Italiana, Rimini, Italy, 25-27 November 2019.
- Shimadzu Workshop "Applicazione analitiche ed innovazioni tecnologiche" Università degli Studi di Torino, Dipartimento di Scienze e Tecnologie del Farmaco, Turin Italy, 5th November 2019.
- "Machine Learning meets chemistry", 17-18th of February 2020 at the Chemistry Department, UNITO.
- Shimadzu Online Workshop "Cannabis: il corretto approccio analitico in ambito analitico e forense"
- Convegno "Collaborazione tra Istituzioni Scientifiche, Aziende ed Enti" 29 Jenuary 2020 Università degli Studi di Torino, Dipartimento di Chimica. Organizer: Dott. Marco Ginepro.

Other activities

Assistant for teaching: Incarico di Supporto alla didattica art.27- Assistenza al laboratorio di "*Controllo Analitico dei prodotti e dei processi industriali*", Laurea Magistrale in Chimica Industriale, Dipartimento di Chimica, Università degli Studi di Torino – 48 h.

3rd year:

Papers

- *Quantitative insights on the interaction between metal ions and water kefir grains: kinetics studies and EPR investigations*
  Giulia Costamagna, Giorgio Volpi, Elena Ghibaudi, Marco Ginepro , **Natural Product Research (Taylor&Francis online); doi: 10.1080/14786419.2020.1855164**

- *One-step sustainable synthesis of cationic high- swelling polymers obtained from starch-derived maltodextrins*

Claudio Cecone and Giulia Costamagna, Marco Ginepro, Francesco Trotta ***RSC Advances, Royal Society of Chemistry [2021];*** RSC Adv., 2021, 11, 7653–7662 ***DOI: 10.1039/d0ra10715h***

- *Catalytic oxidative desulphirization of pyrolytic oils to fuels over different waster derived carbon-based catalysts*

Valentina Tamborrino and Giulia Costamagna, Mattia Bartoli, Massimo Rovere, Pravin Jagdale, Luca Lavagna, Marco Ginepro, Alberto Tagliaferro, ***FUEL, Elsevier [2021];*** **Fuel, 296, (2021), 120693** ***DOI: 10.1016/j.fuel.2021.120693***

- *Combined effect of silicon and non-thermal plasma treatments on yield, mineral content, and nutraceutical proprieties of edible flowers of Begonia cucullata*

Silvia Traversari, Laura Pistelli, Bianca del Ministro, Sonia Cacini, Giulia Costamagna, Marco Ginepro, Ilaria Marchioni, Alessandro Orlandini, Daniele Massa, ***Plant Physiology and Biochemistry, Elsevier [2021]; Fuel, 296, (2021), 120693 DOI: 10.1016/j.fuel.2021.120693***

PhD Courses Attended

Course title	Instructor	University / Department	Hours	CFU
Chemical Sensors for Scientific Research and Everyday Life	Ornella Abollino	Department of Chemistry, University of Turin	8	2
LyondellBasell: from the first Ziegler Natta Catalyst to Polymer Circularity	Paracat	Department of Chemistry, University of Turin	32	4
Bibliography and bibliometrics like pros: Stay up to date and Develop Literature Syntheses in the Biomedical Domain	Paolo Gardois, Nicoletta Colombi	Doctoral School of the University of Turin	14	3,5

Other activities

Assistant for teaching: Incarico di Supporto alla didattica art.27- Assistenza al laboratorio di "*Controllo Analitico dei prodotti e dei processi industriali*", Laurea Magistrale in Chimica Industriale, Dipartimento di Chimica, Università degli Studi di Torino – 36 h.

Due to COVID-19 Pandemic Situation it was not possible to spend my period abroad.